

# CASE FILE COPY

VIBRATION AND DAMPING OF  
LAMINATED, COMPOSITE-MATERIAL PLATES  
INCLUDING THICKNESS-SHEAR EFFECTS

Final Report (Part II)  
NASA Research Grant NGR-37-003-055

by

C.W. Bert & C.C. Siu  
School of Aerospace, Mechanical and Nuclear Engineering  
The University of Oklahoma  
Norman, Oklahoma 73069

Prepared for  
National Aeronautics and Space Administration  
Washington, D.C.

March 1972

1. Report No. <b>NASA CR- 112140</b>		2. Government Accession No.		3. Recipient's Catalog No.	
4. Title and Subtitle <b>VIBRATION AND DAMPING OF LAMINATED, COMPOSITE-MATERIAL PLATES INCLUDING THICKNESS-SHEAR EFFECTS</b>				5. Report Date	
				6. Performing Organization Code	
7. Author(s) <b>C. W. Bert and C. C. Siu</b>				8. Performing Organization Report No.	
				10. Work Unit No. <b>501-22-03-03</b>	
9. Performing Organization Name and Address <b>School of Aerospace, Mechanical, and Nuclear Engineering The University of Oklahoma Norman, Oklahoma 73069</b>				11. Contract or Grant No. <b>NGR-37-003-055</b>	
				13. Type of Report and Period Covered <b>Contractor Report</b>	
12. Sponsoring Agency Name and Address <b>National Aeronautics and Space Administration Washington, D.C. 20546</b>				14. Sponsoring Agency Code	
15. Supplementary Notes					
16. Abstract <p>An analytical investigation of sinusoidally forced vibration of laminated, anisotropic plates including bending-stretching coupling, thickness-shear flexibility, all three types of inertia effects, and material damping was conducted. The analysis begins with the anisotropic stiffness and damping constitutive relations for a single layer and proceeds through the analogous relations for a laminate. Then the various types of energy and work terms are derived and the problem is formulated as an eigenvalue problem by application of the extended Rayleigh-Ritz Method. The effects of thickness-shear deformation are considered by the use of a shear correction factor analogous to that used by Mindlin for homogeneous plates. The general analysis is applicable to plates with any combination of natural boundary conditions at their edges.</p> <p>Natural frequencies of boron/epoxy plates calculated on the basis of two different resonance criteria (peak-amplitude and modified Kennedy-Pancu techniques) and the associated nodal patterns are in good agreement with previously published experimental data.</p>					
17. Key Words (Suggested by Author(s)) <b>Composite materials Vibration damping Stiffness Vibration , Micromechanics</b>				18. Distribution Statement  <b>Unclassified - Unlimited</b>	
19. Security Classif. (of this report) <b>Unclassified</b>		20. Security Classif. (of this page) <b>Unclassified</b>		21. No. of Pages <b>245</b>	
				22. Price*	

VIBRATION AND DAMPING OF  
LAMINATED, COMPOSITE-MATERIAL PLATES INCLUDING THICKNESS-  
SHEAR EFFECTS

CONTENTS

	<u>Page</u>
ABSTRACT	iv
SYMBOLS	vi
I. INTRODUCTION	1
1.1 Introductory Remarks	1
1.2 A Brief Survey of Selected Vibrational Analyses of Laminated Plates	4
II. FORMULATION OF THE THEORY	9
2.1 Hypotheses	9
2.2 Kinematics	10
2.3 Stiffness Constitutive Relations	11
2.4 Strain Energy	15
2.5 Damping Coefficients and Dissipative Energy	17
2.6 Kinetic Energy	18
2.7 Work Done by External Forces	19
2.8 Application of the Extended Rayleigh-Ritz Method	20
2.9 Reduction to Matrix Form	23

III. DERIVATION OF THICKNESS-SHEAR FACTORS FOR LAMINATES	25
3.1 Static Approach	26
3.2 Dynamic Approach	30
IV. MODAL FUNCTIONS USED FOR VARIOUS PLATE BOUNDARY CONDITIONS	32
4.1 Simply Supported on All Edges	32
4.2 Fully Clamped on All Edges	33
4.3 Free on All Edges	34
V. NUMERICAL RESULTS AND COMPARISON WITH RESULTS OF OTHER INVESTIGATORS	35
5.1 Thickness-Shear Factors for Laminates	35
5.2 Plate Simply Supported on All Edges	36
5.3 Plate Free on All Edges	38
VI. CONCLUSIONS	42
APPENDIXES	
A. NOTATION AND TRANSFORMATION FOR ELASTIC COEFFICIENTS	44
B. MODELS AND MEASURES OF MATERIAL DAMPING	50
B1. Mathematical Models for Material Damping	50
B2. Measures of Material Damping	62
B3. Inter-Relationships Among Various Measures of Damping for Homogeneous Materials	67
C. DERIVATION OF ENERGY DIFFERENCE	76
D. COMPLETE ENERGY EXPRESSIONS	79
D1. The Energy Difference	79
D2. Equations for Minimizing the Energy Difference	80
E. DERIVATION OF THICKNESS-SHEAR FACTOR FOR THE THREE-LAYER, SYMMETRICALLY LAMINATED CASE USING THE DYNAMIC APPROACH	85
E1. Dynamic Elasticity Analysis of an Individual Layer Undergoing Pure Thickness-Shear Motion	85

E2. Dynamic Elasticity Analysis for Three-Layer, Symmetrically Laminated Case	86
E3. Dynamic Analysis of a Symmetrically Laminated Timoshenko Beam Undergoing Pure Thickness-Shear Motion	88
E4. Determinations of the Thickness-Shear Factor	91
F. COMPLEX STIFFNESS COEFFICIENTS FOR A LAMINATE HAVING ALTERNATING PLIES OF TWO DIFFERENT COMPOSITE MATERIALS	92
F1. Introduction	92
F2. Analysis	93
G. IDENTIFICATION OF INTEGRAL FORMS	100
G1. Trigonometric Integrals	100
G2. Combination Trigonometric-Beam Type Integrals	107
H. EVALUATION OF EXPERIMENTAL METHODS USED TO DETERMINE MATERIAL DAMPING IN COMPOSITE MATERIALS	109
I. DISCUSSION ON SYMMETRY OF THE ARRAY OF CONSTITUTIVE COEFFICIENTS	123
J. COMPUTER PROGRAM DOCUMENTATION	126
REFERENCES	128
TABLES	147
FIGURES	157
COMPUTER PROGRAM LISTING	180

## ABSTRACT

This report is concerned with analytical investigation of sinusoidally forced vibration of laminated, anisotropic plates including bending-stretching coupling, thickness-shear flexibility, all three types of inertia effects, and material damping.

In the analysis the effects of thickness-shear deformation are considered by the use of a shear correction factor  $K$ , analogous to that used by Mindlin for homogeneous plates. Two entirely different approaches for calculating the thickness-shear factor for a laminate are presented. Numerical examples indicate that the value of  $K$  depends on the layer properties and the stacking sequence of the laminate.

The general analysis is applicable to plates with any combination of natural boundary conditions at their edges. The analysis begins with the anisotropic stiffness and damping constitutive relations for a single layer and proceeds through the analogous relations for a laminate. Then the various types of energy and work terms are derived and the problem is formulated as an eigenvalue problem by application of the extended Rayleigh-Ritz method.

The first five resonant frequencies of boron/epoxy plates with all edges free are calculated on the basis of two different resonance criteria: the peak-amplitude and modified Kennedy-Pancu techniques. The results show that the resonant frequencies obtained by the two techniques differ by only a very small amount, and are in good agreement with the results obtained

both experimentally and analytically by Clary. Furthermore, the nodal patterns obtained agree satisfactorily with those of Clary. Finally, the damping values in this investigation are in good agreement with the experimental ones obtained by Clary.

## SYMBOLS

$A$	cross-sectional area
$A_o$	area involved in shear-stress integration (fig. 8)
$A_i, B_i$	constants depending upon the boundary conditions (Appendix E)
$A_i$	hereditary constants, eq. (B-21)
$A_{ij}$	stretching stiffness of the plate
$a$	length of plate
$a(x_1), a(x_2)$	wave amplitudes at positions $x_1$ and $x_2$
$a_i, a_{i+1}, a_{i+n}$	free-vibration amplitudes corresponding to the $i$ -th, $(i+1)$ th, and $(i+n)$ th cycles
$a_o$	initial amplitude
$B_{ij}$	bending-stretching coupling stiffness of the plate
$\bar{B}_{ij}$	complex stiffness coefficient
$b$	width of plate
$b$	material damping coefficient defined in eq. (B-10)
$b_c$	critical material damping coefficient
$C_d$	damping coefficient defined in eq. (B-22)
$C'_d$	damping coefficient defined in eq. (B-8)
$C_i$	constants depending upon the initial conditions
$C_{ij}$	Cauchy elastic coefficient
$\bar{C}_{ij}$	complex version of $C_{ij}$
$\bar{C}'_{ij}$	effective stiffness coefficients defined following eq. (F-7)
$C_m, C_n$	characteristic parameters tabulated in ref. 44
$c$	viscous damping coefficient



$\bar{c}$	Kelvin-Voigt complex damping coefficient
$c_c$	critical value of $c$
$c_s$	shear wave-propagation velocity
$D$	total dissipative energy
$D_A$	energy dissipated per unit of plate area
$D_{ij}$	bending and twisting stiffnesses of the plate
$\bar{D}_{ij}$	complex version of $D_{ij}$
$E$	Young's modulus
$E_{11}, E_{22}$	Young's moduli in the $x, y$ directions
$Ei(u)$	the exponential integral defined in eq. (B-18)
$e$	base of the natural logarithms, $e \approx 2.7183$
$F_d$	damping force
$F_s$	spring force
$\tilde{F}$	exciting force amplitude
$\Delta F$	horizontal shear force per unit width
$F_{ij}$	thickness-shear stiffnesses of the plate
$\bar{F}_{ij}$	complex stiffness coefficients associated with $F_{ij}$
$\{f\}$	generalized-force column matrix
$g$	loss tangent
$g_1$	parameter of the Biot model
$g_k$	dimensionless geometric parameter defined in ref. 35
$g_{A11}$ , etc.	subscripted loss tangents where the subscripts (i.e. $A_{11}$ ) refer to the associated stiffness; for example, $g_{A11}$ signifies the loss tangent associated with the longitudinal stretching stiffness
$H$	factor $\equiv (h/m)^{\frac{1}{2}}$
HPMF	half-power magnification factor
$\bar{H}$	factor $\equiv H/\omega_n$

$H^{(a)}, H^{(b)}$	thickness fractions of layers a and b, respectively
$h$	total thickness of the plate; parameter in eq. (H-2)
$I$	integral form defined in Appendix G
$i$	unit imaginary number $\equiv \sqrt{-1}$
$K$	thickness shear factor
$\bar{K}$	factor defined in eq. (H-10)
$\bar{K}_c$	complex-flexibility factor defined in eq. (F-15)
$K_{ij}$	composite shear coefficient
$k$	spring rate
$\bar{k}$	complex spring constant
$k'$	stiffness coefficient associated with the total in-plane force
$k''$	$C_1 e^{im}$ ( $C_1$ and $m$ are constants)
$\bar{k}$	Kelvin-Voigt complex stiffness defined in eq. (B-3)
$L$	effective length of spring
$\tilde{L}$	amplitude of Lagrangian energy difference
$\bar{L}_c$	complex-stiffness factor defined in eq. (F-16)
$\ln$	natural logarithm
$\log$	logarithm with base 10
$[M]$	mass matrix
$M_{ij}$	stress couples, moment per unit width
$MF, MF'$	magnification factors defined in eqs. (B-38) and (B-16)
$m$	damping exponent defined in eq. (B-22)
$m$	mass
$m, n$	$\cos \theta, \sin \theta$
$m_0, m_1, m_2$	mass per unit of plate area, first moment of mass per unit area, second moment of mass per unit area

$N_{ij}$	membrane stress resultants, force per unit width
$n$	degree of heredity
$Q$	quality factor $\equiv$ reciprocal of the dimensionless bandwidth
$Q_i$	thickness-shear stress resultant
$Q_{kl}$	reduced stiffness coefficients transformed to plate coordinates $(x,y)$ ; see eq. (A-16)
$Q_{kl}^*$	reduced (plane-stress) stiffness coefficients with respect to material symmetry axes $(X,Y)$ ; defined in eq. (A-6)
$q$	normal pressure acting on plate
$R$	density ratio ( $\equiv \rho^{(1)} / \rho^{(2)}$ )
$\text{RMF}$	resonant magnification factor
$\bar{S}_{ij}$	complex flexibility defined in eq. (F-22)
$[S]$	complex stiffness matrix
$T$	kinetic energy; period of damped oscillation (Appendix B only)
$T_A$	kinetic energy per unit of plate area
$[T_r]$	transformation matrix defined in eq. (A-12)
$t$	time
$t_1, t_2$	two different specific values of time
$U$	strain energy
$U_A$	strain energy per unit of plate area
$U_d$	energy dissipated per cycle
$U_{dv}$	damping energy per cycle and per unit of volume
$U_{mn}$	undetermined longitudinal-displacement parameters
$U_s$	shear strain energy
$U'_s$	shear strain energy associated with equivalent uniform, longitudinal thickness-shear strain
$U_v$	strain energy per unit of plate volume

$u, v, w$	displacements in the $x, y, z$ directions
$u_o, v_o, w_o$	displacements of middle surface in $x, y, z$ directions
$\tilde{u}$	displacement amplitude of vibration
$u'$	transient solution in eq. (B-70)
$u_{st}$	static displacement; see Appendix B
$V$	volume
$V_{mn}$	undetermined transverse-displacement parameter
$v_s$	spatial attenuation constant defined in eq. (B-33)
$v_t$	temporal decay constant defined in eq. (B-30)
$W$	total work done
$W_{mn}$	undetermined normal-displacement parameter
$X, Y, Z$	coordinates of the material-symmetry axes
$x, y, z$	rectangular coordinates in the longitudinal, transverse, and thickness directions
$x_1, x_2$	two different specific values of position
$z_m, z_n$	characteristic parameters tabulated in ref. 44
$z_k, z_{k-1}$	thickness-direction coordinates of outer and inner faces of the $k$ -th layer
$\{ \}$	column matrix
$[ \ ]$	square matrix
$\alpha, \beta$	normalized arguments in the $x, y$ directions
$\bar{\alpha}$	$\alpha_1 / \alpha_n$
$\alpha_i$	heredity constants in eq. (B-21)
$\beta$	$C_{55}^{(1)} / C_{55}^{(2)}$ in Appendix E only
$\gamma$	loss angle defined in eq. (B-27)
$\gamma_s$	spatial attenuation rate defined in eq. (B-34)
$\gamma_t$	decay rate defined in eq. (B-31)

$\bar{\Delta}$	complex factor defined in eq. (F-22)
$\delta$	logarithmic decrement defined in eq. (B-28)
$\delta_s$	logarithmic attenuation defined in eq. (B-32)
$\epsilon$	Biot parameter in eq. (B-17)
$\epsilon_{ij}$	strain components with respect to x,y axes
$\epsilon_{IJ}$	strain components with respect to X,Y axes
$\epsilon_{xz}$	strain corresponding to longitudinal thickness-shear action (Section III and Appendix E)
$\epsilon'_{xz}$	longitudinal thickness-shear strain weighted according to eq. (55)
$\zeta$	damping ratio
$\zeta_2$	$z_2/z_1$ (Appendix E)
$\theta$	angle of orientation of an individual layer
$\kappa_{ij}$	curvature changes
$u$	parameter ( $\approx \epsilon/\mu_n$ )
$\nu$	Poisson's ratio
$\nu_{12}, \nu_{21}$	major and minor in-plane Poisson's ratios
$\xi$	generalized coordinate
$\{F_{mn}\}$	column matrix representing generalized displacements
$\pi$	$\pi \approx 3.1415962$
$\rho$	density
$\sum$	summation symbol
$\bar{\sigma}$	stress amplitude
$\sigma_{ij}$	stress components with respect to x,y axes
$\sigma_{IJ}$	stress components with respect to X,Y axes
$\tau$	dummy time variable in eq. (B-19)
$\psi$	assumed modal function
$\phi(t)$	hereditary kernel defined in eq. (B-21)

$\phi$	phase angle between response and exciting force
$\Psi_{xmn}, \Psi_{ymn}$	undetermined rotation parameters
$\Psi_x, \Psi_y$	angles of rotation in the xz and yz planes
$\Omega$	dimensionless frequency ( $\equiv \omega/\omega_n$ )
$\Omega_{hp}$	$\Omega$ at half-power points
$\Omega_s$	$\omega/c_s$
$\omega$	circular frequency of vibration
$\omega_n$	natural frequency
$\omega_1, \omega_2$	angular frequencies defining the half-power points of the frequency spectrum

#### Superscripts:

(k)	denotes a typical kth layer
$\wedge$	denotes a damping quantity
$\cdot$	denotes differentiation with respect to time
$\sim$	denotes that the quantity is an amplitude
o	refers to the middle surface of the plate
I, R	denote the respective imaginary and real parts of a complex quantity

#### Subscripts:

,	denotes partial differentiation with respect to the variable following the comma, i.e. $u_{0,x} = \partial u_0 / \partial x$
k	integers ; $k = 1, 2, \dots K$
l	integers ; $l = 1, 2, \dots L$
m	integers ; $m = 1, 2, \dots M$
n	integers ; $n = 1, 2, \dots N$
R	denotes resonance

## SECTION I

### INTRODUCTION

#### 1.1 Introductory Remarks

The continuing demand for increased structural efficiency in many advanced aerospace vehicles has resulted in development of laminated structures made of advanced fiber-reinforced composite materials, such as boron-epoxy, graphite-epoxy and boron-aluminum (reference 1). One of the most common structural elements for such vehicles is the rectangular plate or panel, for which numerous stable static, buckling, and free-vibrational analyses have been performed (reference 2). These advanced vehicles must maintain their structural integrity not only during high statically applied mechanical and thermal loadings, but also in a variety of dynamic environments. In order to predict the dynamic stresses to which a structure will be subjected, it is necessary to perform a dynamic response analysis including the effects of damping properties as well as the various stiffnesses. An example of this type of requirement is found in the Space Shuttle now under NASA preliminary development (reference 3).

A composite material is defined as two or more materials joined together to form a nonhomogeneous material, which is used in constructing structures. Although such a material is nonhomogeneous on a micro scale, it behaves macroscopically as if it were a homogeneous, anisotropic material. An anisotropic material is one which exhibits different properties when

tested at different directional orientations within the body. For example, a single layer of composite material containing unidirectionally oriented fibers (hereafter referred to as a unidirectional composite) has considerably greater stiffness and strength in the direction of the fibers than it does in a direction transverse to the fibers (see figure 1). This anisotropic aspect is one of several which makes structural analyses for composite-material structures more complicated (reference 4) than those for ordinary isotropic materials, such as aluminum alloys or many unfilled plastics.

A single layer of unidirectional composite has certain orthogonal axes of material symmetry and thus is said to be orthotropic, and behaves in considerably simpler fashion than a general anisotropic material. If the material is thin it is called plane orthotropic. However, for purposes of obtaining a more efficient design, it is often advantageous to place different layers or plies at different orientations. For the case of a thin plate, this means that we must consider it as a plane anisotropic material. This treatment is intermediate between the complicated general anisotropic case and the much simpler plane orthotropic case.

A laminate consists of two or more layers integrally joined together. It is said to be laminated symmetrically if all of the layers above and below the midplane of the laminate have the same dimensions, properties, and orientation (if the layers are orthotropic); see figure 2. A laminate is said to be balanced if all of the layers oriented at  $+\theta$  are balanced by an equal number of identical layers at an orientation of  $-\theta$ ; see figure 3. If a laminate is not symmetrically laminated, coupling occurs between in-plane (either normal or shear) stress on one hand and either bending or twisting deformation on the other hand. In such a case as a laminate



consisting of a metallic substrate and a few layers of overlaying filamentary composite material, considerable bending-stretching coupling can occur and thus, it is necessary to consider not only the in-plane and bending stiffnesses but also the coupling stiffnesses which couple together the other two effects (reference 4). Obviously, this is considerably more complicated to analyze than a simple single layer.

Unfortunately, it appears that no one has yet succeeded in devising a lamination scheme that is both symmetrical and balanced. However, in the special, yet practical, case of multiple identical layers oriented alternately at  $+0$  and  $-0$ , as the number of layers is increased, the bending-coupling effect diminishes (reference 5). For more than ten such layers, the bending-stretching coupling may be neglected for most engineering purposes and, thus, the laminate may be treated macroscopically as if it were a single-layer plate.

It has long been recognized that, due to the relatively low shear stiffnesses of composite materials in planes normal to the laminating plane, the thickness-shear\* deformations must be included in the analysis, even when the plate is relatively thin (references 6-8), in order to achieve reasonably good predictions of laminate flexural behavior. Although several existing laminated plate theories include thickness-shear flexibility, all of them require an ad hoc assumption of the required shear correction factor. In this report, two different, relatively simple procedures are

---

\* Sometimes referred to as "transverse shear", especially in the case of beams. The terminology used here follows that established by Yu for sandwich plates (reference 9). Here the term, transverse, is reserved for the in-plane direction which is normal to the longitudinal direction.

presented to enable rational prediction of the appropriate composite shear correction factor (K). The frequencies calculated using these values for K in shear-flexible laminated plate vibrational analysis give good agreement with the exact three-dimensional elasticity solution, which is computationally much more complicated.

The use of high-damping polymeric materials in the form of a thin layer or tape has come into widespread use as a structural damper to reduce the vibrational response of aircraft panels, especially in high-noise regions such as in the vicinity of jet engines. When the polymeric material is added on either one side or both sides, it is known as an unconstrained damping layer; when the polymeric material is placed between two or more layers, it is called a constrained damping layer (or layers). Appropriate analyses and design procedures have been developed for including either type of damping layer, assuming all layers (metal and polymer) are isotropic (references 10-12). However, so far as known, no detailed solutions have been published on vibration of laminated composite-material plates which included material damping. Such an analysis is presented in this report and the results are compared with experimental data reported recently by Clary (reference 13).

## 1.2 A Brief Survey of Selected Vibrational Analyses of Laminated Plates

Apparently the first vibrational analysis was carried out by Pister (reference 14) for a thin plate arbitrarily laminated of isotropic layers. In this case, the net effect of the bending-stretching coupling resulted in a reduced flexural stiffness.

Stavsky (reference 15) formulated a coupled bending-stretching dynamic theory for thin plates laminated of composite-material layers, but he did not present any numerical results. Apparently the first published results of the vibrational analysis of such plates is due to Ashton and Waddoups (reference 16), who used the Rayleigh-Ritz method to analyze rectangular plates. These results compared reasonably well with experimental results for the completely free and cantilever cases. A similar analytical and experimental study, but involving simply supported and free boundary conditions, was carried out by Hikami (reference 17). Additional analysis of the free-edge case was carried out by Ashton (reference 18).

For simply supported plates, Whitney and Leissa (references 19,20) presented closed-form solutions for the natural frequencies in the case of cross-ply and angle-ply lamination schemes. As would be expected, their results showed a strong effect of bending-stretching coupling in lowering the natural frequencies.

The case of clamped boundary conditions is more complicated analytically, but more representative of practical aerospace structures. Rayleigh-Ritz and experimental investigations of such structures were carried out independently by Ashton and Anderson (reference 21) and by Bert and Mayberry (reference 22).

The first more accurate vibrational analysis of laminated plates including thickness-shear flexibility was made by Ambartsumyan; see reference 23. He assumed an arbitrary distribution of thickness-shear stresses through the thickness. However, in carrying out his actual calculations, Ambartsumyan assumed a simple parabolic distribution. It can be shown by a simple mechanics-of-materials analysis (Jourawski shear theory; see Section

III) that the thickness-shear stress distribution must be discontinuous from layer to layer; thus, the simple parabolic distribution does not hold. Ambartsumyan did not give any numerical results for vibration of laminated plates; however, Whitney (reference 24) did so, using Ambartsumyan's basic theory.

Using another approach, Yang et al (reference 25) extended the Mindlin homogeneous, isotropic, dynamic plate analysis (reference 26) to the laminated anisotropic case. They assumed a thickness-shear angle which is independent of the thickness coordinate (z) and then integrated the stress equations of motion to obtain the governing partial differential equations. After integration, they introduced a thickness-shear coefficient in an ad hoc fashion to correlate the predicted frequencies with known results.

Also Yang et al introduced the coupling inertial effect (present only in the case of plates laminated unsymmetrically with respect to mass distribution), as well as the familiar translational and rotatory inertia effects present in homogeneous (or mass-symmetrically laminated) plates. The inclusion of these higher-order inertial effects is consistent with the inclusion of thickness-shear flexibility.

The analysis presented in this report is an improvement over both the Ambartsumyan and Yang et al analyses, in that it presents simple rational means for calculating the shear coefficient, rather than assuming it a priori.

An alternative to considering shear deformation per se is to make a microlaminar analysis, such as considered by Biot (reference 27) and Bolotin (reference 28). However, this approach has not been used very extensively so far.

Another approximate approach is to use the Voigt and Reuss models to

determine the properties of an equivalent homogeneous, anisotropic, shear-flexible plate. This method was originated independently by Postma (reference 29), White and Angona (reference 30), and Rytov (reference 31) to investigate wave propagation in a continuum consisting of alternating layers of stiff and flexible isotropic materials. This concept was applied recently to plates with experimental verification for the special case of a beam, by Achenbach and Zerbe (reference 32). A new analysis, extending the Postma approach to the more general case of a laminate consisting of alternating orthotropic layers, is presented in Appendix F.

All of the analyses mentioned above are approximate formulations in this sense: interlaminar compatibility is impossible unless both of the in-plane Poisson's ratios are identical in all of the layers. The reason for this is that, in a plate, one can have discontinuities in the strain component in a given direction in the plane, due to the Poisson contraction caused by a stress resultant or a stress couple acting in the perpendicular direction in the plane. This deficiency can be removed by using the approach introduced recently by Hsu and Wang (reference 33) and Wang (reference 34) for laminated shells. Another technique is to apply the nonhomogeneous three-dimensional elasticity approach, such as used recently by Srinivas et al (references 35-37) for a special case of simply supported edges. Still another method is to use finite elements in the thickness direction, as introduced recently by Tso et al (reference 38). Unfortunately, all of the more accurate analyses mentioned in this paragraph are quite complicated computationally and thus are not amenable to engineering analyses of practical structural elements. Furthermore, the work of reference 37 showed that for structurally reasonable values of the following modal parameter, the Mindlin-type theory (such as extended here) is

sufficiently accurate for determination of natural frequencies, but not for determination of the associated stress distribution.

There are numerous analyses in the literature on vibration of damped plates with isotropic layers; also there are a few vibrational analyses of single-layer, anisotropic plates and a few quasi-static (creep) analyses of laminated, anisotropic plates. However, vibrational analyses of laminated, anisotropic plates are quite limited. Dong (reference 39) indicated the solution for the dynamic response of a simply-supported rectangular plate arbitrarily laminated of orthotropic, viscoelastic plies modeled as a standard linear solid.

## SECTION II

### FORMULATION OF THE THEORY OF LAMINATED, SHEAR-FLEXIBLE PLATES

In this section is presented a theoretical analysis of sinusoidally forced vibration of laminated, anisotropic plates including bending-stretching coupling, thickness-shear, all three types of inertia effects, and material damping. First the assumptions, on which the analysis is based, are stated explicitly. The general analysis is applicable to plates with any combination of natural boundary conditions at their edges. The analysis begins with the anisotropic stress-strain relations for a single layer and proceeds through the stiffness and damping constitutive relations, formulation of the various types of energy and work terms, and culminates in the formulation of an eigenvalue problem by application of the extended Rayleigh-Ritz method.

#### 2.1 Hypotheses

The following assumptions are made in the analysis presented here:

H1. All displacements are assumed to be sufficiently small so that the linear strain-displacement relations are sufficiently accurate.

H2. The layers which make up the plate are linearly elastic and may be isotropic or orthotropic with any arbitrary orientation in the plane of the plate.

H3. The layers are sufficiently thin that thickness-normal-stress

effects may be neglected, i.e. the layers are assumed to have finite stiffnesses which resist membrane, bending, and thickness shearing stresses.

H4. The layers are assumed to be bonded together perfectly.

H5. The plate is assumed to have all components of translational, translational-rotatory coupling, and rotatory inertia.

H6. All material damping effects are assumed to be small. They are incorporated by using stiffnesses which are complex rather than real (see Appendix B); the complex-stiffness array is assumed to be symmetric (see Appendix I). All other thermal effects are neglected.

H7. All initial-stress effects are neglected.

H8. All interactions with a surrounding fluid can be either neglected or considered to be included in the values used for the material-damping coefficients.

H9. The excitation consists of a uniformly distributed normal pressure loading, sinusoidal with respect to time.

## 2.2 Kinematics

The displacement field is assumed to be (hypothesis H3):

$$\begin{aligned}u(x,y,z,t) &= u_0(x,y,t) + z\psi_x(x,y,t) \\v(x,y,z,t) &= v_0(x,y,t) + z\psi_y(x,y,t) \\w(x,y,z,t) &= w_0(x,y,t)\end{aligned}\tag{1}$$

where  $u, v, w$  are the displacement components in the  $x, y, z$  directions (see figure 4);  $u_0, v_0, w_0$  are the displacement components at the middle surface



of the multi-layer plate;  $\psi_x$  and  $\psi_y$  are the weighted middle-surface rotations in the respective  $xz$  and  $yz$  planes; and  $t$  is time.

Within the framework of hypothesis H1, the total engineering strains are given by the following in-plane strain-displacement relations:

$$\epsilon_{ij} = \epsilon_{ij}^0 + z\kappa_{ij} \quad \begin{matrix} \text{(no sum)} \\ (ij = xx, yy, xy) \end{matrix} \quad (2)$$

where

$$\epsilon_{xx}^0 = u_{0,x} \quad ; \quad \epsilon_{yy}^0 = v_{0,y} \quad ; \quad \epsilon_{xy}^0 = v_{0,x} + u_{0,y} \quad (3)$$

$$\kappa_{xx} = \psi_{x,x} \quad ; \quad \kappa_{yy} = \psi_{y,y} \quad ; \quad \kappa_{xy} = \psi_{y,x} + \psi_{x,y} \quad (4)$$

Also the following thickness-shear strain-displacement relations hold:

$$\epsilon_{xz} = w_{0,x} + \psi_x \quad ; \quad \epsilon_{yz} = w_{0,y} + \psi_y \quad (5)$$

where a subscript comma denotes partial differentiation with respect to the variable following the comma, i.e.  $u_{0,x} = \partial u_0 / \partial x$ .

### 2.3 Stiffness Constitutive Relations

In line with hypothesis H2, the following stress-strain relations are assumed to hold for each individual layer of which the plate is comprised:

$$\begin{Bmatrix} \sigma_{xx}^{(k)} \\ \sigma_{yy}^{(k)} \\ \sigma_{yz}^{(k)} \\ \sigma_{xz}^{(k)} \\ \sigma_{xy}^{(k)} \end{Bmatrix} = \begin{bmatrix} Q_{11}^{(k)} & Q_{12}^{(k)} & 0 & 0 & Q_{16}^{(k)} \\ Q_{12}^{(k)} & Q_{22}^{(k)} & 0 & 0 & Q_{26}^{(k)} \\ 0 & 0 & Q_{44}^{(k)} & Q_{45}^{(k)} & 0 \\ 0 & 0 & Q_{45}^{(k)} & Q_{55}^{(k)} & 0 \\ Q_{16}^{(k)} & Q_{26}^{(k)} & 0 & 0 & Q_{66}^{(k)} \end{bmatrix} \begin{Bmatrix} \epsilon_{xx}^{(k)} \\ \epsilon_{yy}^{(k)} \\ \epsilon_{yz}^{(k)} \\ \epsilon_{xz}^{(k)} \\ \epsilon_{xy}^{(k)} \end{Bmatrix} \quad (6)$$

where  $\sigma_{xx}^{(k)}$ ,  $\sigma_{yy}^{(k)}$  are the in-plane normal stresses;  $\sigma_{xz}^{(k)}$ ,  $\sigma_{yz}^{(k)}$  are the thickness-shear stresses;  $\sigma_{xy}^{(k)}$  is the in-plane shear stress; the  $Q_{ij}$  are the reduced stiffness coefficients which are applicable to a thin layer (see Appendix A); superscript (k) denotes a typical layer k, where  $k = 1, 2, 3, \dots, n$ ; and n is the total number of layers of which the plate is comprised.

It is noted that it is more consistent mathematically to write the stress-strain relations in either matrix form as

$$\left\{ \sigma_i^{(k)} \right\} = [Q_{ij}^{(k)}] \left\{ \epsilon_j^{(k)} \right\} \quad (i, j = 1, 2, 4, 5, 6), \quad (7)$$

or in tensor notation as

$$\sigma_{ij}^{(k)} = Q_{ijkl}^{(k)} \epsilon_{kl}^{(k)} \quad (i, j = x, y, z). \quad (8)$$

However, here a mixed notation is used for engineering convenience: double lettered subscripts (xx, yy, yz, xz, xy) following classical elasticity theory notation for stresses and strains, and double numbered subscripts (i, j = 1, 2, 4, 5, 6) to reduce the number of subscripts used on the stiffness coefficients.

As is conventional in plate and shell theory, it is convenient to introduce generalized forces which are applicable to the whole laminate, rather than only a specific distance from the plate middle surface. The stress components,  $\sigma_{ij}^{(k)}$ , are functions of  $x, y, z$ ; therefore, integrating them through the thickness yields the following generalized forces, which are functions of  $x, y$  only:

$$\begin{aligned} \{N_{xx}, N_{yy}, N_{xy}, Q_x, Q_y\} &\equiv \int_{-h/2}^{h/2} \{\sigma_{xx}^{(k)}, \sigma_{yy}^{(k)}, \sigma_{xy}^{(k)}, \sigma_{xz}^{(k)}, \sigma_{yz}^{(k)}\} dz \\ &= \sum_{k=1}^n \int_{z_{k-1}}^{z_k} \{\sigma_{xx}^{(k)}, \sigma_{yy}^{(k)}, \sigma_{xy}^{(k)}, \sigma_{xz}^{(k)}, \sigma_{yz}^{(k)}\} dz \end{aligned} \quad (9)$$

$$\begin{aligned} \{M_{xx}, M_{yy}, M_{xy}\} &\equiv \int_{-h/2}^{h/2} \{\sigma_{xx}^{(k)}, \sigma_{yy}^{(k)}, \sigma_{xy}^{(k)}\} z dz \\ &= \sum_{k=1}^n \int_{z_{k-1}}^{z_k} \{\sigma_{xx}^{(k)}, \sigma_{yy}^{(k)}, \sigma_{xy}^{(k)}\} z dz \end{aligned} \quad (10)$$

where  $h \equiv$  total plate thickness, the quantity  $(z_k - z_{k-1})$  is the thickness of an individual layer (see figure 5),  $N_{ij} \equiv$  membrane stress resultants (force per unit length),  $Q_i \equiv$  thickness-shear stress resultants (force per unit length), and  $M_{ij}$  are the stress couples (moment per unit length).

Inserting the stress-strain relations, given by equations (6) into equations (9) and (10), one obtains the following constitutive relations for the composite:

$$\begin{Bmatrix} N_{xx} \\ N_{yy} \\ N_{xy} \\ \hline M_{xx} \\ M_{yy} \\ M_{xy} \\ \hline Q_y \\ Q_x \end{Bmatrix} = \begin{bmatrix} A_{11} & A_{12} & A_{16} & B_{11} & B_{12} & B_{16} & 0 & 0 \\ A_{12} & A_{22} & A_{26} & B_{12} & B_{22} & B_{26} & 0 & 0 \\ A_{16} & A_{26} & A_{66} & B_{16} & B_{26} & B_{66} & 0 & 0 \\ \hline B_{11} & B_{12} & B_{16} & D_{11} & D_{12} & D_{16} & 0 & 0 \\ B_{12} & B_{22} & B_{26} & D_{12} & D_{22} & D_{26} & 0 & 0 \\ B_{16} & B_{26} & B_{66} & D_{16} & D_{26} & D_{66} & 0 & 0 \\ \hline 0 & 0 & 0 & 0 & 0 & 0 & F_{44} & F_{45} \\ 0 & 0 & 0 & 0 & 0 & 0 & F_{45} & F_{55} \end{bmatrix} \begin{Bmatrix} \epsilon_{xx}^o \\ \epsilon_{yy}^o \\ \epsilon_{xy}^o \\ \hline \kappa_{xx} \\ \kappa_{yy} \\ \kappa_{xy} \\ \hline \epsilon_{yz} \\ \epsilon_{xz} \end{Bmatrix} \quad (11)$$

where the respective stretching, bending-stretching coupling, and bending stiffnesses of the plate are defined as follows:

$$\{A_{ij}, B_{ij}, D_{ij}\} = \int_{-h/2}^{h/2} Q_{ij}^{(k)} \{1, z, z^2\} dz \quad (i, j=1, 2, 6) \quad (12)$$

and the thickness-shear stiffnesses of the plate are as follows:

$$F_{ij} = K_{ij} \int_{-h/2}^{h/2} Q_{ij}^{(k)} dz \quad (i, j=4, 5) \quad (13)$$

where  $K_{ij}$   $\equiv$  composite shear coefficient, introduced to account for the thickness-shear strain variation through the thickness. Section III presents several approximate analyses to predict  $K_{ij}$  analytically.

The  $A_{ij}$ ,  $B_{ij}$ , and  $D_{ij}$  submatrices appearing in equation (11) are present in the classical Kirchhoff-type theory of laminated plates (see refs. 4,5,15-22). In the case of an orthotropic plate all of the terms with subscripts 16 and 26, called the cross-elasticity or shear-coupling terms, vanish. Furthermore, when the layers are all isotropic materials,

only two of each set of the terms with subscripts 11,12,22, and 66 are independent.

If the plate is either homogeneous (i.e. single layer) or laminated symmetrically about the plate middle surface, the bending-stretching coupling stiffness submatrix  $B_{ij}$  vanishes. Then the only remaining terms are the  $A_{ij}$  and  $D_{ij}$  submatrices, which are present in classical, homogeneous thin-plate theory.

The thickness-shear stiffness coefficients  $F_{ij}$  account for the presence of thickness-shear strains, in a manner which can be considered to be a generalization of that used by Mindlin (ref. 26) for homogeneous, isotropic plates. To reduce the present theory to the classical Kirchhoff-type plate theory, the thickness-shear strains would be omitted; thus, from equations (5), one would obtain:

$$\psi_x = -w_{0,x} ; \quad \psi_y = -w_{0,y} \quad (14)$$

Furthermore, one would delete the thickness-shear strains,  $\epsilon_{xz}$  and  $\epsilon_{yz}$ , from equations (11) and the thickness-shear stress resultants,  $Q_x$  and  $Q_y$ , would be computed from equilibrium considerations only.

## 2.4 Strain Energy

The differential of the strain-energy density (strain energy per unit volume) is given by:

$$dU_v^{(k)} = \sigma_{xx}^{(k)} d\epsilon_{xx}^{(k)} + \sigma_{yy}^{(k)} d\epsilon_{yy}^{(k)} + \sigma_{xy}^{(k)} d\epsilon_{xy}^{(k)}$$

$$+\sigma_{xz}^{(k)} d\epsilon_{xz}^{(k)} + \sigma_{yz}^{(k)} d\epsilon_{yz}^{(k)} \quad (15)$$

Integration of equation (15) yields:

$$U_v^{(k)} = (1/2) \left[ \sigma_{xx}^{(k)} \epsilon_{xx}^{(k)} + \sigma_{yy}^{(k)} \epsilon_{yy}^{(k)} + \sigma_{xy}^{(k)} \epsilon_{xy}^{(k)} \right. \\ \left. + \sigma_{yz}^{(k)} \epsilon_{yz}^{(k)} + \sigma_{xz}^{(k)} \epsilon_{xz}^{(k)} \right] \quad (16)$$

The strain energy per unit of plate area ( $U_A$ ) is the integral of  $U_v^{(k)}$  over the total thickness of the plate:

$$U_A = \int_{-h/2}^{h/2} U_v^{(k)} dz = \sum_{k=1}^n \int_{z_{k-1}}^{z_k} U_v^{(k)} dz \quad (17)$$

Substituting equations (16), (6), and (2) into equation (17), performing the integration, and using equations (12) and (13), one obtains the following expression for the strain energy per unit area:

$$U_A = (1/2) \left[ A_{11} (\epsilon_{xx}^o)^2 + 2A_{12} \epsilon_{xx}^o \epsilon_{yy}^o + A_{22} (\epsilon_{yy}^o)^2 + 2A_{16} \epsilon_{xx}^o \epsilon_{xy}^o \right. \\ + 2A_{26} \epsilon_{yy}^o \epsilon_{xy}^o + A_{66} (\epsilon_{xy}^o)^2 + 2B_{11} \epsilon_{xx}^o \kappa_{xx} \\ + 2B_{12} (\epsilon_{xx}^o \kappa_{yy} + \epsilon_{yy}^o \kappa_{xx}) + 2B_{22} \epsilon_{yy}^o \kappa_{yy} \\ + 2B_{16} (\epsilon_{xx}^o \kappa_{xy} + \epsilon_{xy}^o \kappa_{xx}) + 2B_{26} (\epsilon_{yy}^o \kappa_{xy} + \epsilon_{xy}^o \kappa_{yy}) \\ + 2B_{66} \epsilon_{xy}^o \kappa_{xy} + D_{11} \kappa_{xx}^2 + 2D_{12} \kappa_{xx} \kappa_{yy} + D_{22} \kappa_{yy}^2 \\ + 2D_{16} \kappa_{xx} \kappa_{xy} + 2D_{26} \kappa_{yy} \kappa_{xy} + D_{66} \kappa_{xy}^2 + F_{44} \epsilon_{yz}^2 \\ \left. + 2F_{45} \epsilon_{yz} \epsilon_{xz} + F_{55} \epsilon_{xz}^2 \right] \quad (18)$$

## 2.5 Damping Coefficients and Dissipative Energy

For a material with Kimball-Lovell structural damping (see Appendix B), the stress-strain rate relation for sinusoidal motion at a circular frequency  $\omega$  can be expressed as follows:

$$\hat{\sigma} = (b/\omega) \dot{\epsilon} \quad (19)$$

where  $b$  is a material constant and  $\dot{\epsilon}$  is the strain rate.

The strain is given by

$$\epsilon = |\epsilon| e^{i\omega t} \quad (20)$$

where  $i \equiv \sqrt{-1}$ .

Thus,

$$\dot{\epsilon} = i\omega\epsilon \quad (21)$$

Substituting equation (21) into equation (19), one obtains:

$$\hat{\sigma} = \hat{Q}\epsilon \quad (22)$$

where

$$\hat{Q} = ib \quad (23)$$

Generalizing equation (23) to the entire array of stresses and strains in layer "k", in contracted notation analogous to equation (7), we obtain the following expression, where  $\hat{Q}_{ij}^{(k)}$  is symmetric (hypothesis H6):

$$\left\{ \hat{\sigma}_i^{(k)} \right\} = [\hat{Q}_{ij}^{(k)}] \left\{ \epsilon_j^{(k)} \right\} \quad (24)$$

Equation (24) is the same as equation (7), except that here the presence of the hat symbols ( $\hat{\phantom{x}}$ ) denotes damping quantities rather than elastic quantities.

The energy dissipated per unit of plate area, due to damping, is denoted by the symbol  $D_A$ . The expression for it in terms of the midplane strains ( $\epsilon_{ij}^0$ ) and the curvatures ( $\kappa_{ij}$ ) is the same as equation (18), except for the presence of the hat symbols over all of the  $A_{ij}$ ,  $B_{ij}$ ,  $D_{ij}$ , and  $F_{ij}$  quantities, where

$$\begin{aligned}\hat{A}_{ij} &\equiv ig_{ij}^{(A)} A_{ij}, \quad \hat{B}_{ij} \equiv ig_{ij}^{(B)} B_{ij}, \quad \hat{D}_{ij} \equiv ig_{ij}^{(D)} D_{ij}, \\ \hat{F}_{ij} &\equiv ig_{ij}^{(F)} F_{ij}\end{aligned}\tag{25}$$

where  $g_{ij}^{(\phantom{A})}$  are loss tangents (see Appendix B).

## 2.6 Kinetic Energy

The differential kinetic energy of an elemental volume ( $dx$  by  $dy$  by  $dz$ ) is given by:

$$(\rho^{(k)}/2) (\dot{u}^2 + \dot{v}^2 + \dot{w}^2) dx dy dz$$

where  $\rho^{(k)}$  is the density at the point  $(x, y, z)$  and  $\dot{u}, \dot{v}, \dot{w}$  are the velocity components in the  $x, y, z$  directions respectively.

Now the kinetic energy per unit of plate area is obtained from the differential quantity given above by dividing by  $dx dy$  and integrating over the entire thickness of the plate, as follows:



$$T_A = \int_{-h/2}^{h/2} (\rho^{(k)}/2)(\dot{u}^2 + \dot{v}^2 + \dot{w}^2) dz \quad (26)$$

Substituting the kinematic relations, equations (1), into equation (26) and performing the integration, assuming that the density is uniform through the thickness of each individual layer, one arrives at the following expression:

$$\begin{aligned} T_A = & (m_0/2)(\dot{u}_0^2 + \dot{v}_0^2 + \dot{w}_0^2) + m_1 (\dot{u}_0 \dot{\psi}_x + \dot{v}_0 \dot{\psi}_y) \\ & + (m_2/2) (\dot{\psi}_x^2 + \dot{\psi}_y^2) \end{aligned} \quad (27)$$

where  $m_0, m_1$ , and  $m_2$  are respectively the mass per unit of plate area, first moment of mass per unit area (coupling inertia), and second moment of mass per unit area (mass moment of inertia), defined as follows:

$$\{m_0, m_1, m_2\} = \sum_{k=1}^n \int_{z_{k-1}}^{z_k} \rho^{(k)} \{1, z, z^2\} dz \quad (28)$$

Only the coefficient  $m_0$  appears in classical Kirchhoff theory for the dynamics of thin, homogeneous plates. The Mindlin dynamic plate theory of homogeneous plates (ref. 26) contains both  $m_0$  and  $m_2$ , while the dynamic theory originated by Yang et al (ref. 25) for laminated plates contains  $m_0, m_1$ , and  $m_2$ .

## 2.7 Work Done by External Forces

The only external force considered here is a uniformly distributed normal pressure which has a sinusoidal wave form in time. Thus, it can be written in complex variable notation as follows:

$$q(x,y,t) = \tilde{q} e^{i\omega t} \quad (29)$$

where  $\tilde{q} \equiv$  amplitude of the normal pressure.

The following expression for the total work done may be derived easily from the principle of virtual work:

$$W = \int_0^a \int_0^b q(x,y,t) w_0(x,y) dx dy \quad (30)$$

## 2.8 Application of the Extended Rayleigh-Ritz Method

Since the present problem is one of steady-state harmonic excitation denoted in complex-variable exponential forms, the displacements and rotations are proportional to  $e^{i\omega t}$  also. It is noted that the phase angle between the response and the excitation is taken care of by the imaginary components of these quantities. Thus, the time dependence cancels out in all of the energy terms which appear in Lagrange's equation. Therefore, it is necessary to consider only the amplitudes of the respective energy and work terms. Then, as shown in detail in Appendix C, the amplitude of the Lagrangian energy difference can be expressed as follows:

$$\tilde{L} = (\tilde{T} + \tilde{W}) - (\tilde{U} + \tilde{D}) \quad (31)$$

where  $\tilde{D}, \tilde{T}, \tilde{U}, \tilde{W}$  are the amplitudes of the dissipative, kinetic, and strain energies and of the work done by the external forces, respectively.

The strain and damping energy terms can be combined by introducing complex stiffnesses, as discussed in Appendix B. Making this substitution and integrating over the plate area, we obtain the following:

$$\begin{aligned}
 \tilde{U} + \tilde{D} = \frac{1}{2} \int_0^a \int_0^b \{ & \bar{A}_{11} \tilde{u}_{o,x}^2 + 2\bar{A}_{12} \tilde{u}_{o,x} \tilde{v}_{o,y} + \bar{A}_{22} \tilde{v}_{o,y}^2 + 2(\bar{A}_{16} \tilde{u}_{o,x} + \bar{A}_{26} \tilde{v}_{o,y}) (\tilde{v}_{o,x} + \tilde{u}_{o,y}) \\
 & + \bar{A}_{66} (\tilde{v}_{o,x} + \tilde{u}_{o,y})^2 + 2\bar{B}_{11} \tilde{u}_{o,x} \tilde{\psi}_{x,x} + 2\bar{B}_{12} (\tilde{u}_{o,x} \tilde{\psi}_{y,y} + \tilde{v}_{o,y} \tilde{\psi}_{x,x}) + 2\bar{B}_{22} \tilde{v}_{o,y} \tilde{\psi}_{y,y} \\
 & + 2\bar{B}_{16} [\tilde{u}_{o,x} (\tilde{\psi}_{y,x} + \tilde{\psi}_{x,y}) + (\tilde{v}_{o,x} + \tilde{u}_{o,y}) \tilde{\psi}_{x,x}] + 2\bar{B}_{26} [\tilde{v}_{o,y} (\tilde{\psi}_{y,x} + \tilde{\psi}_{x,y}) \\
 & + (\tilde{v}_{o,x} + \tilde{u}_{o,y}) \tilde{\psi}_{y,y}] + 2\bar{B}_{66} (\tilde{v}_{o,x} + \tilde{u}_{o,y}) (\tilde{\psi}_{y,x} + \tilde{\psi}_{x,y}) + \bar{D}_{11} \tilde{\psi}_{x,x}^2 \\
 & + 2\bar{D}_{12} \tilde{\psi}_{x,x} \tilde{\psi}_{y,y} + \bar{D}_{22} \tilde{\psi}_{y,y}^2 + 2\bar{D}_{16} \tilde{\psi}_{x,x} (\tilde{\psi}_{y,x} + \tilde{\psi}_{x,y}) + 2\bar{D}_{26} \tilde{\psi}_{y,y} (\tilde{\psi}_{y,x} + \tilde{\psi}_{x,y}) \\
 & + \bar{D}_{66} (\tilde{\psi}_{y,x} + \tilde{\psi}_{x,y})^2 + \bar{F}_{44} (\tilde{w}_{o,y} + \tilde{\psi}_y)^2 + 2\bar{F}_{45} (\tilde{w}_{o,y} + \tilde{\psi}_y) (\tilde{w}_{o,x} + \tilde{\psi}_x) \\
 & + \bar{F}_{55} (\tilde{w}_{o,x} + \tilde{\psi}_x)^2 \} dx dy \quad (32)
 \end{aligned}$$

where the superscript  $(\sim)$  denotes that the quantity is an amplitude, and

$$\begin{aligned}
 \bar{A}_{ij}, \bar{B}_{ij}, \bar{D}_{ij} &= (A_{ij} + \hat{A}_{ij}), (B_{ij} + \hat{B}_{ij}), (D_{ij} + \hat{D}_{ij}); i, j=1, 2, 6 \\
 \bar{F}_{ij} &= F_{ij} + \hat{F}_{ij}; i, j=4, 5
 \end{aligned} \quad (33)$$

The sum of the amplitudes of the kinetic energy and the work done by external forces can be expressed as follows:

$$\begin{aligned}
\tilde{T} + \tilde{W} = & (\omega^2/2) \int_0^a \int_0^b [m_0 (\tilde{u}_0^2 + \tilde{v}_0^2 + \tilde{w}_0^2) + 2m_1 (\tilde{u}_0 \tilde{\psi}_x + \tilde{v}_0 \tilde{\psi}_y) \\
& + m_2 (\tilde{\psi}_x^2 + \tilde{\psi}_y^2)] dx dy + \int_0^a \int_0^b \tilde{q} \tilde{w}_0 dx dy
\end{aligned} \quad (34)$$

To apply the extended Rayleigh-Ritz method, the assumed functions for the amplitudes of the displacements and rotations are given the following general form:

$$\begin{aligned}
\tilde{u}_0 &= \sum_{m=1}^M \sum_{n=1}^N U_{mn} \phi_{um}(\alpha) \phi_{un}(\beta) \\
\tilde{v}_0 &= \sum_{m=1}^M \sum_{n=1}^N V_{mn} \phi_{vm}(\alpha) \phi_{vn}(\beta) \\
\tilde{w}_0 &= \sum_{m=1}^M \sum_{n=1}^N W_{mn} \phi_{wm}(\alpha) \phi_{wn}(\beta) \\
\tilde{\psi}_y &= \sum_{m=1}^M \sum_{n=1}^N \psi_{ymn} \phi_{ym}(\alpha) \phi_{yn}(\beta) \\
\tilde{\psi}_x &= \sum_{m=1}^M \sum_{n=1}^N \psi_{xmn} \phi_{xm}(\alpha) \phi_{xn}(\beta)
\end{aligned} \quad (35)$$

The modal coefficients  $U_{mn}, V_{mn}, W_{mn}, \psi_{ymn}, \psi_{xmn}$  are the undetermined parameters, the  $\phi$ 's are assumed modal functions,  $\alpha = x/a$ ,  $\beta = y/b$ .

Substituting equations (32), (34), and (35) into equation (31) for the Lagrangian energy-difference amplitude ( $\tilde{L}$ ), one obtains the result presented in Appendix D1.

Hamilton's principle can be stated mathematically as follows:

$$\delta \int_{t_1}^{t_2} \tilde{L} dt = 0 \quad (36)$$

To achieve as close of an approximation as possible to equation (36), the Lagrangian function  $\tilde{L}$  is minimized by setting its partial derivatives with respect to the modal coefficients respectively equal to zero, i.e.

$$\begin{aligned} \partial \tilde{L} / \partial u_{k\ell} = 0 ; \quad \partial \tilde{L} / \partial v_{k\ell} = 0 ; \quad \partial \tilde{L} / \partial w_{k\ell} = 0 ; \quad \partial \tilde{L} / \partial \psi_{xk\ell} = 0 \\ \partial \tilde{L} / \partial \psi_{yk\ell} = 0 \quad ; \quad k = 1, 2, \dots, M \quad ; \quad \ell = 1, 2, \dots, N \end{aligned} \quad (37)$$

Equations (37) represent a set of  $M \times N$  nonhomogeneous, linear algebraic equations.

## 2.9 Reduction to Matrix Form

For computational convenience, it is desirable to express the set of equations (37) in matrix form as follows:

$$[S] \{ \xi_{mn} \} - \omega^2 [M] \{ \xi_{mn} \} = \{ f \} \quad (38)$$

where  $[S]$  = complex stiffness matrix,  $[M]$  = mass matrix, and  $\{ \xi_{mn} \}$  and  $\{ f \}$  are column matrices representing the generalized displacements and generalized forces, respectively, i.e.

$$\left\{ \xi_{mn} \right\} \equiv \begin{Bmatrix} U_{mn} \\ V_{mn} \\ W_{mn} \\ \psi_{ymn} \\ \psi_{xmn} \end{Bmatrix} ; \quad \left\{ f \right\} \equiv \begin{Bmatrix} 0 \\ 0 \\ \tilde{q} \\ 0 \\ 0 \end{Bmatrix} \quad (39)$$

Equation (38) can be written in explicit complex form as follows:

$$[S^{(R)} + iS^{(I)}] \left\{ \xi_{mn}^{(R)} + i\xi_{mn}^{(I)} \right\} - \omega^2 [M^{(R)}] \left\{ \xi_{mn}^{(R)} + i\xi_{mn}^{(I)} \right\} = \left\{ f^{(R)} \right\} \quad (40)$$

where superscripts (R) and (I) denote the real and imaginary parts of the complex quantities appearing in equation (38).

Equation (40) can be solved for the response matrix, partitioned into real and imaginary parts, as follows:

$$\begin{Bmatrix} \xi_{mn}^{(R)} \\ \xi_{mn}^{(I)} \end{Bmatrix} = \begin{bmatrix} S^{(R)} - \omega^2 M^{(R)} & -S^{(I)} \\ S^{(I)} & S^{(R)} - \omega^2 M^{(R)} \end{bmatrix}^{-1} \begin{Bmatrix} f^{(R)} \\ 0 \end{Bmatrix} \quad (41)$$

The modal coefficients are placed in the inverse matrix in equation (41). For the specific numerical case treated  $M=N=2$ , i.e.  $m,n=1,2$ . Thus, the complete matrix is of order  $40 \times 40$  with each submatrix being of order  $2 \times 2$ . Thus, the problem has been reduced to a standard algebraic eigenvalue problem which can be solved by an available computer subroutine for the IBM 360 Series 50 digital computer. Complete computer program documentation is presented in Appendix J.

### SECTION III

#### DERIVATION OF THICKNESS-SHEAR FACTORS FOR LAMINATES

In this section are presented two entirely different approaches for calculating the thickness-shear factors for a laminate. The first approach is to extend the Jourawski static theory of shear-flexible beams (reference 40), as presented in elementary mechanics-of-materials textbooks, to a laminated beam. The other approach is to extend, to the laminate case, Mindlin's method (ref. 26) of matching the pure thickness-shear-mode frequencies predicted by two-dimensional dynamic elasticity and by Timoshenko one-dimensional, shear-flexible beam theory (references 41, 42).

In the case of isotropic plates, there is only one independent thickness-shear factor ( $K$ ), since  $K_{45}=0$  and  $K_{55}=K_{44}=K$ . The static approach mentioned above yields a value of  $K = 0.833$  (reference 43), while Mindlin's dynamic approach results in a value of 0.822 for  $K$ . Srinivas et al. (ref. 35) showed that use of either of these values for  $K$  in Mindlin's plate theory results in a very close approximation to the lower natural frequencies computed by exact, dynamic, three-dimensional theory of elasticity for rather thick, homogeneous isotropic rectangular plates simply supported on all edges.

In the case of orthotropic plates, there are two independent thickness-shear factors ( $K_{44}$  and  $K_{55}$ ), since  $K_{45}=0$  and  $K_{55} \neq K_{44}$ . In the case of a plane anisotropic plate, such as one consisting of a unidirectional

composite material with its major material-symmetry axis oriented at an acute angle ( $\theta$ ) with its edges, there are three independent, non-zero  $K_{ij}$ . However, for this case, Appendix A presents transformations from which the three  $F_{ij}$ , proportional to  $K_{ij}$  and defined in equation (13), can be calculated from the following data:  $F_{44}$  and  $F_{55}$  for the orthotropic case ( $\theta=0^\circ$ ) and the value of  $\theta$  in the anisotropic case. Thus, the general problem of determining  $K_{ij}$  is reduced to one of calculating  $K_{44}$  and  $K_{55}$  for the orthotropic case.

To calculate  $K_{55}$  for an orthotropic laminate by either of the two approaches mentioned above, one considers a beam oriented in the  $x$  direction and laminated of layers having properties  $E_{11}^{(k)*}$  and  $C_{55}^{(k)}$ . To calculate  $K_{44}$ ,  $x \rightarrow y$ ,  $E_{11}^{(k)} \rightarrow E_{22}^{(k)}$ , and  $C_{55}^{(k)} \rightarrow C_{44}^{(k)}$ .

To provide a check for the results, the fundamental eigenvalues for free vibration calculated by laminated, shear-flexible plate theory (Section II), using these values of  $K_{ij}$ , are compared with the exact laminated elasticity theory values given by Srinivas et al. (ref. 35).

### 3.1 Static Approach

To calculate the horizontal shear force per unit width,  $\Delta F$ , acting on a cross section, figures 6 and 7 are used. For consistency plate notation is used, even though the theory is only one dimensional.

The bending stress in typical layer " $k$ ", at a distance  $z$  from the midplane of the laminate, is calculated as follows:

$$\sigma_{xx}^{(k)} = E_{11}^{(k)} \kappa_{xx} z \quad (42)$$

---

\* For thin plates as treated in this report,  $E_{11}^{(k)} \rightarrow Q_{11}^{(k)}$ , where  $Q_{11}^{(k)} = E_{11}^{(k)} / (1 - \nu_{12}^{(k)} \nu_{21}^{(k)})$ .



where  $\kappa_{xx}$   $\equiv$  longitudinal bending curvature and  $E_{11}^{(k)}$   $\equiv$  longitudinal Young's modulus of layer "k".

The longitudinal stress couple (bending moment per unit width) is defined as follows:

$$M_{xx} = \sum_{k=1}^n \int_{z_{k-1}}^{z_k} \sigma_{xx}^{(k)} z \, dz \quad (43)$$

The longitudinal curvature can be expressed in terms of  $M_{xx}$  as follows:

$$\kappa_{xx} = M_{xx} / D_{11} \quad (44)$$

where  $D_{11}$   $\equiv$  longitudinal flexural rigidity.

From equations (42) and (44), the bending stresses acting on the left ( $x=x_1$ ) and right ( $x = x_1 + \Delta x$ ) sides of the elements are:

$$\sigma_{xx}^{(k)}(x_1) = (E_{11}^{(k)} z / D_{11}) M_{xx} ; \quad (45)$$

$$\sigma_{xx}^{(k)}(x_1 + \Delta x) = (E_{11}^{(k)} z / D_{11}) (M_{xx} + \Delta M_{xx})$$

Since both of these bending stress distributions act on identical cross-sectional areas, the horizontal shear force per unit width, which acts on the element, is given by:

$$\Delta F = \int_{A_0} [\sigma_{xx}^{(k)}(x_1 + \Delta x) - \sigma_{xx}^{(k)}(x_1)] \, dA \quad (46)$$

where  $A_0$   $\equiv$  area shown in figure 8.

Combining equations (45) and (46), one obtains:

$$\Delta F = (\Delta M_{xx} / D_{11}) Y(z) \quad (47)$$

where

$$Y(z) \equiv \int_{A_0} E_{11}^{(k)} z \, dA .$$

The force per unit width,  $\Delta F$ , must equilibrate the horizontal shear stress,  $\sigma_{xz}^{(k)}$ , acting on the bottom face of the element shown in figure 7. Thus, we have:

$$\Delta F = \sigma_{xz}^{(k)} \Delta x \quad (48)$$

Hooke's law in shear for layer "k" is

$$\sigma_{xz}^{(k)} = C_{55}^{(k)} \epsilon_{xz}^{(k)} \quad (49)$$

where  $C_{55}^{(k)}$  and  $\epsilon_{xz}^{(k)}$  are the modulus and strain corresponding to longitudinal thickness-shear action in layer "k".

Substituting equation (49) into equation (48), one obtains the following result:

$$\Delta F = C_{55}^{(k)} \epsilon_{xz}^{(k)} \Delta x \quad (50)$$

The following expression for the longitudinal shear strain at a distance  $z$  is obtained by equating the right-hand sides of equation (47) and (50):

$$\epsilon_{xz}^{(k)}(x,z) = [Y(z)/(C_{55}^{(k)} D_{11})] Q_x(x) \quad (51)$$

where  $Q_x$  is the thickness-shear stress resultant (force per unit width), which is related to  $M_{xx}$  by static equilibrium as follows:

$$Q_x = \Delta M_{xx} / \Delta x \quad (52)$$

The shear strain energy for a laminated, rectangular-cross-section beam, shown in figure 9, is:

$$U_s = \frac{1}{2} \int_A C_{55}^{(k)} [\epsilon_{xz}^{(k)}]^2 dA \quad (53)$$

The shear strain energy associated with an equivalent uniform, longitudinal thickness-shear strain in a laminated, rectangular-cross-section beam of cross-sectional area  $A$  is:

$$U'_s = (K_{55}/2) (\epsilon'_{xz})^2 \int_A C_{55}^{(k)} dA \quad (54)$$

where  $K_{55}$  is the longitudinal thickness-shear factor and  $\epsilon'_{xz}$  is weighted according to:

$$\epsilon'_{xz} = \left[ \sum_{k=1}^n \int_{z_{k-1}}^{z_k} \sigma_{xz}^{(k)} \epsilon_{xz}^{(k)} dz \right] \left[ \sum_{k=1}^n \int_{z_{k-1}}^{z_k} \sigma_{xz}^{(k)} dz \right]^{-1} \quad (55)$$

Equating the right-hand sides of equations (53) and (54) yields an equation; then substituting equations (49) and (51) into that equation, one arrives at the following explicit expression for the longitudinal

thickness-shear factor

$$K_{55} = \frac{\left[ \sum_{k=1}^n \int_{z_{k-1}}^{z_k} Y(z) dz \right]^2}{\left[ \sum_{k=1}^n \int_{z_{k-1}}^{z_k} C_{55}^{(k)} dz \right] \left\{ \sum_{k=1}^n \int_{z_{k-1}}^{z_k} (C_{55}^{(k)})^{-1} [Y(z)]^2 dz \right\}} \quad (56)$$

Equation (56) is a general expression for the static, longitudinal thickness-shear factor for an arbitrarily laminated beam. It is a relatively simple algebraic expression which depends upon only the longitudinal Young's and thickness-shear moduli of the individual layers ( $E_{11}^{(k)}$  and  $C_{55}^{(k)}$ ) and the lamination geometry. Numerical results are presented in later examples.

### 3.2 Dynamic Approach

Due to the inherent mathematical form of the equations of dynamic elasticity theory for a multi-material (multi-layer) medium, it is not feasible to present a general solution for the thickness-shear factor obtained by using the dynamic approach. Even in the case of a specific class of laminate, such as the three-layer, symmetrically laminated one, it is not possible to obtain an explicit expression for the thickness-shear factor. In fact, the complexity of the dynamic case, which involves the dynamic elasticity-theory analysis of a shear-flexible laminated beam, approaches that of the shear-flexible laminated plate and thus negates much of the advantage of using the thickness-shear factor

approach to laminated, shear-flexible plate dynamics. However, in order to illustrate the dynamic approach and to provide a numerical comparison with the static approach and with the exact results of Srinivas et al (ref. 35), an analysis for the symmetrical three-layer case is presented in Appendix E.

# SECTION IV

## MODAL FUNCTIONS USED FOR VARIOUS

### PLATE BOUNDARY CONDITIONS

In applying the extended Rayleigh-Ritz method, the approximate modal shapes assumed must satisfy the kinematic boundary conditions. However, to improve convergence, it is desirable to satisfy the force-type boundary conditions also. For a rectangular plate, the three cases of boundary conditions most commonly encountered in practice are discussed in Sections 4.1-4.3.

It should be noted that  $C_m$ ,  $C_n$ ,  $Z_m$ ,  $Z_n$  are characteristic parameters tabulated in reference 44. Also, five boundary conditions per edge need to be prescribed rather than four as in classical theory.

#### 4.1 Simply Supported on All Edges

The boundary conditions considered here are simply-supported edges in the sense that

$$\begin{aligned} N_{xx} = M_{xx} = \tilde{v}_o = \tilde{w}_o = \tilde{\psi}_y = 0 & \quad \text{at } x = 0, a \quad (\alpha=0,1) \\ N_{yy} = M_{yy} = \tilde{u}_o = \tilde{w}_o = \tilde{\psi}_x = 0 & \quad \text{at } y = 0, b \quad (\beta=0,1) \end{aligned} \quad (57)$$

As was pointed out by Wang (reference 45), it is impossible for a separable-form deflection function to satisfy the above boundary conditions for the case of a plate of anisotropic material ( $Q_{16}$  and  $Q_{26} \neq 0$ ). However, the following modal functions permit eqs. (35) to satisfy eq. (57) exactly

in the orthotropic case, but only approximately in the anisotropic case:

$$\begin{aligned}\phi_{um} &= \phi_{\psi xm} = \cos m\pi\alpha ; & \phi_{vm} &= \phi_{wm} = \phi_{\psi ym} = \sin m\pi\alpha \\ \phi_{vn} &= \phi_{\psi yn} = \cos n\pi\beta ; & \phi_{un} &= \phi_{wn} = \phi_{\psi xn} = \sin n\pi\beta\end{aligned}\quad (58)$$

For the simply supported case, we substitute equations (58) into equations (D-1 through D-6). The evaluations of the integral forms are presented in Appendix G.

#### 4.2 Fully Clamped on All Edges

The boundary conditions for a fully clamped laminated plate are as follows:

$$\begin{aligned}\tilde{u}_0 &= \tilde{v}_0 = 0 & \text{at } x = 0, a \text{ and } y = 0, b \\ \tilde{w}_0 &= \tilde{w}_{0,x} = \tilde{\psi}_y = 0 & \text{at } x = 0, a \\ \tilde{w}_0 &= \tilde{w}_{0,y} = \tilde{\psi}_x = 0 & \text{at } y = 0, b\end{aligned}\quad (59)$$

The assumed modal functions selected to permit equations (35) to satisfy equations (59) are as follows:

$$\begin{aligned}\phi_{um} &= \phi_{vm} = \phi_{\psi xm} = \phi_{\psi ym} = \sin 2m\pi\alpha \\ \phi_{un} &= \phi_{vn} = \phi_{\psi xn} = \phi_{\psi yn} = \sin 2n\pi\beta \\ \phi_{wm} &= \cosh Z_m\alpha - \cos Z_m\alpha - C_m (\sinh Z_m\alpha - \sin Z_m\alpha) \\ \phi_{wn} &= \cosh Z_n\beta - \cos Z_n\beta - C_n (\sinh Z_n\beta - \sin Z_n\beta)\end{aligned}\quad (60)$$

For the fully clamped case, we substitute equations (60) into equations (D1 through D6). The evaluations of the integral forms are presented in Appendix G.

#### 4.3 Free on All Edges

The boundary conditions appropriate for a laminated plate free on all edges can be expressed mathematically as follows:

$$\begin{aligned}
 N_{xy} = M_{xy} = 0 & \quad \text{at } x = 0, a \quad \text{and } y = 0, b \\
 N_{xx} = Q_x = M_{xx} = 0 & \quad \text{at } x = 0, a \\
 N_{yy} = Q_y = M_{yy} = 0 & \quad \text{at } y = 0, b
 \end{aligned} \tag{61}$$

The assumed modal functions selected to permit equations (35) to satisfy equations (61) are as follows:

$$\begin{aligned}
 \phi_{um} = \phi_{vm} = \phi_{\psi xm} = \phi_{\psi ym} &= 1 - \cos 2m\pi\alpha \\
 \phi_{un} = \phi_{vn} = \phi_{\psi xn} = \phi_{\psi yn} &= 1 - \cos 2n\pi\alpha \\
 \phi_{wm} = \cos m\pi\alpha ; \quad \phi_{wn} &= \cos n\pi\beta
 \end{aligned} \tag{62}$$

For the free edge case, we substitute equations (62) into equations (D1 through D6). The evaluation of the resulting integral forms are presented in Appendix G.



## SECTION V

### NUMERICAL RESULTS AND COMPARISON WITH RESULTS OF OTHER INVESTIGATORS

In this section a comparison is made between the numerical results obtained in this investigation and those obtained by other investigators.

#### 5.1 Thickness-Shear Factors for Laminates

Two example problems are analyzed and, where possible, results of Example 1 are compared with solutions obtained from other sources. The results of Example 2 are presented for use in design.

Example 1: Three-layer, symmetric, isotropic laminate. - The coordinate system is shown in figure 10. All geometrical and material property ratios correspond to the data of ref. 35 given as follows:

$$z_2/z_1 = h^{(2)} / [h^{(2)} + 2h^{(1)}] = 0.8, \quad E_{11}^{(1)} / E_{11}^{(2)} = 15,$$
$$C_{55}^{(1)} / C_{55}^{(2)} = 15, \quad \rho^{(1)} / \rho^{(2)} = 1, \quad \text{and} \quad \nu^{(1)} = \nu^{(2)} = 0.3$$

Assuming only the x-direction is considered in the static and dynamic approaches which were developed in Section III, then the following results are obtained: (I) static case - the result obtained from equation (56) can be expressed as  $K_{55} = 0.651$ , (II) dynamic case - the result obtained by equating eqs. (E-13) and (E-27) is  $K_{55} = 0.350$ .

When the three-layer, laminate thickness parameter is chosen to be  $z_2/z_1 = 1$ , the analysis given in Section III can be reduced to a single-layer homogeneous, isotropic material. Thus, using the data  $E_{11}^{(1)}/E_{11}^{(2)} = C_{55}^{(1)}/C_{55}^{(2)} = \rho^{(1)}/\rho^{(2)} = 1$  and  $\nu^{(1)} = \nu^{(2)} = 0.3$ , the static case gives  $K_{55} = 0.833$  and dynamic case results in  $K_{55} = 0.822$ . These results are identical with the values of the static and the dynamic shear factors obtained for single-layer plates by previous investigators (refs. 43 and 16).

Example 2: Multiple alternating layers of two materials. - The geometrical and material property ratios are given as

$$h^{(2)}/h^{(1)} = 1, \quad E_{11}^{(1)}/E_{11}^{(2)} = C_{55}^{(1)}/C_{55}^{(2)} = \text{from } 0.01 \text{ to } 100$$

The laminates vary from two layers to nine layers. Since the static case is a relatively simple algebraic expression which considers only longitudinal Young's and thickness-shear moduli of the individual layers ( $E_{11}^{(k)}$  and  $C_{55}^{(k)}$ ) and the laminate geometry, for design purposes, eq. (56) will be used. The results are shown in table 1 and figure 11.

## 5.2 Plate Simply Supported on All Edges

Here we consider only free vibration of plates made of composite material having material-symmetry axes coinciding with the geometric coordinates (plate edges) as shown in figure 12. Neglecting energy dissipation, the time integral of the difference between the potential and kinetic energies attains a stationary value. The displacement and rotations

are proportional to  $e^{i\omega t}$ . The time dependence in the strain and kinetic energies cancel each other, i.e. only the amplitudes of the strain energy and kinetic energy need be considered. Thus, we use only the real part of homogeneous eqs. (D1-D6) with proper boundary conditions, see eq. (57), to apply Example 3.

Example 3: Three-layer, symmetric, isotropic plate. - The elastic coefficients are those of isotropic material:

$$Q_{11}^{(k)} = Q_{22}^{(k)} = E^{(k)} / \{1 - [\nu^{(k)}]^2\}, Q_{12}^{(k)} = \nu^{(k)} E^{(k)} / \{1 - [\nu^{(k)}]^2\}$$

$$Q_{44}^{(k)} = Q_{55}^{(k)} = Q_{66}^{(k)} = E^{(k)} / \{2[1 + \nu^{(k)}]\}, Q_{45}^{(k)} = 0 \quad (k=1,2)$$

Geometrical and material property ratios correspond to the data of ref. 35, given as follows

$$z_2/z_1 = h^{(2)} / [h^{(2)} + 2h^{(1)}] = 0.8, E_{11}^{(1)} / E_{11}^{(2)} = C_{55}^{(1)} / C_{55}^{(2)} = 15,$$

$$\rho^{(1)} / \rho^{(2)} = 1, \nu^{(1)} = \nu^{(2)} = 0.3$$

and the following dimensionless geometric parameter defined in ref. 35:

$$g_k^2 = \{ [m\pi h^{(k)} / a]^2 + [n\pi h^{(k)} / b]^2 \}^{1/2} = \begin{cases} 0.0002\pi^2 & \text{for } k=1 \\ 0.0128\pi^2 & \text{for } k=2 \end{cases}$$

When the thickness of three-ply laminates is chosen to be  $z_2/z_1 = 1$ , it can be reduced to a single-layer material as a special case. Then the material properties are as follows:

$$Q_{ij}^{(1)} = Q_{ij}^{(2)} \quad i, j = 1, 2, 4, 5, 6$$

$$E_{11}^{(1)} / E_{11}^{(2)} = C_{55}^{(1)} / C_{55}^{(2)} = \rho^{(1)} / \rho^{(2)} = 1 ; \nu^{(1)} = \nu^{(2)} = 0.3$$

$$g_1 = 0, \quad g_2 = 12.$$

A FORTRAN IV program is employed to compute the lowest eigenvalues of plates with simply supported edges. The two cases considered are: (1) single-layer homogeneous, isotropic, and (2) three-ply symmetrical construction. The results are shown as a solid line in figures 13 and 14. The static and dynamic shear factors calculated in examples 1 and 2 are also shown for comparison.

The static Jourawski shear theory and dynamic Timoskenko type theory appear to give good results for K as evaluated by inserting in laminated, shear flexible plate theory and comparing the lowest eigenvalues with those given in refs. 35 and 14.

### 5.3 Plate Free on All Edges

The problem considered here is forced vibration of a rectangular plate made of an arbitrary number of composite-material layers each having its major material-symmetry axis oriented at an arbitrary angle with geometrical coordinates as shown in figure A-2.

Since the present problem is one of steady-state harmonic excitation including material damping effects, the complete set of eqs. (D1-D6) with proper boundary conditions, eqs. (61), must be used.

Example 4: Boron/epoxy plate with twenty-four parallel plies oriented at an arbitrary angle. - The input-data material properties are Young's and shear moduli ( $E_{11}$ ,  $E_{22}$ ,  $C_{44}$ ,  $C_{55}$ ,  $C_{66}$ ), major Poisson's ratio ( $\nu_{12}$ ), bending and twisting stiffnesses ( $D_{11}$ ,  $D_{22}$ ,  $D_{12}$ ,  $D_{66}$ ), and their corresponding loss tangents, as generated in ref. 46 from constituent-material experimental properties. It is noticed that all of the above input data are functions of frequency. Geometrical and material properties correspond to the data of ref. 13, as follows:

length,  $a = 18.19$  in ; width,  $b = 2.75$  in.  
 thickness,  $h = 0.034$  in. ; density,  $\rho = 0.000194$  lb-sec<sup>2</sup>/in<sup>4</sup>  
 angle of orientation,  $\theta = 0^\circ, 10^\circ, 30^\circ, 45^\circ, 60^\circ, 90^\circ$

A FORTRAN IV program is employed to compute the eigenvectors of a plate with all edges free. To obtain the resonant frequencies of the first five modes, two different resonance criteria are applied. In the peak-amplitude method, the system is excited harmonically and the amplitude at a particular point ( $\alpha = 0$ ,  $\beta = 1$ ) is measured over a range of frequency. The amplitude of the response depends not only on the dynamic characteristics of the system, but also on the amplitude of the force applied to it. For a linear system the peak amplitude is taken as maximum displacement per unit amplitude of force. Throughout this report, this ratio is referred to as the response. A typical result of response with varying frequency is shown in figure 15 for an angle of orientation,  $\theta = 10^\circ$ . The complete results are as tabulated in Table II.

In the modified Kennedy-Pancu method, the modal shapes, phase relations between motions at various points, and coupling between the

various degrees of freedom are assumed to be unaffected by the presence of a small amount of damping. Vectors are used for the analysis of the results of forced vibration by making a polar plot (called the Argand plane) of the displacement vector (amplitude and phase angle). In the vicinity of resonance, the resulting curve would be an approximately circular arc. Each point on the circle locus corresponds to a value of frequency.

In the modified Kennedy-Pancu method, the resonant frequency is defined to correspond to the point of the Argand-plot curve having maximum change in arc length ( $\Delta s$ ) per fixed change in frequency ( $\Delta \omega$ ). The change in arc length  $\Delta s$  can be determined approximately in analytical fashion as the response amplitude ( $W/\tilde{q}$ ) multiplied by the difference in the phase angles corresponding to the two distinct frequencies (separated by  $\Delta \omega$ ), i.e.

$$\Delta s = (W/\tilde{q}) \Delta \varphi$$

The parameter  $\Delta s/\Delta \omega$  is plotted versus excitation frequency in figure 16 for a specific angle of orientation,  $\theta = 10^\circ$ .

As can be seen in the figure, the curves exhibit sharp spikes and thus the Kennedy-Pancu resonant frequencies, i.e. the frequencies corresponding to the maximum points, can readily be found. The results obtained in this fashion for all of the plates used by Clary are tabulated in Table II.

A discussion of experimental methods used to determine material damping in composite materials is presented in Appendix H. Here the damping ratios are calculated by using the modified Kennedy-Pancu method as expressed in equation (B-69), Appendix B. It is noted that the damping ratio is the

ratio of material damping coefficient to critical material damping coefficient. The results associated with each mode are tabulated completely in Table II.

The nodal patterns of the first five modes are calculated from the response at selected points on the surface of the plate. Twenty-five points in the x direction and five points in the y direction are used. The nodal patterns are shown in figures 17-22. The results appear to be in good agreement with the data of ref. 13.

## VI. CONCLUSIONS

The analyses in Sections II and IV were developed for the vibrational problem of composite-material plates with thickness-shear flexibility and material damping. The theory used in the analyses is that of Yang, Norris, and Stavsky (ref. 25), which can be considered to be the laminated, anisotropic version of Mindlin's dynamic plate theory.

To account for the effects of thickness-shear deformation, a shear correction factor  $K$  was introduced. A variety of methods to arrive at an appropriate shear factor have been proposed for homogeneous plates; the most popular ones resulted in  $K = 0.833$  for a static distribution (ref. 44) and 0.822 for the dynamic case (ref. 26). Srinivas et al. (ref. 35) showed that use of either of these values for  $K$  in Mindlin's plate theory gives a very close approximation to the lower natural frequencies computed by exact, dynamic, three-dimensional elasticity theory for rather thick, homogeneous, isotropic rectangular plates simply supported on all edges.

Unfortunately to date no one has proposed a means of rational calculation of the shear factor for a laminated plate. Srinivas et al. made an exact, dynamic three-dimensional elasticity analysis of simply supported laminated plates. However, their analysis is quite tedious computationally and thus they have presented numerical results for only a very limited number of cases.



In the present investigation, both static (Jourauski shear theory) and dynamic (Mindlin type analysis for pure thickness-shear motion) approaches were used to derive a shear factor  $K$  for laminates.

An assessment of the accuracy of these theories was made by comparing the lowest eigenvalues calculated by the laminated, shear-flexible plate theory with the laminated, three-dimensional exact values given by Srivivas et al. (ref. 35).

It has been found that the shear factor  $K$  for a laminate is not the same value as that for a homogeneous, isotropic member. The numerical examples indicated that the value of  $K$  depends on the layer properties and the stacking sequence of the laminate.

Using peak-amplitude and modified Kennedy-Pancu methods, the first five resonant frequencies were calculated for various laminated boron/epoxy plates with all edges free. The resonant frequencies obtained by the two techniques differed by only a very small amount, and were in good agreement with the results obtained both experimentally and analytically by Clary (ref. 13). Furthermore, the nodal patterns have been found to be satisfactory or as good as the data given by Clary. Finally, the damping-ratio results were in good agreement with the experimental ones obtained by Clary. No comparison with analytical results for laminated-plate damping could be made, since they have not been available previously.

## APPENDIX A

### NOTATION AND TRANSFORMATION FOR ELASTIC COEFFICIENTS

The generalized Hooke's law (Cauchy equations) for a general anisotropic material in terms of rectangular coordinates  $x, y, z$  are as follows:

$$\begin{Bmatrix} \sigma_{xx} \\ \sigma_{yy} \\ \sigma_{zz} \\ \sigma_{yz} \\ \sigma_{xz} \\ \sigma_{xy} \end{Bmatrix} = \begin{bmatrix} C_{11} & C_{12} & C_{13} & C_{14} & C_{15} & C_{16} \\ C_{21} & C_{22} & C_{23} & C_{24} & C_{25} & C_{26} \\ C_{31} & C_{32} & C_{33} & C_{34} & C_{35} & C_{36} \\ C_{41} & C_{42} & C_{43} & C_{44} & C_{45} & C_{46} \\ C_{51} & C_{52} & C_{53} & C_{54} & C_{55} & C_{56} \\ C_{61} & C_{62} & C_{63} & C_{64} & C_{65} & C_{66} \end{bmatrix} \begin{Bmatrix} \epsilon_{xx} \\ \epsilon_{yy} \\ \epsilon_{zz} \\ \epsilon_{yz} \\ \epsilon_{xz} \\ \epsilon_{xy} \end{Bmatrix} \quad (A-1)$$

where  $\sigma_{ij}$  and  $\epsilon_{ij}$  are stress and strain components, and  $C_{kl}$  are the Cauchy stiffness coefficients for a three-dimensional body. It can be shown that the matrix of Cauchy coefficients is symmetric, provided that the material is conservative (elastic), so that

$$C_{lk} = C_{kl} \quad (A-2)$$

Usually a single layer of fiber-reinforced composite material has the fibers oriented more or less parallel to the top and bottom surfaces

of the layer, i.e. material-symmetry plane XY coincides with surface plane xy. Thus, it is orthotropic in the yz and xz planes, and the shear-normal or cross-elasticity coefficients with subscripts i4 and i5 (i=1,2,3,6) vanish:

$$\begin{Bmatrix} \sigma_{xx} \\ \sigma_{yy} \\ \sigma_{zz} \\ \sigma_{yz} \\ \sigma_{xz} \\ \sigma_{xy} \end{Bmatrix} = \begin{bmatrix} C_{11} & C_{12} & C_{13} & 0 & 0 & C_{16} \\ C_{12} & C_{22} & C_{23} & 0 & 0 & C_{26} \\ C_{13} & C_{23} & C_{33} & 0 & 0 & C_{36} \\ 0 & 0 & 0 & C_{44} & C_{45} & 0 \\ 0 & 0 & 0 & C_{45} & C_{55} & 0 \\ C_{16} & C_{26} & C_{36} & 0 & 0 & C_{66} \end{bmatrix} \begin{Bmatrix} \epsilon_{xx} \\ \epsilon_{yy} \\ \epsilon_{zz} \\ \epsilon_{yz} \\ \epsilon_{xz} \\ \epsilon_{xy} \end{Bmatrix} \quad (A-3)$$

The only exception to the above, i.e. the only case when the general form (A-1), rather than (A-3), must be used is the case of a shingle-laminated composite, as shown in figure A-1 (reference 47).

If, in addition to being parallel to the top and bottom faces of the layer, the fibers are also oriented in a direction parallel to one of the coordinate directions in the plane of the layer, the material-symmetry planes XY,YZ,ZX all coincide with the coordinate planes xy, yz, zx and the material is said to be completely orthotropic. In this case the Cauchy relations are:

$$\begin{Bmatrix} \sigma_{XX} \\ \sigma_{YY} \\ \sigma_{ZZ} \end{Bmatrix} = \begin{bmatrix} C_{11}^* & C_{12}^* & C_{13}^* \\ C_{12}^* & C_{22}^* & C_{23}^* \\ C_{13}^* & C_{23}^* & C_{33}^* \end{bmatrix} \begin{Bmatrix} \epsilon_{XX} \\ \epsilon_{YY} \\ \epsilon_{ZZ} \end{Bmatrix} ; \begin{Bmatrix} \sigma_{YZ} \\ \sigma_{XZ} \\ \sigma_{XY} \end{Bmatrix} = \begin{Bmatrix} C_{44}^* & \epsilon_{YZ} \\ C_{55}^* & \epsilon_{XZ} \\ C_{66}^* & \epsilon_{XY} \end{Bmatrix} \quad (A-4)$$

where the asterisks denote the orthotropic case.

In the case of a thin layer of fiber-reinforced composite material in which the thickness-normal stress ( $\sigma_{ZZ}$ ) can be neglected (see Hypothesis H3, Section 2.1), the third equation in set (A-4) can be solved for  $\epsilon_{ZZ}$  in terms of  $\epsilon_{XX}$  and  $\epsilon_{YY}$ . Then equations (A-4) can be simplified as follows:

$$\begin{Bmatrix} \sigma_{XX} \\ \sigma_{YY} \end{Bmatrix} = \begin{bmatrix} Q_{11}^* & Q_{12}^* \\ Q_{12}^* & Q_{22}^* \end{bmatrix} \begin{Bmatrix} \epsilon_{XX} \\ \epsilon_{YY} \end{Bmatrix} ; \begin{Bmatrix} \sigma_{YZ} \\ \sigma_{XZ} \\ \sigma_{XY} \end{Bmatrix} = \begin{bmatrix} Q_{44}^* & \epsilon_{YZ} \\ Q_{55}^* & \epsilon_{XZ} \\ Q_{66}^* & \epsilon_{XY} \end{bmatrix} \quad (A-5)$$

where the reduced orthotropic stiffness coefficients ( $Q_{kl}^*$ ) are related to the Cauchy three-dimensional orthotropic stiffness coefficients ( $C_{kl}^*$ ) as follows:

$$\begin{aligned} Q_{11}^* &= C_{11}^* - (C_{13}^*)^2 / C_{33}^* & ; & \quad Q_{12}^* = C_{12}^* - (C_{13}^* C_{23}^* / C_{33}^*) ; \\ Q_{22}^* &= C_{22}^* - (C_{23}^*)^2 / C_{33}^* & ; & \quad Q_{ij}^* = C_{ij}^* \quad (ij = 44, 55, 66) \end{aligned} \quad (A-6)$$

Equation (A-5) can be written in the form of a single matrix equation as follows:

$$\begin{Bmatrix} \sigma_{IJ} \end{Bmatrix} = [Q_{kl}^*] \begin{Bmatrix} \epsilon_{IJ} \end{Bmatrix} \quad (A-7)$$

where

$$\{\sigma_{IJ}\} \equiv \begin{Bmatrix} \sigma_{XX} \\ \sigma_{YY} \\ \sigma_{YZ} \\ \sigma_{XZ} \\ \sigma_{XY} \end{Bmatrix}, \quad \{\epsilon_{IJ}\} \equiv \begin{Bmatrix} \epsilon_{XX} \\ \epsilon_{YY} \\ \frac{1}{2}\epsilon_{YZ} \\ \frac{1}{2}\epsilon_{XZ} \\ \frac{1}{2}\epsilon_{XY} \end{Bmatrix} \quad (A-8)$$

$$[Q_{kl}^*] \equiv \begin{bmatrix} Q_{11}^* & Q_{12}^* & 0 & 0 & 0 \\ Q_{12}^* & Q_{22}^* & 0 & 0 & 0 \\ 0 & 0 & 2Q_{44}^* & 0 & 0 \\ 0 & 0 & 0 & 2Q_{55}^* & 0 \\ 0 & 0 & 0 & 0 & 2Q_{66}^* \end{bmatrix} \quad (A-9)$$

where the presence of the factor 1/2 in the  $\epsilon_{IJ}$  matrix is used to make it a second-rank tensor and this necessitates the presence of the factor 2 appearing in equation (A-9).

In structural-panel applications of composite materials, usually there are design requirements for multiple orientations of fiber-reinforced composite-material layers. Therefore, it is essential that a set of transformation relations be used to calculate the stiffness coefficients for any desired orientation from that associated with the major material-symmetry direction (fiber direction) as shown in figure A-2. Such relations are developed in the ensuing paragraphs.

Arbitrary orthogonal axes in the plane of the laminate and making an angle  $\theta$  with the material-symmetry axes (X,Y) are designated as the x,y axes. Then the components of stress and strain can be transformed from the x,y axes to the X,Y axes as follows:

$$\{\sigma_{IJ}\} = [T_r] \{\sigma_{ij}\} \quad (A-10)$$

$$\{\epsilon_{IJ}\} = [T_r] \{\epsilon_{ij}\} \quad (A-11)$$

where  $\{\sigma_{IJ}\}$  and  $\{\epsilon_{IJ}\}$  are as defined in equations (A-8);  $\{\sigma_{ij}\}$  and  $\{\epsilon_{ij}\}$  are similar except that the subscripts X,Y,Z are replaced by the subscripts x,y,z; and  $[T_r]$  is the transformation, defined as follows:

$$[T_r] \equiv \begin{bmatrix} m^2 & n^2 & 0 & 0 & -2mn \\ n^2 & m^2 & 0 & 0 & 2mn \\ 0 & 0 & m & -n & 0 \\ 0 & 0 & n & m & 0 \\ mn & -mn & 0 & 0 & m^2 - n^2 \end{bmatrix} \quad (A-12)$$

where

$$m = \cos \theta, \quad n = \sin \theta. \quad (A-13)$$

For the case when  $\theta \neq 0$ , we have

$$\{\sigma_{ij}\} = [Q_{kl}] \{\epsilon_{ij}\} \quad (A-14)$$

In view of equations (A-7,A-10,A-11,A-14),

$$[Q_{kl}] = [T_r]^{-1} [Q_{kl}^*] [T_r] \quad (A-15)$$

By substituting equations (A-9) and (A-12) and then performing the matrix operations indicated in equation (A-15) the elements of the  $[Q_{kl}]$  matrix are related to those of the  $[Q_{kl}^*]$  matrix as follows:

$$\begin{aligned} Q_{11} &= Q_{11}^* m^4 + 2 (Q_{12}^* + 2Q_{66}^*) m^2 n^2 + Q_{22}^* n^4 \\ Q_{12} &= Q_{12}^* m^4 + (Q_{11}^* + Q_{22}^* - 4Q_{66}^*) m^2 n^2 + Q_{12}^* n^4 \\ Q_{22} &= Q_{22}^* m^4 + 2(Q_{12}^* + 2Q_{66}^*) m^2 n^2 + Q_{11}^* n^4 \\ Q_{66} &= Q_{66}^* m^4 + (Q_{11}^* + Q_{22}^* - 2Q_{12}^* - 2Q_{66}^*) m^2 n^2 + Q_{66}^* n^4 \\ Q_{16} &= (2Q_{66}^* + Q_{12}^* - Q_{11}^*) m^3 n - (2Q_{66}^* + Q_{12}^* - Q_{22}^*) mn^3 \\ Q_{26} &= -(2Q_{66}^* + Q_{12}^* - Q_{22}^*) m^3 n + (2Q_{66}^* + Q_{12}^* - Q_{11}^*) mn^3 \\ Q_{44} &= Q_{44}^* m^2 + Q_{55}^* n^2 \\ Q_{45} &= Q_{55}^* mn - Q_{44}^* mn \\ Q_{55} &= Q_{55}^* m^2 + Q_{44}^* n^2 \end{aligned} \quad (A-16)$$

## APPENDIX B

### MODELS AND MEASURES OF MATERIAL DAMPING

#### B1. Mathematical Models for Material Damping

Internal friction or damping in materials can be caused by a variety of combinations of fundamental physical mechanisms, depending upon the specific material. For metals, these mechanisms include thermoelasticity on both the micro and macro scales, grain boundary viscosity, point-defect relaxations, eddy-current effects, stress-induced ordering, interstitial impurities, and electronic effects (reference 48). According to Lazan (ref.48), little is known about the physical micromechanisms operative in most nonmetallic materials. However, for one important class of these, namely polymers and elastomers, considerable phenomenological data have been obtained. Due to the long-range molecular order associated with their giant molecules, polymers exhibit rheological behavior intermediate between that of a crystalline solid and a simple liquid. Of particular importance is the marked dependence of both stiffness and damping on frequency and temperature.

The purpose of developing a mathematical model for the rheological behavior of a solid is to permit realistic results to be obtained from mathematical analyses of complicated structures under various conditions, such as sinusoidal, random, and transient loading. According to reference 48, as early as 1784 Coulomb recognized that the mechanisms of damping



operative at low stresses may be different than those at high stresses. Even today, after more than 2500 publications on damping have appeared, major emphasis is placed on linear models of damping for several reasons: they have sufficient accuracy for the low-stress regime and linear analyses are computationally more economical than nonlinear ones.

The simplest mathematical models of rheological systems are single-parameter models: (1) an idealized spring, which exhibits a restoring force linearly proportional to displacement and thus displays no damping whatsoever, and (2) an idealized dashpot, which produces a force linearly proportional to velocity. Obviously, neither of these models are very appropriate to represent the behavior of most real materials.

The next most complicated models of rheological systems are the two-parameter models: (1) the Maxwell model, which consists of a spring and dashpot in mechanical series, as shown schematically in figure B-1(a); and (2) the Kelvin-Voigt model, which is comprised of a spring in parallel with a dashpot, as shown in figure B-1(b). The Maxwell model is a fair approximation to the behavior of a viscoelastic liquid. However, as a model for a viscoelastic solid, it has several very serious drawbacks (reference 48); there are no means to provide for internal stress and for afterworking. The Kelvin-Voigt model overcomes these deficiencies and is a first approximation to the behavior of a viscoelastic solid. However, it has the following disadvantages (reference 48): there is no elastic response during application or release of loading, the creep rate approaches zero for long durations of loading, and there is no permanent set irrespective of the loading history.

It should be mentioned that the Kelvin-Voigt model is the simplest one which permits representation as a complex quantity when subjected to sinusoidal motion. To show this, one can write the following differential equation governing the motion of a single-degree-of-freedom system consisting of a sinusoidally excited mass attached to a Kelvin-Voigt element:

$$m\ddot{u} + c\dot{u} + k u = \tilde{F} e^{i\omega t} \quad (B-1)$$

where  $m \equiv$  mass,  $c \equiv$  viscous damping coefficient,  $k \equiv$  spring rate,  $\tilde{F} \equiv$  exciting force amplitude,  $\omega \equiv$  circular frequency of exciting force,  $u \equiv$  displacement,  $i \equiv \sqrt{-1}$ ,  $t \equiv$  time, and a dot denotes a derivative with respect to time. Assuming that sufficient time has passed for the transients to die out,\* we can write the steady state solution of equation (B-1) as follows:

$$u = \tilde{u} e^{i(\omega t - \varphi)} = \tilde{F} [(k - m\omega^2) + i\omega c]^{-1} e^{i\omega t} \quad (B-2)$$

where  $\varphi \equiv$  phase angle between the response ( $u$ ) and the exciting force, and  $\tilde{u} \equiv$  displacement amplitude.

It is noted that the terms containing Kelvin-Voigt coefficients  $k$  and  $i\omega c$  can be grouped into a single Kelvin-Voigt complex stiffness ( $\bar{k}$ ) as follows:

---

\*It can be shown that they do die out for a mechanical system, for which  $c$ ,  $m$ , and  $k$  are all positive quantities.

$$\bar{k} = k + i\omega c \quad (B-3)$$

Alternatively, the Kelvin-Voigt element coefficient could have been grouped into a single complex damping coefficient ( $\bar{c}$ ) as follows:

$$\bar{c} = c - (i k/\omega) \quad (B-4)$$

The force ( $F_d$ ) in a dashpot is given by

$$F_d = c \dot{u} = i\omega c \tilde{u} e^{i(\omega t - \phi)} \quad (B-5)$$

The energy dissipated per cycle ( $U_d$ ) is a dashpot undergoing sinusoidal motion can be calculated as follows:

$$U_d = \oint F_d du = \int_0^{2\pi/\omega} F_d \dot{u} dt = \pi c \omega \tilde{u}^2 \quad (B-6)$$

In 1927, Kimball and Lovell (reference 49) observed that many engineering materials exhibited energy losses which were contradictory to equation(B-6). Specifically, they found that  $U_d$  was proportional to  $\tilde{u}^2$  but independent of  $\omega$ , i.e.

$$U_d = C'_d \tilde{u}^2 \quad (B-7)$$

Later work by Wegel and Walther (reference 50) also showed that  $U_d \propto \tilde{u}^2$  but  $C'_d$  was a weak function of  $\omega$ . Still later, for stresses below the fatigue limit of the material, Lazan (references 48,51) showed that  $U_d \propto \tilde{u}^2$  and  $C'_d$  was practically independent of  $\omega$ .

Equating the energy dissipated per cycle in the Kimball-Lovell material, equation (B-7), to that in the dashpot, equation (B-6), one obtains

$$C'_d = \pi c \omega \quad (B-8)$$

To utilize the Kimball-Lovell observation in practical structural dynamic analyses, it was desirable to have an expression for the associated damping force, i.e. an equation analogous to equation (B-5), which governs a dashpot. According to Bishop (reference 52) this was first done by Collar. Combining equations (B-5 , B-8), one obtains the following "frequency-dependent damping" relation:

$$F_d = (b/\omega) \dot{u} \quad (B-9)$$

where  $b$  is a constant given by

$$b = C'_d / \pi \quad (B-10)$$

The kind of damping represented by equation (B-9) has been called frequency-dependent damping, since the usual dashpot coefficient  $c$  is now replaced by the quantity  $b/\omega$ .

For the damper represented by Eq. (B-9), it is convenient to replace  $k$  in the undamped system by the following Kimball-Lovell complex stiffness (reference 53):

$$\bar{k}' = k + ib \quad (B-11)$$

where it is now noted that both  $k$  and  $b$  are assumed to be independent of frequency. This representation has been used extensively in aircraft

structural dynamic and flutter analyses (references 54,55).

An alternative to equation (B-11), is to use the concept of a complex damping coefficient, originated by Myklestad (reference 56), in which the spring constant is replaced by

$$\bar{k}'' = C_1 e^{im} \quad (B-12)$$

where  $C_1$  and  $m$  are constants.

Although Kimball and Lovell's original work was based on data obtained during steady-state sinusoidal motion, the models represented by equations (B-9, B-11, B-12) have been applied to free vibrations as well (refs. 52,53,57). To alleviate the difficulty of the interpreting of  $\omega$  in equation (B-9) for the case of free vibration or for multiple-frequency forced vibration, Reid (reference 58) suggested the following form:

$$F_d = b \left| u/\dot{u} \right| \dot{u} \quad (B-13)$$

where the bars denote that the absolute value of the quantity between them is to be used.

In summary, four different versions of material damping have been discussed. In terms of the differential equation for free vibration, they may be written as follows:

$$m\ddot{u} + (b/\dot{u}) \dot{u} + ku = 0 \quad (B-14a)$$

$$m\ddot{u} + (k + ib) u = 0 \quad (B-14b)$$

$$m\ddot{u} + C_1 e^{im} u = 0 \quad (B-14c)$$

$$m\ddot{u} + b \left| u/\dot{u} \right| \dot{u} + ku = 0 \quad (B-14d)$$

The models represented by equations (B-14) have been criticized by many investigators for various reasons:

1. In equation (B-14a), the interpretation of  $\omega$  is dubious (references 58,60). Milne (reference 59) suggested that it is associated with the imaginary part of the pair of complex roots, but went on to state that there is no clear justification for this interpretation.

2. Equations (B-14b) and (B-14c) are equations with complex coefficients and the meaning of this is not clear (references 57,59). Furthermore, although they have complex exponential solutions, neither the real nor imaginary parts alone are solutions (references 59,60).

3. Equation (B-14d) is a nonlinear differential equation, due to the behavior of  $|u/\dot{u}|$  (reference 59).

4. None of the models represented by equations (B-14) can be simulated, even on a conceptual basis, on an analog computer (references 58, 60).

5. The model represented by equation (B-14a) does not meet the Wiener-Paley condition (references 61, 62) of causality for physically realizable systems, as was shown in references 60, 63-65.

6. Equation (B-14b) fails to give the proper relations of a damping force that is proportional to displacement and in phase with velocity. This can be alleviated by use of a more unwieldy expression proposed in references 66,67.

Incidentally reference 68 claimed that none of the equation (B-14) models result in energy dissipation that is independent of  $\omega$  (the reason for abandoning the Kelvin-Voigt model). However, an error in this reasoning, which makes it invalid, was pointed out in reference 69.

It can be shown that the sinusoidally forced vibration version of free vibration equations (B-14a,b,c) are exactly equivalent. Probably the most popular form for writing this is as follows:

$$m\ddot{u} + (k + ib)u = \tilde{F} e^{i\omega t} \quad (B-15)$$

The major criticism of the use of equation (B-15) is that it results in a conventionally defined magnification factor (see Section B2), corresponding to zero frequency, which is not equal to unity for  $g \neq 0$  (reference 52). This difficulty can be eliminated by redefining the magnification factor as follows:

$$MF' \equiv \tilde{u}/u'_{st} \quad (B-16)$$

where

$$u'_{st} \equiv F/k'$$

and  $k'$  is the stiffness coefficient associated with the total in-plane force amplitude, i.e.

$$k' \equiv (k^2 + b^2)^{\frac{1}{2}}$$

Thus,

$$MF' = (k^2 + b^2)^{\frac{1}{2}} / [(k - m\omega^2)^2 + b^2]^{\frac{1}{2}} = (1 + g^2)^{\frac{1}{2}} / [(1 - \omega^2/\omega_n^2)^2 + g^2]^{\frac{1}{2}}$$

The major advantages of using the equation (B-15) model for steady-state vibrational and flutter analyses are as follows:

1. The analysis is considerably simplified in comparison with that for viscous damping, as pointed out in reference 70.
2. The analysis is linear.
3. The complex-modulus concept has long been in common use, especially

in connection with measurement of the damping properties of elastomers, polymers, etc. (reference 69).

4. The complex-stiffness approach has been used very successfully in flutter analysis for approximately three decades refs. 54, 55, 69, 71).

In view of these considerations, the complex-stiffness approach is used in the main portion of the present report. However, for completeness and comparison, a number of other more complicated approaches are also discussed in this section.

To overcome some of the deficiencies of the Kelvin-Voigt and Maxwell models, they were combined in various ways to obtain the three-parameter models shown in figure B-1(c) and (d). It can be shown (reference 72) that by properly selecting the values of the coefficients, the two models can be used interchangeably. In other words, the model representation is not unique. In fact, both representations have been called the "standard linear solid", "standard linear material," "simple an-elastic model", or "standard model of a viscoelastic body" (references 73-76). Unfortunately, few materials have been characterized by the use of the standard linear solid. Perhaps the most extensive characterization has been carried out for flexural vibration of 2024-T4 aluminum alloy: by Granick and Stern (reference 77,78 ) in air and by Gustafson et al (reference 79) in vacuo.

Obviously one can go on from a three-parameter model to a four-parameter one, etc. Continuing this process, one obtains two well-known models (reference 74): the Kelvin chain, shown in figure B-2(a), and the generalized Maxwell model, shown in figure B-2(b). The behavior of such systems can be written in either differential or integral form, as discussed in detail in reference 74. However, the complexity of



such a model has limited its use both experimentally (in characterizing engineering materials) and analytically (in performing dynamic analyses). Thus, for engineering applications, there is a continuing search for models which are simple, yet represent the behavior of real materials with sufficient accuracy.

A (relatively simple model, which is somewhat similar to the generalized Maxwell one, is due to Biot (reference 80); see figure B-2(c). The number of simple Voigt elements in this model is allowed to increase without bound, so that the damping force is represented by the following expression:

$$F_d = g_1 \int_{t_1}^t Ei [-\epsilon(t-\tau)] (du/d\tau) d\tau \quad (B-17)$$

where  $\tau$  is a dummy variable;  $\epsilon, g_1 \equiv$  parameters, and  $Ei(u)$  is the exponential integral

$$Ei(u) \equiv \int_{\infty}^{-u} (e^{-\xi}/\xi) d\xi \quad (B-18)$$

Caughey (ref. 60) made a detailed study of Biot's model for both free and forced vibration. He showed that for  $u/\epsilon > 10$ , the energy dissipated in Biot's model is within 4% of being independent of frequency ( $\omega$ ) and thus essentially depends only upon the square of the displacement amplitude. Milne (ref. 59) studied the Biot model by means of the convolution integral.

Neubert (reference 81) introduced a variant of the Biot model, in which a different distribution function for the local stiffness-damping ratio is used. Milne (ref. 59) also studied this model via the convolution integral. Milne introduced a new synthesized model of his own. However,

the main conclusion of his investigation was that, for practical engineering purposes, the choice of a rheological model is not critical, provided that the range of constant damping is kept the same and the damping is small.

The linear hereditary theory of material damping was originated in 1876 by Boltzmann (reference 82). In this theory, the energy loss is attributed to the elastic delay by which the deformation lags behind the applied force. It is called a hereditary theory because the instantaneous deformation depends upon all of the stresses applied to the body previously as well as upon the stress at that instant. The damping force is given by

$$F_d = \int_{-\infty}^t \Phi(t, \tau) u(\tau) d\tau \quad (B-19)$$

where  $t \equiv$  actual time,  $\tau \equiv$  an instant of time (dummy variable),  $u \equiv$  displacement, and  $\Phi \equiv$  hereditary kernel or memory function. Often the hereditary kernel depends upon the difference  $(t-\tau)$  only; then equation B-19) becomes:

$$F_d = \int_{-\infty}^t \Phi(t - \tau) u(\tau) d\tau \quad (B-20)$$

It is most advantageous to determine the hereditary kernel from experimental data. It has been found to be a monotonically decreasing function which can be represented mathematically as follows:

$$\Phi(t) = \sum_{i=1}^n A_i e^{-\alpha_i t} \quad (B-21)$$

Such a system is said to have a heredity of degree  $n$  and  $A_i$  and  $\alpha_i$

are called heredity constants. Hobbs (ref. 75) has shown that a first-degree hereditary model is equivalent to a simple anelastic model (standard linear solid).

Volterra (reference 83) has presented a method of determining the hereditary kernel from material response to either suddenly applied loading or to sinusoidal excitation. He also presented plots of magnification factor and phase shift versus frequency for a wide range of parameters of a single-degree-of-freedom system with first-degree hereditary damping. For certain combinations of the parameters, the magnification and phase characteristics are quite different from that of a viscously damped system; yet for certain other combinations, the characteristics are quite similar.

Numerous nonlinear mathematical models have been proposed to permit better correspondence between theory and experiment. However, all of them, by their very nonlinear nature, are more complicated to apply in structural dynamic analyses of practical engineering systems. Perhaps the simplest one is damping energy per unit volume and per cycle proportional to stress to a power (ref. 48):

$$U_{dv} = C_d \tilde{\sigma}^m \quad (B-22)$$

where  $C_d$  and  $m$  are material constants and  $\tilde{\sigma}$  is the cyclic stress amplitude. It is noted that  $m=2$  corresponds to the Kimball-Lovell relation (linear theory) discussed previously. It has been found that  $m$  varies from 1.8 to 6.0, generally being near 2.0 at low stress amplitudes.

The hysteresis loop associated with the complex-modulus model, equation (B-11), is elliptic in shape; see figure B-3(a). However,

the hysteresis loops determined experimentally have sharp corners at both ends and are nearly linear in the low-stress, low-strain region, as shown in figure B-3(b). According to ref. 48 (page 97), in 1938 Davidenkov proposed a nonlinear mathematical model which results in a similar shape of hysteresis loop. Further work on this class of model has been carried out by Pisarenko (reference 84).

Rosenblueth and Herrera (reference 85) proposed a nonlinear model which eliminates the causality difficulties of the complex-modulus model. Chang and Bieber (reference 86) introduced a nonlinear hysteresis model in which there is no hysteresis damping unless the displacement amplitude exceeds a certain threshold value.

## B2. Measures of Material Damping

In this section, various definitions of damping are discussed in the context of a complex-modulus material.

Energy Dissipation Under Steady-State Sinusoidal Vibration. - Energy dissipated per cycle ( $U_d$ ) in the form of internal frictional heating is one measure of damping. However, this quantity depends upon the size, shape, and dynamic stress distribution (which in turn, depends upon the particular mode of vibration). In view of the above difficulties, the specific damping energy ( $U_{dv}$ ) is usually considered to be a more basic property of the material, rather than the structure. The  $U_{dv}$  is defined as the damping energy per cycle and per unit volume, assuming a uniform dynamic stress distribution throughout the volume considered. Thus, the total damping energy is

$$U_d = \oint_V U_{dv} dV \quad (B-23)$$

where  $V$  = volume. The usual units of  $U_d$  are in-lb/cycle and of  $U_{dv}$ , in-lb/in<sup>3</sup>-cycle.

Resonant Magnification Factor Under Steady-State Sinusoidal Excitation. - The resonant magnification factor (RMF) is defined as the dimensionless ratio of the response at resonance to the excitation, where both the response and the excitation must be specified in the same units (see figure B-4). These quantities may be in units of displacement, velocity, acceleration, or strain. Unfortunately, the resonant magnification factor is dependent upon the structural system configuration as well as upon the damping property of the material, so that it is considered to be a system characteristic, rather than a basic material property.

Incidentally RMF is not applicable to nonlinear systems, since then it depends upon the excitation level. (In a linear system, RMF is independent of the level of excitation.)

Bandwidth of Half-Power Points Under Steady-State Sinusoidal Excitation. - The separation  $(\omega_2 - \omega_1)$  between the frequencies associated with the half-power points increases with an increase in damping (see figure B-5) and thus can be used as a measure of damping. A more meaningful definition is to normalize by the associated resonant frequency  $(\omega_n)$ , i.e. use the dimensionless bandwidth given by:

$$(\omega_2 - \omega_1) / \omega_n$$

This measure is the basis for determination of damping by the original Kennedy-Pancu method (reference 87).

The quality factor  $Q$  is defined as the reciprocal of the dimensionless

bandwidth.

Derivative of Phase Angle with Respect to Frequency, at Resonance. -

This measure is the basis for determination of damping by an improvement (reference 88) of the Kennedy-Pancu method.

Loss Tangent Under Steady-State Sinusoidal Excitation. - Applying the complex-stiffness (see Section B1) to the material property representing stiffness, namely the Young's modulus ( $E$ ), we obtain

$$E \rightarrow E^R(1 + ig) \quad (B-24)$$

Thus, the loss tangent<sup>\*</sup> is defined as follows:

$$g = E^I/E^R \quad (B-25)$$

where  $E^I \equiv$  loss modulus<sup>\*\*</sup> and  $E^R$  is called the storage modulus.<sup>\*\*\*</sup>

Referring to figure B-6, we obtain the following relation:

$$g = \tan \gamma = E^I/E^R \quad (B-26)$$

or

$$\gamma = \arctan E^I/E^R \quad (B-27)$$

---

\*Also known as the "loss coefficient", "loss factor", or "damping factor".

\*\*Also sometimes called the "dissipation modulus."

\*\*\*Also sometimes called "elastic modulus" or "real modulus."

The quantity  $\gamma$  is called the loss angle and equation (B-26) explains the origin of the term loss tangent for  $g$ .

Cyclic Decay of Free Vibrations. - In a linear system, free vibrations decay exponentially (see figure B-7). The larger the damping, the faster is the decay. Thus, the logarithmic decrement  $\delta$  is defined as follows:

$$\delta = \ln (a_i / a_{i+1}) \quad (B-28)$$

where  $\ln$  = natural logarithm.

For a power-law material, eq. (B-22), to have  $\delta$  independent of amplitude,  $m$  must be 2 (see Section B3 for proof). When  $m=2$ , the following means of calculating  $\delta$  is more practical, especially when damping is small:

$$\delta = (1/n) \ln (a_i / a_{i+n}) \quad (B-29)$$

where  $n$  is any arbitrary integer.

Temporal Decay of Free Vibrations. - Another measure associated with the decay of free vibrations is the temporal decay constant  $v_t$ , defined as follows (reference 48, foldout opposite p. 35):

$$v_t = (t_2 - t_1)^{-1} \ln [u(t_1) / u(t_2)] \quad (B-30)$$

where  $t_1$  and  $t_2$  are two different values of time, arbitrary except that  $t_2 > t_1$  and  $(t_2 - t_1)$  must be an integer number of periods of damped vibration. The quantities  $u(t_1)$  and  $u(t_2)$  are the respective displacements at times  $t_1$  and  $t_2$ . It is seen that the usual units for  $v_t$  are  $\text{sec}^{-1}$ .

An alternate way of specifying the temporal decay is the decay rate  $\gamma_t$ , which has units of decibals per second (db/sec) and is defined as follows:

$$\gamma_t \equiv 20 (t_2 - t_1)^{-1} \log [u(t_1)/u(t_2)] \quad (\text{B-31})$$

or

$$\gamma_t = 20(t_2 - t_1)^{-1} \log e^{v_t(t_2 - t_1)} = (20 \log e) v_t \approx 8.68 v_t$$

where  $\log \equiv$  logarithm to the base 10.

Spatial Attenuation of a Plane Wave in a Slender Bar. - If one propagates a plane, harmonic wave in a slender bar made of a homogeneous, linear material, the wave exhibits exponential decay with axial position ( $x$ ), analogous to the temporal decay of free vibration (which may be considered as a standing wave). Analogous to the logarithmic decrement (see above), we have the logarithmic attenuation  $\delta_s$ , defined as follows in terms of amplitudes  $a(x_1)$  and  $a(x_2)$  at stations  $x_1$  and  $x_2$ :

$$\delta_s = \ln [a(x_1)/a(x_2)] \quad (\text{B-32})$$

Analogous to the temporal decay constant, we define the spatial attenuation constant  $v_s$  as follows:

$$v_s \equiv (x_2 - x_1)^{-1} \ln [a(x_1)/a(x_2)] \quad (\text{B-33})$$

The unit of  $v_s$  is  $\text{in}^{-1}$ .

Finally, analogous to the decay rate, we define the spatial attenuation rate  $\gamma_s$  as follows:



$$\gamma_s = 20(x_2 - x_1)^{-1} \log [a(x_1)/a(x_2)] \approx 8.68 \gamma_s. \quad (B-34)$$

The unit of  $\gamma_s$  is db per unit length.

It should be cautioned that the determination of damping by wave attenuation requires that the cross section of the bar be compact (preferably round or square) and that the largest cross-sectional dimension be very small compared to the wave length of the traveling wave. Furthermore, the two stations along the bar, at which the wave measurements are made, must be: (1) sufficiently far from the point of impact that initial transients have died out and (2) sufficiently far from each other so that a measurable change in amplitude occurs. Kolsky discussed these points in detail in reference 89.

### B3. Inter-Relationships Among Various Measures of Damping for Homogeneous Materials

Here we consider a single degree-of-freedom system consisting of a mass supported on a massless spring made of a homogeneous Kimball-Lovell or complex-modulus material. Then the governing differential equation for simple harmonic excitation is equation (B-15), which has the following steady-state solution:

$$u = \tilde{u} e^{i(\omega t - \varphi)} \quad (B-35)$$

where

$$\tilde{u} = \tilde{F} [(k - m\omega^2)^2 + b^2]^{-1/2} \quad (B-36)$$

$$\varphi = \arctan [b/(k - m\omega^2)] \quad (B-37)$$

The magnification factor (MF) is defined as follows:

$$MF \equiv \tilde{u}/u_{st} \quad (B-38)$$

where  $u_{st}$  is the so-called static displacement, defined as follows:

$$u_{st} \equiv \tilde{F}/k \quad (B-39)$$

Combining equations (B-36, B-38, and B-39), one obtains the following relation:

$$MF = \left\{ [1 - (\omega/\omega_n)^2]^2 + (b/m\omega_n^2)^2 \right\}^{-1/2} \quad (B-40)$$

where  $\omega_n$  is the natural frequency (i.e. the resonant frequency of the undamped system), given by:

$$\omega_n = (k/m)^{1/2} \quad (B-41)$$

The critical material damping coefficient ( $b_c$ ) is the minimum value of  $b$  for which the free vibratory motion is non-oscillatory. It is obtained from the following relationship:

$$(b_c/2m\omega_n)^2 = k/m = \omega_n^2$$

or

$$b_c = 2m\omega_n^2 \quad (B-42)$$

The damping ratio  $\zeta$  is defined as follows:

$$\zeta \equiv b/b_c \quad (B-43)$$

Combining equations (B-40, B-42, and B-43), one arrives at the following general, dimensionless relationship:

$$MF = \left\{ \left[ 1 - (\omega/\omega_n)^2 \right]^2 + 4\zeta^2 \right\}^{-1/2} \quad (B-44)$$

It is seen easily that MF is a function of only two parameters: the frequency ratio  $(\omega/\omega_n)$  and the damping ratio  $(\zeta)$ . It should be mentioned that equation (B-44) is somewhat different than the known relationship for a single-degree-of-freedom Kelvin-Voigt viscously damped system, even though the damping ratio  $\zeta$  is defined analogously ( $\equiv c/c_c$ , where  $c_c = 2m\omega_n$ ).

The resonant magnification factor (RMF) is defined as the value of MF at resonance, which is taken here to occur when  $\varphi = 90^\circ$ . In view of equation (B-37), this implies that the resonant frequency is  $\omega_n$ . Thus, at resonance, equation (B-44) reduces to the following simple expression:

$$\boxed{RMF = (2\zeta)^{-1}} \quad (B-45)$$

Thus, it is seen that the same simple relationship between the damping ratio and the resonant magnification factor holds as does for a Kelvin-Voigt system. Although the resonant amplitude can be measured accurately, there are problems in measuring the static deflection in complicated structures (due to signal-to-noise ratio limitations of instrumentation). For this reason, in structural dynamics, RMF is seldom used as a measure of damping.

The damping energy, i.e. the energy dissipated per cycle, can be computed as follows:

$$U_d = \oint F_d \, du = \int_0^{2\pi/\omega} F_d \dot{u} \, dt \quad (B-46)$$

where  $F_d$  is the damping force, given by

$$F_d = (b/\omega)\dot{u} \quad (B-47)$$

Substituting equations (B-35) and (B-47) into equation (B-46) and integrating, we obtain the following result:

$$U_d = \pi b \tilde{u}^2 \quad (B-48)$$

To convert equation (B-48) to the form of equation (B-22), with  $m=2$ , it is necessary to divide by the volume and to relate  $\tilde{u}$  to  $\tilde{\sigma}$ . Now the force amplitude is

$$\tilde{F} = A\tilde{\sigma} = k\tilde{u} \quad (B-49)$$

where  $A$  = cross-sectional area.

Assuming the spring is a massless and uniform bar, we have

$$k = AE/L \quad (B-50)$$

where  $L$   $\equiv$  effective length of spring and  $E$  = Young's modulus of the bar.

Combining equations (B-48, B-49, B-50), one obtains the following result:

$$U_{ds} = U_d/V = (\pi bL/A)(\tilde{\sigma}/E)^2 \quad (B-51)$$

Comparing the form of equations (B-22) and (B-51), we see that for a Kimball-Lovell material,  $m = 2$  and

$$C_d = \pi bL/AE^2 \quad (B-52)$$

It should be noted that Lazan (reference 48, chap. II) has shown that these results are independent of the stress distribution and the specimen geometry, provided that  $m = 2$ .

In view of equations (B-42, B-43, and B-44), equation (B-52) can be expressed in the following more useful form:

$$C_d = 2\pi \zeta / E \quad (B-53)$$

According to equation (B-48), the damping energy (and thus, excitation power) is proportional to the square of the displacement amplitude  $u_o$  (and thus, the MF). Then the power is one half of what it is at resonance when  $MF = RMF/\sqrt{2}$ . In view of equation (B-45), the half-power magnification factor (HPMF) is related to the damping ratio as follows:

$$HPMF = RMF/\sqrt{2} = (2/\sqrt{2} \zeta)^{-1} \quad (B-54)$$

To determine the two sideband frequencies ( $\omega = \omega_1$  and  $\omega_2$ ) corresponding to half power, we combine equations (B-44) and (B-54) to obtain the following quadratic expression in  $\omega^2$ :

$$(2/\sqrt{2} \zeta)^2 = [1 - (\omega/\omega_n)^2]^2 + 4\zeta^2$$

which has the following positive roots:

$$\omega_{1,2} = \omega_n (1 \pm 2\zeta)^{\frac{1}{2}} \quad (B-55)$$

It is interesting to note that equation (B-55) is identical to the analogous expression for the lightly damped Kelvin-Voigt system, i.e.  $(c/c_c)^2 \ll 1$ .

For small damping ( $\zeta \ll \frac{1}{2}$ ),

$$\omega_{1,2} \approx (1 \pm \zeta) \omega_n$$

Thus, we get the following relation between the dimensionless bandwidth and the damping ratio  $\zeta$ :

$$\boxed{(\omega_2 - \omega_1) / \omega_n \approx 2\zeta} \quad (B-56)$$

In the original Kennedy-Pancu method (reference 87), this relationship is used to determine the damping ratio from the geometry of an experimentally determined Argand plot (a polar-coordinate plot of response amplitude versus phase angle).

In terms of the quality factor  $Q$ , equation (B-56) may be rewritten as follows:

$$\boxed{Q \approx (2\zeta)^{-1}} \quad (B-57)$$

It is interesting to note that in order for the half-power frequencies to be real, the damping ratio  $\zeta$  must be no greater than  $\sqrt{2}/2 \approx 0.707$ . However, this is not a severe limitation for actual structural materials.

The potential energy (strain energy) stored in our single-degree-of-freedom mathematical model is given by:

$$U = \oint F_s \, du \quad (B-58)$$

where  $F_s$  is the spring force, given by

$$F_s = ku \quad (B-59)$$

Thus,

$$U = k \int_0^{\tilde{u}} u \, du = k\tilde{u}^2/2 \quad (B-60)$$

Combining equations (B-48) and (B-60), we obtain

$$U_d/U = 2\pi b/k \quad (B-61)$$

Using equations (B-41, B-42, B-43), we can rewrite equation (B-61) in the following more useful form:

$$U_d/U = 4\pi\zeta \quad (B-62)$$

or

$$\boxed{\zeta = (1/4\pi)(U_d/U)} \quad (B-63)$$

The loss tangent is defined as follows for the system considered here:

$$g \equiv b/k \quad (B-64)$$

Inserting equations (B-41, B-42, B-43) into equation (B-64) we obtain the following useful relationship:

$$\boxed{g = 2\zeta} \quad (B-65)$$

The following useful relationship, which is sometimes taken as a fundamental definition of damping (reference 66), is obtained here by combining equations (B-63) and (B-65):

$$\boxed{g = (1/2\pi)(U_d/U)} \quad (B-66)$$

Taking the derivative of phase angle  $\varphi$  with respect to frequency  $\omega$ , one obtains the following result from equation (B-37):

$$d\varphi/d\omega = 2b\omega / [(k - m\omega^2)^2 + b^2] \quad (B-67)$$

At resonance (subscript R), defined by  $\omega = \omega_n = \sqrt{k/m}$ , equation (B-67) becomes:

$$(d\varphi/d\omega)_R = 2m\omega_n/b \quad (B-68)$$

Combining equations (B-42, B-43, and B-68), we obtain the following

very useful result:

$$\zeta = [\omega_n (d\varphi/d\omega)_R]^{-1} \quad (B-69)$$

It is interesting to note that although the MF vs.  $\omega$  relation, equation (B-44), is different than the corresponding relation for a Kelvin-Voigt viscously damped system, equation (B-69) is identical to its corresponding relationship for a Kelvin-Voigt system. Equation (B-69) is used to determine the damping ratio from an experimentally determined Argand diagram in the improved Kennedy-Pancu method (reference 88).

The transient solution of the system represented by equation (B-14a) can be written as follows:

$$u' = \tilde{u}' e^{-\zeta \omega_n t} \sin(\sqrt{1-\zeta^2} \omega_n t - \varphi) \quad (B-70)$$

From its definition in equation (B-28), the logarithmic decrement  $\delta$  can be determined as follows:

$$\delta = \ln \frac{e^{-\zeta \omega_n t_1}}{e^{-\zeta \omega_n (t_1 + T)}} = \ln e^{\zeta \omega_n T} = \zeta \omega_n T \quad (B-71)$$

where  $T$  is the period of damped oscillation, given by

$$T = (2\pi/\omega_n) (1-\zeta^2)^{-1/2} \quad (B-72)$$

Thus, we now have

$$\delta = 2\pi\zeta (1-\zeta^2)^{-1/2} \quad (B-73)$$

For small damping ( $\zeta^2 \ll 1$ ), equation (B-73) can be replaced by the following approximate expression:

$$\delta \approx 2\pi\zeta \quad (B-74)$$



Combining equations (B-65) and (B-74), one obtains the following:

$$\boxed{\delta = \pi g} \quad (B-75)$$

In view of equation (B-63) and since the specific energies are given by:

$$U_{ds} \equiv U_d/V, \quad U_s \equiv U/V, \quad (B-76)$$

we have

$$\zeta' = U_{ds} / 4\pi U_s \quad (B-77)$$

However, the specific strain energy is

$$U_s = \tilde{\sigma}^2 / 2E \quad (B-78)$$

A power-law-damping material is defined by equation (B-22).

Combining this relation with equation (B-78), one obtains:

$$\zeta = (E C_d / 8\pi) \tilde{\sigma}^{m-2} \quad (B-79)$$

Thus, it is clear that  $\zeta$  is independent of stress amplitude only for a KL (Kimball-Lovell) material ( $m=2$ ). Then

$$\boxed{\zeta = E C_d / 8\pi} \quad (B-80)$$

or, in view of equation (B-65),

$$\boxed{g = E C_d / 4\pi} \quad (B-81)$$

Furthermore, since the logarithmic decrement of a KL material with small damping is approximately proportional to the damping ratio as shown by equation (B-74), the following approximate relation holds:

$$\boxed{\delta \approx E C_d / 4} \quad (B-82)$$

## APPENDIX C

### DERIVATION OF ENERGY DIFFERENCE

It is assumed that the generalized coordinate  $\xi$  and generalized force  $f$  have the following forms:

$$\begin{aligned}\xi &= \tilde{\xi} e^{i\omega t} \\ f &= \tilde{q} e^{i\omega t}\end{aligned}\tag{C-1}$$

where  $\tilde{\xi}$  is a complex form representing  $\tilde{u}_o, \tilde{v}_o, \tilde{w}_o, \tilde{v}_x$  and  $\tilde{v}_y$ .

The strain energy can be expressed as

$$U = (1/2) \sum_{i=1}^n \sum_{j=1}^n Q_{ij} \xi_i \xi_j = \tilde{U} e^{2i\omega t}\tag{C-2}$$

where  $Q_{ij}$  are stiffness coefficients and  $\tilde{U}$  is the amplitude of the strain energy given by:

$$\tilde{U} = (1/2) \sum_{i=1}^n \sum_{j=1}^n Q_{ij} \tilde{\xi}_i \tilde{\xi}_j\tag{C-3}$$

For the damping energy, a dissipation function suitable for material damping (reference 90) is developed. Hence, we introduce a dissipation energy function for material damping as follows:

$$D = \frac{1}{2} \sum_{i=1}^n \sum_{j=1}^n (b_{ij}/\omega) \dot{\xi}_i \dot{\xi}_j = (i\omega/2) \sum_{i=1}^n \sum_{j=1}^n \hat{Q}_{ij} \tilde{\xi}_i \tilde{\xi}_j e^{2i\omega t} = (i\omega) \tilde{D} e^{2i\omega t}\tag{C-4}$$

where  $b_{ij}$  are structural damping coefficients,  $\hat{Q}_{ij} = ib_{ij}$  and  $\tilde{D}$  is the amplitude of dissipation energy given by:

$$\tilde{D} = \frac{1}{2} \sum_{i=1}^n \sum_{j=1}^n \hat{Q}_{ij} \tilde{\xi}_i \tilde{\xi}_j \quad (C-5)$$

The kinetic energy of the system is

$$T = \frac{1}{2} \sum_{i=1}^n \sum_{j=1}^n m_{ij} \dot{\xi}_i \dot{\xi}_j = -(\omega^2/2) \sum_{i=1}^n \sum_{j=1}^n m_{ij} \tilde{\xi}_i \tilde{\xi}_j e^{2i\omega t} = -\tilde{T} e^{2i\omega t} \quad (C-6)$$

where  $m_{ij}$  are inertia coefficients and  $\tilde{T}$  is the amplitude of kinetic energy given by

$$\tilde{T} = (\omega^2/2) \sum_{i=1}^n \sum_{j=1}^n m_{ij} \tilde{\xi}_i \tilde{\xi}_j \quad (C-7)$$

The work done by the uniformly distributed normal force is

$$W = f \sum_{i=1}^n \xi_i = \tilde{q} e^{i\omega t} \sum_{i=1}^n \xi_i = \tilde{W} e^{2i\omega t} \quad (C-8)$$

where  $\tilde{q}$  is the amplitude of the normal pressure and  $\tilde{W}$  is the amplitude of the work done

$$\tilde{W} = \tilde{q} \sum_{i=1}^n \tilde{\xi}_i \quad (C-9)$$

The Lagrangian equation takes the following form (reference 91)

$$\frac{d}{dt} \left( \frac{\partial T}{\partial \dot{\xi}} \right) + \frac{\partial D}{\partial \dot{\xi}} + \frac{\partial U}{\partial \xi} = f \quad (C-10)$$

Each term of equation (C-10) can be expressed in terms of its amplitude as follows:

$$\frac{d}{dt} \left( \frac{\partial T}{\partial \dot{\xi}} \right) = - \frac{\partial \tilde{T}}{\partial \tilde{\xi}} e^{i\omega t}, \quad \frac{\partial D}{\partial \dot{\xi}} = \frac{\partial \tilde{D}}{\partial \tilde{\xi}} e^{i\omega t} \quad (C-11)$$

$$\frac{\partial U}{\partial \xi} = \frac{\partial \tilde{U}}{\partial \tilde{\xi}} e^{i\omega t}, \quad f = \frac{\partial W}{\partial \xi} = \frac{\partial \tilde{W}}{\partial \tilde{\xi}} e^{i\omega t}$$

With equations (C-11) introduced, one can rewrite equation (C-10) as follows:

$$\frac{\partial}{\partial \tilde{\xi}} (\tilde{T} + \tilde{W} - \tilde{U} - \tilde{D}) e^{i\omega t} = 0 \quad (C-12)$$

or

$$\frac{\partial}{\partial \tilde{\xi}} (\tilde{T} + \tilde{W} - \tilde{U} - \tilde{D}) = 0 \quad (C-13)$$

Equation (C-13) is analogous to one presented by Volterra (reference 83).

Thus, the amplitude of the Lagrangian energy difference can be expressed as follows

$$\tilde{L} = (\tilde{T} + \tilde{W}) - (\tilde{U} + \tilde{D}) \quad (C-14)$$

when used in conjunction with Hamilton's principle, expressed in equation (36).

# APPENDIX D

## COMPLETE ENERGY EXPRESSIONS

### D1. The Energy Difference

$$\begin{aligned}
 \tilde{L} = & \frac{1}{2} \sum_{m=1}^M \sum_{n=1}^N \int_0^1 \int_0^1 \left\{ (\bar{A}_{11}/a^2) (U_{mn} \phi'_{um} \phi_{un})^2 + (2\bar{A}_{12}/ab) (U_{mn} \phi'_{um} \phi_{un}) (V_{mn} \phi_{vm} \phi'_{vn}) \right. \\
 & + 2\bar{A}_{16} (a^{-1} U_{mn} \phi'_{um} \phi_{un}) (a^{-1} V_{mn} \phi'_{vm} \phi_{vn} + b^{-1} U_{mn} \phi_{um} \phi'_{un}) \\
 & + 2\bar{A}_{26} (b^{-1} V_{mn} \phi_{vm} \phi'_{vn}) (a^{-1} V_{mn} \phi'_{vm} \phi_{vn} + b^{-1} U_{mn} \phi_{um} \phi'_{un}) + \bar{A}_{66} (a^{-1} V_{mn} \phi'_{vm} \phi_{vn} + b^{-1} U_{mn} \phi_{um} \phi'_{un})^2 \\
 & + 2\bar{B}_{11} (a^{-1} U_{mn} \phi'_{um} \phi_{un}) (a^{-1} \psi_{xmn} \phi'_{\psi xm} \phi_{\psi xn}) + 2\bar{B}_{12} [(a^{-1} U_{mn} \phi'_{um} \phi_{un}) (b^{-1} \psi_{ymn} \phi_{\psi ym} \phi'_{\psi yn}) \\
 & + b^{-1} V_{mn} \phi_{vm} \phi'_{vn}) (a^{-1} \psi_{xmn} \phi'_{\psi xm} \phi_{\psi xn})] + 2\bar{B}_{22} (b^{-1} V_{mn} \phi_{vm} \phi'_{vn}) (b^{-1} \psi_{ymn} \phi_{\psi ym} \phi'_{\psi yn}) \\
 & + 2\bar{B}_{16} [(a^{-1} U_{mn} \phi'_{um} \phi_{un}) (a^{-1} \psi_{ymn} \phi'_{\psi ym} \phi_{\psi yn} + b^{-1} \psi_{xmn} \phi_{\psi xm} \phi'_{\psi xn}) + a^{-1} V_{mn} \phi'_{vm} \phi_{vn} \\
 & + b^{-1} U_{mn} \phi_{um} \phi'_{un}) (a^{-1} \psi_{xmn} \phi'_{\psi xm} \phi_{\psi xn})] + 2\bar{B}_{26} [b^{-1} V_{mn} \phi_{vm} \phi'_{vn}) (a^{-1} \psi_{ymn} \phi'_{\psi ym} \phi_{\psi yn} \\
 & + b^{-1} \psi_{xmn} \phi_{\psi xm} \phi'_{\psi xn}) + (a^{-1} V_{mn} \phi'_{vm} \phi_{vn} + b^{-1} U_{mn} \phi_{um} \phi'_{un}) (b^{-1} \psi_{ymn} \phi_{\psi ym} \phi'_{\psi yn})] \\
 & + 2\bar{B}_{66} (a^{-1} V_{mn} \phi'_{vm} \phi_{vn} + b^{-1} U_{mn} \phi_{um} \phi'_{un}) (a^{-1} \psi_{ymn} \phi_{\psi ym} \phi'_{\psi yn} + b^{-1} \psi_{xmn} \phi_{\psi xm} \phi'_{\psi xn}) \\
 & + (\bar{D}_{11}/a^2) (\psi_{xmn} \phi'_{\psi xm} \phi_{\psi xn})^2 + (2\bar{D}_{12}/ab) (\psi_{xmn} \phi'_{\psi xm} \phi_{\psi xn}) (\psi_{ymn} \phi_{\psi ym} \phi'_{\psi yn}) \\
 & + (\bar{D}_{22}/b^2) (\psi_{ymn} \phi_{\psi ym} \phi'_{\psi yn})^2 + 2\bar{D}_{16} (a^{-1} \psi_{xmn} \phi'_{\psi xm} \phi_{\psi xn}) (a^{-1} \psi_{ymn} \phi_{\psi ym} \phi'_{\psi yn}) \\
 & + b^{-1} \psi_{xmn} \phi_{\psi xm} \phi'_{\psi xn}) + 2\bar{D}_{26} (b^{-1} \psi_{ymn} \phi_{\psi ym} \phi'_{\psi yn}) (a^{-1} \psi_{ymn} \phi_{\psi ym} \phi'_{\psi yn} + b^{-1} \psi_{xmn} \phi_{\psi xm} \phi'_{\psi xn}) \\
 & + \bar{D}_{66} (a^{-1} \psi_{ymn} \phi_{\psi ym} \phi'_{\psi yn} + b^{-1} \psi_{xmn} \phi_{\psi xm} \phi'_{\psi xn})^2 + K_{55} \bar{A}_{55} (a^{-1} W_{mn} \phi'_{wm} \phi_{wn} + \psi_{xmn} \phi_{\psi xm} \phi'_{\psi xn})^2 \\
 & + 2K_{45} \bar{A}_{45} (a^{-1} W_{mn} \phi'_{wm} \phi_{wn} + \psi_{xmn} \phi_{\psi xm} \phi'_{\psi xn}) (b^{-1} W_{mn} \phi_{wm} \phi'_{wn} + \psi_{ymn} \phi_{\psi ym} \phi'_{\psi yn}) \\
 & + K_{44} \bar{A}_{44} (b^{-1} W_{mn} \phi_{wm} \phi'_{wn} + \psi_{ymn} \phi_{\psi ym} \phi'_{\psi yn})^2 \} ab d\alpha d\beta \\
 & - (\omega^2/2) \sum_{m=1}^M \sum_{n=1}^N \int_0^1 \int_0^1 \left\{ m_o [(U_{mn} \phi_{um} \phi_{un})^2 + (V_{mn} \phi_{vm} \phi_{vn})^2 + (W_{mn} \phi_{wm} \phi_{wn})^2] \right. \\
 & \left. + 2m_1 [(U_{mn} \phi_{um} \phi_{un}) (\psi_{xmn} \phi_{\psi xm} \phi_{\psi xn}) + (V_{mn} \phi_{vm} \phi_{vn}) (\psi_{ymn} \phi_{\psi ym} \phi_{\psi yn})] \right\}
 \end{aligned}$$

$$\begin{aligned}
& +m_2 [ (\psi_{xmn} \phi_{\psi x m} \phi_{\psi x n})^2 + (\psi_{ymn} \phi_{\psi y m} \phi_{\psi y n})^2 ] \} ab \, d\alpha \, d\beta \\
& - \sum_{m=1}^M \sum_{n=1}^N \int_0^1 \int_0^1 \tilde{q} W_{mn} \phi_{wm} \phi_{wn} \, ab \, d\alpha \, d\beta
\end{aligned} \tag{D-1}$$

where

$$\phi'_m = \partial \phi_m / \partial \alpha, \quad \phi'_n = \partial \phi_n / \partial \beta$$

## D2. Equations for Minimizing the Energy Difference

$$\begin{aligned}
\partial \tilde{L} / \partial U_{k\ell} = & (b/a) \bar{A}_{11} \sum_{m=1}^M \sum_{n=1}^N U_{mn} \int_0^1 \phi'_{um} \phi'_{uk} \, d\alpha \int_0^1 \phi_{un} \phi_{u\ell} \, d\beta \\
& + \bar{A}_{12} \sum_{m=1}^M \sum_{n=1}^N V_{mn} \int_0^1 \phi_{vm} \phi'_{uk} \, d\alpha \int_0^1 \phi'_{vn} \phi_{u\ell} \, d\beta \\
& + (b/a) \bar{A}_{16} \sum_{m=1}^M \sum_{n=1}^N V_{mn} \int_0^1 \phi'_{vm} \phi'_{uk} \, d\alpha \int_0^1 \phi_{vn} \phi_{u\ell} \, d\beta \\
& + \bar{A}_{16} \sum_{m=1}^M \sum_{n=1}^N U_{mn} \int_0^1 \phi_{um} \phi'_{uk} \, d\alpha \int_0^1 \phi'_{un} \phi_{u\ell} \, d\beta \\
& + \bar{A}_{16} \sum_{m=1}^M \sum_{n=1}^N U_{mn} \int_0^1 \phi'_{um} \phi_{uk} \, d\alpha \int_0^1 \phi_{un} \phi'_{u\ell} \, d\beta \\
& + (a/b) \bar{A}_{26} \sum_{m=1}^M \sum_{n=1}^N V_{mn} \int_0^1 \phi_{vm} \phi_{uk} \, d\alpha \int_0^1 \phi'_{vn} \phi'_{u\ell} \, d\beta \\
& + \bar{A}_{66} \sum_{m=1}^M \sum_{n=1}^N V_{mn} \int_0^1 \phi'_{vm} \phi_{uk} \, d\alpha \int_0^1 \phi_{vn} \phi'_{u\ell} \, d\beta \\
& + (a/b) \bar{A}_{66} \sum_{m=1}^M \sum_{n=1}^N U_{mn} \int_0^1 \phi_{um} \phi_{uk} \, d\alpha \int_0^1 \phi'_{un} \phi'_{u\ell} \, d\beta \\
& + (b/a) \bar{B}_{11} \sum_{m=1}^M \sum_{n=1}^N \psi_{xmn} \int_0^1 \phi'_{\psi x m} \phi'_{uk} \, d\alpha \int_0^1 \phi_{\psi x n} \phi_{u\ell} \, d\beta
\end{aligned}$$

$$\begin{aligned}
& +\bar{B}_{12} \sum_{m=1}^M \sum_{n=1}^N \Psi_{ymn} \int_0^1 \phi_{ym} \phi'_{uk} d\alpha \int_0^1 \phi'_{yn} \phi_{ul} d\beta \\
& + (b/a) \bar{B}_{16} \sum_{m=1}^M \sum_{n=1}^N \Psi_{ymn} \int_0^1 \phi'_{ym} \psi'_{uk} d\alpha \int_0^1 \phi_{yn} \phi_{ul} d\beta \\
& +\bar{B}_{16} \sum_{m=1}^M \sum_{n=1}^N \Psi_{xmn} \int_0^1 \phi_{xm} \phi'_{uk} d\alpha \int_0^1 \phi'_{xn} \phi_{ul} d\beta \\
& +\bar{B}_{16} \sum_{m=1}^M \sum_{n=1}^N \Psi_{xmn} \int_0^1 \phi'_{xm} \phi_{uk} d\alpha \int_0^1 \phi_{xn} \phi'_{ul} d\beta \\
& + (a/b) \bar{B}_{26} \sum_{m=1}^M \sum_{n=1}^N \Psi_{ymn} \int_0^1 \phi_{ym} \phi_{uk} d\alpha \int_0^1 \phi'_{yn} \phi'_{ul} d\beta \\
& +\bar{B}_{66} \sum_{m=1}^M \sum_{n=1}^N \Psi_{ymn} \int_0^1 \phi'_{ym} \phi_{uk} d\alpha \int_0^1 \phi_{yn} \phi'_{ul} d\beta \\
& + (a/b) \bar{B}_{66} \sum_{m=1}^M \sum_{n=1}^N \Psi_{xmn} \int_0^1 \phi_{xm} \phi_{uk} d\alpha \int_0^1 \phi'_{xn} \phi'_{ul} d\beta \\
& -ab \omega^2 \sum_{m=1}^M \sum_{n=1}^N m_o U_{mn} \int_0^1 \phi_{um} \phi_{uk} d\alpha \int_0^1 \phi_{un} \phi_{ul} d\beta \\
& -ab \omega^2 \sum_{m=1}^M \sum_{n=1}^N m_l \Psi_{xmn} \int_0^1 \phi_{xm} \phi_{uk} d\alpha \int_0^1 \phi_{xn} \phi_{ul} d\beta = 0 \quad (D-2)
\end{aligned}$$

There is another equation, for  $\partial \tilde{L} / \partial v_{kl} = 0$ , which is analogous to eq. (D-2) with the following substitutions:

$$u \leftrightarrow v, \quad U \leftrightarrow V, \quad x \leftrightarrow y, \quad l \leftrightarrow 2, \quad \phi \leftrightarrow \phi', \quad a \leftrightarrow b. \quad (D-3)$$

$$\begin{aligned}
\partial \tilde{L} / \partial w_{k\ell} = & (b/a) K_{55} \bar{A}_{55} \sum_{m=1}^M \sum_{n=1}^N w_{mn} \int_0^1 \phi'_{wm} \phi'_{wk} d\alpha \int_0^1 \phi_{wn} \phi_{w\ell} d\beta \\
& + b K_{55} \bar{A}_{55} \sum_{m=1}^M \sum_{n=1}^N \psi_{xmn} \int_0^1 \phi_{\psi xm} \phi'_{wk} d\alpha \int_0^1 \phi_{\psi xn} \phi_{wxn} \phi_{w\ell} d\beta \\
& + K_{45} \bar{A}_{45} \sum_{m=1}^M \sum_{n=1}^N w_{mn} \int_0^1 \phi'_{wm} \phi_{wk} d\alpha \int_0^1 \phi_{wn} \phi'_{w\ell} d\beta \\
& + K_{45} \bar{A}_{45} \sum_{m=1}^M \sum_{n=1}^N w_{mn} \int_0^1 \phi_{wm} \phi'_{wk} d\alpha \int_0^1 \phi'_{wn} \phi_{w\ell} d\beta \\
& + a K_{45} \bar{A}_{45} \sum_{m=1}^M \sum_{n=1}^N \psi_{xmn} \int_0^1 \phi_{\psi xm} \phi_{wk} d\alpha \int_0^1 \phi_{\psi xn} \phi'_{w\ell} d\beta \\
& + b K_{45} \bar{A}_{45} \sum_{m=1}^M \sum_{n=1}^N \psi_{ymn} \int_0^1 \phi_{\psi ym} \phi'_{wk} d\alpha \int_0^1 \phi_{\psi yn} \phi_{w\ell} d\beta \\
& + (a/b) K_{44} \bar{A}_{44} \sum_{m=1}^M \sum_{n=1}^N w_{mn} \int_0^1 \phi_{wm} \phi_{wk} d\alpha \int_0^1 \phi'_{wn} \phi'_{w\ell} d\beta \\
& + a K_{44} \bar{A}_{44} \sum_{m=1}^M \sum_{n=1}^N \psi_{ymn} \int_0^1 \phi_{\psi ym} \phi_{wk} d\alpha \int_0^1 \phi_{\psi yn} \phi'_{w\ell} d\beta \\
& - ab \omega^2 \sum_{m=1}^M \sum_{n=1}^N m_o w_{mn} \int_0^1 \phi_{wm} \phi_{wk} d\alpha \int_0^1 \phi_{wn} \phi_{w\ell} d\beta \\
& - ab \tilde{q} \sum_{m=1}^M \sum_{n=1}^N \int_0^1 \phi_{wk} d\alpha \int_0^1 \phi_{w\ell} d\beta = 0 \tag{D-4}
\end{aligned}$$

$$\partial \tilde{L} / \partial \psi_{xk\ell} = (b/a) \bar{B}_{11} \sum_{m=1}^M \sum_{n=1}^N u_{mn} \int_0^1 \phi'_{um} \phi'_{\psi xk} d\alpha \int_0^1 \phi_{un} \phi_{\psi x\ell} d\beta$$



$$\begin{aligned}
& +\bar{B}_{12} \sum_{m=1}^M \sum_{n=1}^N v_{mn} \int_0^1 \bar{\phi}_{vm} \bar{\phi}'_{\psi xk} d\alpha \int_0^1 \bar{\phi}'_{vn} \bar{\phi}_{\psi x\ell} d\beta \\
& +\bar{B}_{16} \sum_{m=1}^M \sum_{n=1}^N u_{mn} \int_0^1 \bar{\phi}'_{um} \bar{\phi}_{\psi xk} d\alpha \int_0^1 \bar{\phi}_{un} \bar{\phi}'_{\psi x\ell} d\beta \\
& +(b/a) \bar{B}_{16} \sum_{m=1}^M \sum_{n=1}^N v_{mn} \int_0^1 \bar{\phi}'_{vm} \bar{\phi}'_{\psi xk} d\alpha \int_0^1 \bar{\phi}_{vn} \bar{\phi}_{\psi x\ell} d\beta \\
& +\bar{B}_{16} \sum_{m=1}^M \sum_{n=1}^N u_{mn} \int_0^1 \bar{\phi}_{um} \bar{\phi}'_{\psi xk} d\alpha \int_0^1 \bar{\phi}'_{un} \bar{\phi}_{\psi x\ell} d\beta \\
& +(a/b) \bar{B}_{26} \sum_{m=1}^M \sum_{n=1}^N v_{mn} \int_0^1 \bar{\phi}_{vm} \bar{\phi}_{\psi xk} d\alpha \int_0^1 \bar{\phi}'_{vn} \bar{\phi}'_{\psi x\ell} d\beta \\
& +\bar{B}_{66} \sum_{m=1}^M \sum_{n=1}^N v_{mn} \int_0^1 \bar{\phi}'_{vm} \bar{\phi}_{\psi xk} d\alpha \int_0^1 \bar{\phi}_{vn} \bar{\phi}'_{\psi x\ell} d\beta \\
& +(a/b) \bar{B}_{66} \sum_{m=1}^M \sum_{n=1}^N u_{mn} \int_0^1 \bar{\phi}_{um} \bar{\phi}_{\psi xk} d\alpha \int_0^1 \bar{\phi}'_{un} \bar{\phi}'_{\psi x\ell} d\beta \\
& +(b/a) \bar{D}_{11} \sum_{m=1}^M \sum_{n=1}^N \psi_{xmn} \int_0^1 \bar{\phi}'_{\psi xm} \bar{\phi}'_{\psi xk} d\alpha \int_0^1 \bar{\phi}_{\psi xn} \bar{\phi}_{\psi x\ell} d\beta \\
& +\bar{D}_{12} \sum_{m=1}^M \sum_{n=1}^N \psi_{ymn} \int_0^1 \bar{\phi}_{\psi ym} \bar{\phi}'_{\psi xk} d\alpha \int_0^1 \bar{\phi}'_{\psi yn} \bar{\phi}_{\psi x\ell} d\beta \\
& +(b/a) \bar{D}_{16} \sum_{m=1}^M \sum_{n=1}^N \psi_{ymn} \int_0^1 \bar{\phi}'_{\psi ym} \bar{\phi}'_{\psi xk} d\alpha \int_0^1 \bar{\phi}_{\psi yn} \bar{\phi}_{\psi x\ell} d\beta \\
& +\bar{D}_{16} \sum_{m=1}^M \sum_{n=1}^N \psi_{xmn} \int_0^1 \bar{\phi}'_{\psi xm} \bar{\phi}_{\psi xk} d\alpha \int_0^1 \bar{\phi}_{\psi xn} \bar{\phi}'_{\psi x\ell} d\beta \\
& +\bar{D}_{16} \sum_{m=1}^M \sum_{n=1}^N \psi_{xmn} \int_0^1 \bar{\phi}_{\psi xm} \bar{\phi}'_{\psi xk} d\alpha \int_0^1 \bar{\phi}'_{\psi xn} \bar{\phi}_{\psi x\ell} d\beta
\end{aligned}$$

$$\begin{aligned}
& +(a/b)\bar{D}_{26} \sum_{m=1}^M \sum_{n=1}^N \psi_{ymn} \int_0^1 \bar{\phi}_{\psi ym} \bar{\phi}_{\psi xk} d\alpha \int_0^1 \bar{\phi}'_{\psi yn} \bar{\phi}'_{\psi x\ell} d\beta \\
& +\bar{D}_{66} \sum_{m=1}^M \sum_{n=1}^N \psi_{ymn} \int_0^1 \bar{\phi}'_{\psi ym} \bar{\phi}_{\psi x\ell} d\alpha \int_0^1 \bar{\phi}_{\psi yn} \bar{\phi}'_{\psi x\ell} d\beta \\
& +(a/b)\bar{D}_{66} \sum_{m=1}^M \sum_{n=1}^N \psi_{xmn} \int_0^1 \bar{\phi}_{\psi xm} \bar{\phi}_{\psi xk} d\alpha \int_0^1 \bar{\phi}'_{\psi xn} \bar{\phi}'_{\psi x\ell} d\beta \\
& +bK_{55}\bar{A}_{55} \sum_{m=1}^M \sum_{n=1}^N w_{mn} \int_0^1 \bar{\phi}'_{wm} \bar{\phi}_{\psi xk} d\alpha \int_0^1 \bar{\phi}_{wn} \bar{\phi}_{\psi x\ell} d\beta \\
& +ab K_{55}\bar{A}_{55} \sum_{m=1}^M \sum_{n=1}^N \psi_{xmn} \int_0^1 \bar{\phi}_{\psi xm} \bar{\phi}_{\psi xk} d\alpha \int_0^1 \bar{\phi}_{\psi xn} \bar{\phi}_{\psi x\ell} d\beta \\
& +a K_{45}\bar{A}_{45} \sum_{m=1}^M \sum_{n=1}^N w_{mn} \int_0^1 \bar{\phi}_{wm} \bar{\phi}_{\psi xk} d\alpha \int_0^1 \bar{\phi}'_{wn} \bar{\phi}_{\psi x\ell} d\beta \\
& +ab K_{45}\bar{A}_{45} \sum_{m=1}^M \sum_{n=1}^N \psi_{ymn} \int_0^1 \bar{\phi}_{\psi ym} \bar{\phi}_{\psi xk} d\alpha \int_0^1 \bar{\phi}_{\psi yn} \bar{\phi}_{\psi x\ell} d\beta \\
& -ab \omega^2 \sum_{m=1}^M \sum_{n=1}^N m_1 u_{mn} \int_0^1 \bar{\phi}_{um} \bar{\phi}_{\psi xk} d\alpha \int_0^1 \bar{\phi}_{un} \bar{\phi}_{\psi x\ell} d\beta \\
& -ab \omega^2 \sum_{m=1}^M \sum_{n=1}^N m_2 \psi_{xmn} \int_0^1 \bar{\phi}_{\psi xm} \bar{\phi}_{\psi xk} d\alpha \int_0^1 \bar{\phi}_{\psi xn} \bar{\phi}_{\psi x\ell} d\beta = 0 \quad (D-5)
\end{aligned}$$

There is an analogous expression for  $\partial\tilde{L}/\partial\psi_{y k \ell}=0$ , using the transformations (D-3), plus the following additional one:

$$45 \leftrightarrow 55 \quad (D-6)$$

## APPENDIX E

### DERIVATION OF THICKNESS-SHEAR FACTOR FOR THE THREE-LAYER, SYMMETRICALLY LAMINATED CASE USING THE DYNAMIC APPROACH

#### E1. Dynamic Elasticity Analysis of an Individual Layer Undergoing Pure Thickness-Shear Motion

For an individual layer undergoing pure thickness-shear motion in the  $xz$  plane, the only non-zero strain component is  $\epsilon_{xz}$ . Now it is assumed that the layer is orthotropic, so that the only non-zero stress component is  $\sigma_{xz}$ , given by equation (49). Then the general stress equations of motion for three-dimensional, dynamic elastic theory reduce to the following two equations:

$$\sigma_{xz,z} = \rho u_{,tt} \quad ; \quad \sigma_{xz,x} = \rho w_{,tt} \quad (E-1)$$

The longitudinal thickness-shear strain can be calculated from the displacements  $(u,w)$  in the  $x,z$  directions, respectively, as follows:

$$\epsilon_{xz} = u_{,z} + w_{,x} \quad (E-2)$$

The following displacement equations of motion are obtained by substituting equations (49) and (E-2) into equations (E-1):

$$c_s^2(u_{,zz} + w_{,xz}) = u_{,tt} \quad ; \quad c_s^2(u_{,xz} + w_{,xx}) = w_{,tt} \quad (E-3)$$

where  $c_s$  is the shear wave-propagation velocity defined by:

$$c_s^2 = C_{55}/\rho \quad (E-4)$$

However, for pure longitudinal thickness-shear motion, the displacements are independent of axial position  $x$ . Thus, all derivatives of displacements with respect to  $x$  vanish and equations (E-3) reduce to the following single expression:

$$c_s^2 u_{,zz} = u_{,tt} \quad (E-5)$$

Equation (E-5) is the familiar, one-dimensional wave equation, which is solved easily by the separation-of-variables method, with the following solution for simple harmonic motion:

$$u(z,t) = (A \cos \Omega_s z + B \sin \Omega_s z)(C_1 \cos \omega t + C_2 \sin \omega t) \quad (E-6)$$

where  $\Omega_s \equiv \omega/c_s$ ,  $A$  and  $B$  are constants depending upon the boundary conditions, and  $C_1$  and  $C_2$  are constants which depend upon the initial conditions.

## E2. Dynamic Elasticity Analysis for Three-Layer, Symmetrically Laminated Case

Here we consider the special case of a three-layer, symmetrically laminated member, in which the two identical outer layers are designated by superscript 1 and the middle layer is denoted by superscript 2, as

shown in figure E-1. The proper boundary conditions for the anti-symmetric modes in pure thickness-shear motion are

$$\begin{aligned} u^{(1)}(z_2, t) &= u^{(2)}(z_2, t) ; u_{,z}^{(1)}(z_1, t) = 0 ; \\ u_{,z}^{(1)}(z_2, t) &= u_{,z}^{(2)}(z_2, t) ; u^{(2)}(0, t) = 0 \end{aligned} \quad (E-7)$$

where  $z_1$  and  $z_2$  are dimensions shown in figure E-1.

Substituting equation (E-6) into equations (E-7) yields the following set of expressions:

$$\begin{aligned} A_1 \cos \Omega_s^{(1)} z_2 + B_1 \sin \Omega_s^{(1)} z_2 &= A_1 \cos \Omega_s^{(2)} z_2 \\ + B_2 \sin \Omega_s^{(2)} z_2 ; -\Omega_s^{(1)} A_1 \sin \Omega_s^{(1)} z_2 + \Omega_s^{(1)} B_1 \cos \Omega_s^{(1)} z_2 &= \\ -\Omega_s^{(2)} A_2 \sin \Omega_s^{(2)} z_2 + \Omega_s^{(2)} B_2 \cos \Omega_s^{(2)} z_2 ; -\Omega_s^{(1)} A_1 \sin \Omega_s^{(1)} z_1 &= \\ + \Omega_s^{(1)} B_1 \cos \Omega_s^{(1)} z_1 = 0 ; A_2 = 0 \end{aligned} \quad (E-8)$$

or

$$\begin{bmatrix} \cos \Omega_s^{(1)} z_2 & \sin \Omega_s^{(1)} z_2 & -\sin \Omega_s^{(2)} z_2 \\ -\Omega_s^{(1)} \sin \Omega_s^{(1)} z_2 & \Omega_s^{(1)} \cos \Omega_s^{(1)} z_2 & -\Omega_s^{(2)} \cos \Omega_s^{(2)} z_2 \\ -\Omega_s^{(1)} \sin \Omega_s^{(1)} z_1 & \Omega_s^{(1)} \cos \Omega_s^{(1)} z_1 & 0 \end{bmatrix} \begin{Bmatrix} A_1 \\ B_1 \\ B_2 \end{Bmatrix} = \begin{Bmatrix} 0 \\ 0 \\ 0 \end{Bmatrix} \quad (E-9)$$

The homogeneous system of linear algebraic equations (E-9) has a nontrivial solution if, and only if, the determinant of its coefficient

matrix is equal to zero. The resulting determinantal equation has as its solutions the roots of the following transcendental equation:

$$\Omega_s^{(1)} \tan \Omega_s^{(2)} z_2 = - \Omega_s^{(2)} \cot (\Omega_s^{(1)} z_2 - \Omega_s^{(1)} z_1) \quad (E-10)$$

From the definitions of  $\Omega^{(k)}$  and  $c_s^{(k)}$ , we have

$$\Omega_s^{(1)} / \Omega_s^{(2)} = c_s^{(2)} / c_s^{(1)} = (C_{55}^{(2)} / C_{55}^{(1)})^{1/2} (\rho^{(1)} / \rho^{(2)})^{1/2} = (R/\beta)^{1/2} \quad (E-11)$$

where

$$\beta \equiv C_{55}^{(1)} / C_{55}^{(2)} \quad ; \quad R \equiv \rho^{(1)} / \rho^{(2)} \quad (E-12)$$

Then equation (E-10) can be expressed as follows:

$$(R/\beta)^{1/2} \tan [(\zeta_2 \Omega_s^{(1)} z_1 (\beta/R)^{1/2})] = \cot [(1-\zeta_2) \Omega_s^{(1)} z_1] \quad (E-13)$$

where

$$\zeta_2 \equiv z_2 / z_1 \quad (E-14)$$

### E3. Dynamic Analysis of a Symmetrically Laminated Timoshenko Beam Undergoing Pure Thickness-Shear Motion

Here we consider a symmetrically laminated Timoshenko beam<sup>\*</sup>. The

---

<sup>\*</sup>A beam exhibiting both thickness-shear flexibility and rotatory inertia is generally referred to as a Timoshenko beam (refs. 41,42).

axial and thickness (or depth) directions are designated as the  $x$  and  $z$  axes, respectively. Such a beam could be analyzed as a special case of the laminated plate theory presented in Section II by merely deleting all derivatives with respect to  $y$ . However, the beam case is so much simpler and pure thickness-shear motion is such a simple type of motion; therefore, it was decided to make an exact analysis for the present case.

The following kinematic relations hold throughout the entire thickness of the laminate:

$$\kappa_{xx} = \psi_{x,x} \quad ; \quad \epsilon_{xz} = w_{o,x} + \psi_x \quad (E-15)$$

The following stress-strain relations are applicable to a typical layer "k":

$$\sigma_{xx}^{(k)} = E_{11}^{(k)} \epsilon_{xx} = E_{11}^{(k)} \kappa_{xx} z \quad ; \quad \sigma_{xz}^{(k)} = C_{55}^{(k)} \epsilon_{xz} \quad (E-16)$$

The bending moment and shear force, expressed on the basis of a unit width as in plate theory (Section 2.3) are:

$$M_{xx} = \sum_{k=1}^n \int_{z_{k-1}}^{z_k} \sigma_{xx}^{(k)} z \, dz \quad ; \quad Q_x = \sum_{k=1}^n \int_{z_{k-1}}^{z_k} \sigma_{xz}^{(k)} \, dz \quad (E-17)$$

Substituting equations (E-15) and (E-16) into equation (E-17) and introducing the shear factor  $K_{55}$  as a correction factor to be determined later, one obtains:

$$M_{xx} = D_{11} \psi_{x,x} \quad ; \quad Q_x = K_{55} A_{55} (w_{o,x} + \psi_x) \quad (E-18)$$

where

$$\{D_{11}, A_{55}\} \equiv \sum_{k=1}^n \int_{z_{k-1}}^{z_k} \{E_{11}^{(k)} z^2, C_{55}^{(k)}\} dz \quad (E-19)$$

The equations of motion for a symmetrically laminated Timoshenko beam are identical in form to those governing a homogeneous Timoshenko beam (refs. 41,42), namely:

$$Q_{x,x} = m_o w_{o,tt} ; M_{xx,x} - Q_x = m_2 \psi_{x,tt} \quad (E-20)$$

where  $m_o$  and  $m_2$  are defined in equations (28).

Inserting equations (E-18) into equation (E-20), one obtains the following set of two coupled equations of motion in terms of the generalized displacements  $w_o$  and  $\psi_x$ :

$$K_{55} A_{55} (w_{o,xx} + \psi_{x,x}) = m_o w_{o,tt} \quad (E-21)$$

$$D_{11} \psi_{x,xx} - K_{55} A_{55} (w_{o,x} + \psi_x) = m_2 \psi_{x,tt} \quad (E-22)$$

For pure thickness-shear motion,  $w_o$  and  $\psi_x$  are independent of axial position  $x$ , so that equations (E-21) and (E-22) uncouple and become:

$$w_{o,tt} = 0 \quad (E-23)$$

$$m_2 \psi_{x,tt} + K_{55} A_{55} \psi_x = 0 \quad (E-24)$$

Since equation (E-23) does not contain  $K_{55}$  and since  $w_o$  is not



in equation (E-24), we have no further need for equation (E-23).

For steady-state harmonic motion, the solution of equation (E-24) can be expressed as follows:

$$\psi_x = \tilde{\psi}_x e^{i\omega t} \quad (E-25)$$

where  $\tilde{\psi}_x$  is a constant.

Substituting equation (E-25) into equation (E-24), we are led to the following relationship:

$$\omega^2 = K_{55} A_{55} / m_2 \quad (E-26)$$

This equation is applicable to any symmetrical laminate. For the special case of a three-layer one, using the notation depicted in figure 10 and the definitions of  $A_{55}$  and  $m_2$  from equations (E-19) and (28), one obtains:

$$\omega^2 = 3K_{55} z_1^{-2} (C_{55}^{(1)} / \rho^{(1)}) [(\zeta_2 / \beta) + 1 - \zeta_2] \quad (E-27)$$

$$\cdot [(\zeta_2^3 / R) + 1 - \zeta_2^3]^{-1}$$

where  $\beta, R$ , and  $\zeta_2$  are as defined previously.

#### E4. Determinations of the Thickness-Shear Factor

The longitudinal thickness-shear factor,  $K_{55}$ , is determined implicitly by equating  $\omega^2$  associated with the lowest non-trivial solution of equation (E-13) to that given by equation (E-27).

APPENDIX F

COMPLEX STIFFNESS COEFFICIENTS FOR A LAMINATE HAVING  
ALTERNATING PLIES OF TWO DIFFERENT COMPOSITE MATERIALS\*

F1. Introduction

The theory presented in Section II can be used to calculate the stiffness and damping coefficients for an arbitrary laminate, i.e. one consisting of any number of plies of any thickness, material, and orientation. However, in many cases of practical importance, laminates are designed to have many plies of two alternating materials. In such cases, the approximate approach used in refs. 29-31 is sufficiently accurate. Although this approach was originated for application to wave propagation in an infinite medium, it is applicable also to plates. In the latter configuration, it has been verified experimentally in several instances. By comparison with static experimental results, Rose and Tshirschnitz (reference 92) found that it gave good predictions of the in-plane elastic modulus and in-plane shear modulus. Also Achenbach and Zerbe (ref. 32) found that it gave a frequency versus wavelength relationship for longitudinal vibration of a laminated beam which was in excellent agreement with experimental results.

In all of the work mentioned above, all of the individual layers were isotropic. However, in many cases of increasing importance, at least one of the sets of layers may be made of composite materials. Some examples

\*After completion of this derivation, the work of Chou et al. (Reference 149) came to the attention of the authors. In their work, Chou et al. derived purely elastic equations which are analogous to the complex ones derived here.

are as follows:

1. Alternating layers of an isotropic material and an orthotropic material. Examples: armor plate consisting of alternating layers of a hard ceramic material (isotropic) and a lossy glass fiber-epoxy matrix composite (orthotropic); a laminate consisting of alternate layers of high-modulus orthotropic composite material (such as boron-epoxy or graphite-epoxy) and low-modulus, high-damping polymer (to increase the damping capacity of the laminate).

2. Alternating layers of two different orthotropic composite materials. Example: Boron-epoxy (for high stiffness) and glass-epoxy (for low cost). The lamination scheme may be either parallel ply (unidirectional) or cross ply.

3. Alternating layers of the same composite material and thickness, but oriented alternately at  $+\theta$  and  $-\theta$ , where  $0 < \theta < 90^\circ$ . This is the so-called angle-ply lamination arrangement, which is very popular in a variety of aerospace structures.

An original derivation is presented here which is applicable to determination of both the stiffness and damping of the above three classes of laminates. It may be considered to be a generalization of the work of refs. 29-31; necessarily the resulting equations reduce to theirs in the case when both materials are isotropic.

## F2. Analysis

The bases for the present analysis, as well as that of refs. 29-31, are the following hypotheses:

1. Strains in the plane of the laminations are equal.

2. Stresses in the direction normal to lamination planes are equal.

Hypothesis 1 leads to the Voigt upper-bound estimate (reference 93) of the equivalent macroscopic properties of a two-phase material having arbitrary geometrical configuration of individual constituents. Except for the presence of an additional Poisson's ratio effects term, this is known also as the "rule of mixtures". Hypothesis 2 leads to the corresponding Reuss lower-bound estimate (reference 94), which is almost identical with the so-called "inverse rule of mixtures".

Here we consider a medium consisting of repeating alternating layers denoted by "a" and "b", as shown in figure F-1. The plane of the laminations is designated as the xy plane and z is the normal to this plane. Then the two hypotheses mentioned above can be stated mathematically as follows in contracted notation:

$$\epsilon_j^{(a)} = \epsilon_j^{(b)} = \epsilon_j \quad (j=1,2,6) \quad (F-1)$$

$$\sigma_i^{(a)} = \sigma_i^{(b)} = \sigma_i \quad (i=3,4,5) \quad (F-2)$$

where the  $\epsilon_j$  are strain components, the  $\sigma_i$  are stress components, and superscripts (a) and (b) refer to layers "a" and "b". Subscripts 1 and 2 refer to normal strain (or normal stress) in the plane of the layers, 3 refers to thickness-normal effects, 4 and 5 refer to thickness shear, and 6 refers to in-plane shear. This notation is consistent with that most widely used in the field of composite-material mechanics (ref. 4) but differs from the mixed notation used in the body of this report.

As a consequence of the complex, orthotropic version of Hooke's law

and static equilibrium, equations (F-1) and (F-2) imply the following relations:

$$\sigma_j = H^{(a)} \sigma_j^{(a)} + H^{(b)} \sigma_j^{(b)} \quad (j=1,2,6) \quad (F-3)$$

$$\epsilon_i = H^{(a)} \epsilon_i^{(a)} + H^{(b)} \epsilon_i^{(b)} \quad (i=3,4,5) \quad (F-4)$$

where  $H^{(a)}$  and  $H^{(b)}$  are the thickness fractions of layers "a" and "b", respectively. Thus,

$$H^{(a)} + H^{(b)} = 1 \quad (F-5)$$

The complex, orthotropic version of Hooke's law, alluded to above, holds for each type of layer as follows:

$$\begin{Bmatrix} \sigma_1^{(k)} \\ \sigma_2^{(k)} \\ \sigma_3^{(k)} \\ \sigma_4^{(k)} \\ \sigma_5^{(k)} \\ \sigma_6^{(k)} \end{Bmatrix} = \begin{bmatrix} \bar{C}_{11}^{(k)} & \bar{C}_{12}^{(k)} & \bar{C}_{13}^{(k)} & 0 & 0 & \bar{C}_{16}^{(k)} \\ \bar{C}_{12}^{(k)} & \bar{C}_{22}^{(k)} & \bar{C}_{23}^{(k)} & 0 & 0 & \bar{C}_{26}^{(k)} \\ \bar{C}_{13}^{(k)} & \bar{C}_{23}^{(k)} & \bar{C}_{33}^{(k)} & 0 & 0 & \bar{C}_{36}^{(k)} \\ 0 & 0 & 0 & \bar{C}_{44}^{(k)} & \bar{C}_{45}^{(k)} & 0 \\ 0 & 0 & 0 & \bar{C}_{45}^{(k)} & \bar{C}_{55}^{(k)} & 0 \\ \bar{C}_{16}^{(k)} & \bar{C}_{26}^{(k)} & \bar{C}_{36}^{(k)} & 0 & 0 & \bar{C}_{66}^{(k)} \end{bmatrix} \begin{Bmatrix} \epsilon_1^{(k)} \\ \epsilon_2^{(k)} \\ \epsilon_3^{(k)} \\ \epsilon_4^{(k)} \\ \epsilon_5^{(k)} \\ \epsilon_6^{(k)} \end{Bmatrix} \quad (k=a,b) \quad (F-6)$$

where the  $\bar{C}_{ij}^{(k)}$  are the complex stiffness coefficients.

$$\begin{Bmatrix} \sigma_1 \\ \sigma_2 \\ \sigma_3 \\ \sigma_3 \end{Bmatrix} = \begin{bmatrix} \bar{c}'_{11} & \bar{c}'_{12} & \bar{c}'_{13} & \bar{c}'_{13} & \bar{c}'_{16} \\ \bar{c}'_{12} & \bar{c}'_{22} & \bar{c}'_{23} & \bar{c}'_{23} & \bar{c}'_{26} \\ \bar{c}^{(a)}_{13} & \bar{c}^{(a)}_{23} & \bar{c}^{(a)}_{33} & 0 & \bar{c}^{(a)}_{36} \\ \bar{c}^{(b)}_{13} & \bar{c}^{(b)}_{23} & 0 & \bar{c}^{(b)}_{33} & \bar{c}^{(b)}_{36} \end{bmatrix} \begin{Bmatrix} \epsilon_1 \\ \epsilon_2 \\ \epsilon_3^{(a)} \\ \epsilon_3^{(b)} \\ \epsilon_6 \end{Bmatrix} \quad (F-7)$$

where

$$\bar{c}'_{ij} = H^{(a)} \bar{c}^{(a)}_{ij} + H^{(b)} \bar{c}^{(b)}_{ij} ; \quad i, j = 11, 12, 16, 22, 26$$

$$\bar{c}'_{ij} = H^{(a)} \bar{c}^{(a)}_{ij} ; \quad i, j = 13, 23$$

$$\bar{c}'_{ij} = H^{(b)} \bar{c}^{(b)}_{ij} ; \quad i, j = 13, 23$$

Combining equations (F-4) and the last two of equations (F-7), we get the following relations:

$$\begin{aligned} \epsilon_3^{(a)} = & [C_{33}^{(b)} \epsilon_3 - H^{(b)} (\bar{c}^{(a)}_{13} - \bar{c}^{(b)}_{13}) \epsilon_1 - H^{(b)} (\bar{c}^{(a)}_{23} - \bar{c}^{(b)}_{23}) \epsilon_2 \\ & - H^{(b)} (\bar{c}^{(b)}_{36} - \bar{c}^{(a)}_{36}) \epsilon_6] [H^{(a)} \bar{c}^{(b)}_{33} + H^{(b)} \bar{c}^{(a)}_{33}]^{-1} \end{aligned} \quad (F-8)$$

$$\begin{aligned} \epsilon_3^{(b)} = & [\bar{c}^{(a)}_{33} \epsilon_3 - H^{(a)} (C_{13}^{(b)} - \bar{c}^{(a)}_{13}) \epsilon_1 - H^{(a)} (\bar{c}^{(b)}_{23} - \bar{c}^{(a)}_{23}) \epsilon_2 \\ & - H^{(a)} (\bar{c}^{(b)}_{36} - \bar{c}^{(a)}_{36}) \epsilon_6] [H^{(a)} \bar{c}^{(b)}_{33} + H^{(b)} \bar{c}^{(a)}_{33}]^{-1} \end{aligned} \quad (F-9)$$

Substituting equations (F-8) and (F-9) into the first of equations (F-7), one is led to the following result:

$$\sigma_1 = \bar{c}_{11} \epsilon_1 + \bar{c}_{12} \epsilon_2 + \bar{c}_{13} \epsilon_3 + \bar{c}_{16} \epsilon_6 \quad (F-10)$$

where

$$\bar{C}_{11} \equiv H^{(a)} \bar{C}_{11}^{(a)} + H^{(b)} \bar{C}_{11}^{(b)} - \bar{K}_c (\bar{C}_{13}^{(a)} - \bar{C}_{13}^{(b)})^2 \quad (F-11)$$

$$\bar{C}_{12} \equiv H^{(a)} \bar{C}_{12}^{(a)} + H^{(b)} \bar{C}_{12}^{(b)} - \bar{K}_c (\bar{C}_{13}^{(a)} - \bar{C}_{13}^{(b)}) (\bar{C}_{23}^{(a)} - \bar{C}_{23}^{(b)}) \quad (F-12)$$

$$\bar{C}_{13} \equiv [\bar{C}_{13}^{(a)} (H^{(a)} / \bar{C}_{33}^{(a)}) + \bar{C}_{13}^{(b)} (H^{(b)} / \bar{C}_{33}^{(b)})] \bar{L}_c \quad (F-13)$$

$$\bar{C}_{16} \equiv H^{(a)} \bar{C}_{16}^{(a)} + H^{(b)} \bar{C}_{16}^{(b)} - \bar{K}_c (\bar{C}_{13}^{(a)} - \bar{C}_{13}^{(b)}) (\bar{C}_{36}^{(a)} - \bar{C}_{36}^{(b)}) \quad (F-14)$$

$$\bar{K}_c \equiv [(\bar{C}_{33}^{(a)} / H^{(a)}) + (\bar{C}_{33}^{(b)} / H^{(b)})]^{-1} \quad (F-15)$$

$$\bar{L}_c \equiv [ (H^{(a)} / \bar{C}_{33}^{(a)}) + (H^{(b)} / \bar{C}_{33}^{(b)}) ]^{-1} \quad (F-16)$$

Analogous equations to equations (F-10) - (F-14) can be obtained readily by interchanging the roles of subscripts 1 and 2.

From the last two of equations (F-7), one gets:

$$\begin{aligned} 2\sigma_3 = & (\bar{C}_{13}^{(a)} + \bar{C}_{13}^{(b)}) \epsilon_1 + (\bar{C}_{23}^{(a)} + \bar{C}_{23}^{(b)}) \epsilon_2 + \bar{C}_{33}^{(a)} \epsilon_3^{(a)} + \bar{C}_{33}^{(b)} \epsilon_3^{(b)} \\ & + (\bar{C}_{36}^{(a)} + \bar{C}_{36}^{(b)}) \epsilon_6 \end{aligned} \quad (F-17)$$

Then substituting equations (F-8) and (F-9) into equation (F-17), one finds the following result:

$$\sigma_3 = \bar{C}_{13} \epsilon_1 + \bar{C}_{23} \epsilon_2 + \bar{C}_{33} \epsilon_3 + \bar{C}_{36} \epsilon_6 \quad (F-18)$$

where  $\bar{C}_{13}$  and  $\bar{C}_{23}$  are given by equation (F-13) and an analogous equation, and

$$\bar{C}_{33} = \bar{L}_c \quad (F-19)$$

$$\bar{c}_{36} = [\bar{c}_{36}^{(a)} (H^{(a)} / \bar{c}_{33}^{(a)}) + \bar{c}_{36}^{(b)} (H^{(b)} / \bar{c}_{33}^{(b)})] \bar{L}_c \quad (F-20)$$

Still another set of equations analogous to equations (F-10)-(F-14) can be obtained by interchanging the roles of subscripts 1 and 6.

As the first step toward determining expressions involving the composite coefficients with subscripts 44, 45, and 55, it is expedient to invert the pertinent equations in set (F-6), thus arriving at the following expressions:

$$\begin{Bmatrix} \epsilon_4^{(k)} \\ \epsilon_5^{(k)} \end{Bmatrix} = \begin{bmatrix} \bar{s}_{44}^{(k)} & \bar{s}_{45}^{(k)} \\ \bar{s}_{45}^{(k)} & \bar{s}_{55}^{(k)} \end{bmatrix} \begin{Bmatrix} \sigma_4 \\ \sigma_5 \end{Bmatrix} \quad (F-21)$$

where

$$\bar{s}_{44}^{(k)} \equiv \bar{c}_{55}^{(k)} / \bar{\Delta}^{(k)}, \quad \bar{s}_{45}^{(k)} \equiv - \bar{c}_{45}^{(k)} / \bar{\Delta}^{(k)}, \quad (F-22)$$

$$\bar{s}_{55}^{(k)} \equiv \bar{c}_{44}^{(k)} / \bar{\Delta}^{(k)}, \quad \bar{\Delta}^{(k)} \equiv \bar{c}_{44}^{(k)} \bar{c}_{55}^{(k)} - (\bar{c}_{45}^{(k)})^2$$

Inserting equations (F-21) into equations (F-4), we arrive at the following expressions:

$$\begin{Bmatrix} \epsilon_4 \\ \epsilon_5 \end{Bmatrix} = \begin{bmatrix} \bar{s}_{44} & \bar{s}_{45} \\ \bar{s}_{45} & \bar{s}_{55} \end{bmatrix} \begin{Bmatrix} \sigma_4 \\ \sigma_5 \end{Bmatrix} \quad (F-23)$$

where

$$\bar{s}_{44} = H^{(a)} \bar{s}_{44}^{(a)} + H^{(b)} \bar{s}_{44}^{(b)} \quad (F-24)$$



There are three expressions, analogous to equation (F-24), which are obtained by merely substituting subscripts 45 and 55, respectively, for subscript 44 in equation (F-24).

We now have derived expressions for all twenty of the laminate coefficients which appear in equation (F-23), above, and in the following expression:

$$\begin{Bmatrix} \sigma_1 \\ \sigma_2 \\ \sigma_3 \\ \sigma_6 \end{Bmatrix} = \begin{bmatrix} \bar{c}_{11} & \bar{c}_{12} & \bar{c}_{13} & \bar{c}_{16} \\ \bar{c}_{12} & \bar{c}_{22} & \bar{c}_{23} & \bar{c}_{26} \\ \bar{c}_{13} & \bar{c}_{23} & \bar{c}_{33} & \bar{c}_{36} \\ \bar{c}_{16} & \bar{c}_{26} & \bar{c}_{36} & \bar{c}_{66} \end{bmatrix} \begin{Bmatrix} \epsilon_1 \\ \epsilon_2 \\ \epsilon_3 \\ \epsilon_6 \end{Bmatrix} \quad (\text{F-25})$$

The effective density of the laminate is given by the following expression:

$$\rho = H^{(a)} \rho^{(a)} + H^{(b)} \rho^{(b)} \quad (\text{F-26})$$

## APPENDIX G

### IDENTIFICATION OF INTEGRAL FORMS

#### G1. Trigonometric Integrals

The integral forms for three boundary conditions are tabulated in the following form, where  $m, k, n, l = 1$  to  $2$ :

Integral Form	<u>Evaluation for Boundary Condition Listed</u>		
	Simply Supported	Clamped Edges	Free Edges
$I_{1mk} \equiv \int_0^1 \phi_{um} \phi_{uk} d\alpha$	$\frac{1}{2} ; m=k \neq 0$ $0 ; m \neq k$	$\frac{1}{2} ; m=k \neq 0$ $0 ; m \neq k$	$3/2 ; m=k \neq 0$ $1 ; m \neq k$
$I_{1nl} \equiv \int_0^1 \phi_{un} \phi_{ul} d\beta$	$\frac{1}{2} ; n=l \neq 0$ $0 ; n \neq l$	$\frac{1}{2} ; n=l \neq 0$ $0 ; n \neq l$	$3/2 ; n=l \neq 0$ $1 ; n \neq l$
$I_{2mk} \equiv \int_0^1 \phi_{vm} \phi_{vk} d\alpha$	$\frac{1}{2} ; m=k \neq 0$ $0 ; m \neq k$	$I_{1mk}$	$I_{1mk}$
$I_{2nl} \equiv \int_0^1 \phi_{vn} \phi_{vl} d\beta$	$\frac{1}{2} ; n=l \neq 0$ $0 ; n \neq l$	$I_{1nl}$	$I_{1nl}$
$I_{3mk} \equiv \int_0^1 \phi_{um} \phi_{vk} d\alpha$	$0$	$I_{1mk}$	$I_{1mk}$
$I_{3nl} \equiv \int_0^1 \phi_{un} \phi_{vl} d\beta$	$0$	$I_{1nl}$	$I_{1nl}$
$I_{4mk} \equiv \int_0^1 \phi_{um} \phi'_{uk} d\alpha$	$k\pi/2 ; m=k \neq 0$ $0 ; m \neq k$	$0 ; m=k \neq 0$ $0 ; m \neq k$	$0 ; m=k \neq 0$ $0 ; m \neq k$
$I_{4nl} \equiv \int_0^1 \phi_{un} \phi'_{vl} d\beta$	$n\pi/2 ; n=l \neq 0$ $0 ; n \neq l$	$0 ; n=l \neq 0$ $0 ; n \neq l$	$0 ; n=l \neq 0$ $0 ; n \neq l$

Integral Form	<u>Evaluation for Boundary Condition Listed</u>		
	Simply Supported	Clamped Edges	Free Edges
$I_{5mk} \equiv \int_0^1 \Phi_{vm} \Phi'_{uk} d\alpha$	$k\pi/2 ; m=k \neq 0$ $0 ; m \neq k$	$I_{4mk}$	$I_{4mk}$
$I_{5nl} \equiv \int_0^1 \Phi_{vn} \Phi'_{ul} d\beta$	$n\pi/2 ; n=l \neq 0$ $0 ; n \neq l$	$I_{4nl}$	$I_{4nl}$
$I_{6mk} \equiv \int_0^1 \Phi_{um} \Phi'_{uk} d\alpha$	0	$I_{4mk}$	$I_{4mk}$
$I_{6nl} \equiv \int_0^1 \Phi_{un} \Phi'_{ul} d\beta$	0	$I_{4nl}$	$I_{4nl}$
$I_{7mk} \equiv \int_0^1 \Phi_{vm} \Phi'_{vk} d\alpha$	0	$I_{4mk}$	$I_{4mk}$
$I_{7nl} \equiv \int_0^1 \Phi_{vn} \Phi'_{vl} d\beta$	0	$I_{4nl}$	$I_{4nl}$
$I_{8mk} \equiv \int_0^1 \Phi'_{um} \Phi'_{uk} d\alpha$	$mk\pi^2/2 ; m=k \neq 0$ $0 ; m \neq k$	$2mk\pi^2 ; m=k \neq 0$ $0 ; m \neq k$	$2mk\pi^2 ; m=k \neq 0$ $0 ; m \neq k$
$I_{8nl} \equiv \int_0^1 \Phi'_{un} \Phi'_{ul} d\beta$	$nl\pi^2/2 ; n=l \neq 0$ $0 ; n \neq l$	$2nl\pi^2 ; n=l \neq 0$ $0 ; n \neq l$	$2nl\pi^2 ; n=l \neq 0$ $0 ; n \neq l$
$I_{9mk} \equiv \int_0^1 \Phi'_{vm} \Phi'_{vk} d\alpha$	$mk\pi^2/2 ; m=k \neq 0$ $0 ; m \neq k$	$I_{8mk}$	$I_{8mk}$
$I_{9nl} \equiv \int_0^1 \Phi'_{vn} \Phi'_{vl} d\beta$	$nl\pi^2/2 ; n=l \neq 0$ $0 ; n \neq l$	$I_{8nl}$	$I_{8nl}$
$I_{10mk} \equiv \int_0^1 \Phi'_{um} \Phi'_{vk} d\alpha$	0	$I_{8mk}$	$I_{8mk}$
$I_{10nl} \equiv \int_0^1 \Phi'_{un} \Phi'_{vl} d\beta$	0	$I_{8nl}$	$I_{8nl}$
$I_{11mk} \equiv \int_0^1 \Phi'_{\psi xm} \Phi'_{wk} d\alpha$	0	See G2 for clamped case	0
$I_{11nl} \equiv \int_0^1 \Phi'_{\psi xn} \Phi'_{wl} d\beta$	$\frac{1}{2} ; n=l \neq 0$ $0 ; n \neq l$	See G2	0

Integral Form	Evaluation for Boundary Condition Listed		
	Simply Supported	Clamped Edges	Free Edges
$I_{12mk} = \int_0^1 \phi \psi_{ym} \phi_{wk} d\alpha$	$\frac{1}{2} ; m=k \neq 0$ $0 ; m \neq k$	$I_{11mk}$	$I_{11mk}$
$I_{12nl} = \int_0^1 \phi \psi_{yn} \phi_{wl} d\beta$	$0$	$I_{11nl}$	$I_{11nl}$
$I_{13mk} = \int_0^1 \phi \psi_{xm} \phi'_{wk} d\alpha$	$k\pi/2 ; m=k \neq 0$ $0 ; m \neq k$	See G2	$0$
$I_{13nl} = \int_0^1 \phi \psi_{xn} \phi'_{wl} d\beta$	$0$	See G2	$0$
$I_{14mk} = \int_0^1 \phi' \psi_{xm} \phi_{wk} d\alpha$	$k\pi/2 ; m=k \neq 0$ $0 ; m \neq k$	$I_{13mk}$	$I_{13mk}$
$I_{14nl} = \int_0^1 \phi' \psi_{xn} \phi_{wl} d\beta$	$0$	$I_{13nl}$	$I_{13nl}$
$I_{15mk} = \int_0^1 \phi \psi_{ym} \phi'_{wk} d\alpha$	$0$	$I_{13mk}$	$I_{13mk}$
$I_{15nl} = \int_0^1 \phi \psi_{yn} \phi'_{wl} d\beta$	$n\pi/2 ; n=l \neq 0$ $0 ; n \neq l$	$I_{13nl}$	$I_{13nl}$
$I_{16mk} = \int_0^1 \phi' \psi_{ym} \phi_{wk} d\alpha$	$0$	$I_{13mk}$	$I_{13mk}$
$I_{16nl} = \int_0^1 \phi' \psi_{yn} \phi_{wl} d\beta$	$n\pi/2 ; n=l \neq 0$ $0 ; n \neq l$	$I_{13nl}$	$I_{13nl}$
$I_{17mk} = \int_0^1 \phi \psi_{wm} \phi_{wk} d\alpha$	$\frac{1}{2} ; m=k \neq 0$ $0 ; m \neq k$	$1$	$\frac{1}{2} ; m=k \neq 0$ $0 ; m \neq k$
$I_{17nl} = \int_0^1 \phi \psi_{wn} \phi_{wl} d\beta$	$\frac{1}{2} ; n=l \neq 0$ $0 ; n \neq l$	$1$	$\frac{1}{2} ; n=l \neq 0$ $0 ; n \neq l$
$I_{18mk} = \int_0^1 \phi' \psi_{wm} \phi_{wk} d\alpha$	$0$	$0$	$0$
$I_{18nl} = \int_0^1 \phi' \psi_{wn} \phi_{wl} d\beta$	$0$	$0$	$0$

Integral Form	<u>Evaluation for Boundary Condition Listed</u>		
	Simply Supported	Clamped Edges	Free Edges
$I_{19mk} \equiv \int_0^1 \phi'_{wm} \phi_{wk} d\alpha$	0	$I_{18mk}$	$I_{18mk}$
$I_{19nl} \equiv \int_0^1 \phi'_{wn} \phi_{wl} d\beta$	0	$I_{18nl}$	$I_{18nl}$
$I_{20mk} \equiv \int_0^1 \phi'_{wm} \phi'_{wk} d\alpha$	$mk\pi^2/2 ; m=k \neq 0$ 0 ; $m \neq k$	$C_m Z_m (C_m Z_m - 2)$	$mk\pi^2/2 ; m=k \neq 0$ 0 ; $m \neq k$
$I_{20nl} \equiv \int_0^1 \phi'_{wn} \phi'_{wl} d\beta$	$nl\pi^2/2 ; n=l \neq 0$ 0 ; $n \neq l$	$C_n Z_n (C_n Z_n - 2)$	$nl\pi^2/2 ; n=l \neq 0$ 0 ; $n \neq l$
$I_{21mk} \equiv \int_0^1 \phi_{\psi xm} \phi_{\psi xk} d\alpha$	$\frac{1}{2} ; m=k \neq 0$ 0 ; $m \neq k$	$I_{1mk}$	$I_{1mk}$
$I_{21nl} \equiv \int_0^1 \phi_{\psi xn} \phi_{\psi xl} d\beta$	$\frac{1}{2} ; n=l \neq 0$ 0 ; $n \neq l$	$I_{1nl}$	$I_{1nl}$
$I_{22mk} \equiv \int_0^1 \phi_{\psi ym} \phi_{\psi yk} d\alpha$	$\frac{1}{2} ; m=k \neq 0$ 0 ; $m \neq k$	$I_{1mk}$	$I_{1mk}$
$I_{22nl} \equiv \int_0^1 \phi_{\psi yn} \phi_{\psi yl} d\beta$	$\frac{1}{2} ; n=l \neq 0$ 0 ; $n \neq l$	$I_{1nl}$	$I_{1nl}$
$I_{23mk} \equiv \int_0^1 \phi_{\psi xm} \phi_{\psi yk} d\alpha$	0	$I_{1mk}$	$I_{1mk}$
$I_{23nl} \equiv \int_0^1 \phi_{\psi xn} \phi_{\psi yl} d\beta$	0	$I_{1nl}$	$I_{1nl}$
$I_{24mk} \equiv \int_0^1 \phi_{\psi xm} \phi'_{\psi yk} d\alpha$	$k\pi/2 ; m=k \neq 0$ 0 ; $m \neq k$	$I_{4mk}$	$I_{4mk}$
$I_{24nl} \equiv \int_0^1 \phi_{\psi xn} \phi'_{\psi yl} d\beta$	$n\pi/2 ; n=l \neq 0$ 0 ; $n \neq l$	$I_{4nl}$	$I_{4nl}$
$I_{25mk} \equiv \int_0^1 \phi_{\psi ym} \phi'_{\psi xk} d\alpha$	$k\pi/2 ; m=k \neq 0$ 0 ; $m \neq k$	$I_{4mk}$	$I_{4mk}$
$I_{25nl} \equiv \int_0^1 \phi_{\psi yn} \phi'_{\psi xl} d\beta$	$n\pi/2 ; n=l \neq 0$ 0 ; $n \neq l$	$I_{4nl}$	$I_{4nl}$

Integral Form	<u>Evaluation for Boundary Condition Listed</u>		
	Simply Supported	Clamped Edges	Free Edges
$I_{26mk} \equiv \int_0^1 \Phi_{\psi xm} \Phi'_{\psi xk} d\alpha$	0	$I_{4mk}$	$I_{4mk}$
$I_{26nl} \equiv \int_0^1 \Phi_{\psi xn} \Phi'_{\psi xl} d\beta$	0	$I_{4nl}$	$I_{4nl}$
$I_{27mk} \equiv \int_0^1 \Phi_{\psi ym} \Phi'_{\psi yk} d\alpha$	0	$I_{4mk}$	$I_{4mk}$
$I_{27nl} \equiv \int_0^1 \Phi_{\psi yn} \Phi'_{\psi yl} d\beta$	0	$I_{4nl}$	$I_{4nl}$
$I_{28mk} \equiv \int_0^1 \Phi'_{\psi xm} \Phi'_{\psi xk} d\alpha$	$mk\pi^2/2; m=k \neq 0$ 0 ; $m \neq k$	$I_{8mk}$	$I_{8mk}$
$I_{28nl} \equiv \int_0^1 \Phi'_{\psi xn} \Phi'_{\psi xl} d\beta$	$nl\pi^2/2; n=l \neq 0$ 0 ; $n \neq l$	$I_{8nl}$	$I_{8nl}$
$I_{29mk} \equiv \int_0^1 \Phi'_{\psi ym} \Phi'_{\psi yk} d\alpha$	$mk\pi^2/2; m=k \neq 0$ 0 ; $m \neq k$	$I_{8mk}$	$I_{8mk}$
$I_{29nl} \equiv \int_0^1 \Phi'_{\psi yn} \Phi'_{\psi yl} d\beta$	$nl\pi^2/2; n=l \neq 0$ 0 ; $n \neq l$	$I_{8nl}$	$I_{8nl}$
$I_{30mk} \equiv \int_0^1 \Phi'_{\psi xm} \Phi'_{\psi yk} d\alpha$	0	$I_{8mk}$	$I_{8mk}$
$I_{30nl} \equiv \int_0^1 \Phi'_{\psi xn} \Phi'_{\psi yl} d\beta$	0	$I_{8nl}$	$I_{8nl}$
$I_{31mk} \equiv \int_0^1 \Phi_{\psi xm} \Phi_{uk} d\alpha$	$\frac{1}{2}; m=k \neq 0$ 0 ; $m \neq k$	$I_{1mk}$	$I_{1mk}$
$I_{31nl} \equiv \int_0^1 \Phi_{\psi xn} \Phi_{ul} d\beta$	$\frac{1}{2}; n=l \neq 0$ 0 ; $n \neq l$	$I_{1nl}$	$I_{1nl}$
$I_{32mk} \equiv \int_0^1 \Phi_{um} \Phi_{\psi xk} d\alpha$	$\frac{1}{2}; m=k \neq 0$ 0 ; $m \neq k$	$I_{1mk}$	$I_{1mk}$
$I_{32nl} \equiv \int_0^1 \Phi_{un} \Phi_{\psi xl} d\beta$	$\frac{1}{2}; n=l \neq 0$ 0 ; $n \neq l$	$I_{1nl}$	$I_{1nl}$

Integral Form	<u>Evaluation for Boundary Condition Listed</u>		
	Simply Supported	Clamped Edges	Free Edges
$I_{33mk} \equiv \int_0^1 \Phi'_{\psi xm} \Phi_{uk} d\alpha$	0	$I_{4mk}$	$I_{4mk}$
$I_{33nl} \equiv \int_0^1 \Phi'_{\psi xn} \Phi_{ul} d\beta$	0	$I_{4nl}$	$I_{4nl}$
$I_{34mk} \equiv \int_0^1 \Phi_{\psi xm} \Phi'_{uk} d\alpha$	0	$I_{4mk}$	$I_{4mk}$
$I_{34nl} \equiv \int_0^1 \Phi_{\psi xn} \Phi'_{ul} d\beta$	0	$I_{4nl}$	$I_{4nl}$
$I_{35mk} \equiv \int_0^1 \Phi_{\psi ym} \Phi_{uk} d\alpha$	0	$I_{1mk}$	$I_{1mk}$
$I_{35nl} \equiv \int_0^1 \Phi_{\psi yn} \Phi_{ul} d\beta$	0	$I_{1nl}$	$I_{1nl}$
$I_{36mk} \equiv \int_0^1 \Phi'_{\psi ym} \Phi_{uk} d\alpha$	$k\pi/2$ ; $m=k \neq 0$ 0 ; $m \neq k$	$I_{4mk}$	$I_{4mk}$
$I_{36nl} \equiv \int_0^1 \Phi'_{\psi yn} \Phi_{ul} d\beta$	$n\pi/2$ ; $n=l \neq 0$ 0 ; $n \neq l$	$I_{4nl}$	$I_{4nl}$
$I_{37mk} \equiv \int_0^1 \Phi_{\psi ym} \Phi'_{uk} d\alpha$	$k\pi/2$ ; $m=k \neq 0$ 0 ; $m \neq k$	$I_{4mk}$	$I_{4mk}$
$I_{37nl} \equiv \int_0^1 \Phi_{\psi yn} \Phi'_{ul} d\beta$	$n\pi/2$ ; $n=l \neq 0$ 0 ; $n \neq l$	$I_{4nl}$	$I_{4nl}$
$I_{38mk} \equiv \int_0^1 \Phi_{\psi xm} \Phi_{vk} d\alpha$	0	$I_{1mk}$	$I_{1mk}$
$I_{38nl} \equiv \int_0^1 \Phi_{\psi xn} \Phi_{vl} d\beta$	0	$I_{1nl}$	$I_{1nl}$
$I_{39mk} \equiv \int_0^1 \Phi'_{\psi xm} \Phi_{vk} d\alpha$	$k\pi/2$ ; $m=k \neq 0$ 0 ; $m \neq k$	$I_{4mk}$	$I_{4mk}$

Integral Form	Evaluation for Boundary Condition Listed		
	Simply Supported	Clamped Edges	Free Edges
$I_{39nl} \equiv \int_0^1 \phi'_{\psi xn} \phi'_{vl} d\beta$	$n\pi/2 ; n=l \neq 0$ $0 ; n \neq l$	$I_{4nl}$	$I_{4nl}$
$I_{40mk} \equiv \int_0^1 \phi_{\psi xm} \phi'_{vk} d\alpha$	$k\pi/2 ; m=k \neq 0$ $0 ; m \neq k$	$I_{4mk}$	$I_{4mk}$
$I_{40nl} \equiv \int_0^1 \phi_{\psi xn} \phi'_{vl} d\beta$	$n\pi/2 ; n=l \neq 0$ $0 ; n \neq l$	$I_{4nl}$	$I_{4nl}$
$I_{41mk} \equiv \int_0^1 \phi_{\psi ym} \phi'_{vk} d\alpha$	$\frac{1}{2} ; m=k \neq 0$ $0 ; m \neq k$	$I_{1mk}$	$I_{1mk}$
$I_{41nl} \equiv \int_0^1 \phi_{\psi yn} \phi'_{vl} d\beta$	$\frac{1}{2} ; n=l \neq 0$ $0 ; n \neq l$	$I_{1nl}$	$I_{1nl}$
$I_{42mk} \equiv \int_0^1 \phi'_{\psi ym} \phi'_{vk} d\alpha$	0	$I_{4mk}$	$I_{4mk}$
$I_{42nl} \equiv \int_0^1 \phi'_{\psi yn} \phi'_{vl} d\beta$	0	$I_{4nl}$	$I_{4nl}$
$I_{43mk} \equiv \int_0^1 \phi_{\psi ym} \phi'_{vk} d\alpha$	0	$I_{4mk}$	$I_{4mk}$
$I_{43nl} \equiv \int_0^1 \phi_{\psi yn} \phi'_{vl} d\beta$	0	$I_{4nl}$	$I_{4nl}$
$I_{44mk} \equiv \int_0^1 \phi'_{\psi xm} \phi'_{uk} d\alpha$	$mk\pi^2/2 ; m=k \neq 0$ $0 ; m \neq k$	$I_{8mk}$	$I_{8mk}$
$I_{44nl} \equiv \int_0^1 \phi'_{\psi xn} \phi'_{ul} d\beta$	$nl\pi^2/2 ; n=l \neq 0$ $0 ; n \neq l$	$I_{8nl}$	$I_{8nl}$
$I_{55mk} \equiv \int_0^1 \phi'_{\psi ym} \phi'_{uk} d\alpha$	0	$I_{8mk}$	$I_{8mk}$
$I_{55nl} \equiv \int_0^1 \phi'_{\psi yn} \phi'_{ul} d\beta$	0	$I_{8nl}$	$I_{8nl}$
$I_{56mk} \equiv \int_0^1 \phi'_{\psi xm} \phi'_{vk} d\alpha$	0	$I_{8mk}$	$I_{8mk}$



Integral Form	<u>Evaluation for Boundary Condition Listed</u>		
	Simply Supported	Clamped Edges	Free Edges
$I_{56nl} \equiv \int_0^1 \Phi'_{\psi xn} \Phi'_{v\ell} d\beta$	0	$I_{8nl}$	$I_{8nl}$
$I_{57mk} \equiv \int_0^1 \Phi'_{\psi ym} \Phi'_{vk} d\alpha$	$mk\pi^2/2 ; m=k \neq 0$ 0 ; $m \neq k$	$I_{8mk}$	$I_{8mk}$
$I_{57nl} \equiv \int_0^1 \Phi'_{\psi yn} \Phi'_{v\ell} d\beta$	$n\ell\pi^2/2 ; n=\ell \neq 0$ 0 ; $n \neq \ell$	$I_{8nl}$	$I_{8nl}$

## G2. Combination Trigonometric-Beam Type Integrals

These integrals are related to  $I_{11mk}$ ,  $I_{11nl}$ ,  $I_{13mk}$ , and  $I_{13nl}$  for clamped and free edges of the plate mentioned in Appendix G1. Therefore, these integrals were evaluated and are listed below:

### All Edges Clamped.

$$\begin{aligned}
 I_{11mk} &\equiv \int_0^1 \Phi_{\psi xm} \Phi_{wk} d\alpha \\
 &= \frac{1}{(Z_k)^2 + (2m\pi)^2} \left\{ Z_k \sinh Z_k \sin 2m\pi - 2m\pi \cosh Z_k \cos 2m\pi + 2m\pi \right\} \\
 &\quad + \left\{ \frac{\cos[2m\pi + Z_k] - 1}{2[2m\pi + Z_k]} + \frac{\cos[2m\pi - Z_k] - 1}{2[2m\pi - Z_k]} \right. \\
 &\quad \left. - \frac{C_k}{(Z_k)^2 + (2m\pi)^2} \left\{ Z_k \cosh Z_k \sin 2m\pi - 2m\pi \sinh Z_k \cos 2m\pi \right\} \right. \\
 &\quad \left. + C_k \left\{ \frac{\sin[2m\pi - Z_k]}{2[2m\pi - Z_k]} - \frac{\sin[2m\pi + Z_k]}{2[2m\pi + Z_k]} \right\} \right\}
 \end{aligned}$$

$I_{11nl}$  is analogous to  $I_{11mk}$  with the following substitutions:

$$m \leftrightarrow n, \quad k \leftrightarrow l, \quad \alpha \leftrightarrow \beta$$

$$\begin{aligned} I_{13mk} &\equiv \int_0^1 \phi_{\psi xm} \phi'_{wk} d\alpha = \frac{Z_k}{(Z_k)^2 + (2m\pi)^2} \left\{ Z_k \cosh Z_k \sin 2m\pi \right. \\ &\quad \left. - 2m\pi \sinh Z_k \cos 2m\pi \right\} + Z_k \left\{ \frac{\sin[2m\pi - Z_k]}{2[2m\pi - Z_k]} - \frac{\sin[2m\pi + Z_k]}{2[2m\pi + Z_k]} \right\} \\ &\quad - \frac{Z_k C_k}{(Z_k)^2 + (2m\pi)^2} \left\{ Z_k \sinh Z_k \sin 2m\pi - 2m\pi \cosh Z_k \cos 2m\pi + 2m\pi \right\} \\ &\quad - Z_k C_k \left\{ \frac{\cos[2m\pi + Z_k] - 1}{2[2m\pi + Z_k]} + \frac{\cos[2m\pi - Z_k] - 1}{2[2m\pi - Z_k]} \right\} \end{aligned}$$

$I_{13nl}$  is analogous to  $I_{13mk}$  with the following substitutions:

$$m \leftrightarrow n, \quad k \leftrightarrow l, \quad \alpha \leftrightarrow \beta$$

## APPENDIX H

### EVALUATION OF EXPERIMENTAL METHODS USED TO DETERMINE MATERIAL DAMPING IN COMPOSITE MATERIALS

#### H1. Specimens and Experimental Techniques

The following experimental techniques and specimen types have been used to determine material damping by experimental means (references 48, 79):

1. Decay of free vibration:
  - a. Torsional pendulum
  - b. Axially vibrating bar<sup>\*</sup> (reference 95)
  - c. Beam
    - (1) Free-free<sup>\*</sup> (reference 96)
    - (2) Cantilever<sup>\*</sup> (references 97, 98)
2. Resonant response:
  - a. Torsional<sup>\*</sup> (reference 99)
  - b. Axial
  - c. Beam
    - (1) Free-free<sup>\*</sup> (references 99, 100)
    - (2) Cantilever<sup>\*</sup> (references 101-104)

---

<sup>\*</sup> Apparently only these methods have been applied to measurement of damping in composite materials; each is discussed briefly in succeeding paragraphs.

- d. Cubic block
- e. Plate<sup>\*</sup> (reference 13)
- f. Shell<sup>\*</sup> (reference 105)
- 3. Rotating-beam deflection<sup>\*</sup> (reference 106)
- 4. Composite oscillator
- 5. Ultrasonic methods
- 6. Thermal methods

Pottinger (reference 95) measured the temporal decay of axial vibrations of bars (Type 1b, above) of glass fiber-epoxy and boron fiber-aluminum composites in the frequency range of 1 kHz to 100 kHz.

Among the earliest uses of free vibration to determine the logarithmic decrement of a composite material were the free-free beam experiments reported by Bert et al. (reference 96). The specimens were sandwich beams with glass-epoxy facings and hexagonal-cell honeycomb cores of either aluminum or glass-phenolic. Good correlation was obtained between the measured values of  $\delta$  and those predicted by an energy analysis of a Timoshenko beam, which includes thickness-shear flexibility and rotatory inertia. However, the complexity of the analysis prevents explicit determination of the  $\delta$ 's of the facings and core.

Later Schultz and Tsai (references 97, 98) used free flexural vibration of very thin cantilever beams to determine  $\delta$  for glass-epoxy in two configurations: (1) unidirectional with the fibers at an arbitrary orientation  $\theta$  with respect to the longitudinal axis of the beam, and (2) symmetrically laminated quasi-isotropic layups (layer orientations of  $0^\circ$ ,  $-60^\circ$ ,  $60^\circ$ ,  $-60^\circ$ ,  $0^\circ$  and of  $0^\circ$ ,  $90^\circ$ ,  $45^\circ$ ,  $-45^\circ$ ,  $-45^\circ$ ,  $45^\circ$ ,  $90^\circ$ ,  $0^\circ$ ). In the  $\theta \neq 0^\circ$ ,  $90^\circ$  case, the coupling between bending and twisting significantly invalidated the simple flexural theory used in the data reduction.

Adams et al. (reference 99) used torsional and flexural resonant response to determine the damping of glass fiber-epoxy and carbon fiber-epoxy. The magnetic-coil driver was located at the one end of the test bar to excite torsion, Type 2a, and at the center to excite flexure, Type 2c(1). Similar tests were conducted by Wells et al. (reference 100) on graphite-epoxy.

Cantilever beams, Type 2c(2), were used by Keer and Lazan (reference 101), Gustafson et al. (reference 102), Mazza et al. (reference 103), and Tauchert and Moon (reference 104). It is noted that Keer and Lazan used sandwich-type beams with glass reinforced plastic facings and core, and determined the resonant energy dissipated per cycle as the measure of damping, and found it to be proportional approximately to the square of the stress amplitude, i.e. Kimball-Lovell behavior (see Appendix B).

Clary (ref. 13) conducted resonant response tests on long free-edge plates (Type 2e) made of unidirectional boron fiber-epoxy. He used the modified Kennedy-Pancu method of data reduction, and studied the effect of fiber orientation. The analytical results of the present study are compared with his experimental results in Section 5.3.

Bert and Ray (reference 105) carried out resonant response measurements on a free-edge, circular, truncated conical shell (Type 2f) with an aluminum honeycomb core and glass fiber-epoxy facings. They used the original Kennedy-Pancu data reduction method.

Richter (reference 106) used the rotating-beam deflection technique (Type 3) to determine the damping characteristics of glass fiber-epoxy at low frequency (0.01 to 1.67 Hz).

It is apparent that the most popular techniques that have been used

in connection with measurement of composite-material damping are the free-vibration decay and resonant-response methods. Differences in results obtained by these two methods have been studied analytically by Parke (reference 73), using a standard linear solid, and by Heller and Nederveen (reference 107), using a generalized Maxwell model.

## H2. Excitation and Data-Reduction Techniques for Modal Resonant Response of Complicated Structures

The experimental and data-reduction techniques for determining damping from free-vibration decay are rather straight forward. In contrast, a great variety of techniques are in use for modal response at resonance, especially in regard to data reduction.

One approach is to use multiple shakers located at various locations on the structure and having controlled force amplitudes and phase relationships. This approach was originated by Lewis and Wrisley (reference 108) and has been used and extended by Fraeijs de Veubeke (reference 109), Asher (references 110,111), Traill-Nash et al (references 112,113), Hawkins et al (references 114,115), and de Vries (reference 116). The major disadvantage of this approach is the complexity and expense, in time and cost, of installing multiple shakers.

Another approach is to use a single excitation, even when the structure is complicated. In conjunction with this method, there are a variety of resonance-determination methods; these are discussed in the paragraphs which follow. Comparative critical evaluations of a number of these methods have been presented by Bishop and Gladwell (reference 117), Pendered and Bishop (reference 41), and Pendered (reference 118).

Peak-Amplitude Method. - In this simple, classical method, resonance is defined very simply to occur when the amplitude response reaches a peak. The major disadvantage of this method is that it is limited to lightly damped systems without closely spaced frequencies. The reason for this is that both of two closely-spaced-frequency modes may contribute to the amplitude at an intermediate frequency resulting in an indication of only one mode (a pseudo mode, of course). In an analytical study of a typical system with two natural frequencies, closely spaced, Turner (reference 119) showed that the peak-amplitude method results in a 130% error in determination of the resonant amplitude.

In general, there is no direct means of determining the modal damping, i.e. the magnitude of damping associated with various vibrational modes. However, it can be determined from the response at the anti-resonant frequencies, using the equations derived by Brann et al (reference 120). Also, for the special case of a base-excited system, the ratio of the tip-to-base amplitude to the base amplitude is related to the damping, as was shown in references 121,122.

Peak-Quadrature-Component Method. - This method was originated by Stahle and Forlifer (reference 123) in 1958. In this method, resonance is defined to occur when the quadrature component ( $90^\circ$  out of phase with the excitation) of the response peaks in either a positive or negative direction. Damping is determined from the in-phase-component peaks which occur at a frequency below resonance and another frequency above resonance. Applications of the method are discussed in references 124-126.

Quadrature-Response Method. - In this method, resonance is defined to occur when the in-phase component of the response vanishes. The errors associated with this method have been discussed by Pendered (ref. 118).

Kennedy-Pancu Method and Its Modifications. - This method was originated by Kennedy and Pancu (reference 87) in 1947. Its basis is the geometry of the theoretical Argand diagram for a single-degree-of-freedom damped system, which is a circle (see figure H-1). The data-reduction procedure is to fair a circle through an Argand diagram obtained from experimental data corresponding to a range of frequencies. The tacit assumptions inherent in the method are:

1. The system is a lightly damped, linear system.
2. In the vicinity of a particular resonance, the extraneous contributions from the off-resonant modes are either negligible or invariant with respect to frequency.
3. There is no damping between the normal modes, i.e. the inertia, damping and stiffness matrices are all diagonal.

Advantages of the method are:

1. It permits resonant frequencies, modal amplitudes, and modal damping values all to be determined from the Argand plot.
2. It has been demonstrated on a comparative basis that the KP (Kennedy-Pancu) has better capability in separating closely spaced resonant frequencies.

In the KP method, two ways to determine the resonant frequencies are possible. One way is to use the frequency associated with the point (on the faired-in circle) which is most distant from the real axis. The other way is to use the maximum frequency spacing technique, in which resonance is defined to occur when the rate of change of the arc length (of the Argand plot) with respect to frequency attains a local maximum.

In the original Kennedy-Pancu method, the damping ratio was determined from the half-power points, which are two ends of the diameter (of the



Argand circle) which is parallel to the real axis. See equation (B-56). Pendered and Bishop (reference 88) introduced an improved method, based upon the change in phase with respect to frequency, evaluated at resonance. See equation (B-69).

Gladwell (reference 127) proposed a method of determining the true response peaks and their associated damping ratios, using three points on the frequency-response curve. However, Pendered and Bishop (ref. 88) showed that variations of the two side-points caused changes of 135% in the damping coefficient of the system that they investigated.

Keller (reference 128), Smart (reference 129), and Pallett (reference 130), discussed improvements in instrumentation used in conjunction with the KP method. In his analytical investigation of a typical two-degree-of freedom system with closely spaced natural frequencies, Turner (ref. 119) indicated a 26% error in resonant amplitude determination, which is a considerable improvement over the 130% error for the peak-amplitude method. The modal-shape-determination aspects of the KP method were discussed in reference 131.

The KP method has been applied successfully to a great variety of vibrating systems, including:

1. Aircraft ground and flight testing (ref. 87)
2. Beam-type structures (ref. 88)
3. Two-degree-of-freedom system (ref. 120)
4. Liquid-propellant launch-vehicle axial vibration (refs. 132,133)
5. Unstiffened, stringer-stiffened, and ring-stiffened sandwich cylindrical shells( refs. 103,130,134,135).
6. Sandwich conical shell with composite-material facings (refs. 102-104)

## 7. Composite-material plates (ref. 13).

The last three categories listed above are particularly useful applications of the mode-separating capability of the KP method, since they often have numerous closely spaced natural frequencies. Pendered and Bishop (reference 136) used the KP method in connection with determination of the dynamic characteristics of a sub-system from resonance test results on a complete system consisting of two sub-systems.

Woodcock (reference 137) extended the KP method by providing for any arbitrary amount of damping of the classical viscous type and by making no assumptions about the form of the damping, stiffness, and inertia matrices. However, as pointed out by Nissim (reference 138), it is necessary that the inertia matrix be known a priori in order to determine experimentally the complete dynamic description of the system. (It is noted here that the inertia matrix could be determined experimentally, at the cost of additional tests, by the displaced-frequency method, reference 139). Nissim went on to present a set of data-reduction equations with which the disadvantages of ref. 138 are eliminated. It should be pointed out that apparently no actual applications of the methods of refs. 137 and 138 have been documented so far.

### H3. New Equations for Applying Two Different Versions of the Kennedy-Pancu Method to Two More Realistic Classes of Solids

From linear vibration theory, it is well known that the largest value of the damping ratio  $\zeta$  for which free vibrations can occur is  $\zeta = \zeta_{cr} = 1$ ; at higher values of  $\zeta$ , the motion is nonperiodic. For a standard linear solid, Zener (reference 140) showed that the critical loss tangent is  $53^\circ$ , which corresponds to approximately 1.183 for  $g_{cr}$ . (This compares with a

value of 2.00 for  $g_{cr}$  of a Kelvin-Voigt or Kimball-Lovell solid, since equation (B-65) is assumed to hold for such materials). Parks (ref. 73) showed the error resulting from the use of equation (B-75) for a standard linear solid.

As mentioned previously in the preceding section, in applying the Kennedy-Pancu method, it is tacitly assumed that the inertia, damping and stiffness matrices are all diagonal. Although this assumption may be satisfied in the case of a simple structure made of one material, it is certainly not justified in the case of a laminated composite-material structure. However, if the damping is sufficiently small that it does not affect the modal shapes (although, of course, it affects the modal amplitudes) and the intermodal damping coupling is negligible, then the KP method should still be sufficiently accurate to justify its use for engineering purposes.

It was mentioned in Section B3 that, in order for two half-power points to exist for a Kimball-Lovell material, the damping ratio  $\zeta$  must be less than  $\sqrt{2}/2$ . However, when the damping is greater than this value, one half-power point (denoted as  $\omega_2$ ) still exists. Thus, the method can be modified to accommodate this by using equation (B-55) rewritten as follows:

$$\zeta = (1/2)[(\omega_2/\omega_n)^2 - 1] \quad (H-1)$$

Just as the modification of the original KP method as described above, equation (H-1), permits its use regardless of the amount of damping, other appropriate equations can be derived to extend the use of the method to linear systems composed of materials represented by other damping models.

Here we present original equations for two cases: the standard linear solid (or first-degree hereditary mode 1) and the Biot model. Since these models contain two parameters rather than one as in the cases of viscous and Kimball-Lovell damping, more experimental data will be necessary, of course.

Standard Linear Solid (or First-Degree Hereditary Model). -

Volterra (ref. 83) presented an analysis of the sinusoidally forced vibration of a single-degree-of-freedom system exhibiting first-degree hereditary damping, which is equivalent to a standard linear solid. The equation of motion can be written in the present notation as follows:

$$m\ddot{u} + ku + h \int_0^t e^{-\alpha_1(t-\tau)} [du(\tau)/d\tau] d\tau = F_o \sin \omega t \quad (H-2)$$

or

$$m\ddot{u} + \alpha_1 m \dot{u} + (k+h)u = F_o (\omega \cos \omega t + \alpha_1 \sin \omega t) \quad (H-3)$$

The steady-state-response solution of equation (H-3) is of the form:

$$u = u_o \sin (\omega t - \varphi) \quad (H-4)$$

where

$$u_o \equiv (F_o/m) \left\{ [\alpha_1^2 \omega_n^2 - (\alpha_1^2 - H^2 - \omega_n^2) \omega^2 - \omega^4]^2 + [\alpha_1 H^2 \omega]^2 \right\}^{1/2} \\ \cdot \left\{ \alpha_1^2 (\omega_n^2 - \omega^2)^2 + \omega^2 (\omega^2 - \omega_n^2 - H^2)^2 \right\}^{-1} \quad (H-5)$$

$$\varphi = \arctan \left\{ \alpha_1 H^2 \omega [\alpha_1^2 \omega_n^2 - (\alpha_1^2 - H^2 - \omega_n^2) \omega^2 - \omega^4]^{-1} \right\} \quad (H-6)$$

$$H^2 \equiv h/m, \quad \omega_n^2 \equiv k/m.$$

Equation (H-5) can be written in dimensionless form as follows:

$$MF = \left\{ [\bar{\alpha}^2 - (\bar{\alpha}^2 - \bar{H}^2 - 1)\Omega^2 - \Omega^4]^2 + (\bar{\alpha} \bar{H}^2 \Omega)^2 \right\}^{1/2} \cdot \left\{ \bar{\alpha}^2 (1 - \Omega^2)^2 + \Omega^2 (\Omega^2 - 1 - \bar{H}^2)^2 \right\}^{-1} \quad (H-7)$$

where

$$\bar{\alpha} \equiv \alpha_1 / \omega_n, \quad \bar{H} \equiv H / \omega_n.$$

At resonance defined by  $\omega = \omega_n$  ( $\Omega=1$ ), the resonant magnification factor is:

$$RMF = [1 + (\bar{\alpha}\bar{H})^2]^{1/2} / \bar{H}^3 \quad (H-8)$$

At the half-power points

$$HPMF = RMF / \sqrt{2} \quad (H-9)$$

Combining equations (H-7, H-8, H-9), we obtain the following result:

$$\bar{K} [\bar{\alpha}^2 (1 - \Omega_{hp}^2)^2 + \Omega_{hp}^2 (\Omega_{hp}^2 - 1 - \bar{H}^2)^2]^2 = [\bar{\alpha}^2 - (\bar{\alpha}^2 - \bar{H}^2 - 1)\Omega_{hp}^2 - \Omega_{hp}^4]^2 + (\bar{\alpha}\bar{H}^2\Omega_{hp}^2)^2 \quad (H-10)$$

where

$$\bar{K} \equiv [1 + (\bar{\alpha}\bar{H})^2] (2\bar{H}^6)^{-1}$$

Unfortunately, equation (H-10) is quartic in  $\Omega_{hp}^2$  and thus is very unwieldy for practical use.

To develop equations for the Pendered improvement of the KP method for a standard linear solid, we differentiate equation (H-6) with respect to time, obtaining the following result:

$$d\phi/d\omega = \alpha^2 h^2 \omega \left\{ [\alpha^2 \omega_n^2 - (\alpha^2 - h^2 - \omega_n^2) \omega^2 - \omega^4]^2 + \alpha^2 b^4 \omega^2 \right\}^{-1} \quad (H-11)$$

At resonance defined by  $\omega = \omega_n$  and denoted by subscript R, we can simplify equation (H-11) as follows:

$$(d\phi/d\omega)_R = \left\{ [1 + (\omega_n/\alpha)^2] \omega_n \right\}^{-1}$$

or

$$\alpha = \omega_n \left\{ [\omega_n (d\phi/d\omega)_R]^{-1} - 1 \right\}^{-1/2} \quad (H-12)$$

It is interesting to note that at resonance, the parameter  $h$  drops out, so that  $\alpha$  can be determined directly from equation (H-12). To determine  $h$ , it is necessary to measure  $d\phi/d\omega$  at some other frequency (say  $\omega'$ ) and then use equation (H-11), with  $\alpha$  known from equation (H-12). The second frequency  $\omega'$  should not be too close to  $\omega_n$  to avoid inaccuracy. However, it should not be too far from  $\omega_n$  that the MF has dropped down to such a low value that signal-to-noise-ratio difficulties develop.

Biot Solid. - Caughey (ref. 60) presented an analysis of the sinusoidally forced vibration of a single-degree-of-freedom system with Biot damping. In the present notation, the equation of motion is:

$$m\ddot{u} + ku - g_1 k \int_0^t \text{Ei} [-\epsilon(t-\tau)] (du/d\tau) d\tau = \tilde{F} \sin \omega t \quad (\text{H-13})$$

where  $g_1$  and  $\epsilon$  are parameters of the model.

The steady-state-response solution of equation (H-13) is of the same form as equation (H-4), where here

$$\tilde{u} \equiv (\tilde{F}/k) \left\{ [1 + g_1 \ln \sqrt{1 + (\Omega/\mu)^2} - \Omega^2]^2 + [g_1 \arctan(\Omega/\mu)]^2 \right\}^{-1/2} \quad (\text{H-14})$$

$$\varphi \equiv \arctan (\pi/2) g_1 [1 + (g_1/2) \ln (1/\mu) - \Omega^2]^{-1} \quad (\text{H-15})$$

where

$$\Omega \equiv \omega/\omega_n, \mu \equiv \epsilon/\omega_n.$$

Equation (H-14) may be rewritten in terms of the magnification factor as follows:

$$\text{MF} = \left\{ [1 + g_1 \ln \sqrt{1 + (\Omega/\mu)^2} - \Omega^2]^2 + [g_1 \arctan (\Omega/\mu)]^2 \right\}^{-1/2} \quad (\text{H-16})$$

At resonance defined by  $\omega = \omega_n$  (i.e.  $\Omega = 1$ ), the resonant magnification factor is:

$$\boxed{\text{RMF} = g_1^{-1} [(\ln \sqrt{1 + \mu^{-2}})^2 + (\arctan \mu^{-1})^2]^{-1/2}} \quad (\text{H-17})$$

It is noted that the RMF defined in this way is not the peak MF, but it is very close to it in practical systems. Also, it is emphasized that the RMF is a function of both parameters,  $g$  and  $\mu$ . Thus, data from some other frequency is required. At the half-power points (subscript hp)

defined by  $\text{HPMF} = \text{RMF}/\sqrt{2}$ , the following relation must hold:

$$\boxed{[1 + g_1 \ln \sqrt{1 + (\Omega_{hp}/\mu)^2 - \Omega_{hp}^2}]^2 + [g_1 \arctan (\Omega_{hp}/\mu)]^2 = 2/(\text{RMF})^2} \quad (\text{H-18})$$

Using the necessary experimental data, equations (H-17) and (H-18) can be used to determine the Biot material parameters  $g$  and  $\mu$ .

To derive Pendered type KP relations, we take the derivative of equation (H-15) with respect to time, with the following result:

$$\boxed{d\varphi/d\omega = -(\pi g_1 \Omega/\omega_n) \left\{ [1 - \Omega^2 + (g_1/2) \ln \mu^{-1}]^2 + (\pi/2)^2 g_1^2 \right\}^{-1}} \quad (\text{H-19})$$

At resonance defined by  $\Omega = 1$  and denoted by subscript R, we can simplify equation (H-19) to the following result:

$$\boxed{(d\varphi/d\omega)_R = -(4/g_1 \omega_n) [1 + (\pi^{-1} \ln \mu^{-1})^2]^{-1}} \quad (\text{H-20})$$

Since equation (H-20) contains both parameters ( $g_1$  and  $\mu$ ), it is necessary to measure  $d\varphi/d\omega$  at some other frequency (say  $\Omega'$ ) and then use equations (H-19) and (H-20) to solve for the two parameters.



## APPENDIX I

### DISCUSSION ON SYMMETRY OF THE ARRAY OF CONSTITUTIVE COEFFICIENTS

In the analyses made in the body of this report, we have assumed that the arrays of both the elastic coefficients and the damping coefficients are symmetric, i.e.

$$Q_{lk} = Q_{kl}$$

$$\hat{Q}_{lk} = \hat{Q}_{kl}$$

In the present appendix, we discuss both classical and modern thinking, as well as experimental results which are pertinent to this topic of symmetry of the constitutive-coefficient arrays. In recent years, the validity of the symmetry hypothesis has been questioned for a wide variety of materials such as soil, geological formations, laminated wood, fabrics subjected to membrane loads, and certain composite materials (references 141-144).

#### 11. Elastic Coefficients

More than a century ago, there was considerable controversy regarding the symmetry of the stiffness matrix (or the compliance matrix) of a perfectly elastic material. About a century ago, the argument was supposedly resolved by the brilliant mathematical analysis due to George Green and

the experimental work of Woldemar Voigt; see reference 145. Although Green's analysis was purely mathematical, its importance to modern energy methods of static and dynamic stress analysis was recognized by Love (reference 146), who stated that symmetry of the elastic coefficient array is a necessary condition for the existence of the strain energy function. Voigt verified that symmetry did hold, within experimental accuracy, for the wide variety of single crystals which he investigated. Thus, this hypothesis became well established in anisotropic elasticity theory and it was tacitly assumed to hold for all materials.

Incidentally symmetry of the compliance matrix array requires that the following so-called reciprocal relationship must hold among four of the engineering elastic properties:

$$\nu_{lk}/E_l = \nu_{kl}/E_k \quad (k, l=1, 2, 3; \text{ no sum}) \quad (\text{I-1})$$

where the E's are Young's moduli and the  $\nu$ 's are Poisson's ratios.

Recently Alley and Faison (ref. 143) clearly demonstrated experimentally that equation (I-1) does not hold for fabrics subjected to biaxial loadings. They attributed this result to fiber friction, which is a nonconservative process. Table III lists some filamentary-composite-material test values for which eq. (I-1) does not hold. The viscosity of the epoxy matrix may have been the nonconservative process operative in the case of the glass-epoxy and boron-epoxy composites; see Section I2 of this Appendix. Also, the glass was in fabric form, so fabric friction could have played a part. Furthermore, in the case of the boron-epoxy composite, the minor Poisson's ratio is so very small that it is difficult to measure

with a high degree of confidence and experimental scatter effects become highly magnified. However, none of these explanations account for the case of graphite-graphite composite. It does not creep at the test temperature (room temperature); the fibers were filament wound, not in fabric form; and the minor Poisson's ratio is large enough to be measured accurately (especially since strain-gage transverse sensitivity was provided for in the data reduction). Thus, so far, there has not been a satisfactory explanation for this anomaly.

## 12. Viscoelastic Material

For viscoelastic materials which are homogeneous and anisotropic on a macroscopic basis, Rogers and Pipkin (ref. 141) claimed that there are no thermodynamic bases which require symmetry of the array of constitutive coefficients. Thus, they indicated that for such materials, symmetry can be established by experiment only. For composite materials having a viscoelastic (epoxy resin) matrix, some experimental data suggest that symmetry may not hold in the case of reinforcement by glass fibers and boron fibers (see table III). However, other experimental data on a viscoelastic composite (nylon-fiber-reinforced rubber) suggest that symmetry does hold.

In view of the lack of a definite proof regarding symmetry of a viscoelastic material, symmetry is assumed to hold in the present investigation (see hypothesis H6, Section 2.1).

## APPENDIX J

### COMPUTER PROGRAM DOCUMENTATION

The program described in this appendix was programmed to accomplish the following three computations:

1. Calculate the shear factor  $K$  for laminates, using Jourawski static shear theory.
2. Calculate the lowest eigenvalue for a simply supported laminated plate without damping.
3. Calculate the amplitude frequency response and modified Kennedy-Pancu frequency response and damping data for a free-edge anisotropic plate with material damping.

Computation 1 was accomplished by using an explicit algebraic expression. Computation 2 was performed by using IBM System/360 Scientific Subroutine Packages NROOT and EIGEN. Computation 3 was performed by Package SMIQ. A complete description of the variables, operations, etc. may be found in IBM Manual 360A-CM-03X, version III, for the subroutines NROOT, EIGEN and SMIQ.

The program was written in FORTRAN IV language as prescribed in IBM System Reference Library Form C-28-6274-3.

The input-data deck was set up as follows:

Computation 1 -

- (a) Thickness of each layer (lower and upper limit)
- (b) Elastic and shear moduli

Computation 2 -

- (a) Plate geometry
- (b) Lamination geometry (specially orthotropic)
- (c) Moduli and Poisson's ratio data for each ply
- (d) Density for each ply
- (e) Shear factor (as calculated in Computation 1)

Computation 3 -

- (a) Young's and shear moduli for each layer
- (b) Poisson's ratios for each layer
- (c) Bending and twisting stiffnesses for each layer
- (d) Loss tangents corresponding to moduli, Poisson's ratios, and stiffnesses for each layer
- (e) Plate geometry
- (f) Lamination geometry, including angle of orientation for each layer
- (g) Density of each layer
- (h) Shear factor (as calculated in Computation 1)
- (i) Mode numbers of the assumed modes.

A complete listing of the computer program is presented at the end of this report.

## REFERENCES

1. Engler, E.E.; and Cataldo, C.E.: Design and Test of Advanced Structural Components and Assemblies. NASA Space Shuttle Technology Conference, vol. II, NASA TM X-2273, Apr. 1971, pp. 527-583.
2. Ashton, J.E.; and Whitney, J.M.: Theory of Laminated Plates. Technomic Publishing Co., Inc., 1970.
3. Ojalvo, I.U.; and Arcas, N.: Approximate Analysis and Dynamic Tests for a Thermal Protection System Panel. NASA Space Shuttle Technology Conference, vol. III, NASA TM X-2274, Apr. 1971, pp. 49-93.
4. Ashton, J.E.; Halpin, J.C.; and Petit, P.H.: Primer on Composite Materials: Analysis. Technomic Publishing Co., Inc., 1969.
5. Tsai, S.W.: Structural Behavior of Composite Materials. NASA CR-71, July 1964.
6. Chambers, R.E.; and McGarry, F.J.: Shear Effects in Glass Fiber Reinforced Plastics Laminates. ASTM Bull., no. 238, May 1959, pp. 38-41.
7. Khischenko, Yu. M.: Effect of Shear on the Modulus of Elasticity of Specimens of Glas-Fiber Reinforced Plastics Tested in Transverse Bending. Indust. Lab., vol. 30, no. 6, June 1964, pp. 937-939.
8. Tarnopol'skii, Yu. .; Roze, A.V.; and Polyakov, V.A.: Shear Effects During Bending of Oriented Glass Reinforced Plastics. Polymer Mechanics,

vol. 1, no. 2, Mar.-Apr. 1965, pp. 31-37.

9. Yu., Y.-Y.: Simple Thickness-Shear Modes of Vibration of Infinite Sandwich Plates. J. Appl. Mech., vol. 26, no. 4, Dec. 1959, pp. 679-681.
10. Ross, D.; Ungar, E.E.; and Kerwin, E.M., Jr.: Damping of Plate Flexural Vibrations by Means of Viscoelastic Laminae. Structural Damping, J.E. Ruzicka, ed., Amer. Soc. Mech. Engrs., 1959, pp. 49-87.
11. Ruzicka, J.E.; Derby, T.F.; Schubert, D.W.; and Pepi, J.S.: Damping of Structural Composites with Viscoelastic Shear-Damping Mechanisms. NASA CR-742, Mar. 1967.
12. Derby, T.F.; and Ruzicka, J.E.: Loss Factor and Resonant Frequency of Viscoelastic Shear-Damped Structural Composites. NASA CR-1269, Feb. 1969.
13. Clary, R.R.: Vibration Characteristics of Unidirectional Filamentary Composite Material Panels. Composite Materials: Testing and Design (Second Conference), Amer. Soc. Testing & Matls., Spec. Tech. Publ. 497, 1972, pp. 415-438.
14. Pister, K.S.: Flexural Vibration of Thin Laminated Plates. J. Acoust. Soc. Amer., vol. 31, no. 2, Feb. 1959, pp. 233-234.
15. Stavsky, Y.: Thermoelastic Vibrations of Heterogeneous Membranes and Inextensional Plates. AIAA J., vol. 1, no. 3, Mar. 1963, pp. 722-723.

16. Ashton, J.E.: Analysis of Anisotropic Plates. J. Composite Matls., vol. 3, no. 1, Jan. 1969, pp. 148-165.
17. Hikami, Y.: Transverse Vibrations of Laminated Orthotropic Plates. Rept. No. 32, Div. of Solid Mech., Structures, & Mech. Design, Case Western Reserve Univ., Apr. 1969.
18. Ashton, J.E.: Natural Modes of Free-Free Anisotropic Plates. Shock & Vib. Bull., Bull. 39, Pt. 4, U.S. Dept. Defense, Apr. 1969, pp. 93-97.
19. Whitney, J.M.; and Leissa, A.W.: Analysis of Heterogeneous Anisotropic Plates. J. Appl. Mech., vol. 36, no. 2, June 1969, pp. 261-266.
20. Whitney, J.M.; and Leissa, A.W.: Analysis of a Simply Supported Laminated Anisotropic Rectangular Plate. AIAA J., vol. 8, no. 1, Jan. 1970, pp. 28-33.
21. Ashton, J.E.; and Anderson, J.D.: The Natural Modes of Vibration of Boron-Epoxy Plates. Shock & Vib. Bull., Bull. 39, Pt. 4, U.S. Dept. Defense, Apr. 1969, pp. 81-91.
22. Bert, C.W.; and Mayberry, B.L.: Free Vibrations of Unsymmetrically Laminated Anisotropic Plates with Clamped Edges. J. Composite Matls., vol. 3, no. 2, Apr. 1969, pp. 282-293.
23. Ambartsumyan, S.A.: Theory of Anisotropic Plates. Technomic Publishing Co., Inc., 1970.
24. Whitney, J.M.: The Effect of Transverse Shear Deformation on the Bending of Laminated Plates. J. Composite Matls., vol. 3, no. 3,



July 1969, pp. 534-547.

25. Yang, P.C.; Norris, C.H.; and Stavsky, Y.: Elastic Wave Propagation in Heterogeneous Plates. *Int. J. Solids & Struct.*, vol. 2, no. 4, Oct. 1966, pp. 665-684.
26. Mindlin, R.D.: Influence of Rotatory Inertia and Shear on Flexural Motions of Isotropic, Elastic Plates. *J. Appl. Mech.*, vol. 18, no. 1, Mar. 1951, pp. 31-38.
27. Biot, M.A.: Continuum Dynamics of Elastic Plates and Multilayered Solids Under Initial Stress. *J. Math. & Mech.*, vol. 12, no. 6, Nov. 1963, pp. 793-803.
28. Bolotin, V.V.: Vibration of Layered Elastic Plates. *Proc. Vib. Probs. (Pol. Acad. Sci.)*, vol. 4, no. 4, 1963, pp. 331-345.
29. Postma, G.W.: Wave Propagation in a Stratified Medium. *Geophysics*, vol. 20, no. 4, Oct. 1955, pp. 780-806.
30. White, J.E.; and Angona, F.A.: Elastic Wave Velocities in Laminated Media. *J. Acoust. Soc. Amer.*, vol. 27, no. 2, Mar. 1955, pp. 310-317.
31. Rytov, S.M.: Acoustical Properties of a Thinly Laminated Medium. *Sov. Phys.-Acoust.*, vol. 2, no. 1, Jan. 1956, pp. 68-80.
32. Achenbach, J.D.; and Zerbe, T.R.: Flexural Vibrations of Laminated Plate. *J. Eng. Mech. Div., Proc. ASCE*, vol. 97, no. EM3, June 1971, pp. 619-628.
33. Hsu, T.M.; and Wang, J.T.: A Theory of Laminated Cylindrical Shells Consisting of Layers of Orthotropic Laminae. *AIAA J.*, vol. 8, no. 12,

Dec. 1970, pp. 2141-2146.

34. Wang, J.T.-S.: Axisymmetric Deformation Theory of Orthotropic Layered Cylindrical Shells. Developments in Mechanics, vol. 6 (Proc. 12th. Midwestern Mech. Conf., Aug. 1971), Univ. of Notre Dame Press, 1971, pp. 787-800.
35. Srinivas, S.; Joga Rao, C.V.; and Rao, A.K.: An Exact Analysis for Vibration of Simply-Supported Homogeneous and Laminated Thick Rectangular Plates. J. Sound & Vib., vol. 12, no. 2, June 1970, pp. 187-200.
36. Srinivas, S.; Joga Rao, C.V.; and Rao, A.K.: Some Results from an Exact Analysis of Thick Laminates in Vibration and Buckling. J. Appl. Mech., vol. 37, no. 3, Sept. 1970, pp. 868-870.
37. Srinivas, S.; and Rao, A.K.: Bending, Vibration and Buckling of Simply Supported Thick Orthotropic Rectangular Plates and Laminates. Int. J. Solids & Structures, vol. 6, no. 11, Nov. 1970, pp. 1463-1481.
38. Tso, F.K.W.; Dong, S.B.; and Nelson, R.B.: Natural Vibrations of Rectangular Laminated Orthotropic Plates. Developments in Mechanics, vol. 6 (Proc. 12th. Midwestern Mech. Conf., Aug. 1971), Univ. of Notre Dame Press, 1971, pp. 891-905.
39. Dong, S.B.: Behavior of Laminated Orthotropic Viscoelastic Plates. J. Spacecraft & Rkts., vol. 4, no. 10, Oct. 1967, pp. 1385-1388.
40. Timoshenko, S.P.: History of Strength of Materials. McGraw-Hill

Book Co., Inc., 1953, p. 141.

41. Timoshenko, S.: On the Correction for Shear of the Differential Equation for Transverse Vibrations of Prismatic Bars. *Phil. Mag.*, ser. 6, vol. 41, 1921, pp. 744-746.
42. Timoshenko, S.: *Vibration Problems in Engineering*, 3rd. Ed. D. Van Nostrand Co., Inc., 1955, p. 329.
43. Reissner, E.: The Effect of Transverse-Shear Deformation on the Bending of Elastic Plates. *J. Appl. Mech.*, vol. 12, no. 1, Mar. 1945, pp. A69-A77.
44. Young, E.; and Felgar, R.P., Jr.: Tables of Characteristic Functions Representing Normal Modes of Vibration of a Beam. Bulletin No. 4913, Bureau of Engineering Research, University of Texas, Austin, Tex., July 1, 1949.
45. Wang, J.T.: On the Solution of Plates of Composite Materials. *J. Composite Matls.*, vol. 3, no. 3, July 1969, pp. 590-592.
46. Bert, C.W.; and Chang, S.: In-Plane, Flexural, Twisting and Thickness-Shear Coefficients for Stiffness and Damping of a Monolayer Filamentary Composite. Final Report (Part I) on NASA Research Grant NGR-37-003-055, School of Aerospace, Mechanical and Nuclear Engineering, University of Oklahoma, Norman, Okla., Mar. 1972.
47. Ganov, E.V.: Investigation of Bending Stresses in Shingle-Laminated Glass Reinforced Plastic. *Polymer Mech.*, vol. 1, no. 5, Sept.-Oct.

1965, pp. 101-102.

48. Lazan, B.J.: Damping of Materials and Members of Structural Mechanics. Pergamon Press, 1968.
49. Kimball, A.L.; and Lovell, D.E.: Internal Friction in Solids. Physical Rev., ser. 2, vol. 30, 1927, pp. 948-959.
50. Wegel, R.L.; and Walther, H.: Internal Dissipation in Solids for Small Cyclic Strains. Physics, vol. 6, 1935, pp. 141-157.
51. Lazan, B.J.: A Study with New Equipment of the Effects of Fatigue Stress on the Damping Capacity and Elasticity of Mild Steel. Trans. Am. Soc. Metals, vol. 42, 1950, pp. 499-549.
52. Bishop, R.E.D.: The Theory of Damping Forces in Vibration Theory. J. Roy. Aeron. Soc., vol. 59, no. 539, Nov. 1955, pp. 738-742.
53. Soroka, W.W.: Note on the Relations Between Viscous and Structural Damping Coefficients. J. Aeron. Sci., vol. 16, no. 7, Jul. 1949, pp. 409-410, 448.
54. Theodorsen, T.; and Garrick, I.E.: Mechanism of Flutter - a Theoretical and Experimental Investigation of the Flutter Problem. NACA TR 685, 1940.
55. Scanlan, R.H.; and Rosenbaum, R.: Introduction to the Study of Aircraft Vibration and Flutter. Macmillan, 1951; Dover, 1968.
56. Myklestad, N.O.: The Concept of Complex Damping. J. Appl. Mech., vol. 19, no. 3, Sep. 1952, pp. 284-286.

57. Lancaster, P.: Free Vibration and Hysteretic Damping. J. Roy. Aeron. Soc., vol. 64, no. 592, Apr. 1960, p. 229.
58. Reid, T.J.: Free Vibration and Hysteretic Damping. J. Roy. Aeron. Soc., vol. 60, no. 544, Apr. 1956, p. 283.
59. Milne, R.D.: A Constructive Theory of Linear Damping. Paper C.4, Symposium on Structural Dynamics, Loughborough Univ. of Technology, Loughborough, England, 1970.
60. Caughey, T.K.: Vibration of Dynamic Systems with Linear Hysteretic Damping (Linear Theory). Proc. 4th. U.S. Nat. Congr. Appl. Mech., vol. 1, 1962, pp. 87-97.
61. Paley, R.E.A.C.; and Wiener, N.: Fourier Transforms in the Complex Domain. Am. Math. Soc. Colloquium Publicat., vol. 19, 1934.
62. Garcia-Moliner, F.; and Thomson, R.: Linear Response Functions and the Phenomenological Equations of Internal Friction. J. Appl. Phys., vol. 37, no. 1, Jan. 1966, pp. 83-89.
63. Fraeijs de Veubeke, B.M.: Influence of Internal Damping on Aircraft Resonance. AGARD Manual on Elasticity, vol. 1, chap. 3, 1960.
64. Crandall, S.H.: Dynamic Response of Systems with Structural Damping. Air, Space, and Instruments (C.S. Draper Anniv. Vol.), S. Lees, ed. McGraw-Hill Book Co., 1963, pp. 183-193.
65. Crandall, S.H.: The Role of Damping in Vibration Theory. J. Sound & Vib., vol. 11, no. 1, Jan. 1970, pp. 3-18.

66. Pinsker, W.: Structural Damping. J. Aeron. Sci., vol. 16, no. 11,  
Nov. 1949, p. 699.
67. Scanlan, R.H.; and Mendelson, A.: Structural Damping. AIAA J., vol.  
1, no. 4, Apr. 1963, pp. 938-939.
68. Naylor, V.D.: Some Fallacies in Modern Damping. J. Sound & Vib.,  
vol. 11, no. 2, Feb. 1970, pp. 278-280.
69. Scanlan, R.H.: Linear Damping Models and Causality in Vibrations.  
J. Sound & Vib., vol. 13, no. 4, Dec. 1970, pp. 499-509.
70. Bishop, R.E.D.: The Behavior of Damped Linear Systems in Steady  
Oscillation. Aeron. Quart., vol. 7, no. 2, May 1956, pp. 156-168.
71. Cunningham, H.J.: In Defense of Modern Damping Theory in Flutter  
Analysis. J. Sound & Vib., vol. 14, no. 1, Jan. 1971, pp. 142-144.
72. Bland, D.R.: The Theory of Linear Viscoelasticity. Pergamon Press,  
1960, pp. 3-4.
73. Parke, S.: Logarithmic Decrements at High Damping. Brit. J. Appl.  
Phys., vol. 17, no. 2, Feb. 1966, pp. 271-273.
74. Flügge, W.: Viscoelasticity. Blaisdell Publishing Company, 1967,  
p. 14.
75. Hobbs, G.K.: Methods of Treating Damping in Structures. AIAA Paper  
71-349, presented at the AIAA/ASME 12th Structures, Structural  
Dynamics and Materials Conference, Anaheim, Calif., Apr. 19-21, 1971.

76. Huang, T.C.; and Huang, C.C.: Free Vibrations of Viscoelastic Timoshenko Beams. J. Appl. Mech., vol. 38, no. 2, June 1971, pp. 515-521.
77. Granick, N. and Stern, J.E.: Material Damping of Aluminum by a Resonance-Dwell Technique. NASA TN D-2893, Aug. 1965.
78. Granick, N.; and Stern, J.E.: Material Damping of Aluminum by Resonance-Dwell Technique. Shock & Vib. Bull., Bull. 34, Pt. 5, U.S. Dept. Defense, Feb. 1965, pp. 177-195.
79. Gustafson, A.J.; Mazza, L.T.; Rodgers, R.L.; and McIlwean, E.A.: Development of Test Methods for Measuring Damping of Fiber-Reinforced Materials. Rept. USAAVLABS TR 70-42, U.S. Army Aviation Materiel Laboratories, Ft. Eustis, Va., June 1970 (AD-873990).
80. Biot, M.A.: Linear Thermodynamics and the Mechanics of Solids. Proc. 3rd. U.S. Nat. Congr. Appl. Mech., 1958, pp. 1-18.
81. Neubert, H.K.P.: A Simple Model Representing Internal Damping in Solid Materials. Aeron. Quart., vol. 14, no. 2, May 1963, pp. 187-210.
82. Boltzmann, L.: Zur Theorie der elastische Nachwirkung. Annalen der Physik und Chemie, suppl. 7, 1876, pp. 624-654.
83. Volterra, E.: Vibrations of Elastic Systems Having Hereditary Characteristics. J. Appl. Mech., vol. 17, no.4, Dec. 1950, pp. 363-371.

84. Pisarenko, G.S.: Vibrations of Elastic Systems Taking Account of Energy Dissipation in the Material. Kiev, 1955; Engl. transl., WADD TR-60-582, Wright Air Development Div., Feb. 1962 (AD-274743).
85. Rosenblueth, E.; and Herrera, I.: On a Kind of Hysteretic Damping. J. Eng. Mech. Div., Proc. ASCE, vol. 90, no. EM4, Aug. 1964, pp. 37-48.
86. Chang, C.S.; and Bieber, R.E.: Synthesis of Structural Damping. AIAA J., vol. 6, no. 4, Apr. 1968, pp. 718-719.
87. Kennedy, C.C.; and Pancu, C.D.P.: Use of Vectors in Vibration Measurement and Analysis. J. Aeron. Sci., vol. 14, no. 11, Nov. 1947, pp. 603-625.
88. Pendered, J.W.; and Bishop, R.E.D.: A Critical Introduction to Some Industrial Resonance Testing Techniques. J. Mech. Eng. Sci., vol. 5, no. 4, Dec. 1963, pp. 345-367.
89. Kolsky, H.: Stress Waves in Solids. Oxford Univ. Press, 1953; Dover, 1963.
90. Bishop, R.E.D.: The General Theory of "Hysteretic Damping". Aeron. Quart., vol. 7, no. 1, Feb. 1956, pp. 60-70.
91. Meirovitch, L.: Analytical Methods in Vibrations. Macmillan, 1967, p. 40.
92. Rose, J.L.; and Tshirschnitz, R.: Static Material Constants for a Layered Composite Material. Paper No. 1845A, Spring Meeting,



Soc. for Exper. Stress Anal., Salt Lake City, Utah, May 18-21, 1971.

93. Voigt, W.: Lehrbuch der Kristallphysik. B.G. Teubner, Leipzig, Germany, 1928, pp. 738-741.
94. Reuss, A.: Berechnung der Fließsgrenze von Mischkristallen auf Grund der Plastizitätsbedingung für Einkristalle. Zeits. f. ang. Math. u. Mech., vol. 9, no. 1, Feb. 1929, pp. 48-58.
95. Pottinger, M.G.: Material Damping of Glass Fiber-Epoxy and Boron Fiber-Aluminum Composites. Rept. ARL 70-0237, Aerospace Research Laboratories, Wright-Patterson Air Force Base, Ohio, Oct. 1970 (AD-721191).
96. Bert, C.W.; Wilkins, D.J., Jr.; and Crisman, W.C.: Damping in Sandwich Beams with Shear-Flexible Cores. J. Eng. Industry, Trans. ASME, vol. 89B, no. 4, Nov. 1967, pp. 662-670.
97. Schultz, A.B.; and Tsai, S.W.: Dynamic Moduli and Damping Ratios in Fiber-Reinforced Composites. J. Composite Matls., vol. 2, no. 3, July 1968, pp. 368-379.
98. Schultz, A.B.; and Tsai, S.W.: Measurements of Complex Dynamic Moduli for Laminated Fiber-Reinforced Composites. J. Composite Matls., vol. 3, no. 3, July 1969, pp. 434-443.
99. Adams, R.D.; Fox, M.A.O.; Floord, R.J.L.; Friend, R.J.; and Hewitt, R.L.: The Dynamic Properties of Unidirectional Carbon and Glass Fiber Reinforced Plastics in Torsion and Flexure. J. Composite Matls., vol. 3, no. 4, Oct. 1969, pp. 594-603.
100. Wells, H.; Colclough, W.J.; and Goggin, P.R.: Some Mechanical Properties

of Carbon Fibre Composites. Proc. 24th. Ann. Tech. & Mgt. Conf.,  
Reinf. Plastics/Composites Div., Soc. Plastics Industry, Inc.,  
1969, sect. 2-C.

102. Gustafson, A.J.; Mazza, L.T.; Rodgers, R.L.; and McIlwean, E.H.:  
Development of Test Methods for Measuring Damping of Fiber-Re-  
inforced Materials. Rept. USAAVLABS TR 70-42, U.S. Army Aviation  
Materiel Laboratories, Ft. Eustis, Va., 1970 (AD-873990).
103. Mazza, L.T.; Paxson, E.B.; and Rodgers, R.L.: Measurement of  
Damping Coefficients and Dynamic Modulus of Fiber Composites. Rept.  
USAAVLABS-TN-2, U.S. Army Aviation Materiel Laboratories, Ft. Eustis,  
Va., 1971 (AD-869025).
104. Tauchert, T.R.; and Moon, F.C.: Propagation of Stress Waves in Fiber-  
Reinforced Composite Rods. AIAA J., vol. 9, no. 8, Aug. 1971, pp.  
1492-1498.
105. Bert, C.W.; and Ray, J.D.: Vibrations of Orthotropic Sandwich Conical  
Shells with Free Edges. Int. J. Mech. Sci., vol. 11, no. 9, Sept.  
1969, pp. 767-779.
106. Richter, H.P.H.: Photographic Method for Measuring Material Damp-  
ing and Dynamic Young's Modulus at Low Frequencies Applied to  
a Fiberglass Reinforced Resin Structure. Proc. 18th. Ann. Tech.  
& Mgt. Conf., Reinf. Plastics Div., Soc. Plastics Industry, Inc.,  
1963, sect. 4-D.

107. Heller, R.A.; and Nederveen, C.J.: Comparison of Complex Moduli Obtained from Forced and Free Damped Oscillations. Trans. Soc. Rheology, vol. 11, no. 1, 1967, pp. 113-123.
108. Lewis, A.C.; and Wrisley, D.L.: A System for the Excitation of Pure Modes of Complex Structures. J. Aeron. Sci., vol. 17, no. 11, Nov. 1950, pp. 705-722.
109. Fraeijs de Veubeke, B.M.: A Variational Approach to Pure Mode Excitation Based on Characteristic Phase Lag Theory. AGARD Rept. 39, Advisory Group for Aeron. Res. & Dev., North Atlantic Treaty Org., Apr. 1956.
110. Asher, G.W.: A Method of Normal Mode Excitation Utilizing Admittance Measurements. Proc. Nat. Specialists Meeting on Dynamics & Aeroelasticity, Ft. Worth, Tex., Nov. 6-7, 1958; Inst. of Aeron. Sci., 1959, pp. 69-76.
111. Asher, G.W.: A Note on the Effective Degrees of Freedom of a Vibrating Structure. AIAA J., vol. 5, no. 4, Apr. 1967, pp. 822-824.
112. Traill-Nash, R.W.: On the Excitation of Pure Natural Modes in Aircraft Resonance Testing. J. Aero/Space Sci., vol. 25, no. 12, Dec. 1958, pp. 775-778.
113. Traill-Nash, R.W.; Long, G.; and Bailey, C.M.: Experimental Determination of the Complete Dynamical Properties of a Two-Degree-of-Freedom Model Having Nearly Coincident Natural Frequencies. J. Mech. Eng. Sci., vol. 9, no. 5, Dec. 1967, pp. 402-413.
114. Hawkins, F.J.: An Automatic Shake Testing Technique for Exciting the Normal

Modes of Vibration of Complex Structures. AIAA Sympos. on Struct. Dynamics & Aeroelasticity, Boston, Mass., Aug. 30-Sept. 1, 1965, pp. 452-464.

115. Hawkins, F.J.; Skingle, C.W.; and Taylor, G.A.: A Multiple-Frequency, Shake-Testing Technique for Structures with Rapidly-Changing Dynamic Characteristics. Shock & Vib. Bull., Bull. 35, Pt. 2, U.S. Dept. Defense, Jan. 1966, pp. 107-116.
116. de Vries, G.: The Principles of Global Tests of a Structure. NASA TT F-10,003, Feb. 1966.
117. Bishop, R.E.D.; and Gladwell, G.M.L.: An Investigation into the Theory of Resonance Testing. Phil. Trans. Roy. Soc., London, ser. A, vol. 255, no. 1055, Jan. 17, 1963, pp. 241-280.
118. Pendered, J.W.: Theoretical Investigation into the Effects of Close Natural Frequencies in Resonance Testing. J. Mech. Eng. Sci., vol. 7, no. 4, Dec. 1965, pp. 372-379.
119. Turner, L.J., Jr.: An Analytical Investigation of a Vector Technique for Determining Normal Mode Amplitudes from Vibration Data. M.S. Thesis, Virginia Polytech. Inst., May 1968.
120. Brann, R.P., Devney, A.J.; and Robinson, C.D.: Harmonic Excitation of a Lightly Damped Multi-Degree System. Bull. Mech. Eng. Education, vol. 5, no. 2, 1966, pp. 95-111.
121. Rodden, W.P.; and Whittier, J.S.: Damping of Shaker-Excited Beams Calculated Solely from Displacement-Amplitude Measurements. J.

Acoust. Soc. Amer., vol. 34, no. 4, Apr. 1962, pp. 469-471.

122. Wambsganss, M.W., Jr.; Boers, B.L.; and Rosenberg, G.S.: Method for Identifying and Evaluating Linear Damping Models in Beam Vibrations. Shock & Vib. Bull., Bull. 36, Pt. 4, U.S. Dept. Defense, Jan. 1967, pp. 65-74.
123. Stahle, C.V.; and Forlifer, W.R.: Ground Vibration Testing of Complex Structures. Proc. AIA-AFOSR Flight Flutter Testing Sympos., May 1958.
124. Stahle, C.V.: A Phase Separation Technique for the Experimental Determination of Normal Vibration Modes of Flight Vehicles. Shock & Vib. Bull., Bull. 29, Pt. 4, U.S. Dept. Defense, 1961, pp. 30-42.
125. Stahle, C.V., Jr.: Phase Separation Technique for Ground Vibration Testing. Aerospace Eng., vol. 21, no. 7, July 1962, pp. 56-57, 91-96.
126. Hutton, F.E.: The Application of the Component Analyzer in Determining Modal Patterns, Modal Frequencies, and Damping Factors of Lightly Damped Structures. Shock & Vib. Bull., Bull. 33, Pt. 2, U.S. Dept. Defense, Feb. 1964, pp. 264-272.
127. Gladwell, G.M.L.: A Refined Estimate for the Damping Coefficient. J. Roy. Aeron. Soc., vol. 66, no. 614, Feb. 1962, pp. 124-125.
128. Keller, A.C.: Vector Component Techniques: A Modern Way to Measure Modes. Sound & Vib., vol. 3, no. 3, Mar. 1969, pp. 18-26.
129. Smart, T.E.: Dynamic Phase Plotting. Shock & Vib. Bull., Bull. 37, Pt. 2, U.S. Dept. Defense, Jan. 1968, pp. 77-85.

130. Pallett, D.S.: System for the Complex Plane Representation of Mechanical Vibration Response Parameters. Rept. TM 107.2811-06, Ord. Res. Lab., Penn. State Univ., State College, Pa., Mar. 13, 1969.
131. Pendered, J.W.; and Bishop, R.E.D.: The Determination of Modal Shapes in Resonance Testing. J. Mech. Eng. Sci., vol. 5, no. 4, Dec. 1965, pp. 379-385.
132. Schoenster, J.A.; and Clary, R.R.: Experimental Investigation of the Longitudinal Vibration of a Representative Launch Vehicle with Simulated Propellants. NASA TN D-4502, May 1968.
133. Clary, R.R.; and Turner, L.J., Jr.: Measured and Predicted Longitudinal Vibrations of a Liquid Propellant Two-Stage Launch Vehicle. NASA TN D-5943, Aug. 1970.
134. Bray, F.M.; and Egle, D.M.: An Experimental Investigation of the Vibration of Thin Cylindrical Shells with Discrete Longitudinal Stiffening. Jour. Sound & Vib., vol. 12, no. 2, June 1970, pp. 152-164.
135. Schoenster, J.A : Measured and Calculated Vibration Properties of Ring-Stiffened Honeycomb Cylinders. NASA TN D-6090, Jan. 1971.
136. Pendered, J.W.; and Bishop, R.E.D.: Extraction of Data for a Sub-System from Resonance Test Results. J. Mech. Eng. Sci., vol. 5, no. 4, Dec. 1965, pp. 368-378.
137. Woodcock, D.L.: On the Interpretation of the Vector Plots of Forced Vibrations of a Linear System with Viscous Damping. Aeron. Quart.,

vol. 14, no. 1, Feb. 1963, pp. 45-62.

138. Nissim, E.: On a Simplified Technique for the Determination of the Dynamic Properties of a Linear System with Damping. J. Roy. Aeron. Soc., vol. 71, no. 674, Feb. 1967, pp. 126-128.
139. de Vries, G.: Sondage des systemes vibrants par masses additionnelles. La Recherche Aeronautique, no. 30, Nov.-Dec. 1952, pp. 47-49.
140. Zener, C.: Mechanical Behavior of High Damping Metals. J. Appl. Phys., vol. 18, no. 11, Nov. 1947, pp. 1022-1025.
141. Rogers, T.G.; and Pipkin, A.C.: Asymmetric Relaxation or Compliance Matrices in Linear Viscoelasticity. Zeits. f. angew. Math. u. Physik, vol. 14, 1963, pp. 334-343.
142. Busching, H.W.: Mechanical Behavior of Transversely Anisotropic Materials. Proc. (First) Canadian Congr. Appl. Mech., Laval Univ., Quebec, Canada, May 22-26, 1967, vol. 1.
143. Alley, V.L., Jr.; and Faison, R.W.: Decelerator Fabric Constants Required by the Generalized Form of Hooke's Law. AIAA Paper 70-1179, presented at the AIAA 3rd. Aerodynamic Deceleration Systems Conference, Wright-Patterson Air Force Base, Ohio, Sept. 14-16, 1970.
144. Bert, C.W.; and Guess, T.R.: Mechanical Behavior of Carbon-Carbon Filamentary Composites. Composite Materials: Testing and Design (Second Conference); Amer. Soc. Testing & Matls. Spec. Tech.

Publ. 497, 1972, pp. 89-106.

145. Todhunter, I.; and Pearson, K.: A History of the Theory of Elasticity and of the Strength of Materials. Dover Publications, Inc., New York, 1960.
146. Love, A.E.H.: A Treatise on the Mathematical Theory of Elasticity, 4th. Ed. Dover Publications, Inc., New York, 1944, chap. III.
147. Bert, C.W.; Mayberry, B.L.; and Ray, J.D.: Behavior of Fiber-Reinforced Plastic Laminates Under Biaxial Loading. Composite Materials: Testing and Design, Amer. Soc. Testing & Matls., Spec. Tech. Publ. 460, 1969, pp. 362-380.
148. Hadcock, R.N.: Boron-Epoxy Aircraft Structures. Handbook of Fiber-glass and Advanced Plastics Composites, ed. by G. Lubin, Van Nostrand Reinhold, 1969, pp. 628-660.
149. Chou, P.C., Carleone, J., and Hsu, C.M.: Elastic Constants of Layered Media. J. Composite Matls., vol. 6, no. 1, Jan. 1972, pp. 80-93.



TABLE I. SHEAR FACTOR FOR LAMINATES WITH MULTIPLE ALTERNATING

LAYERS OF TWO MATERIALS

Modulus ratio, $E_{11}^{(1)} / E_{11}^{(2)} = C_{55}^{(1)} / C_{55}^{(2)}$	Number of Layers, n							
	2	3	4	5	6	7	8	9
1	0.833	0.833	0.833	0.833	0.833	0.833	0.833	0.833
10	0.173	0.190	0.203	0.201	0.195	0.193	0.188	0.186
20	0.091	0.087	0.087	0.082	0.072	0.069	0.063	0.062
30	0.062	0.056	0.050	0.047	0.037	0.036	0.032	0.031
40	0.047	0.041	0.033	0.031	0.023	0.022	0.019	0.018
50	0.038	0.032	0.022	0.016	0.015	0.011	0.013	0.012
60	0.032	0.027	0.017	0.016	0.011	0.011	0.009	0.009
70	0.027	0.023	0.014	0.013	0.009	0.008	0.007	0.006
80	0.024	0.020	0.011	0.010	0.008	0.007	0.005	0.005
90	0.021	0.018	0.009	0.008	0.005	0.005	0.004	0.004
100	0.020	0.016	0.007	0.007	0.004	0.004	0.003	0.003

Table II. FREQUENCIES AND DAMPING FOR A LAMINATED COMPOSITE-MATERIAL PLATES

Angle, deg.	Mode No.	Reference 13			Present Results		
		Exp. freq., Hz.	Anal. freq., Hz.	Exp. damping ratio, %	Peak-ampl. freq., Hz.	Kennedy- Pancu freq., Hz.	Calc. damping ratio, %
0	1	141.8	138.2	0.1	138.9	140.0	0.22
	2	182.2	164.0	1.9	170.0	170.4	1.83
	3	386.2	365.4	0.9	359.4	360.1	0.97
	4	401.1	381.1	0.2	389.7	390.2	0.24
	5	649.5	639.4	1.4	639.0	639.6	0.95
10	1	100.6	93.4	0.6	93.0	92.0	1.19
	2	234.0	226.9	3.4	226.1	225.2	1.28
	3	275.2	257.9	0.9	264.0	265.5	1.06
	4	485.3	497.5	1.6	495.2	495.0	0.09
	5	523.4	512.8	0.9	512.3	511.0	0.66
30	1	57.2	56.1	1.0	57.7	58.7	1.37
	2	163.4	164.2	1.0	166.1	165.0	0.82
	3	314.9	325.9	1.1	320.0	320.0	1.03
	4	378.4	385.9	1.6	388.0	387.2	1.64
	5	534.2	572.1	1.4	564.3	565.0	0.97

TABLE II. CONTINUED

Angle, deg.	Mode No.	Reference 13			Present Results		
		Exp. freq., Hz.	Anal. freq., Hz.	Exp. damping ratio, %	Peak-ampl. freq., Hz.	Kennedy- Pancu freq., Hz.	Calc. damping ratio, %
45	1	46.2	42.4	0.9	45.2	45.1	0.98
	2	131.4	122.0	1.2	124.0	124.0	1.25
	3	257.6	250.0	1.1	249.6	251.0	0.95
	4	278.4	291.5	2.2	293.0	293.4	1.59
	5	433.3	432.0	1.5	429.9	430.0	1.18
60	1	44.1	42.4	0.9	43.0	42.3	1.00
	2	127.0	119.0	1.5	121.5	122.0	1.60
	3	260.8	226.3	3.9	228.0	228.1	2.05
	4	239.9	239.3	1.1	237.0	237.6	1.06
	5	405.1	404.0	1.5	402.3	401.5	1.17
90	1	48.0	49.3	0.8	48.1	48.0	0.87
	2	137.6	136.0	1.2	136.0	136.1	1.23
	3	188.9	161.6	5.3	165.6	164.4	3.31
	4	250.6	267.1	1.0	259.8	259.0	1.10
	5	331.7	331.7	2.1	332.3	331.0	1.98

TABLE III. EXPERIMENTAL EXAMPLES OF COMPOSITE MATERIALS WHICH APPEAR TO HAVE UNSYMMETRIC

## CONSTITUTIVE-COEFFICIENT ARRAYS

Composite	$E_{11}$ ( $\text{psix}10^{-6}$ )	$E_{22}$ ( $\text{psix}10^{-6}$ )	$\nu_{12}$	$\nu_{21}$	$\nu_{12}/E_{11}$	$\nu_{21}/E_{22}$	$100 \times \frac{(\nu_{12}/E_{11}) - (\nu_{21}K_{22})}{(\nu_{12}/E_{11}) + (\nu_{21}/E_{22})}$
Glass cloth-epoxy (ref. 147)	3.30	3.15	0.141	0.188	0.0427	0.0597	16.6
Boron-epoxy (ref. 148)	30.6	3.5	0.36	0.033	0.01177	0.00944	-11.0
Graphite-graphite (ref. 144)							
$\pm 60^\circ$ wrap	2.98	2.47	0.21	0.18	0.070	0.073	- 2.1
$\pm 70^\circ$ wrap	3.44	2.28	0.16	0.15	0.046	0.066	-17.8
$\pm 85^\circ$ wrap	4.10	1.83	0.11	0.13	0.027	0.071	-43.1
$90^\circ$ wrap	4.30	1.35	0.09	0.20	0.021	0.148	-75.0

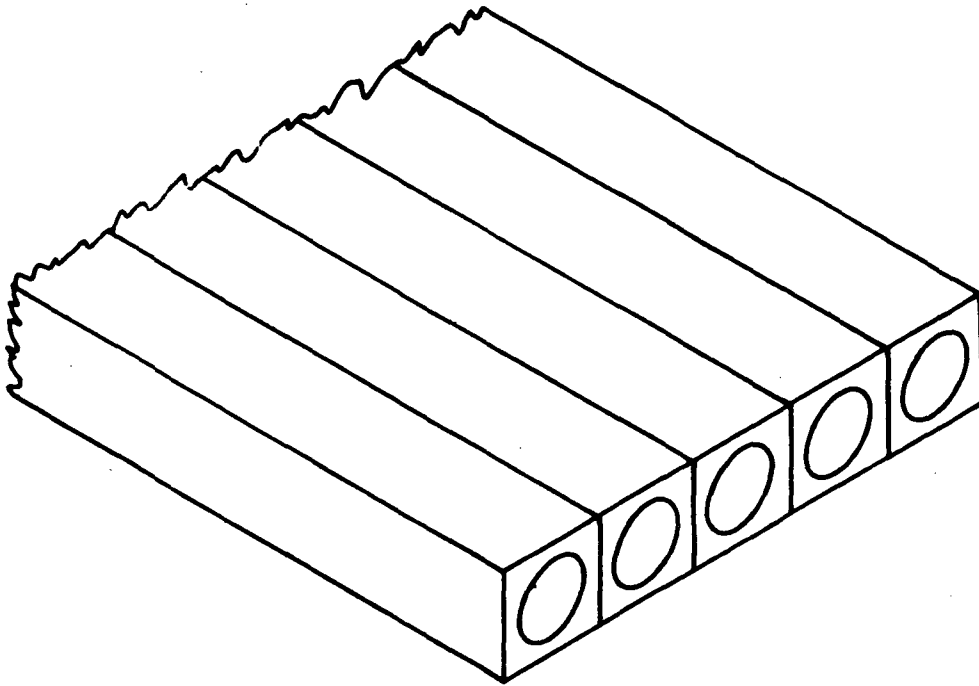
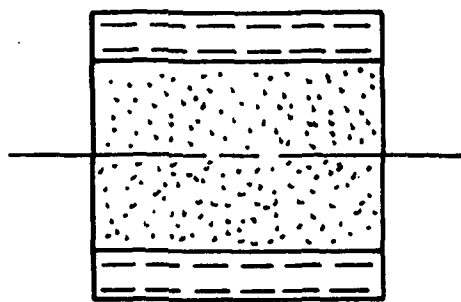
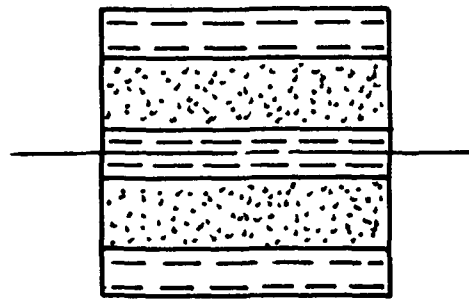


Figure 1. Composite containing unidirectional fibers.



**THICK MIDDLE PLY WITH  
IDENTICAL OUTER PLIES**



**ODD NUMBER OF  
ALTERNATING PLIES**

Figure 2. Examples of symmetrical laminates.

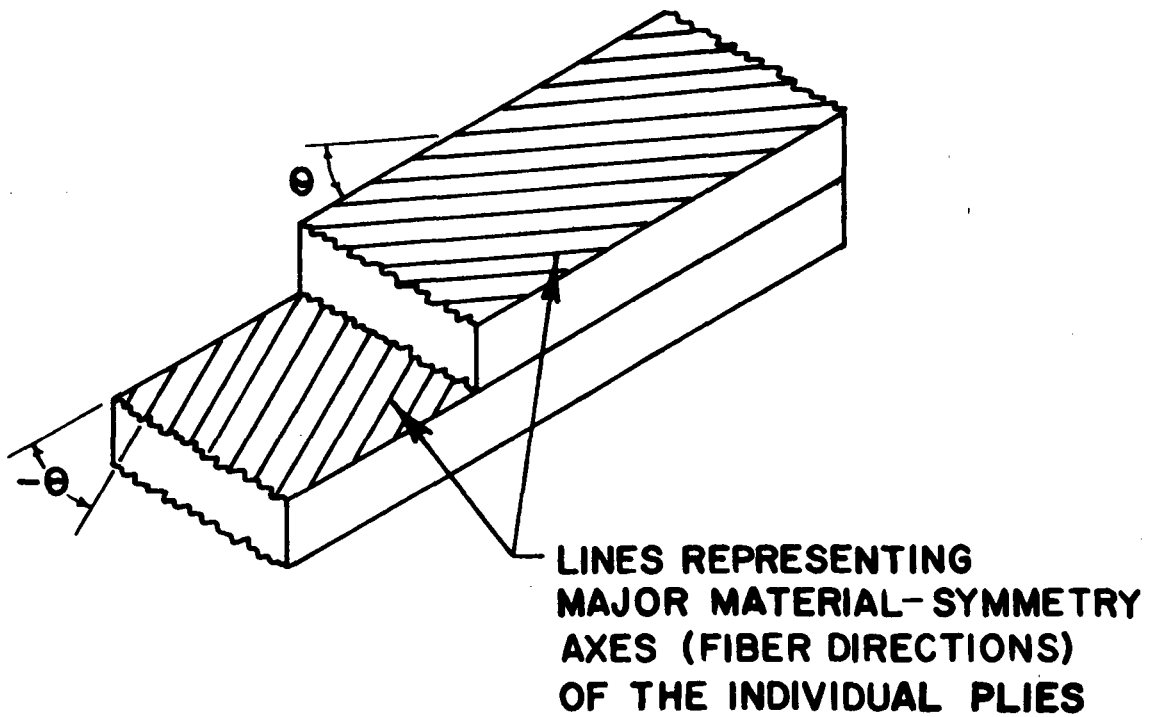


Figure 3. An example of a balanced laminate.

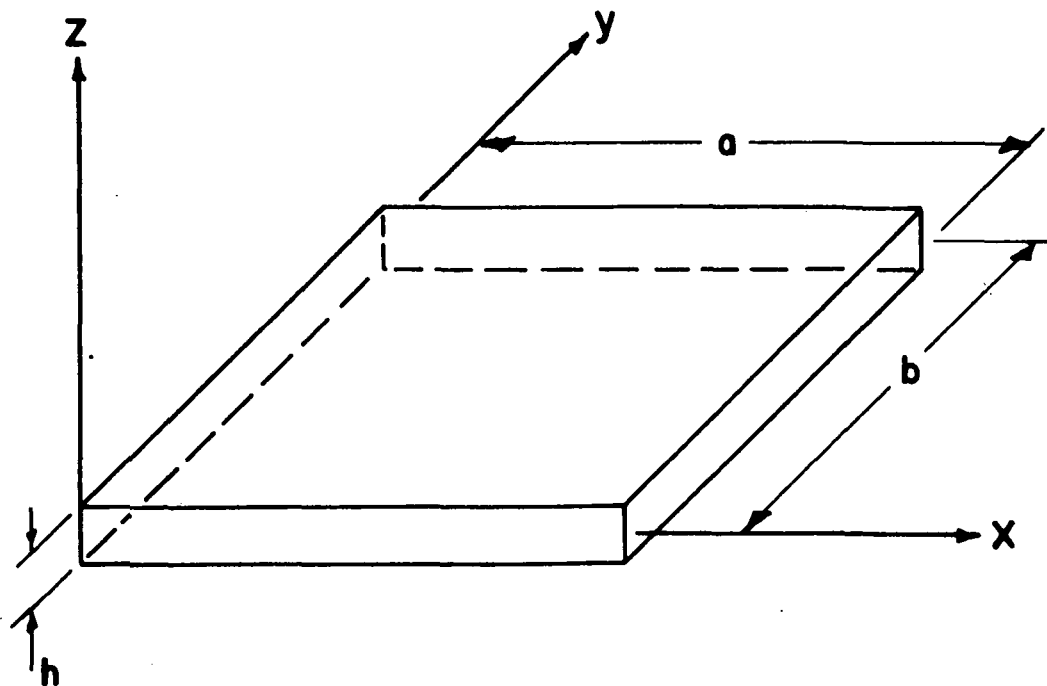


Figure 4. Plate coordinate system.

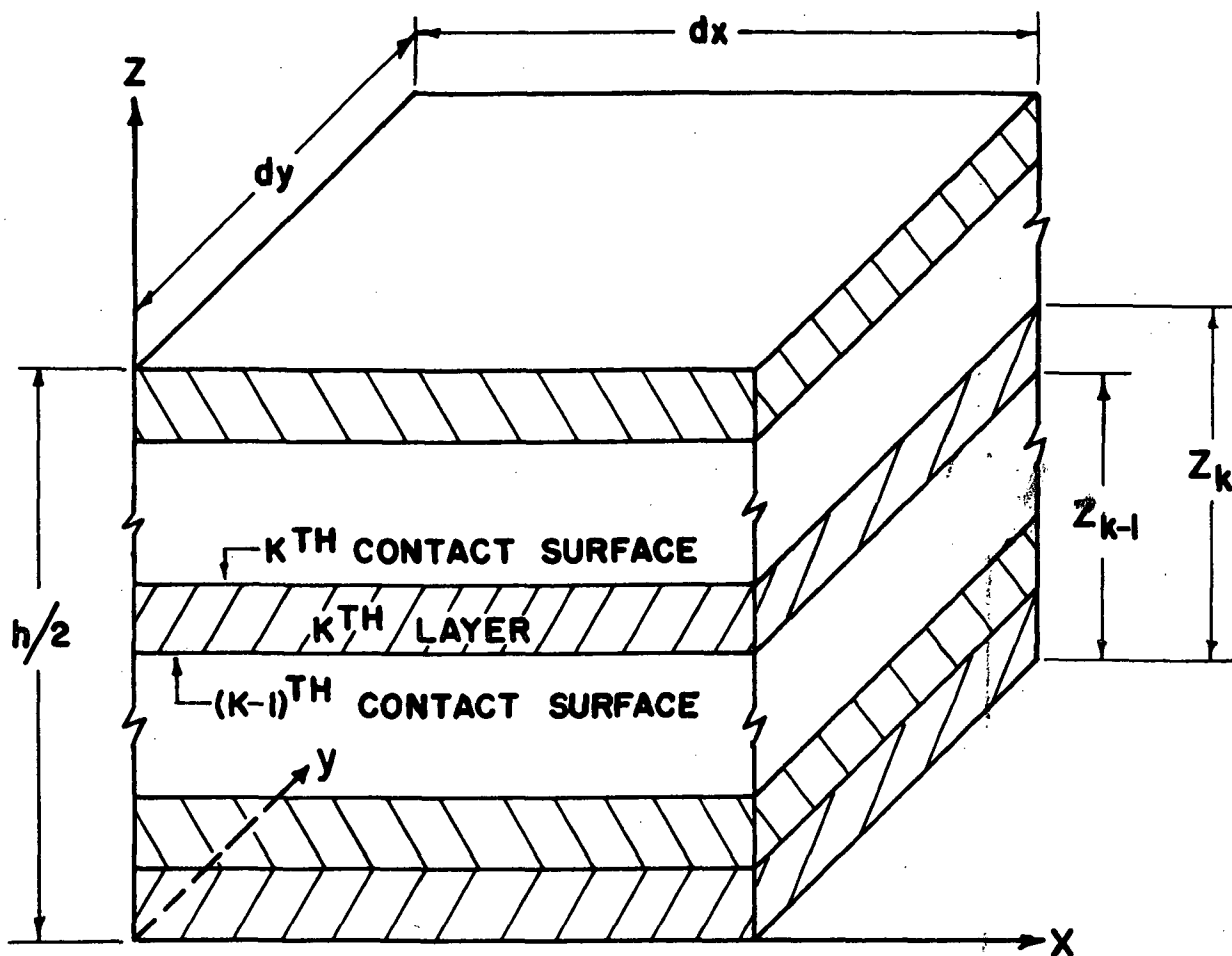


Figure 5. Lamination geometry, showing upper half of plate. (Plane  $xy$  is the midplane of the plate).

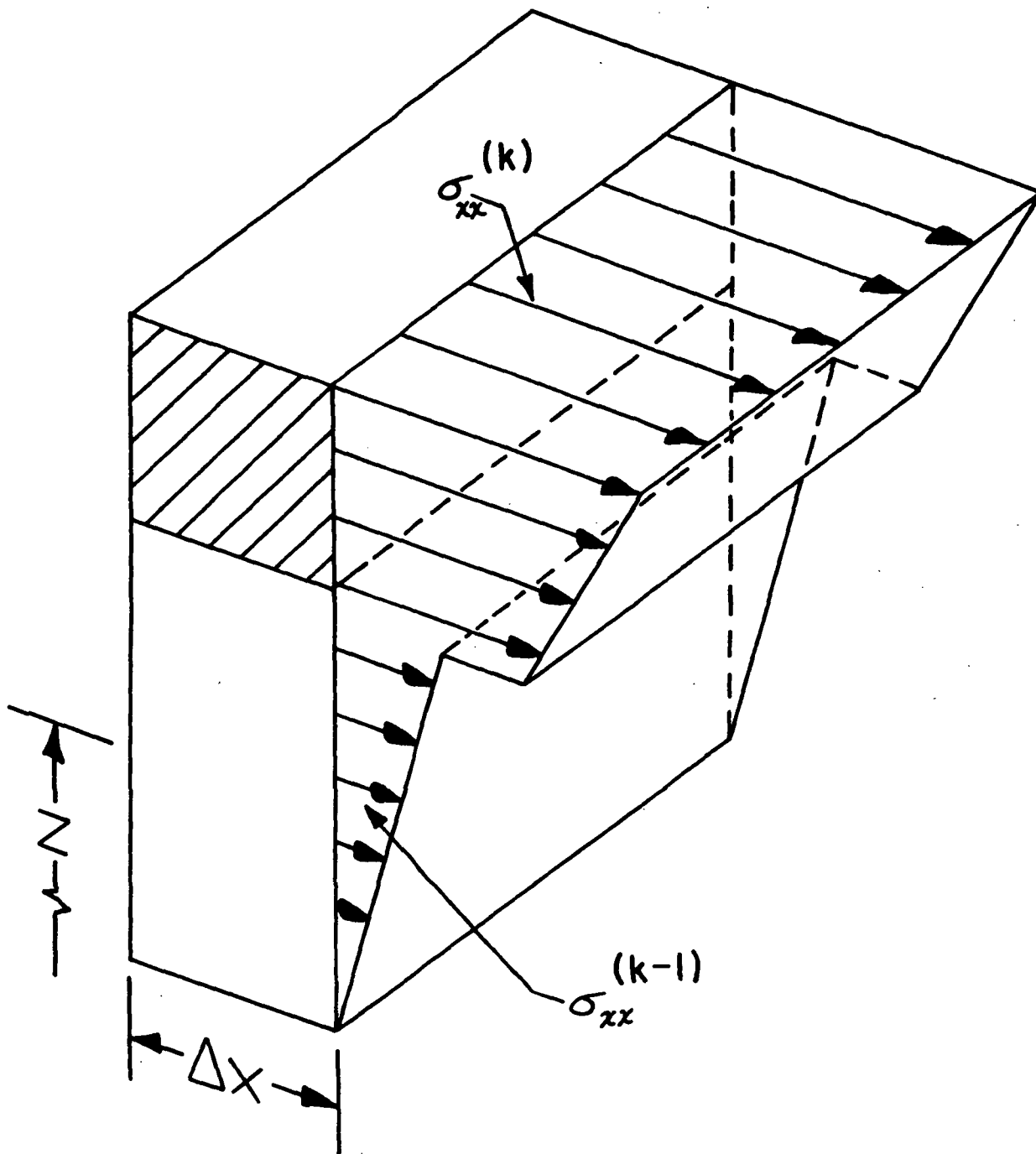


Figure 6. Bending-stress distribution.



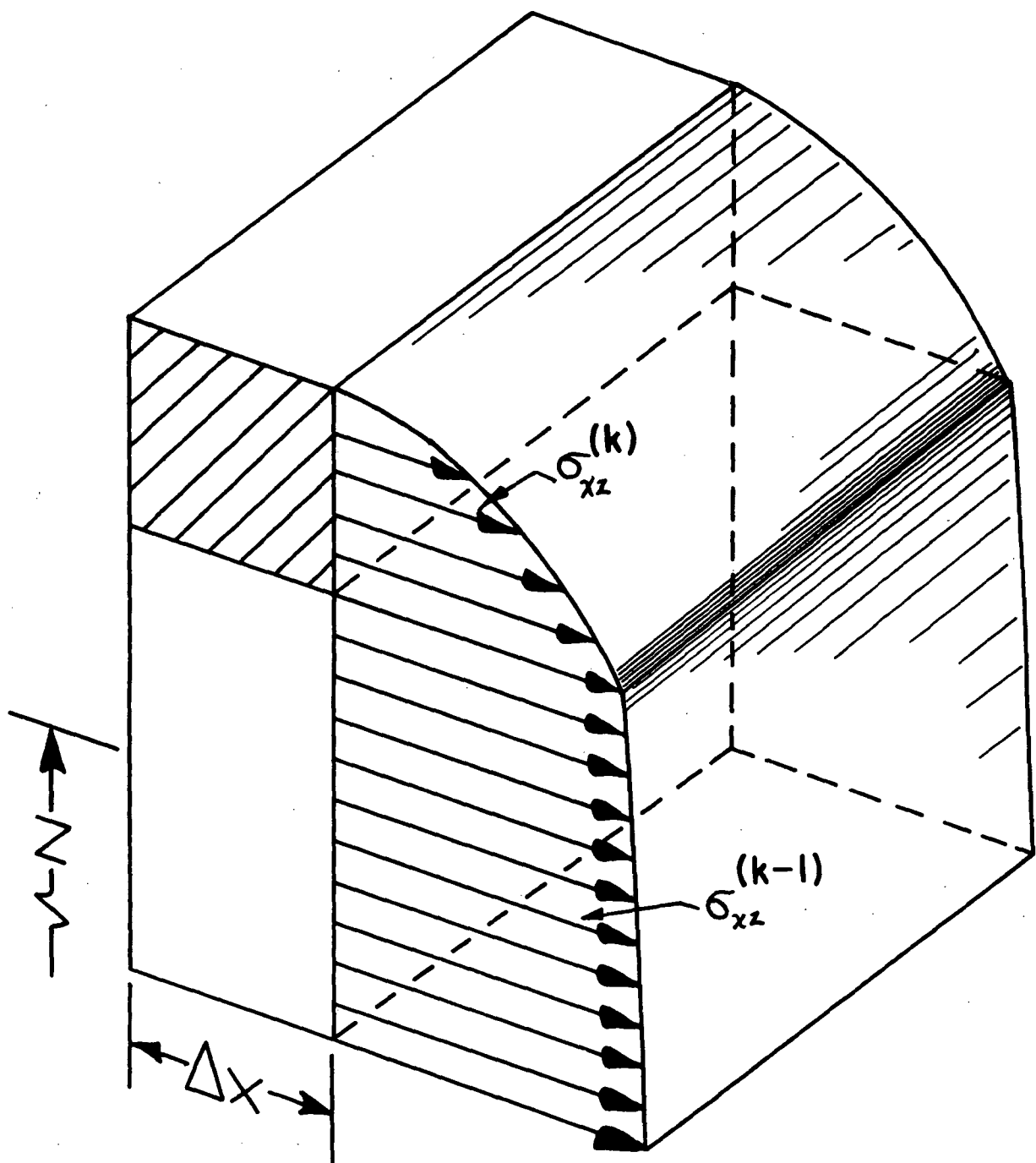


Figure 7. Shear-stress distribution.

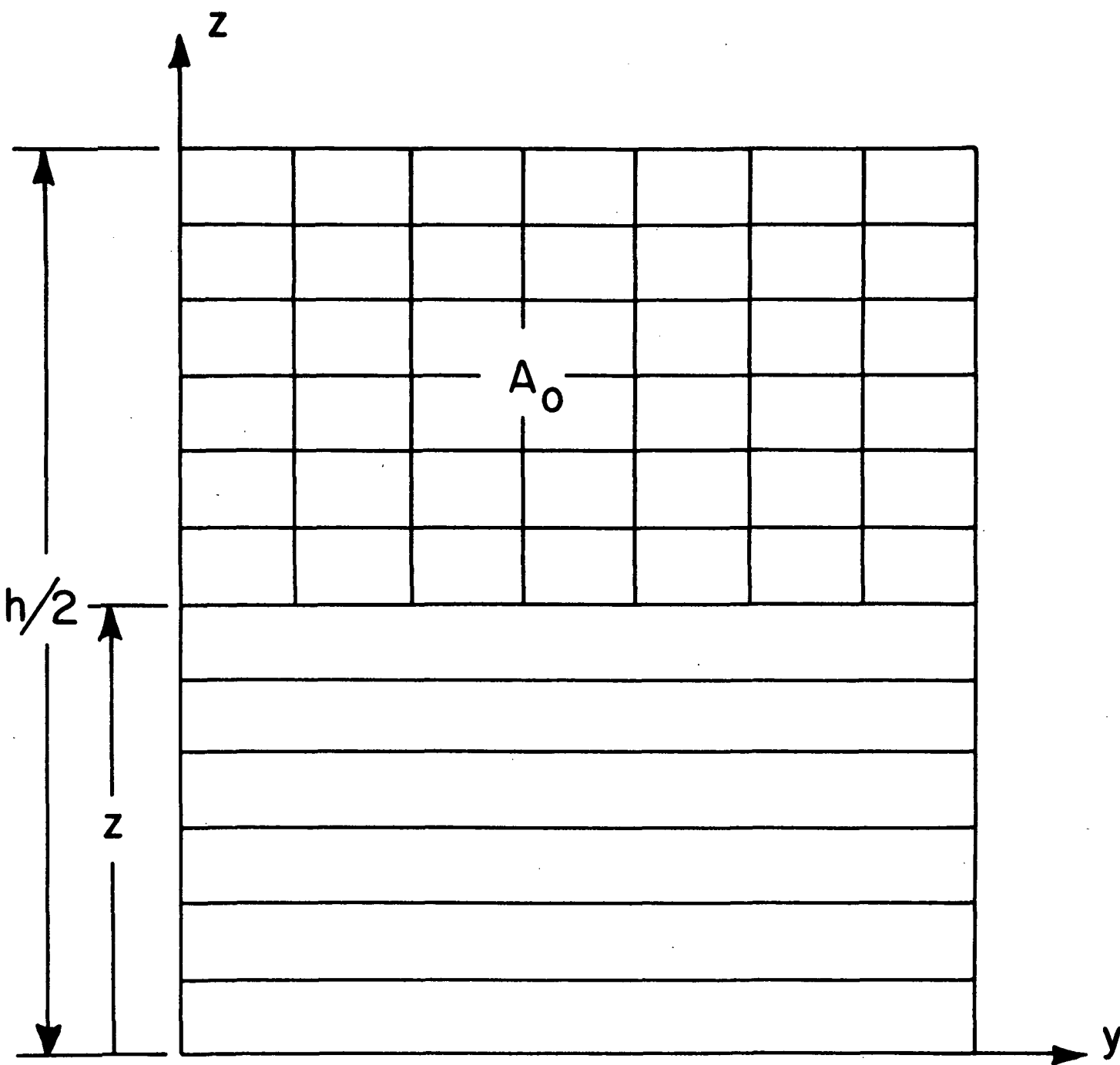


Figure 8. Area of integration  $A_0$ .

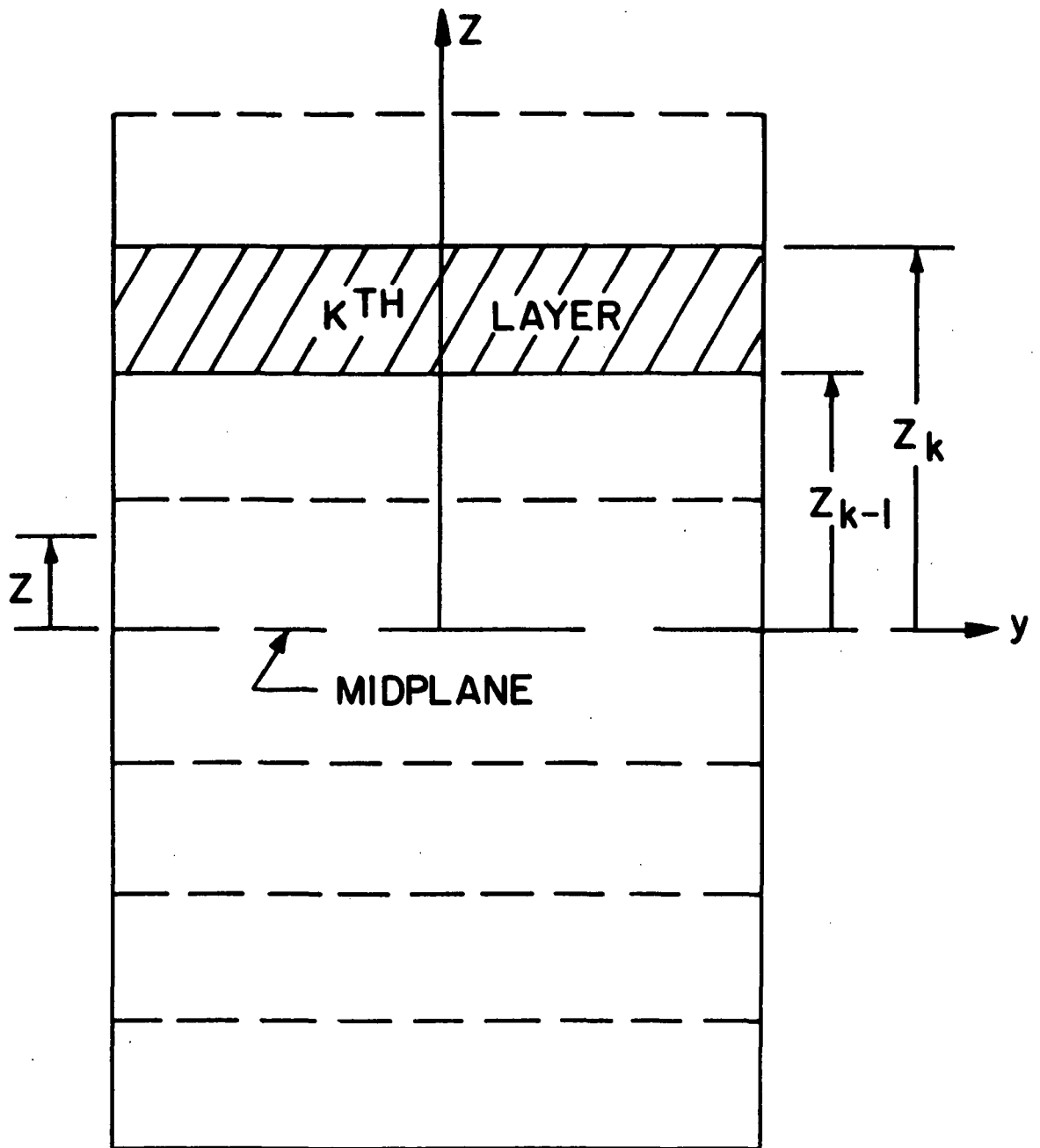


Figure 9. Cross section of laminated beam.

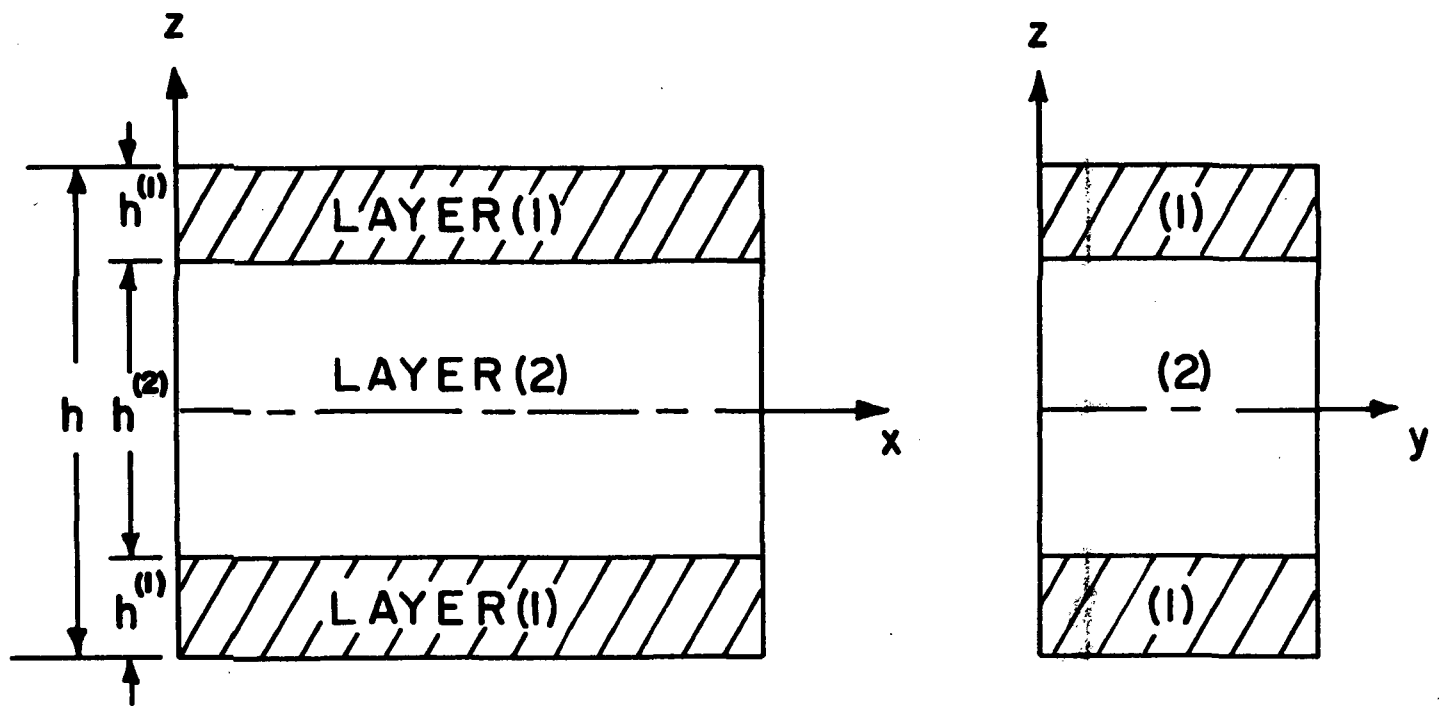


Figure 10. Three-ply symmetrically laminated plate.

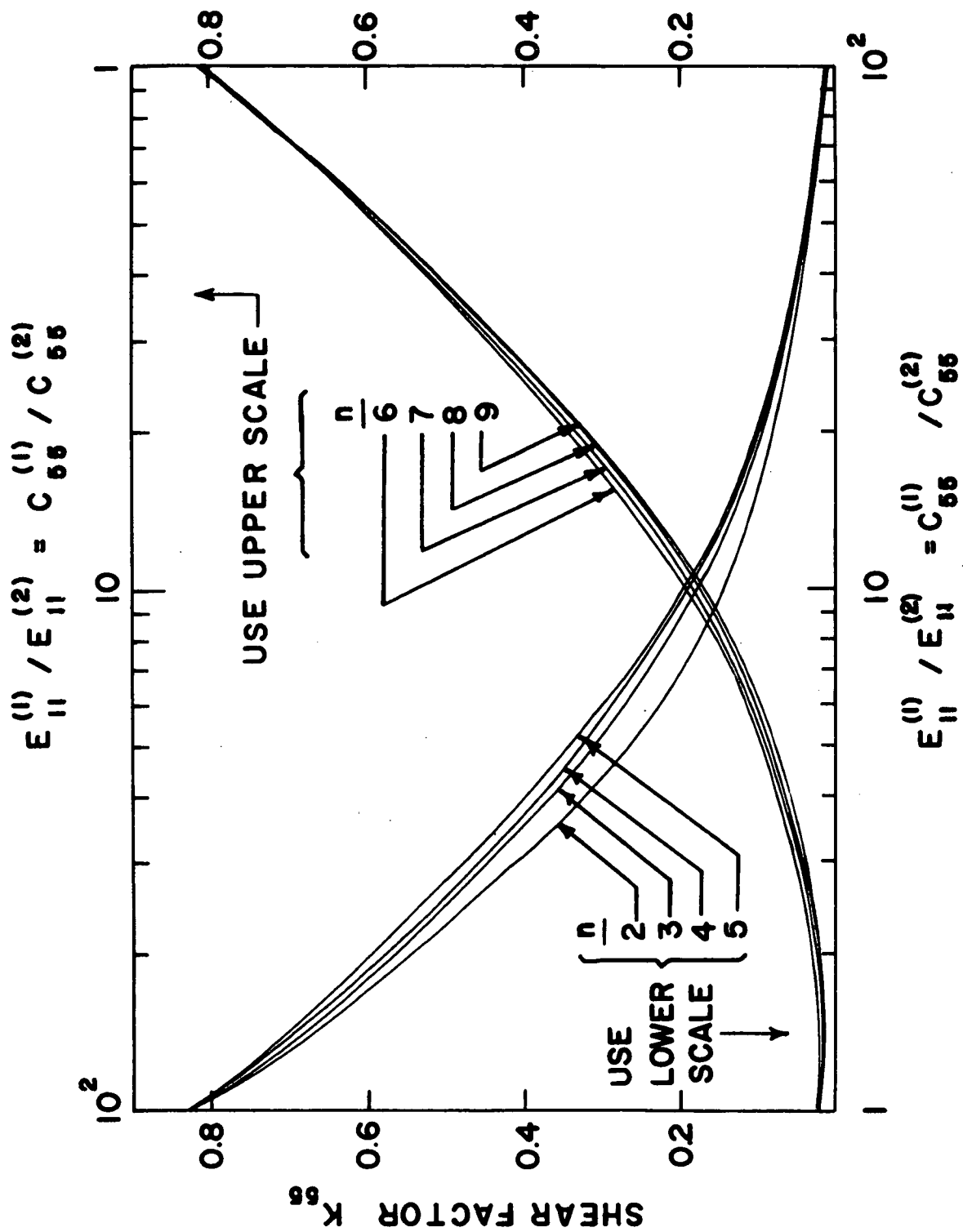


Figure 11. Shear factor for laminates consisting of multiple alternating layers of two materials.

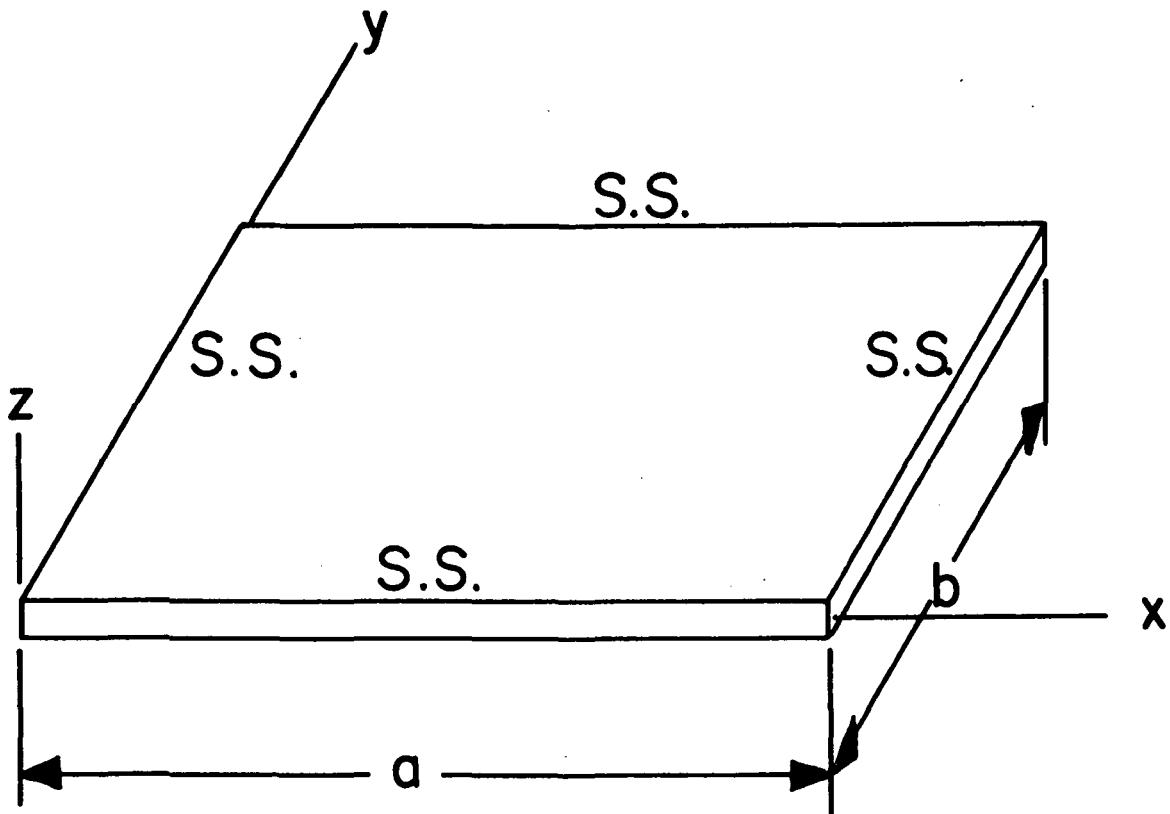


Figure 12. Rectangular plate with simply supported edges.

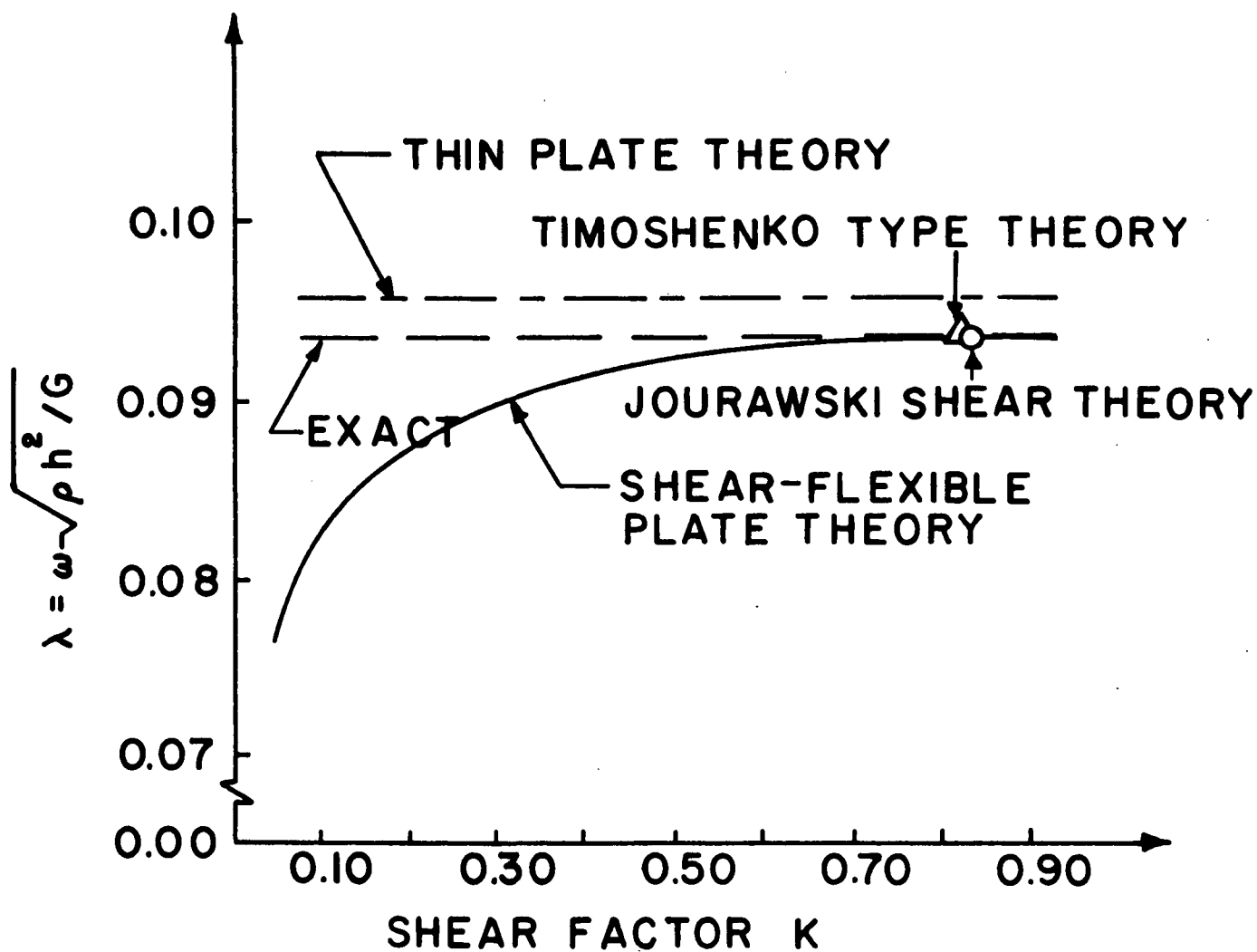


Figure 13. Lowest Eigenvalue ( $\lambda$ ) for homogeneous, isotropic plate.

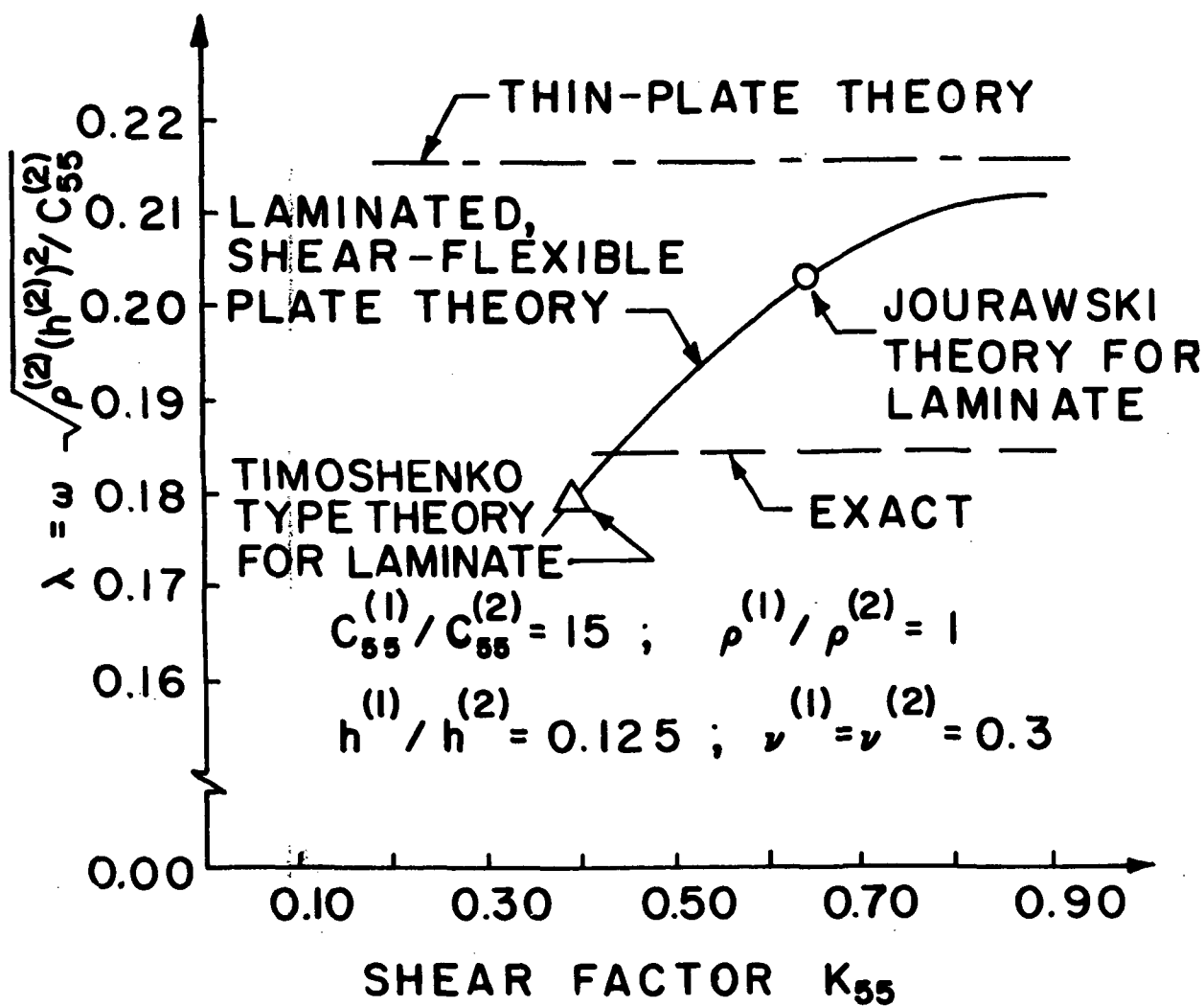


Figure 14. Lowest eigenvalues ( $\lambda$ ) for three-ply symmetrically laminated plate.



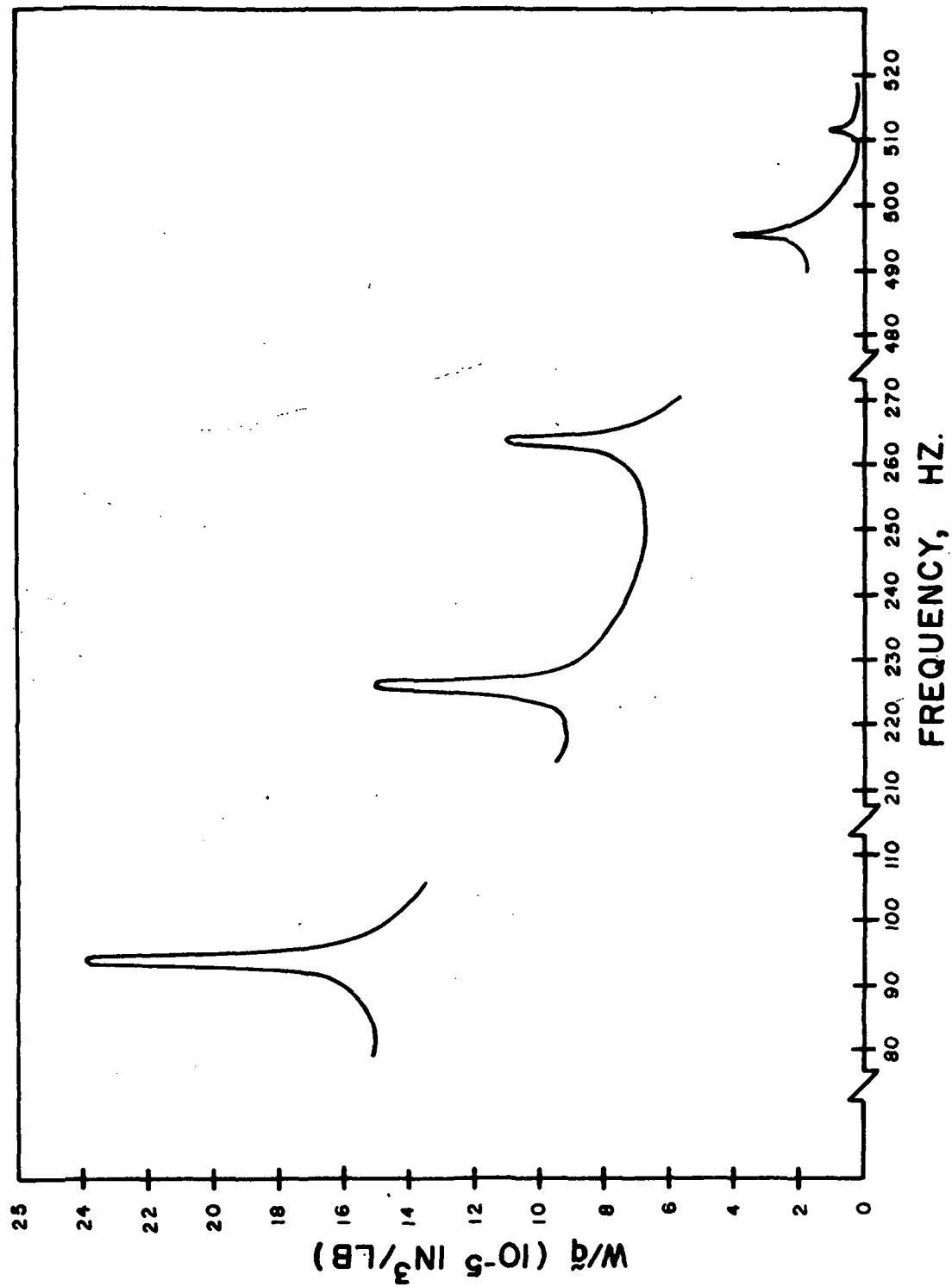
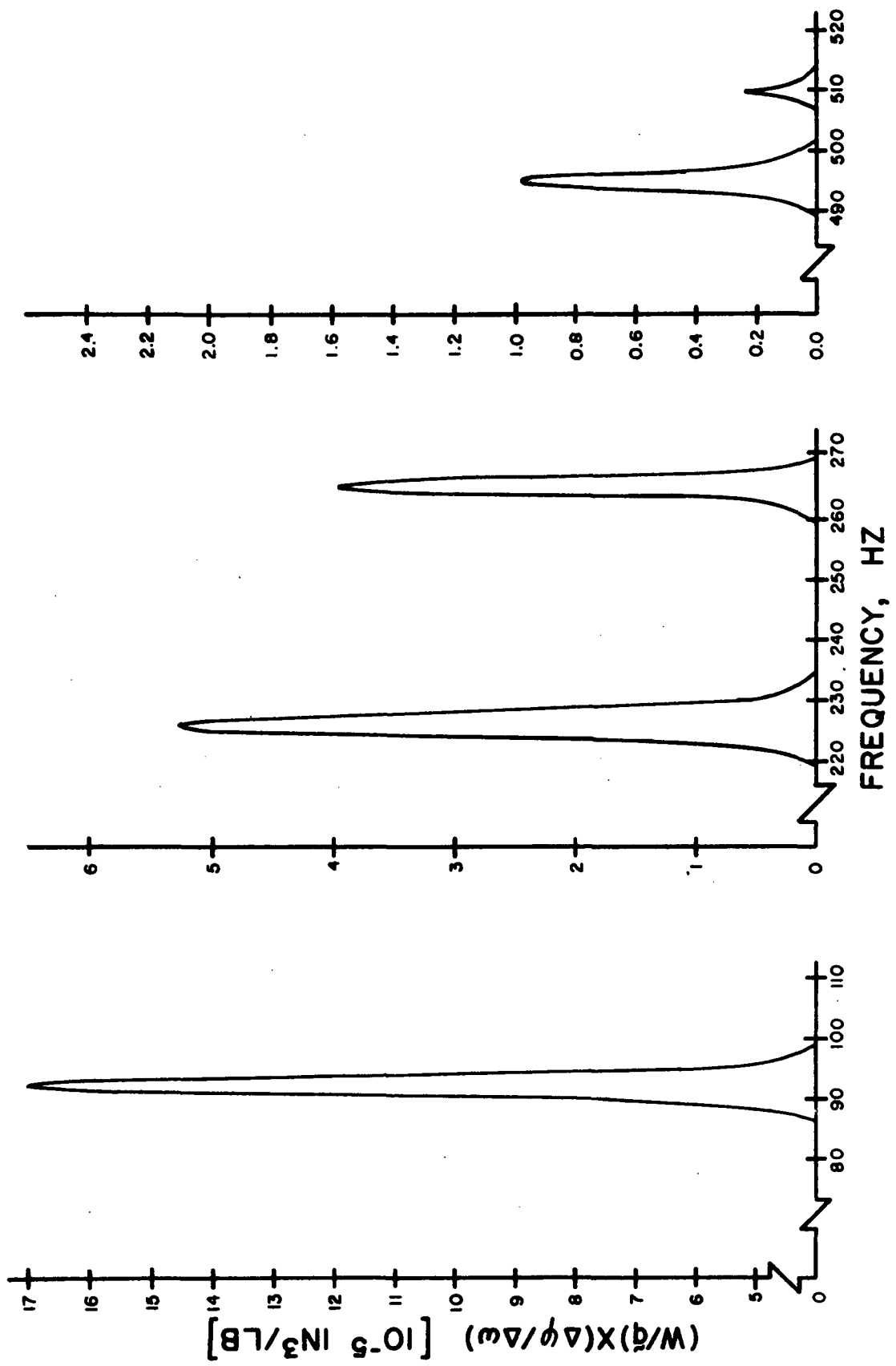


Figure 19. Amplitude frequency response

... M ... K ... Pa ... es ... s ...



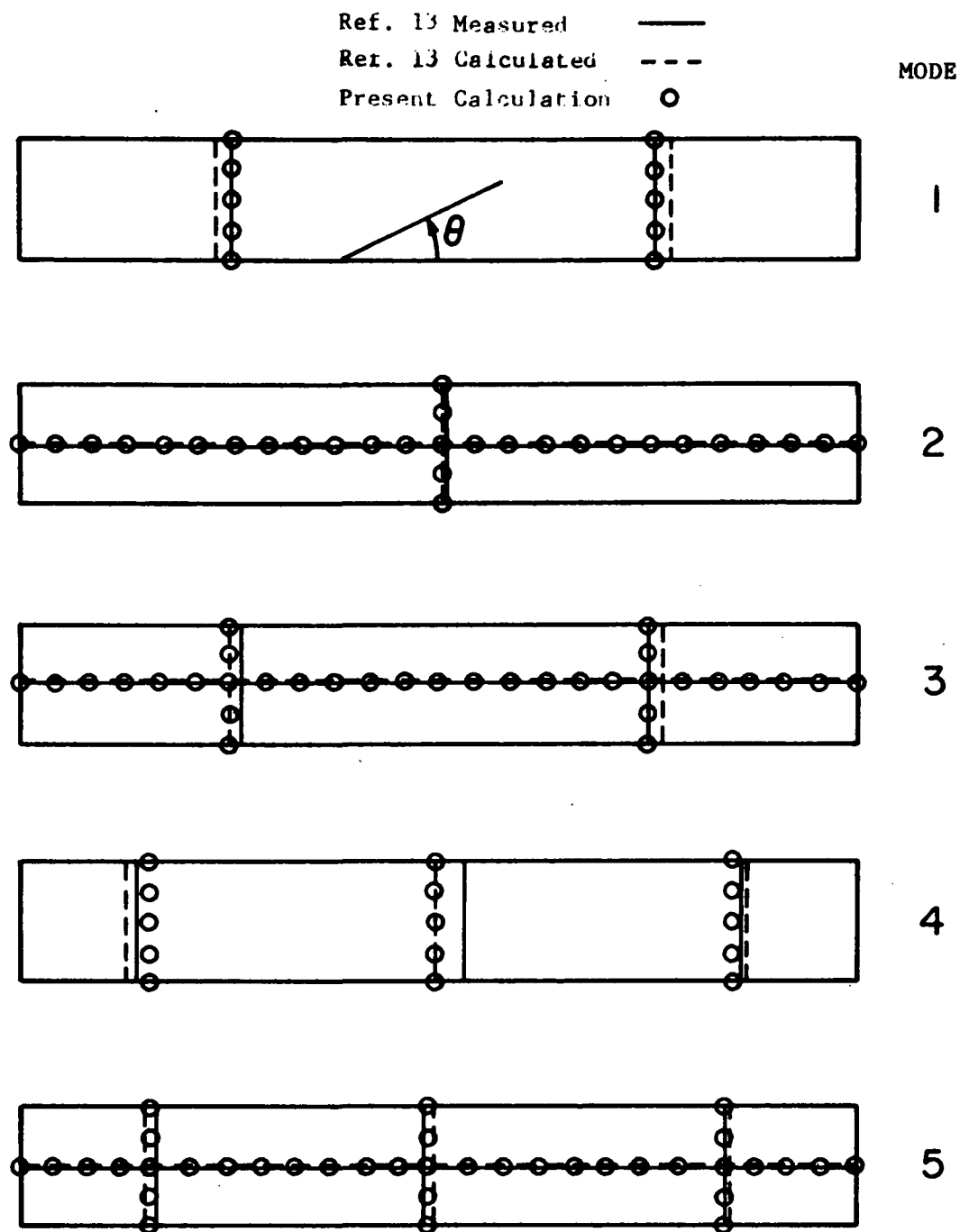


Figure 17. Nodal patterns of the first five modes of composite material plates at angle of orientation  $\theta = 0^\circ$

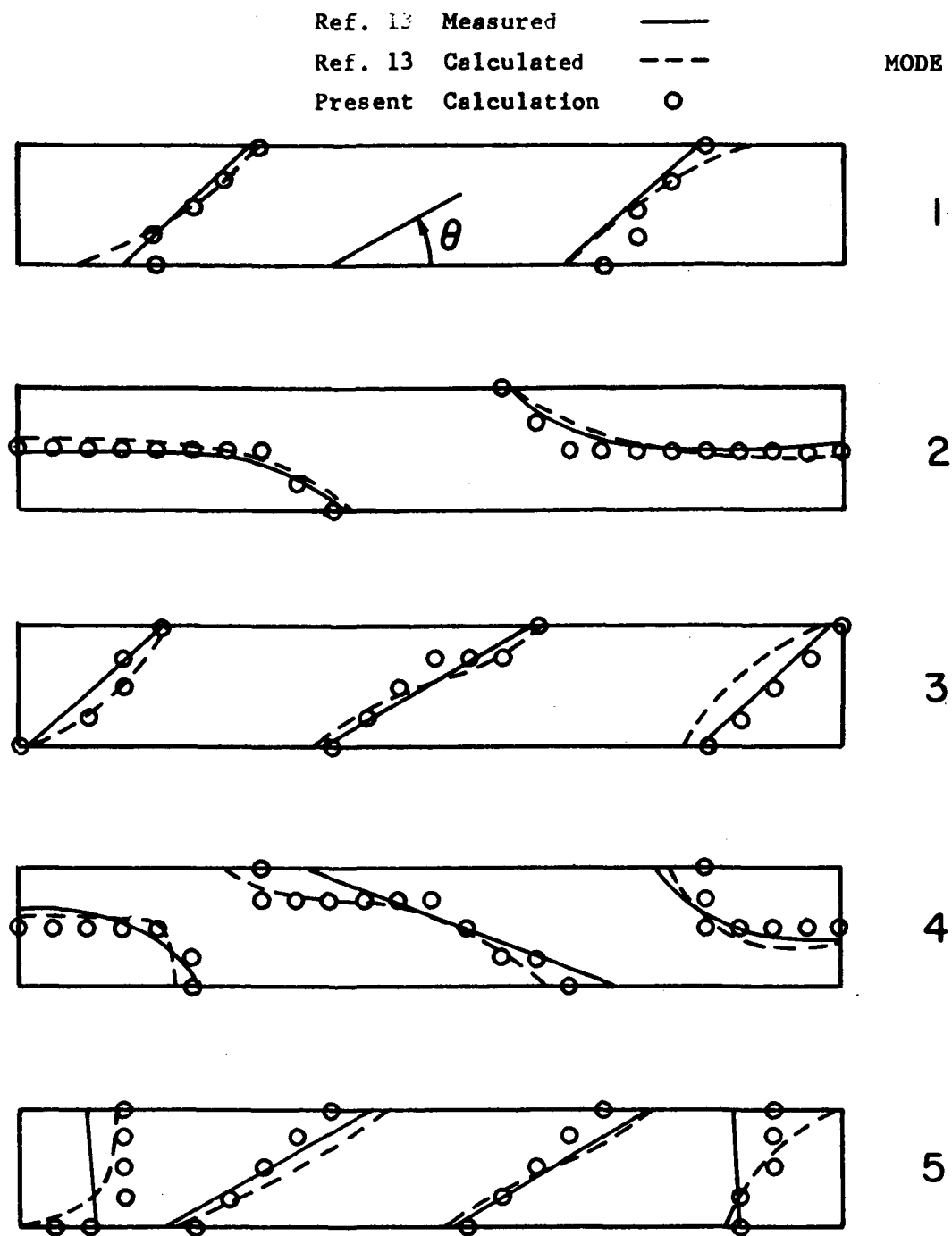


Figure 18. Nodal patterns of the first five modes of composite material plates at angle of orientation  $\theta = 10^\circ$

Ref. 13 Calculated ---

MODE

Present Calculation O

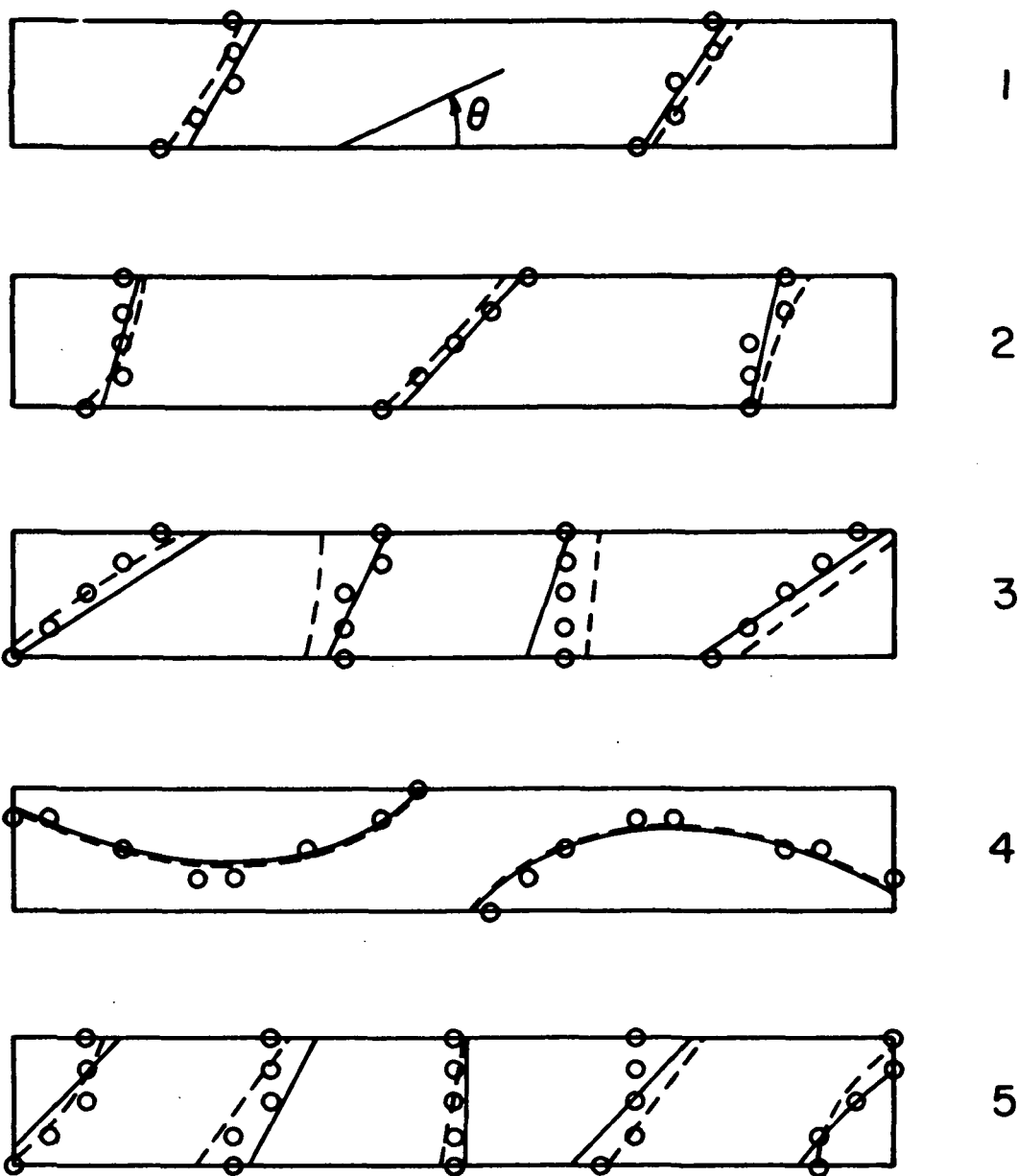


Figure 19. Nodal patterns of the first five modes of composite material plates at angle of orientation  $\theta = 30^\circ$

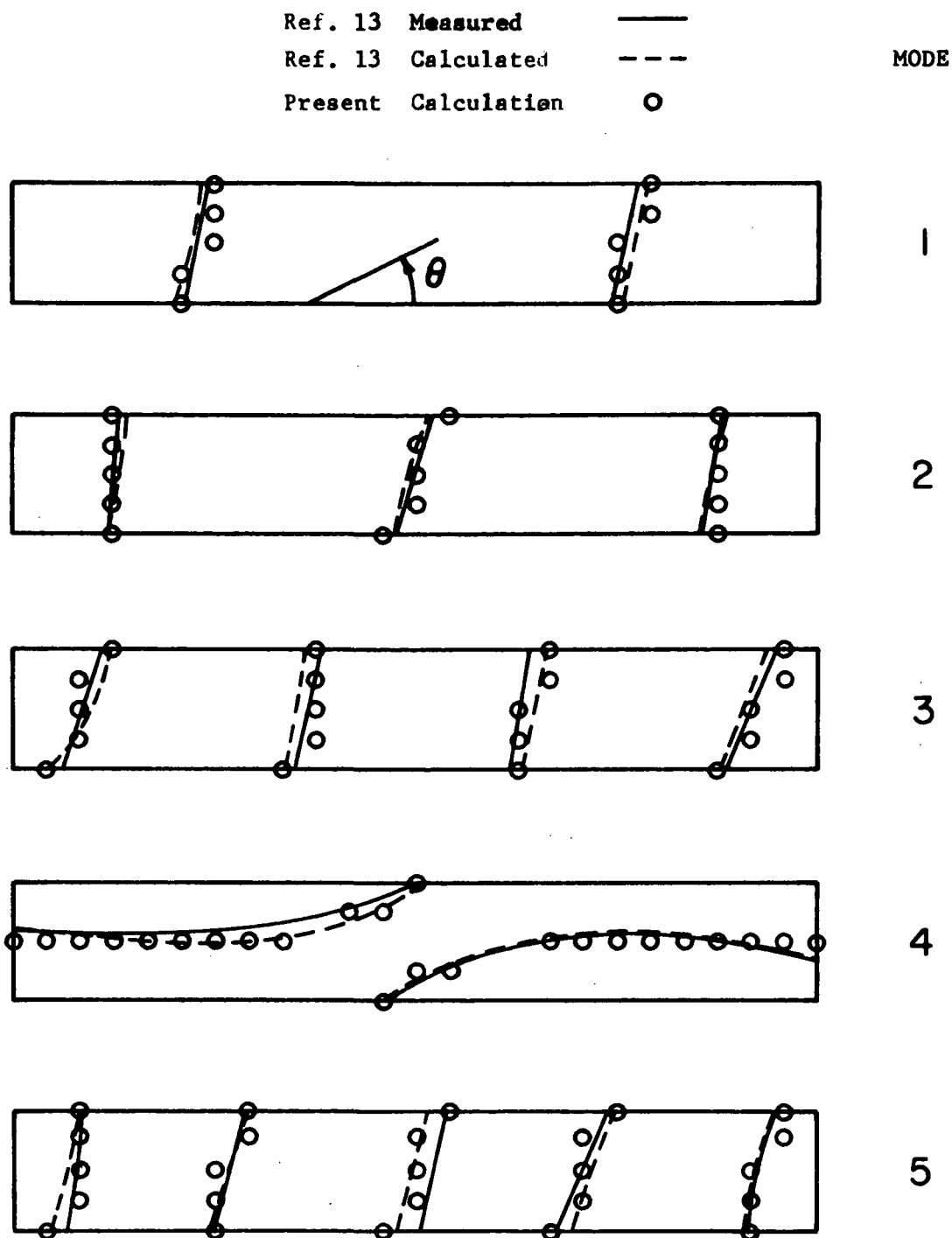


Figure 20. Nodal patterns of the first five modes of composite material plates at angle of orientation  $\theta = 45^\circ$

Ref. 13	Measured	—
Ref. 13	Calculated	- - -
Present	Calculation	○

MODE

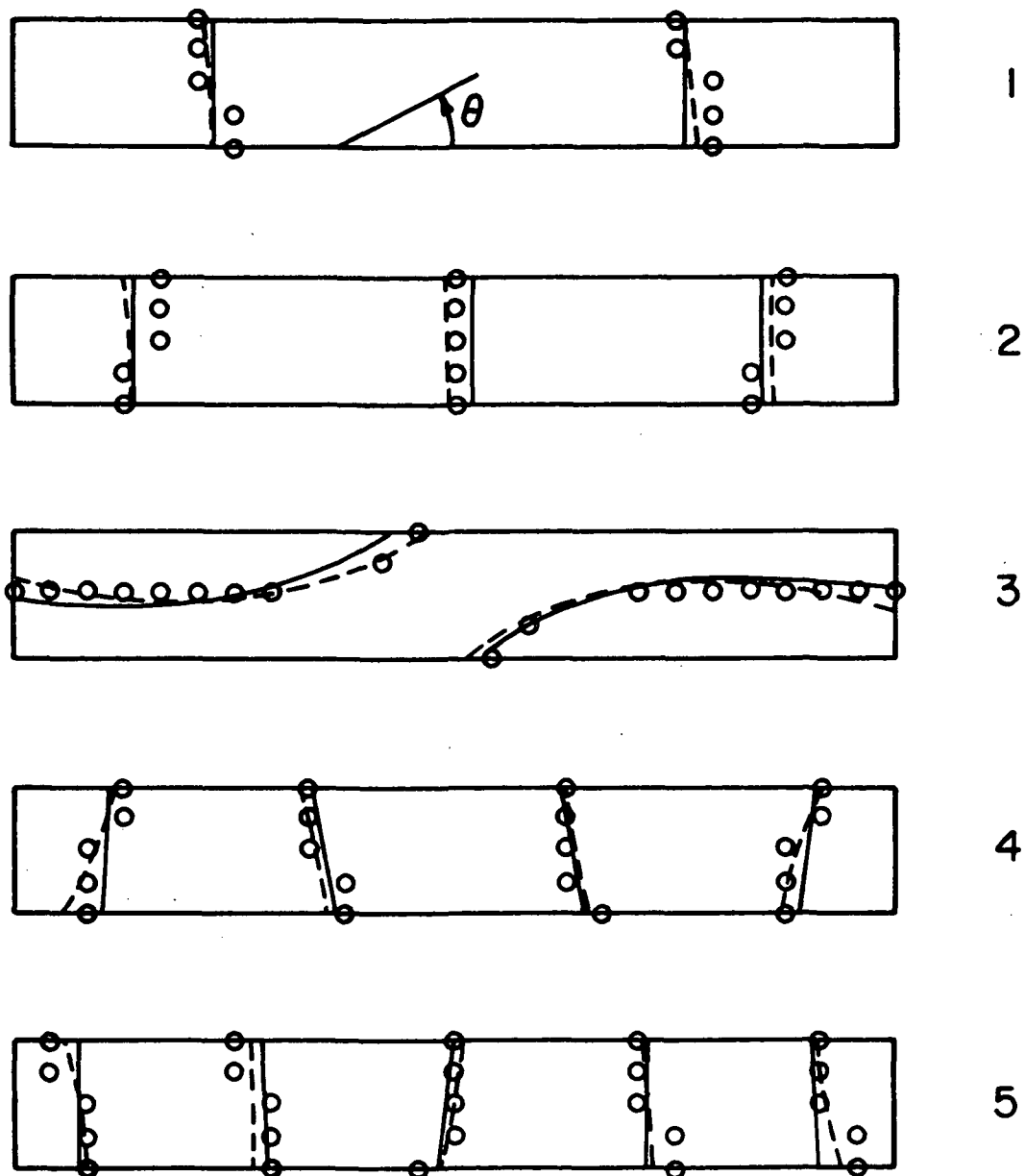


Figure 21. Nodal patterns of the first five modes of composite material plates at angle of orientation  $\theta = 60^\circ$

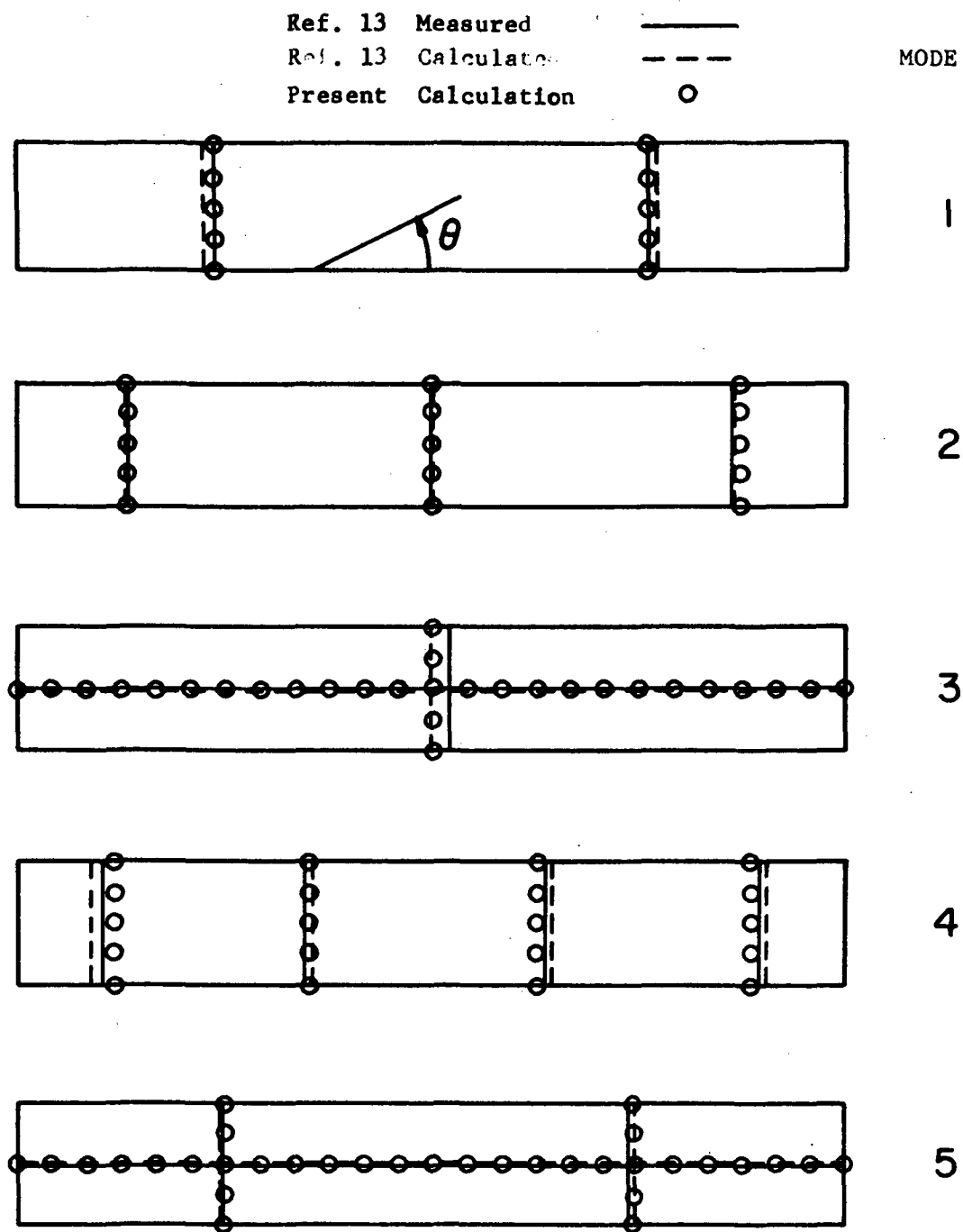


Figure 22. Nodal patterns of the first five modes of composite material plates at angle of orientation  $\theta = 90^\circ$



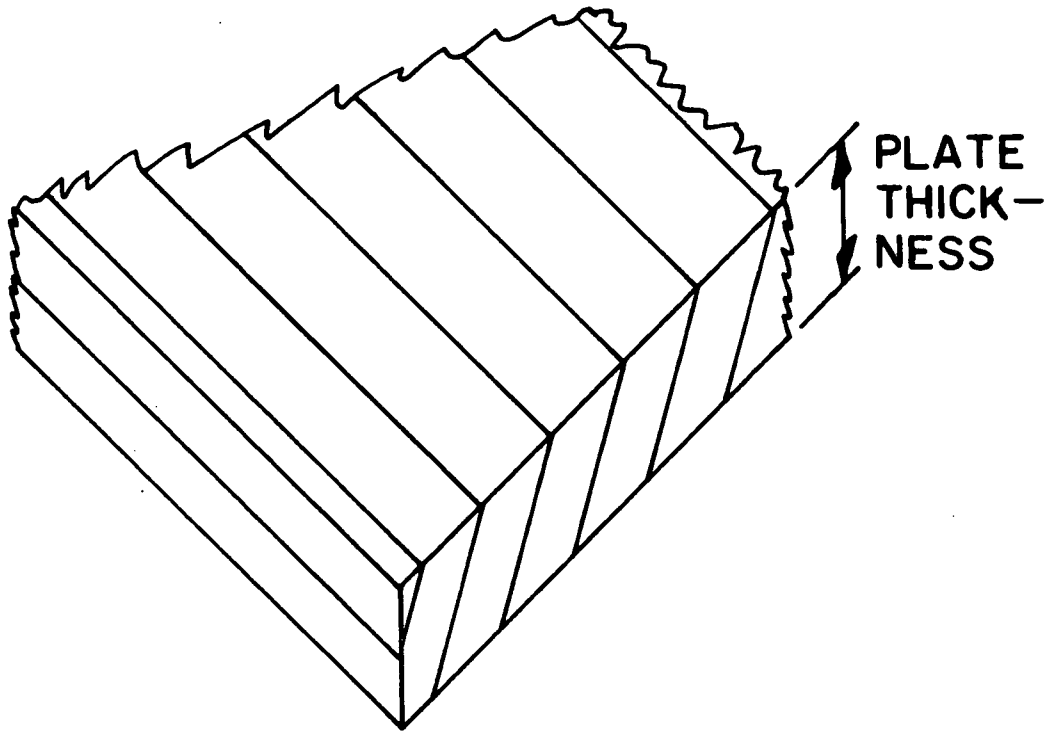


Figure A-1. Shingle-laminated plate.

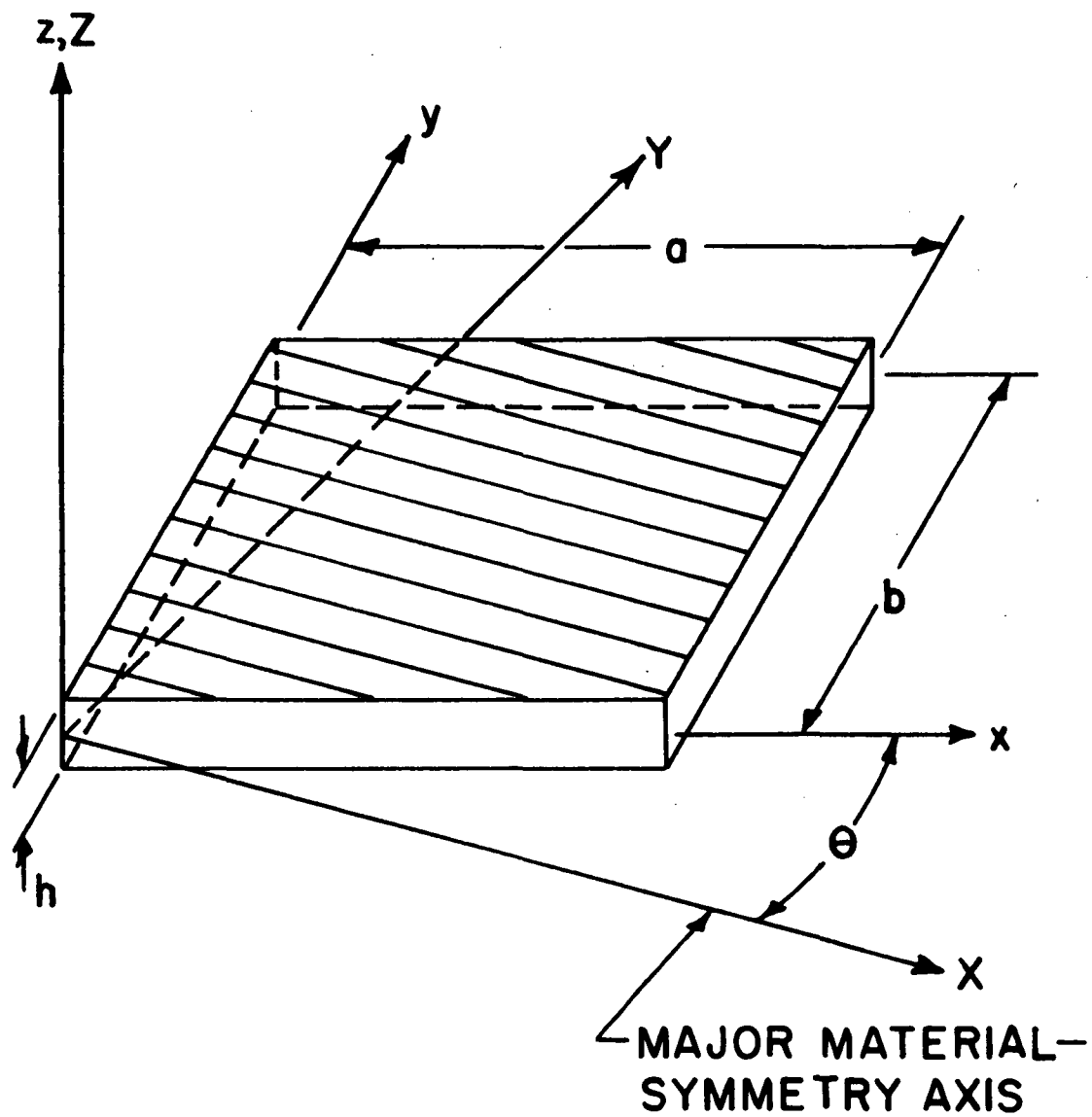
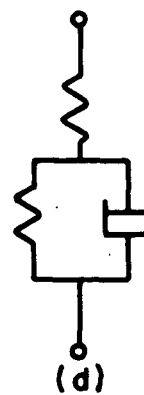
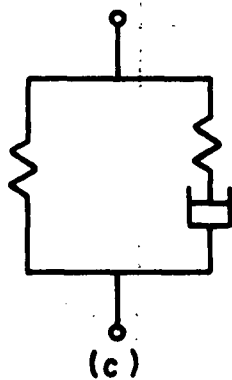
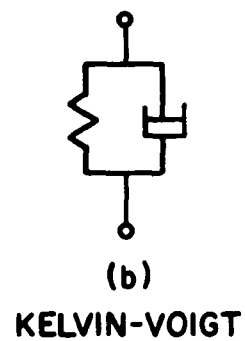
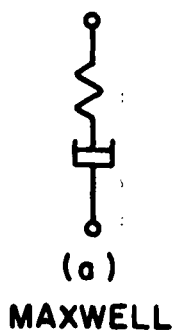


Figure A-2. Major Material-Symmetry Axis Direction.



**THREE-PARAMETER MODELS  
(STANDARD LINEAR SOLID)**

Figure B-1. Two-and three-parameter viscoelastic models.

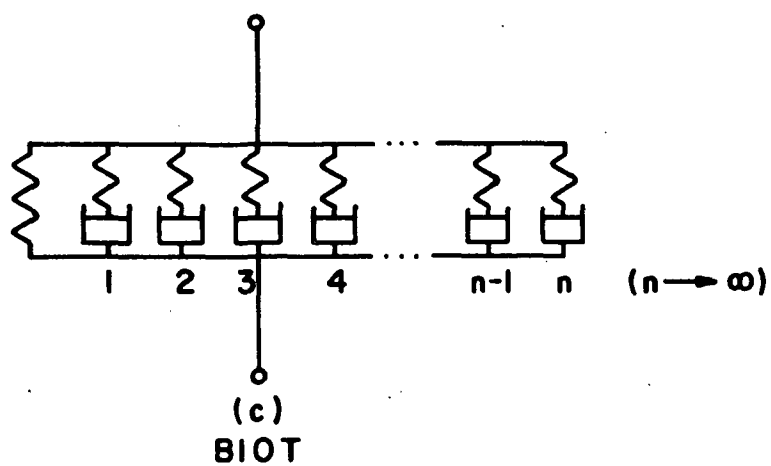
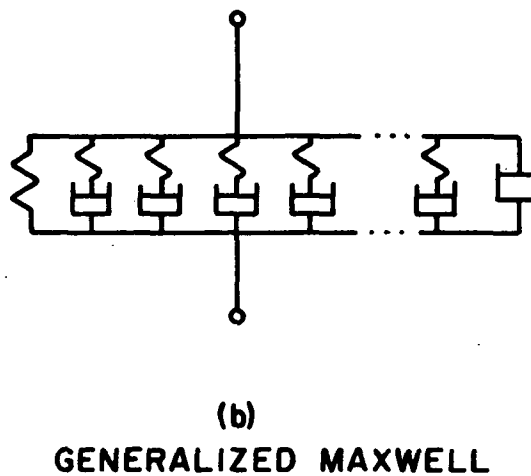
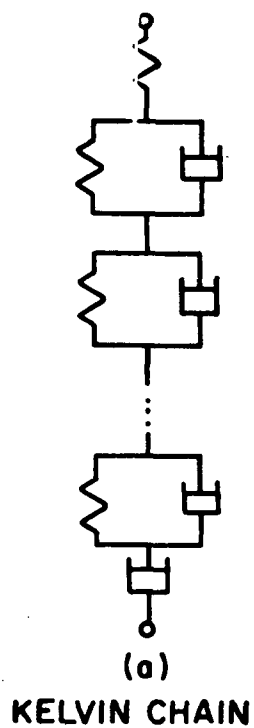
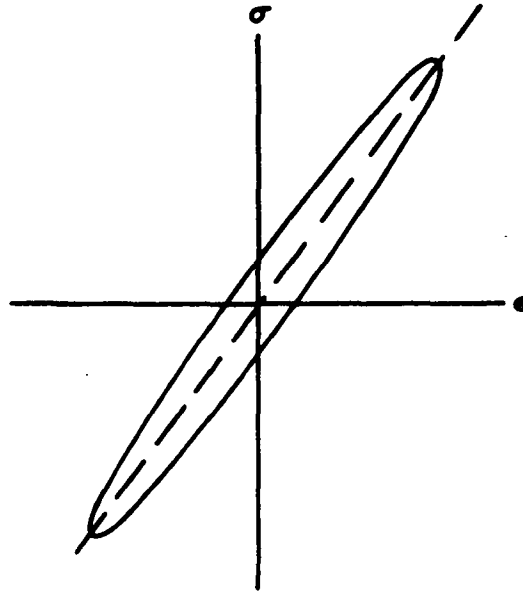
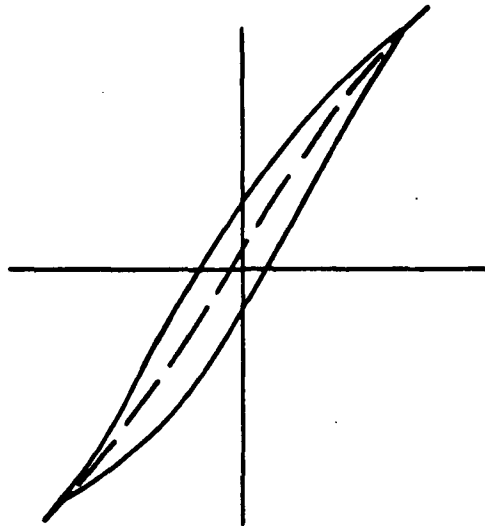


Figure B-2. Many-element viscoelastic models.



**(a) ELLIPTICAL HYSTERESIS LOOP**



**(b) POINTED-END, STRAIGHT-SIDED HYSTERESIS LOOP**

Figure B-3. Hysteresis-loop shapes.

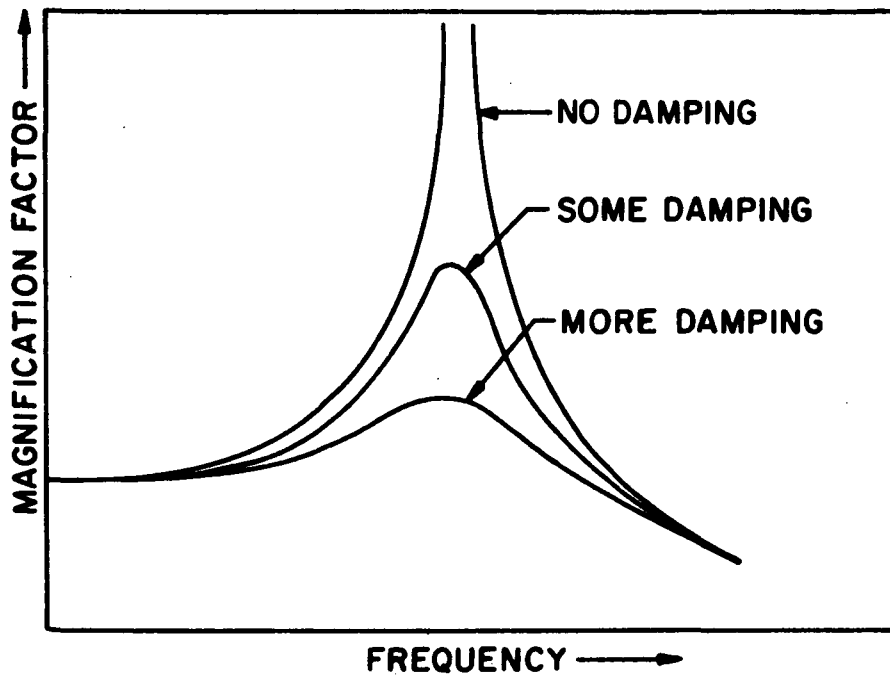


Figure B-4. Effect of damping on magnification factor. (Not drawn to scale).

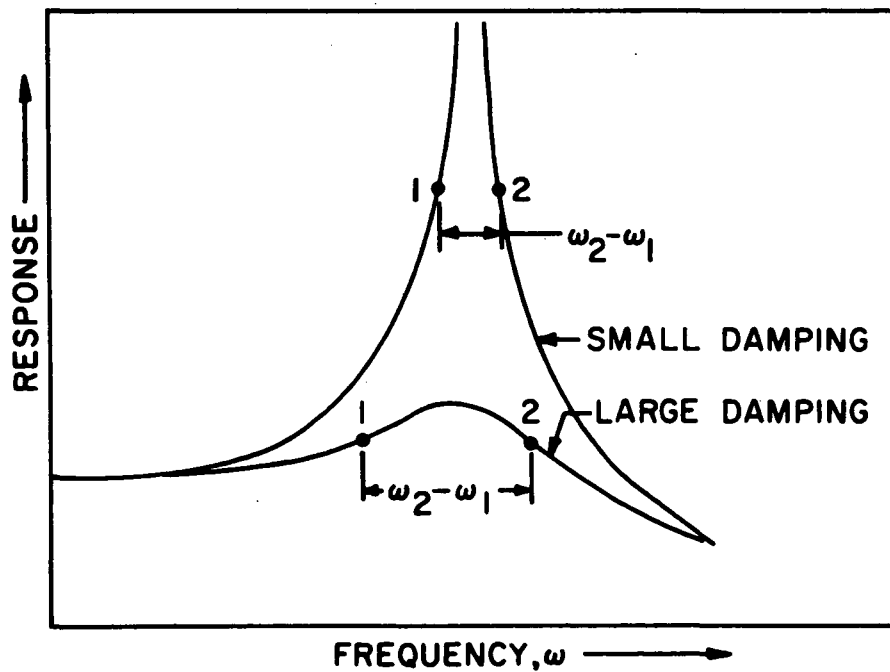


Figure B-5. Effect of damping on half-power-point frequency separation ( $\omega_2 - \omega_1$ ). (Not drawn to scale).

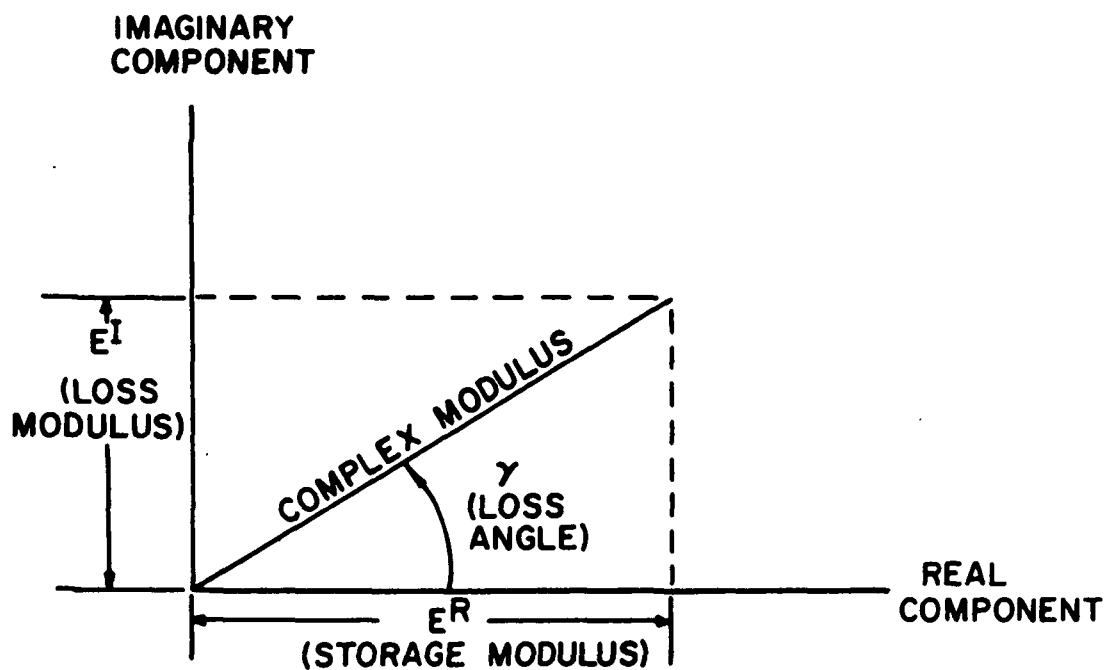


Figure B-6. Concept of complex modulus and loss angle.

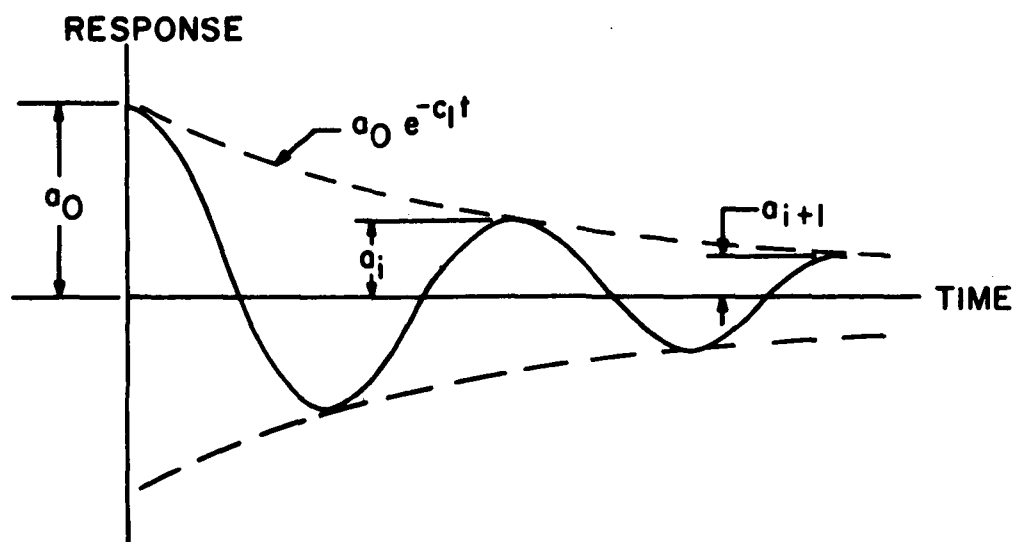


Figure B-7. Exponential decay. (Not drawn to scale).

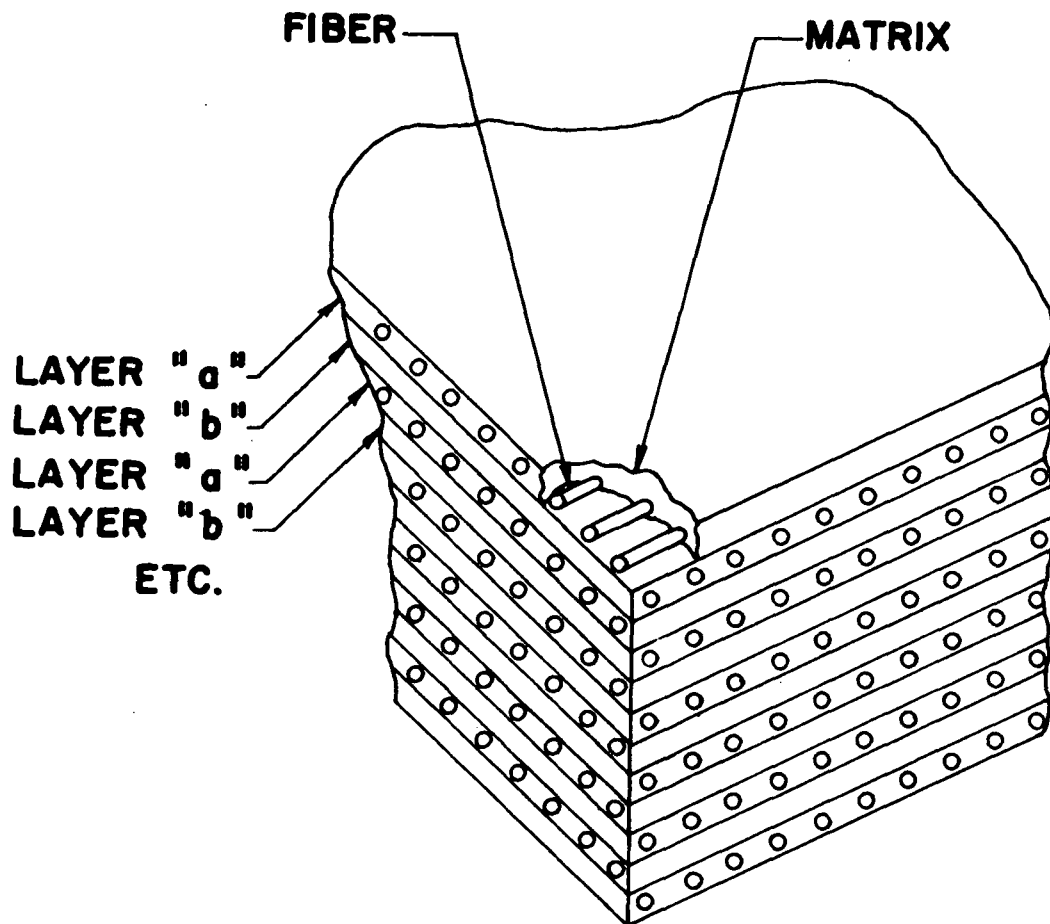


Figure F-1. Medium containing many repeating alternating layers of two different types.



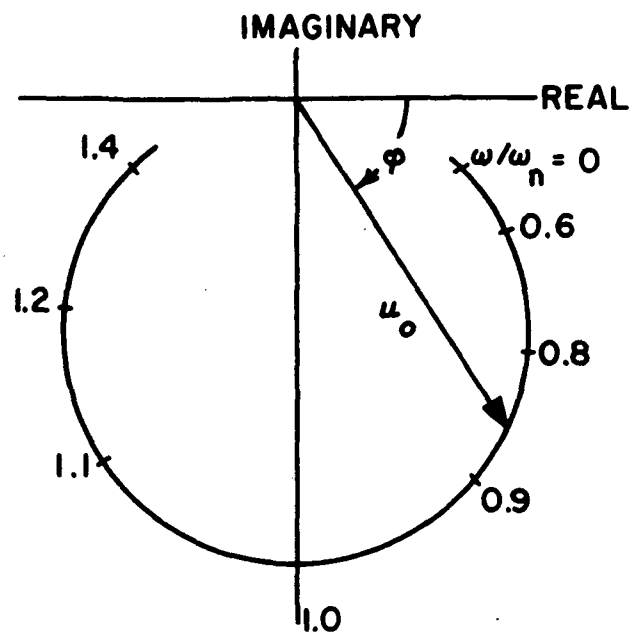


Figure H-1. Theoretical Argand diagram.

```

120 READ(5,10)N
10  FORMAT(I3)
   IF(N) 130,130,140
140 NN=N-1
   READ(5,20)(E(J),G(J),Z(J),J=1,N)
20  FORMAT(3F10.5)
   SUMGZ=G(1)*Z(1)
   DO 30 J=2,N
   SUMGZ=SUMGZ+G(J)*(Z(J)-Z(J-1))
30  CONTINUE
   GE2Z5=E(1)**2/(4.*G(1))*(8./15.*Z(1)**5)
   DO 40 J=2,N
   GE2Z5=GE2Z5+E(J)**2/(4.*G(J))*(Z(J)**4*(Z(J)-Z(J-1))-
40  12./3.*Z(J)**2
   2*(Z(J)**3-Z(J-1)**3)+0.2*(Z(J)**5-Z(J-1)**5))
   E2Z4=E(1)*E(1)*Z(1)**4
   DO 50 J=2,N
   E2Z4=E2Z4+E(J)*E(J)*(Z(J)**2-Z(J-1)**2)**2
50  E2Z4=E2Z4-E(1)*E(1)*Z(1)**4
   GE2Z4=1.0/(4.0*G(1))*E2Z4*Z(1)
   DO 60 J=2,NN
   E2Z4=E2Z4-E(J)*E(J)*(Z(J)**2-Z(J-1)**2)**2
60  GE2Z4=GE2Z4+1.0/(4.0*G(J))*E2Z4*(Z(J)-Z(J-1))
   A(1,1)=E(1)*(2./3.)*Z(1)**3
   DO 70 K=2,NN
   A(1,K)=E(K)*(Z(K)**2*(Z(K)-Z(K-1))-1./3.*(Z(K)**3-Z(K-1)**3))
70
   DO 71 J=2,N
   A(J,1)=E(J)*(Z(J)**2-Z(J-1)**2)
71  LL=1
   DO 72 K=2,NN
   DO 73 J=2,N
   A(J,K)=A(J+LL,K-LL)
73  CONTINUE
72  LL=LL+1
   GEZ=0.0

```

```

11=N
KK=NN
DO 74 M=1,NN
AA=0.0
DO 75 I=1,KK
L=I+1
DO 75 J=L,II
B=A(I,M)*A(J,M)
AA=AA+B
75 CONTINUE
C=0.5*G(M)*AA
GEZ=GEZ+C
II=II-1
KK=KK-1
74 SGEZ=GEZ*4+GEZ*5+GEZ
E1Z3=(1./3.)*E(1)*Z(1)**3
DO 80 J=2,N
E1Z3=E1Z3+0.5*E(J)*(Z(J)**2*(Z(J)-Z(J-1))-1./3.*(Z(J)**3-Z(J-1)
1**3))
80 CONTINUE
E1Z2Z=0.5*E(1)*Z(1)**2
DO 90 J=2,N
E1Z2Z=E1Z2Z+0.5*E(J)*(Z(J)**2-Z(J-1)**2)
E1Z2Z=E1Z2Z-0.5*E(1)*Z(1)**2
AE1Z3=E1Z2Z*Z(1)
DO 100 J=2,NN
E1Z2Z=E1Z2Z-0.5*E(J)*(Z(J)**2-Z(J-1)**2)
AE1Z3=AE1Z3+E1Z2Z*(Z(J)-Z(J-1))
100 CONTINUE
SE1Z3=(E1Z3+AE1Z3)**2
SFK=SE1Z3/(SUMGZ*SGEZ)
WRITE(6,110)N,SFK
110 FORMAT(' N=',I2.5X,'SHEAR FACTOR K =',F7.4//)
GO TO 120
130 CALL EXIT
END

```



```

C44I1=C44I*(1.D0/AN)
C45I=0.D0
C45I1=0.D0
C55I=C44I
C55I1=C44I1
C66I=C44I
C66I1=C44I1
PI=3.1415926536D0
G1=0.0001**0.5*PI
G2=0.0064**0.5*PI
H1=1.D0
H2=8.D0
H=10.D0
R01=1.D0
R02=1.D0
RA=1
RB=2
RC=3
RD=4
RE=5
CA=1
CB=2
CC=3
CD=4
CE=5

```

# CALCULATE STIFFNESS MATRIX

```

AS(RA,CA)=25.D0*(C11I/C66I1+C66I/C66I1)*G1**2
1+25.D0/16.D0*(C11I/C66I1+1.D0)*G2**2
AS(RA,CB)=25.D0*(C12I/C66I1+C66I/C66I1)*G1**2
1+25.D0/16.D0*(C12I/C66I1+1.D0)*G2**2
AS(RA,CC)=0.D0
AS(RA,CD)=0.D0
AS(RA,CE)=0.D0
AS(RB,CA)=25.D0*(C12I/C66I1+C66I/C66I1)*G1**2

```

C  
C  
C

```

1+25.D0/16.D0*(C12I1/C66I1+1.D0)*G2**2
AS(RB,CH)=25.D0*(C22I1/C66I1+C66I1/C66I1)*G1**2
1+25.D0/16.D0*(C22I1/C66I1+1.D0)*G2**2
AS(RB,CC)=0.D0
AS(RB,CD)=0.D0
AS(RB,CE)=0.D0
AS(RC,CA)=0.D0
AS(RC,CB)=0.D0
AS(RC,CC)=(200.D0*K11X2*(H1/H2)*(C44I/C66I1)+200.D0*K22X2*
1(H1/H2)*(C55I/C66I1)+400.D0*K12X2*(H1/H2)*(C45I/C66I1))*G1**2
2+(25.D0/16.D0*K11X2*(C44I/C66I1)+25.D0/16.D0*K22X2*(C55I/C66I1)
3+25.D0/8.D0*K12X2*(C45I/C66I1))*G2**2
AS(RC,CD)=20.D0*K11X2*(H1/H2)*(C44I/C66I1)*G1
1+(5.D0/4.D0)*K11X2*(C44I/C66I1)*G2
AS(RC,CE)=20.D0*K22X2*(H1/H2)*(C55I/C66I1)*G1
1+(5.D0/4.D0)*K22X2*(C55I/C66I1)*G2
AS(RD,CA)=0.D0
AS(RD,CB)=0.D0
AS(RD,CC)=20.D0*K11X2*(H1/H2)*(C44I/C66I1)*G1
1+(5.D0/4.D0)*K11X2*(C44I/C66I1)*G2
AS(RD,CD)=61.D0/12.D0*(C11I/C66I1+C66I1/C66I1)*G1**2+1.D0/12.D0*
1(C11I/C66I1+1.D0)*G2**2+K11X2*(2.D0*(H1/H2)*(C44I/C66I1)+(C44I
2/C66I1))
AS(RD,CE)=61.D0/12.D0*(C12I/C66I1+C66I1/C66I1)*G1**2+1.D0/12.D0*
1(C12I/C66I1+1.D0)*G2**2
AS(RE,CA)=0.D0
AS(RE,CB)=0.D0
AS(RE,CC)=20.D0*K22X2*(H1/H2)*(C55I/C66I1)*G1
1+(5.D0/4.D0)*K22X2*(C55I/C66I1)*G2
AS(RE,CD)=61.D0/12.D0*(C12I/C66I1+C66I1/C66I1)*G1**2+1.D0/12.D0*
1(C12I/C66I1+1.D0)*G2**2
AS(RE,CE)=61.D0/12.D0*(C22I/C66I1+C66I1/C66I1)*G1**2+1.D0/12.D0*
1(C22I/C66I1+1.D0)*G2**2+K22X2*(2.D0*(H1/H2)*(C55I/C66I1)+(C55I
2/C66I1))

```

C  
C

CALCULATE INERTIA MATRIX

C

```

AI(RA,CA)=(H/H2)**2*(2.D0*(H1/H2)*R01/R02+1.D0)
AI(RA,CB)=0.D0
AI(RA,CC)=0.D0
AI(RA,CD)=0.D0
AI(RA,CE)=0.D0
AI(RB,CA)=0.D0
AI(RB,CB)=(H/H2)**2*(2.D0*(H1/H2)*R01/R02+1.D0)
AI(RB,CC)=0.D0
AI(RB,CD)=0.D0
AI(RB,CE)=0.D0
AI(RC,CA)=0.D0
AI(RC,CB)=0.D0
AI(RC,CC)=(H/H2)**2*(2.D0*(H1/H2)*R01/R02+1.D0)
AI(RC,CD)=0.D0
AI(RC,CE)=0.D0
AI(RD,CA)=0.D0
AI(RD,CB)=0.D0
AI(RD,CC)=0.D0
AI(RD,CD)=1.D0/12.D0+61.D0/768.D0*(R01/R02)
AI(RD,CE)=0.D0
AI(RE,CA)=0.D0
AI(RE,CB)=0.D0
AI(RE,CC)=0.D0
AI(RE,CD)=0.D0
AI(RE,CE)=1.D0/12.D0+61.D0/768.D0*(R01/R02)

```

C

CALL DNRROOT

C

CALL DNRROOT(S,AS,AI,EVAL,EVEC)

C

WRITE EIGENVALUES

C

DO 910 I=1,5

EVAL(I)=DSQRT(EVAL(I))

910 WRITE(6,933)I,EVAL(I)

```

933 FORMAT('0'.40X,'EIGENVALUE('.,I2.>')='.,D16.8)
JJJ=JJJ+1
IF(50-JJJ)951,5,5
951 STOP
END
SUBROUTINE DNROOT (M,A,B,XL,X)
SEE WRITE-UP IN IBM SSP, PAGE 31
DIMENSION A(1),B(1),XL(1),X(1)
DOUBLE PRECISION A,B,XL,X,SUMV
C COMPUTE EIGENVALUES AND EIGENVECTORS OF B
K=1
DO 100 J=2,M
L=M*(J-1)
DO 100 I=1,J
L=L+1
K=K+1
100 B(K)=B(L)
C THE MATRIX B IS A REAL SYMMETRIC MATRIX
MV=0
CALL DEIGEN (B,X,M,MV)
C FORM RECIPROCAL OF SQUARE ROOT OF EIGENVALUES. THE RESULTS
C ARE PREMULTIPLIED BY THE ASSOCIATED EIGENVECTORS.
L=0
DO 110 J=1,M
L=L+J
110 XL(J)=1.0/DSORT(DABS(B(L)))
K=0
DO 115 J=1,M
DO 115 I=1,M
K=K+1
115 B(K)=X(K)*XL(J)
C FORM (B**(-1/2))PRIME * A * (B**(-1/2))
DO 120 I=1,M
N2=0
DO 120 J=1,M
N1=M*(I-1)

```



```

L=M*(J-1)+I
X(L)=0.0
DO 120 K=1,M
N1=N1+1
N2=N2+1
120 X(L)=X(L)+B(N1)*A(N2)
L=0
DO 130 J=1,M
DO 130 I=1,J
N1=I-M
N2=M*(J-1)
L=L+1
A(L)=0.0
DO 130 K=1,M
N1=N1+M
N2=N2+1
130 A(L)=A(L)+X(N1)*B(N2)
C   COMPUTE EIGENVALUES AND EIGENVECTORS OF A
CALL DEIGEN (A,X,M,MV)
L=0
DO 140 I=1,M
L=L+1
140 XL(I)=A(L)
C   COMPUTE THE NORMALIZED EIGENVECTORS
DO 150 I=1,M
N2=0
DO 150 J=1,M
N1=I-M
L=M*(J-1)+I
A(L)=0.0
DO 150 K=1,M
N1=N1+M
N2=N2+1
150 A(L)=A(L)+B(N1)*X(N2)
I=0
K=0

```

```

DO 180 J=1,M
SUMV=0.0
DO 170 I=1,M
L=L+1
170 SUMV=SUMV+A(L)*A(L)
175 SUMV=DSQRT(SUMV)
DO 180 I=1,M
K=K+1
180 X(K)=A(K)/SUMV
RETURN
END
.....

SUBROUTINE DEIGEN

PURPOSE
  COMPUTE EIGENVALUES AND EIGENVECTORS OF A REAL SYMMETRIC
  MATRIX

USAGE
  CALL DEIGEN(A,R,N,MV)

DESCRIPTION OF PARAMETERS
  A - ORIGINAL MATRIX (SYMMETRIC), DESTROYED IN COMPUTATION.
      RESULTANT EIGENVALUES ARE DEVELOPED IN DIAGONAL OF
      MATRIX A IN DESCENDING ORDER.
  R - RESULTANT MATRIX OF EIGENVECTORS (STORED COLUMNWISE,
      IN SAME SEQUENCE AS EIGENVALUES)
  N - ORDER OF MATRICES A AND R
  MV- INPUT CODE
      0 COMPUTE EIGENVALUES AND EIGENVECTORS
      1 COMPUTE EIGENVALUES ONLY (R NEED NOT BE
          DIMENSIONED BUT MUST STILL APPEAR IN CALLING
          SEQUENCE)

```

C	REMARKS	EIGEN026
C	ORIGINAL MATRIX A MUST BE REAL SYMMETRIC (STORAGE MODE=1)	EIGEN027
C	MATRIX A CANNOT BE IN THE SAME LOCATION AS MATRIX K	EIGEN028
C		EIGEN029
C	SUBROUTINES AND FUNCTION SUBPROGRAMS REQUIRED	EIGEN030
C	NONE	EIGEN031
C		EIGEN032
C	METHOD	EIGEN033
C	DIAGONALIZATION METHOD ORIGINATED BY JACOBI AND ADAPTED	EIGEN034
C	BY VON NEUMANN FOR LARGE COMPUTERS AS FOUND IN 'MATHEMATICAL	EIGEN035
C	METHODS FOR DIGITAL COMPUTERS', EDITED BY A. RALSTON AND	EIGEN036
C	H.S. WILF, JOHN WILEY AND SONS, NEW YORK, 1962, CHAPTER 7	EIGEN037
C		EIGEN038
C	.....	EIGEN039
C		EIGEN040
C	SUBROUTINE DEIGEN(A,R,N,MV)	EIGEN041
C	DIMENSION A(1),R(1)	EIGEN042
C		EIGEN043
C	.....	EIGEN044
C		EIGEN045
C	IF A DOUBLE PRECISION VERSION OF THIS ROUTINE IS DESIRED, THE	EIGEN046
C	C IN COLUMN 1 SHOULD BE REMOVED FROM THE DOUBLE PRECISION	EIGEN047
C	STATEMENT WHICH FOLLOWS.	EIGEN048
C		EIGEN049
C	DOUBLE PRECISION A,K,ANORM,ANRMX,THR,X,Y,SINX,SINX2,COSX,	EIGEN050
C	COSX2,SINCS	EIGEN051
C		EIGEN052
C	THE C MUST ALSO BE REMOVED FROM DOUBLE PRECISION STATEMENTS	EIGEN053
C	APPEARING IN OTHER ROUTINES USED IN CONJUNCTION WITH THIS	EIGEN054
C	ROUTINE.	EIGEN055
C		EIGEN056
C	THE DOUBLE PRECISION VERSION OF THIS SUBROUTINE MUST ALSO	EIGEN057
C	CONTAIN DOUBLE PRECISION FORTRAN FUNCTIONS. SORT IN STATEMENT	EIGEN058
C	40, 68, 75, AND 78 MUST BE CHANGED TO DSORT. ABS IN STATEMENT	EIGEN059
C	62 MUST BE CHANGED TO DABS.	EIGEN060
C		EIGEN061

```

C .....EIGEN062
C .....EIGEN063
C .....EIGEN064
C .....EIGEN065
C .....EIGEN066
C .....EIGEN067
C .....EIGEN068
C .....EIGEN069
C .....EIGEN070
C .....EIGEN071
C .....EIGEN072
C .....EIGEN073
C .....EIGEN074
C .....EIGEN075
C .....EIGEN076
C .....EIGEN077
C .....EIGEN078
C .....EIGEN079
C .....EIGEN080
C .....EIGEN081
C .....EIGEN082
C .....EIGEN083
C .....EIGEN084
C .....EIGEN085
C .....EIGEN086
C .....EIGEN087
C .....EIGEN088
C .....EIGEN089
C .....EIGEN090
C .....EIGEN091
C .....EIGEN092
C .....EIGEN093
C .....EIGEN094
C .....EIGEN095
C .....EIGEN096
C .....EIGEN097

      GENERATE IDENTITY MATRIX

      IF(MV-1) 10,25,10
10  IQ=-N
    DO 20 J=1,N
      IQ=IQ+N
    DO 20 I=1,N
      IJ=IQ+I
      R(IJ)=0.0+00
      IF(I-J) 20,15,20
15  R(IJ)=1.0+00
20  CONTINUE

      COMPUTE INITIAL AND FINAL NORMS (ANORM AND ANORMX)

25  ANORM=0.0+00
    DO 35 I=1,N
      DO 35 J=1,N
        IF(I-J) 30,35,30
30  IA=I+((J-J-J))/2
      ANORM=ANORM+A(IA)*A(IA)
35  CONTINUE
      IF(ANORM) 165,165,40
40  ANORM=1.414D+00*DSQRT(ANORM)
    ANRMX=ANORM*1.0D-06/FLOAT(N)

      INITIALIZE INDICATORS AND COMPUTE THRESHOLD, THR

C .....
C .....
C .....
      IND=0
      THR=ANORM
45  THR=THR/FLOAT(N)
50  L=1
55  M=L+1
C .....

```

```

C          COMPUTE SIN AND COS
C
60  MQ=(M*M-M)/2
   LQ=(L*L-L)/2
   LM=L+MQ
62  IF(DABS(A(LM))-THR) 130,65,65
65  IND=1
   LL=L+LQ
   MM=M+MQ
   X=0.5D+00*(A(LL)-A(MM))
68  Y=-A(LM)/DSQRT(A(LM)*A(LM)+X*X)
   IF(X) 70,75,75
70  Y=-Y
75  SINX=Y/DSQRT(2.D+C0*(1.D+00+(DSQRT(1.D+00-Y*Y))))
   SINX2=SINX*SINX
78  COSX=DSQRT(1.0D+00-SINX2)
   COSX2=COSX*COSX
   SINCX =SINX*COSX

C          ROTATE L AND M COLUMNS
C
C
   ILQ=N*(L-1)
   IMQ=N*(M-1)
   DO 125 I=1,N
     IQ=(I+1-I)/2
     IF(I-L) 80,115,80
     IF(I-M) 85,115,90
80    IM=I+MQ
85    GO TO 95
90    IM=M+IQ
95    IF(I-L) 100,105,105
100   IL=I+LQ
     GO TO 110
105   IL=L+IQ
110   X=A(IL)*COSX-A(IM)*SINX
     A(IM)=A(IL)*SINX+A(IM)*COSX
EIGEN098
EIGEN099
EIGEN100
EIGEN101
EIGEN102
EIGEN103
EIGEN104
EIGEN105
EIGEN106
EIGEN107
EIGEN108
EIGEN109
EIGEN110
EIGEN111
EIGEN112
EIGEN113
EIGEN114
EIGEN115
EIGEN116
EIGEN117
EIGEN118
EIGEN119
EIGEN120
EIGEN121
EIGEN122
EIGEN123
EIGEN124
EIGEN125
EIGEN126
EIGEN127
EIGEN128
EIGEN129
EIGEN130
EIGEN131
EIGEN132
EIGEN133

```

```

A(IL)=X
115 IF(MV-1) 120,125,120
120 ILR=ILQ+I
    IMR=IMQ+I
    X=R(ILR)*COSX-R(IMR)*SINX
    R(IMR)=R(ILR)*SINX+R(IMR)*COSX
    R(ILR)=X
125 CONTINUE
    X=2.D+00*A(LM)*SINCS
    Y=A(LL)*COSX2+A(MM)*SINX2-X
    X=A(LL)*SINX2+A(MM)*COSX2+X
    A(LM)=(A(LL)-A(MM))*SINCS+A(LM)*(COSX2-SINX2)
    A(LL)=Y
    A(MM)=X
C
C      TESTS FOR COMPLETION
C
C      TEST FOR M = LAST COLUMN
C
130 IF(M-N) 135,140,135
135 M=M+1
    GO TO 60
C
C      TEST FOR L = SECOND FROM LAST COLUMN
C
140 IF(L-(N-1)) 145,150,145
145 L=L+1
    GO TO 55
150 IF(IND-1) 160,155,160
155 IND=0
    GO TO 50
C
160 IF(THR-ANRMX) 165,165,45
    COMPARE THRESHOLD WITH FINAL NORM
C
C
C
EIGEN134
EIGEN135
EIGEN136
EIGEN137
EIGEN138
EIGEN139
EIGEN140
EIGEN141
EIGEN142
EIGEN143
EIGEN144
EIGEN145
EIGEN146
EIGEN147
EIGEN148
EIGEN149
EIGEN150
EIGEN151
EIGEN152
EIGEN153
EIGEN154
EIGEN155
EIGEN156
EIGEN157
EIGEN158
EIGEN159
EIGEN160
EIGEN161
EIGEN162
EIGEN163
EIGEN164
EIGEN165
EIGEN168
EIGEN166
EIGEN167
EIGEN169

```

# C SORT EIGENVALUES AND EIGENVECTORS

EIGEN170  
EIGEN171  
EIGEN172  
EIGEN173  
EIGEN174  
EIGEN175  
EIGEN176  
EIGEN177  
EIGEN178  
EIGEN179  
EIGEN180  
EIGEN181  
EIGEN182  
EIGEN183  
EIGEN184  
EIGEN185  
EIGEN186  
EIGEN187  
EIGEN188  
EIGEN189  
EIGEN190  
EIGEN191  
EIGEN192  
EIGEN193

```

165 IQ=-N
    DO 185 I=1,N
      IQ=IQ+N
      LL=I+(I*I-I)/2
      JQ=N*(I-2)
      DO 185 J=I,N
        JQ=JQ+N
        MM=J+(J*J-J)/2
        IF(A(LL)-A(MM)) 170,185,185
170 X=A(LL)
      A(LL)=A(MM)
      A(MM)=X
      IF(MV-1) 175,185,175
175 DO 130 K=1,N
      ILR=IQ+K
      IMR=JQ+K
      X=R(ILR)
      R(ILR)=R(IMR)
180 R(IMR)=X
185 CONTINUE
      RETURN
    END
  SUBROUTINE CHECK (I)
    WRITE (3,1) I
1  FORMAT (' CHECK ',I3)
    RETURN
  END

```

```

C
C
C
C
VIBRATION OF LAMINATED ANISOTROPIC PLATES
CONSIDERING THICKNESS SHEAR AND DAMPING EFFECTS

DIMENSION S(40,40),T(40)
DIMENSION ANGLE(8),H(24),RO(24)
DIMENSION ER11(24),ER22(24),GE11(24),GE22(24)
DIMENSION VR12(24),VR21(24)
DIMENSION GR12(24),GR13(24),GR23(24),GG12(24),GG13(24),GG23(24)
DIMENSION CRT11(24),CIT11(24),CRT12(24),CIT12(24)
DIMENSION CRT22(24),CIT22(24),CRT66(24),CIT66(24)
DIMENSION CRT16(24),CIT16(24),CRT26(24),CIT26(24)
DIMENSION CRT44(24),CIT44(24),CRT45(24),CIT45(24)
DIMENSION CRT55(24),CIT55(24)
REAL K11,K22,K12
READ(5,15)J,NN,INPU1,INPU2
15 FORMAT(4I5)
READ(5,32)A,B,K11,K22,K12
32 FORMAT(5F10.4)
10 READ(5,35,END=3333)F
35 FORMAT(F10.4)
READ(5,36)(ANGLE(I),H(I),H(I+1),RO(I),I=1,J)
36 FORMAT(4F10.0)
READ(5,37)(ER11(I),ER22(I),GE11(I),GE22(I),I=1,J)
37 FORMAT(4E10.4)
READ(5,39)(VR12(I),VR21(I),I=1,J)
39 FORMAT(2F10.6)
READ(5,40)(GR12(I),GR13(I),GR23(I),GG12(I),GG13(I),GG23(I),I=1,J)
40 FORMAT(6E10.4)

C
C
C
CALCULATE STIFFNESS,DAMPING, AND DENSITY COEFFICIENTS

SMAR11=0.
SMAI11=0.
SMAR12=0.
SMAI12=0.

```



SMAR16=0.  
SMAI16=0.  
SMAR22=0.  
SMAI22=0.  
SMAR26=0.  
SMAI26=0.  
SMAR66=0.  
SMAI66=0.  
SMAR44=0.  
SMAI44=0.  
SMAR45=0.  
SMAI45=0.  
SMAR55=0.  
SMAI55=0.  
SMBR11=0.  
SMBI11=0.  
SMBR12=0.  
SMBI12=0.  
SMBR16=0.  
SMBI16=0.  
SMBR22=0.  
SMBI22=0.  
SMBR26=0.  
SMBI26=0.  
SMBR66=0.  
SMBI66=0.  
SMDR11=0.  
SMDI11=0.  
SMDR12=0.  
SMDI12=0.  
SMDR16=0.  
SMDI16=0.  
SMDR22=0.  
SMDI22=0.  
SMDR26=0.  
SMDI26=0.

```

SMDR66=0.
SMDI66=0.
SUMP0=0.
SUMP1=0.
SUMP2=0.
PI=3.141592653589793
DO 150 I=1,J
  CR11=ER11(I)/(1.-VR12(I)*VR21(I))
  CI11=ER11(I)/(1.-VR12(I)*VR21(I))*GE11(I)
  CR22=ER22(I)/(1.-VR12(I)*VR21(I))
  CI22=ER22(I)/(1.-VR12(I)*VR21(I))*GE22(I)
  CR12=VR12(I)*ER22(I)/(1.-VR12(I)*VR21(I))
  CR12=VR12(I)*ER22(I)/(1.-VR12(I)*VR21(I))*GE22(I)
  CR44=GR13(I)
  CI44=GR13(I)*GG13(I)
  CR55=GR23(I)
  CI55=GR23(I)*GG23(I)
  CR66=GR12(I)
  CI66=GR12(I)*GG12(I)
  THETA=ANGLE(I)*PI/180.
  C4=COS(THETA)*COS(THETA)*COS(THETA)*COS(THETA)
  S4=SIN(THETA)*SIN(THETA)*SIN(THETA)*SIN(THETA)
  C3S1=COS(THETA)*COS(THETA)*COS(THETA)*SIN(THETA)
  S3C1=SIN(THETA)*SIN(THETA)*SIN(THETA)*COS(THETA)
  C2S2=COS(THETA)*COS(THETA)*SIN(THETA)*SIN(THETA)
  C2=COS(THETA)*COS(THETA)
  S2=SIN(THETA)*SIN(THETA)
  CS=COS(THETA)*SIN(THETA)
  CRT11(I)=CR11*C4+2.*(CR12+2.*CR66)*C2S2+CR22*S4
  CIT11(I)=CI11*C4+2.*(CI12+2.*CI66)*C2S2+CI22*S4
  CRT22(I)=CR22*C4+2.*(CR12+2.*CR66)*C2S2+CR11*S4

```

C  
C  
C

CIT22(I)=CI22\*C4+2.\*(CI12+2.\*CI66)\*C2S2+CI11\*S4  
 CRT66(I)=CR66\*C4+(CR11+CR22-2.\*CR12-2.\*CR66)\*C2S2+CR66\*S4  
 CIT66(I)=CI66\*C4+(CI11+CI22-2.\*CI12-2.\*CI66)\*C2S2+CI66\*S4  
 CRT16(I)=(2.\*CR66+CR12-CR11)\*C3S1-(2.\*CR66+CR12-CR22)\*S3C1  
 CIT16(I)=(2.\*CI66+CI12-CI11)\*C3S1-(2.\*CI66+CI12-CI22)\*S3C1  
 CRT26(I)=- (2.\*CR66+CR12-CR22)\*C3S1+(2.\*CR66+CR12-CR11)\*S3C1  
 CIT26(I)=- (2.\*CI66+CI12-CI22)\*C3S1+(2.\*CI66+CI12-CI11)\*S3C1  
 CRT44(I)=CR44\*C2+CR55\*S2  
 CIT44(I)=CI44\*C2+CI55\*S2  
 CRT45(I)=CR55\*CS-CR44\*CS  
 CIT45(I)=CI55\*CS-CI44\*CS  
 CRT55(I)=CR55\*C2+CR44\*S2  
 CIT55(I)=CI55\*C2+CI44\*S2  
 AARI1=CRT11(I)\*(H(I+1)-H(I))  
 SMARI1=SMARI1+AARI1  
 AAI11=CIT11(I)\*(H(I+1)-H(I))  
 SMAI11=SMARI1+AAI11  
 AARI2=CRT12(I)\*(H(I+1)-H(I))  
 SMARI2=SMARI2+AARI2  
 AAI12=CIT12(I)\*(H(I+1)-H(I))  
 SMAI12=SMARI2+AAI12  
 AAR22=CRT22(I)\*(H(I+1)-H(I))  
 SMAR22=SMAR22+AAR22  
 AAI22=CIT22(I)\*(H(I+1)-H(I))  
 SMAI22=SMARI22+AAI22  
 AAR66=CRT66(I)\*(H(I+1)-H(I))  
 SMAR66=SMAR66+AAR66  
 AAI66=CIT66(I)\*(H(I+1)-H(I))  
 SMAI66=SMARI66+AAI66  
 AARI6=CRT16(I)\*(H(I+1)-H(I))  
 SMARI6=SMARI6+AARI6  
 AAI16=CIT16(I)\*(H(I+1)-H(I))  
 SMAI16=SMARI16+AAI16  
 AAR26=CRT26(I)\*(H(I+1)-H(I))  
 SMAR26=SMAR26+AAR26  
 AAI26=CIT26(I)\*(H(I+1)-H(I))

SMAI26=SMAI26+AAI26  
 AAR44=CRT44(I)\*(H(I+1))-H(I)  
 SMAR44=SMAR44+AAI44  
 AAI44=CIT44(I)\*(H(I+1))-H(I)  
 SMAI44=SMAI44+AAI44  
 AAR45=CRT45(I)\*(H(I+1))-H(I)  
 SMAR45=SMAR45+AAI45  
 AAI45=CIT45(I)\*(H(I+1))-H(I)  
 SMAI45=SMAI45+AAI45  
 AAR55=CRT55(I)\*(H(I+1))-H(I)  
 SMAR55=SMAR55+AAI55  
 AAI55=CIT55(I)\*(H(I+1))-H(I)  
 SMAI55=SMAI55+AAI55  
 BBR11=CRT11(I)\*(H(I+1))\*H(I+1)-H(I)\*H(I)  
 SMBR11=SMBR11+BBR11  
 BBI11=CIT11(I)\*(H(I+1))\*H(I+1)-H(I)\*H(I)  
 SMBI11=SMBI11+BBI11  
 BBR12=CRT12(I)\*(H(I+1))\*H(I+1)-H(I)\*H(I)  
 SMBR12=SMBR12+BBR12  
 BBI12=CIT12(I)\*(H(I+1))\*H(I+1)-H(I)\*H(I)  
 SMBI12=SMBI12+BBI12  
 BBR22=CRT22(I)\*(H(I+1))\*H(I+1)-H(I)\*H(I)  
 SMBR22=SMBR22+BBR22  
 BBI22=CIT22(I)\*(H(I+1))\*H(I+1)-H(I)\*H(I)  
 SMBI22=SMBI22+BBI22  
 BBR66=CRT66(I)\*(H(I+1))\*H(I+1)-H(I)\*H(I)  
 SMBR66=SMBR66+BBR66  
 BBI66=CIT66(I)\*(H(I+1))\*H(I+1)-H(I)\*H(I)  
 SMBI66=SMBI66+BBI66  
 BBR16=CRT16(I)\*(H(I+1))\*H(I+1)-H(I)\*H(I)  
 SMBR16=SMBR16+BBR16  
 BBI16=CIT16(I)\*(H(I+1))\*H(I+1)-H(I)\*H(I)  
 SMBI16=SMBI16+BBI16  
 BBR26=CRT26(I)\*(H(I+1))\*H(I+1)-H(I)\*H(I)  
 SMBR26=SMBR26+BBR26  
 BBI26=CIT26(I)\*(H(I+1))\*H(I+1)-H(I)\*H(I)

```

SMBI26=SMBI26+BBI26
DDR11=CRT11(I)*(H(I+1))*H(I+1)*H(I+1)-H(I)*H(I)*H(I)
SMDR11=SMDR11+DDR11
DDI11=CIT11(I)*(H(I+1))*H(I+1)*H(I+1)-H(I)*H(I)*H(I)
SMDI11=SMDI11+DDI11
DDR12=CRT12(I)*(H(I+1))*H(I+1)*H(I+1)-H(I)*H(I)*H(I)
SMDR12=SMDR12+DDR12
DDI12=CIT12(I)*(H(I+1))*H(I+1)*H(I+1)-H(I)*H(I)*H(I)
SMDI12=SMDI12+DDI12
DDR22=CRT22(I)*(H(I+1))*H(I+1)*H(I+1)-H(I)*H(I)*H(I)
SMDR22=SMDR22+DDR22
DDI22=CIT22(I)*(H(I+1))*H(I+1)*H(I+1)-H(I)*H(I)*H(I)
SMDI22=SMDI22+DDI22
DDR66=CRT66(I)*(H(I+1))*H(I+1)*H(I+1)-H(I)*H(I)*H(I)
SMDR66=SMDR66+DDR66
DDI66=CIT66(I)*(H(I+1))*H(I+1)*H(I+1)-H(I)*H(I)*H(I)
SMDI66=SMDI66+DDI66
DDR16=CRT16(I)*(H(I+1))*H(I+1)*H(I+1)-H(I)*H(I)*H(I)
SMDR16=SMDR16+DDR16
DDI16=CIT16(I)*(H(I+1))*H(I+1)*H(I+1)-H(I)*H(I)*H(I)
SMDI16=SMDI16+DDI16
DDR26=CRT26(I)*(H(I+1))*H(I+1)*H(I+1)-H(I)*H(I)*H(I)
SMDR26=SMDR26+DDR26
DDI26=CIT26(I)*(H(I+1))*H(I+1)*H(I+1)-H(I)*H(I)*H(I)
SMDI26=SMDI26+DDI26
PPO=RO(I)*(H(I+1))-H(I)
SUMPO=SUMPO+PPO
PPI=RO(I)*(H(I+1))*H(I+1)-H(I)*H(I)
SUMPI=SUMPI+PPI
PP2=RU(I)*(H(I+1))*H(I+1)*H(I+1)-H(I)*H(I)*H(I)
SUMP2=SUMP2+PP2
150
AR11=SMAR11
AI11=SMAI11
AR12=SMAR12
AI12=SMAI12
AR22=SMAR22

```

AI22=SMAI22  
AR66=SMAR66  
AI66=SMAI66  
AR16=SMAR16  
AI16=SMAI16  
AR26=SMAR26  
AI26=SMAI26  
AR44=SMAR44  
AI44=SMAI44  
AR45=SMAR45  
AI45=SMAI45  
AR55=SMAR55  
AI55=SMAI55  
BRI1=0.5\*SMBRI1  
BI11=0.5\*SMBI11  
BRI2=0.5\*SMBRI2  
BI12=0.5\*SMBI12  
BR22=0.5\*SMBR22  
BI22=0.5\*SMBI22  
BR66=0.5\*SMBR66  
BI66=0.5\*SMBI66  
BRI6=0.5\*SMBRI6  
BI16=0.5\*SMBI16  
BR26=0.5\*SMBR26  
BI26=0.5\*SMBI26  
URI1=SMURI1/3.  
DI11=SMDI11/3.  
URI2=SMURI2/3.  
DI12=SMDI12/3.  
UR22=SMUR22/3.  
DI22=SMDI22/3.  
UR66=SMUR66/3.  
DI66=SMDI66/3.  
URI6=SMURI6/3.  
DI16=SMDI16/3.  
UR26=SMUR26/3.

```

DI26=SMDI26/3.
P0=SUMPO
P1=0.5*SUMP1
P2=SUMP2/3.

C
C
C
WRITE MATERIAL PROPERTIES AND STIFFNESS COEFFICIENTS
CONSIDERING THICKNESS SHEAR AND DAMPING EFFECTS
WRITE (6,50) AR11,BR11,DI11
50 FORMAT('0',18X,'AR11= ',E12.5,5X, 'BR11= ',E12.5,5X,
1'DR11= ',E12.5)
WRITE(6,55)AI11,BI11,DI11
55 FORMAT('0',18X,'AI11= ',E12.5,5X, 'BI11= ',E12.5,5X,
1'DI11= ',E12.5)
WRITE(6,60)AR12,BR12,DR12
60 FORMAT('0',18X,'AR12= ',E12.5,5X, 'BR12= ',E12.5,5X,
1'DR12= ',E12.5)
WRITE(6,65)AI12,BI12,DI12
65 FORMAT('0',18X,'AI12= ',E12.5,5X, 'BI12= ',E12.5,5X,
1'DI12= ',E12.5)
WRITE(6,70)AR22,BR22,DR22
70 FORMAT('0',18X,'AR22= ',E12.5,5X, 'BR22= ',E12.5,5X,
1'DR22= ',E12.5)
WRITE(6,75)AI22,BI22,DI22
75 FORMAT('0',18X,'AI22= ',E12.5,5X, 'BI22= ',E12.5,5X,
1'DI22= ',E12.5)
WRITE(6,80)AR66,BR66,DR66
80 FORMAT('0',18X,'AR66= ',E12.5,5X, 'BR66= ',E12.5,5X,
1'DR66= ',E12.5)
WRITE(6,85)AI66,BI66,DI66
85 FORMAT('0',18X,'AI66= ',E12.5,5X, 'BI66= ',E12.5,5X,
1'DI66= ',E12.5)
WRITE(6,90)AR16,BR16,DR16
90 FORMAT('0',18X,'AR16= ',E12.5,5X, 'BR16= ',E12.5,5X,
1'DR16= ',E12.5)
WRITE(6,95)AI16,BI16,DI16
95 FORMAT('0',18X,'AI16= ',E12.5,5X, 'BI16= ',E12.5,5X,

```

**Page Intentionally Left Blank**



```

JXI=8*NN**2
JYI=9*NN**2
JJUR=JJUR+1
DO 500 M1=1,NN
M=M1+INPU1
DO 500 N2=1,NN
N=N2+INPU2
JUR=JUR+1

```

C C

```

      INTEGRAL CI8MK,CI8NL
      IF(M-K)502,504,502
502 CI8MK=0.
      GO TO 505
504 CI8MK=2.*M*K*PI**2
505 CONTINUE
      IF(N-L)506,508,506
506 CI8NL=0.
      GO TO 509
508 CI8NL=2.*N*L*PI**2
509 CONTINUE

```

C C C

```

      INTEGRAL CI1MK, CI1NL

```

```

      IF(M-K)512,514,512
512 CI1MK=1.
      GO TO 515
514 CI1MK=1.5
515 CONTINUE
      IF(N-L)516,518,516
516 CI1NL=1.
      GO TO 519
518 CI1NL=1.5
519 CONTINUE

```

C C C

```

      INTEGRAL CI6MK,CI6NL

```



```

C      INTEGRAL CI31MK,CI31NL
C
C      CI31MK=CI11MK
C      CI31NL=CI11NL
C
C      INTEGRAL CI34MK,CI34NL
C
C      CI34MK=CI44MK
C      CI34NL=CI44NL
C
C      INTEGRAL CI33MK, CI33NL
C
C      CI33MK=CI44MK
C      CI33NL=CI44NL
C
C      INTEGRAL CI37MK, CI37NL
C
C      CI37MK=CI44MK
C      CI37NL=CI44NL
C
C      //216 CI17NL=1.
C      JYI=JYI+1
C      800 S(JJXR,JYI)=-((DI12*CI25MK*CI24NL+(B/A)*DI16*CI30MK*CI23NL+(A/B)
C      1*DI26*CI23MK*CI30NL+DI66*CI24MK*CI25NL+A*B*K12*AI45*CI23MK
C      2*CI23NL)
C      CALCULATE SUBMATRIX
C      YRUR,YRVR,YRWR,YRZR,YRUI,YRVI,YRWI,YRXI,YRYI
C      JJYR=4*NN**2
C      DO 900 K1=1,NN
C      K=K1+INPU1
C      DO 900 L2=1,NN
C      L=L2+INPU2
C      JUR=0
C      JVR=1*NN**2
C      JWK=2*NN**2
C      JXR=3*NN**2

```

```

JYR=4*NN**2
JUI=5*NN**2
JVI=6*NN**2
JWI=7*NN**2
JXI=8*NN**2
JYI=9*NN**2
JJYR=JJYR+1
DO 900 M1=1,NN
M=M1+INPUI
DO 900 N2=1,NN
N=N2+INPU2
JUR=JUR+1

C
C
C
      INTEGRAL CI37MK, CI37NL
      IF(M-K)902,904,902
      902 CI37MK=0.
      GO TO 905
      904 CI37MK=0.
      905 CONTINUE
      IF(N-L)906,908,906
      906 CI37NL=0.
      GO TO 909
      908 CI37NL=0.
      909 CONTINUE

C
C
C
      INTEGRAL CI36MK, CI36NL
      CI36MK=CI37MK
      CI36NL=CI37NL

C
C
C
      INTEGRAL CI55MK, CI55NL
      IF(M-K)912,914,912
      912 CI55MK=0.
      GO TO 915

```

```

914 CI55MK=2.*M*K*PI**2
915 CONTINUE
    IF(N-L)916,918,916
916 CI55NL=0.
    GO TO 919
918 CI55NL=2.*N*L*PI**2
919 CONTINUE
C
C    INTEGRAL CI35MK, CI35NL
C
    IF(M-K)922,924,922
922 CI35MK=1.
    GO TO 925
924 CI35MK=1.5
925 CONTINUE
    IF(N-L)926,928,926
926 CI35NL=1.0
    GO TO 929
928 CI35NL=1.5
929 CONTINUE
C
C    INTEGRAL CI41MK, CI41NL
C
    CI41MK=CI35MK
    CI41NL=CI35NL
C
    INTEGRAL CI57MK, CI57NL
C
    CI57MK=CI55MK
    CI57NL=CI55NL
C
    INTEGRAL CI42MK, CI42NL
C
    CI42MK=CI37MK
    CI42NL=CI37NL
C

```

C	INTEGRAL CI43MK, CI43NL
C	
	CI43MK=CI37MK
	CI43NL=CI37NL
C	
C	INTEGRAL CI15MK, CI15NL
C	
	CI15MK=0.
	CI15NL=0.
C	
C	INTEGRAL CI12MK, CI12NL
C	
	CI12MK=CI35MK
	CI12NL=CI35NL
C	
C	INTEGRAL CI24MK, CI24NL
C	
	CI24MK=CI37MK
	CI24NL=CI37NL
C	
C	INTEGRAL CI25MK, CI25NL
C	
	CI25MK=CI37MK
	CI25NL=CI37NL
C	
C	INTEGRAL CI23MK, CI23NL
C	
	CI23MK=CI35MK
	CI23NL=CI35NL
C	
C	INTEGRAL CI30MK, CI30NL
C	
	CI30MK=CI55MK
	CI30NL=CI55NL
C	
C	INTEGRAL CI22MK, CI22NL



```

S(JJYR,JWI)=- (B*K12*AI45*CI15MK*CI12NL+A*K22*AI55*CI12MK*CI15NL)
JXI=JXI+1
S(JJYR,JXI)=- (DI12*CI25MK*CI24NL+(B/A)*DI16*CI30MK*CI23NL+(A/B)
1*DI26*CI23MK*CI30NL+DI66*CI24MK*CI25NL+A*B*K12*AI45*CI23MK
2*CI23NL)
JYI=JYI+1
900 S(JJYR,JYI)=- ((A/B)*DI22*CI22MK*CI29NL+2.*DI26*CI27MK*CI27NL+(B/A)
1*DI66*CI29MK*CI22NL+A*B*K22*AI55*CI22MK*CI22NL)
C CALCULATE SUBMATRIX
C UIUR,UIVR,UIWR,UIXR,UIYR,UIUI,UIVI,UIWI,UIXI,UIYI
JJUI=5*NN**2
DO 1000 KI=1,NN
K=K1+INPU1
DO 1000 L2=1,NN
L=L2+INPU2
JUR=0
JVR=1*NN**2
JWR=2*NN**2
JXR=3*NN**2
JYR=4*NN**2
JUI=5*NN**2
JVI=6*NN**2
JWI=7*NN**2
JXI=8*NN**2
JYI=9*NN**2
JJUI=JJUI+1
DO 1000 M1=1,NN
M=M1+INPU1
DO 1000 N2=1,NN
N=N2+INPU2
JUR=JUR+1

C
C INTEGRAL CI8MK,CI8NL
IF(M-K)1002,1004,1002
1002 CI8MK=0.
GO TO 1005

```



```

1004 CI8MK=2.*M*K*PI**2
1005 CONTINUE
      IF(N-L)1006,1008,1006
1006 CI8NL=0.
      GO TO 1009
1008 CI8NL=2.*N*L*PI**2
1009 CONTINUE
C
C      INTEGRAL CI1MK, CI1NL
C
      IF(M-K)1012,1014,1012
1012 CI1MK=1.
      GO TO 1015
1014 CI1MK=1.5
1015 CONTINUE
      IF(N-L)1016,1018,1016
1016 CI1NL=1.
      GO TO 1019
1018 CI1NL=1.5
1019 CONTINUE
C
C      INTEGRAL CI6MK, CI6NL
C
      IF(M-K)1022,1024,1022
1022 CI6MK=0.
      GO TO 1025
1024 CI6MK=0.
1025 CONTINUE
      IF(N-L)1026,1028,1026
1026 CI6NL=0.
      GO TO 1029
1028 CI6NL=0.
1029 CONTINUE
C
C      INTEGRAL CI5MK, CI5NL
C

```

CI5MK=CI6MK  
CI5NL=CI6NL

C

INTEGRAL CI4MK,CI4NL

C

C

CI4MK=CI6MK  
CI4NL=CI6NL

C

INTEGRAL CI10MK,CI10NL

C

C

CI10MK=CI8MK  
CI10NL=CI8NL

C

INTEGRAL CI3MK,CI3NL

C

C

CI3MK=CI1MK  
CI3NL=CI1NL

C

INTEGRAL CI44MK,CI44NL

C

C

CI44MK=CI8MK  
CI44NL=CI8NL

C

INTEGRAL CI31MK,CI31NL

C

C

CI31MK=CI1MK  
CI31NL=CI1NL

C

INTEGRAL CI34MK,CI34NL

C

C

CI34MK=CI4MK  
CI34NL=CI4NL

C

INTEGRAL CI33MK, CI33NL

C

C

CI33MK=CI4MK

C

C	CI33NL=CI4NL
C	INTEGRAL CI37MK, CI37NL
C	
	CI37MK=CI4MK
	CI37NL=CI4NL
C	
C	INTEGRAL CI36MK, CI36NL
C	
	CI36MK=CI4MK
	CI36NL=CI4NL
C	
C	INTEGRAL CI55MK, CI55NL
C	
	CI55MK=CI8MK
	CI55NL=CI8NL
C	
C	INTEGRAL CI35MK, CI35NL
C	
	CI35MK=CI1MK
	CI35NL=CI1NL
	S(JJUI, JUR)=+((B/A)*AI11*CI8MK*CI1NL+2.*AI16*CI6MK*CI6NL+(A/B)
	1*AI66*CI1MK*CI8NL)
	JVR=JVR+1
	S(JJUI, JVR)=+(AI12*CI5MK*CI4NL+(B/A)*AI16*CI10MK*CI3NL+(A/B)
	1*AI26*CI3MK*CI10NL+AI66*CI4MK*CI5NL)
	JWR=JWR+1
	S(JJUI, JWR)=0.
	JXR=JXR+1
	S(JJUI, JXR)=+((B/A)*BI11*CI44MK*CI31NL+BI16*CI34MK*CI33NL+BI16
	1*CI33MK*CI34NL+(A/B)*BI66*CI31MK*CI44NL)
	JYR=JYR+1
	S(JJUI, JYR)=+(BI12*CI37MK*CI36NL+(B/A)*BI16*CI55MK*CI35NL+(A/B)
	1*BI26*CI35MK*CI55NL+BI66*CI36MK*CI37NL)
	JUI=JUI+1
	S(JJUI, JUI)=(B/A)*AR11*CI8MK*CI1NL+2.*AR16*CI6MK*CI6NL+(A/B)

```

1*AR66*CI1MK*CI8NL-W2*A*B*P0*CI1MK*CI1NL
  JVI=JVI+1
  S(JJUI,JVI)=ARI2*CI5MK*CI4NL+(B/A)*ARI6*CI10MK*CI3NL+(A/B)
1*AR26*CI3MK*CI10NL+AR66*CI4MK*CI5NL
  JWI=JWI+1
  S(JJUI,JWI)=0.
  JXI=JXI+1
  S(JJUI,JXI)=(B/A)*BR11*CI44MK*CI31NL+BR16*CI34MK*CI33NL
1*BR16*CI33MK*CI34NL+(A/B)*BR66*CI31MK*CI44NL-W2*A*B*PI*CI31MK
2*CI31NL
  JYI=JYI+1
1000 S(JJUI,JYI)=BR12*CI37MK*CI36NL+(B/A)*BR16*CI55MK*CI35NL+(A/B)
1*BR26*CI35MK*CI55NL+BR66*CI36MK*CI37NL
C  CALCULATE SUHMATRIX
C  VIUR,VIVR,VIVR,VIXR,VIXR,VIVR,VIVI,VIVI,VIVI,VIVI
  JJVI=6*NN**2
  DO 1100 KI=1,NN
    K=KI+INPU1
  DO 1100 L2=1,NN
    L=L2+INPU2
  JUR=0
  JVR=1*NN**2
  JWR=2*NN**2
  JXR=3*NN**2
  JYR=4*NN**2
  JUI=5*NN**2
  JVI=6*NN**2
  JWI=7*NN**2
  JXI=8*NN**2
  JYI=9*NN**2
  JJVI=JJVI+1
  DO 1100 M1=1,NN
    M=M1+INPU1
  DO 1100 N2=1,NN
    N=N2+INPU2
  JUR=JUR+1

```

```

C      INTEGRAL CI4MK, CI4NL
C
C      IF(M-K)1102,1104,1102
1102 CI4MK=0.
      GO TO 1105
1104 CI4MK=0.
1105 CONTINUE
      IF(N-L)1106,1108,1106
1106 CI4NL=0.
      GO TO 1109
1108 CI4NL=0.
1109 CONTINUE
C
C      INTEGRAL CI5MK, CI5NL
C
C      CI5MK=CI4MK
C      CI5NL=CI4NL
C
C      INTEGRAL CI3MK, CI3NL
C
C      IF(M-K)1112,1114,1112
1112 CI3MK=1.
      GO TO 1115
1114 CI3MK=1.5
1115 CONTINUE
      IF(N-L)1116,1118,1116
1116 CI3NL=1.
      GO TO 1119
1118 CI3NL=1.5
1119 CONTINUE
C
C      INTEGRAL CI10MK, CI10NL
C
C      IF(M-K)1122,1124,1122
1122 CI10MK=0.

```

```

GO TO 1125
1124 CI10MK=2.*MK*PI**2
1125 CONTINUE
IF(N-L)1126,1128,1126
1126 CI10NL=0.
GO TO 1129
1128 CI10NL=2.*NL*PI**2
1129 CONTINUE
C
C   INTEGRAL CI2MK, CI2NL
C
C12MK=CI3MK
C12NL=CI3NL
C
C   INTEGRAL CI9MK, CI9NL
C
C19MK=CI10MK
C19NL=CI10NL
C
C   INTEGRAL CI7MK, CI7NL
C
C17MK=CI4MK
C17NL=CI4NL
C
C   INTEGRAL CI39MK, CI39NL
C
C139MK=CI4MK
C139NL=CI4NL
C
C   INTEGRAL CI40MK, CI40NL
C
C140MK=CI4MK
C140NL=CI4NL
C
C   INTEGRAL CI56MK, CI56NL
C
C

```

CI56MK=CI10MK  
 CI56NL=CI10NL  
 C  
 C  
 C  
 INTEGRAL CI38MK, CI38NL  
 C  
 C  
 C  
 CI38MK=CI3MK  
 CI38NL=CI3NL  
 C  
 C  
 C  
 INTEGRAL CI41MK, CI41NL  
 C  
 C  
 C  
 CI41MK=CI3MK  
 CI41NL=CI3NL  
 C  
 C  
 C  
 INTEGRAL CI57MK, CI57NL  
 C  
 C  
 C  
 CI57MK=CI10MK  
 CI57NL=CI10NL  
 C  
 C  
 C  
 INTEGRAL CI42MK, CI42NL  
 C  
 C  
 C  
 CI42MK=CI4MK  
 CI42NL=CI4NL  
 C  
 C  
 C  
 INTEGRAL CI43MK, CI43NL  
 C  
 C  
 C  
 CI43MK=CI4MK  
 CI43NL=CI4NL  
 S(JJVI, JUR)=+(AI12\*CI5MK\*CI4NL+(B/A)\*AI16\*CI10MK\*CI3NL+(A/B)  
 1\*AI26\*CI3MK\*CI10NL+AI66\*CI4MK\*CI5NL)  
 JVR=JVR+1  
 S(JJVI, JVR)=+((A/H)\*AI22\*CI2MK\*CI9NL+2.\*AI26\*CI7MK\*CI7NL+(B/A)  
 1\*AI66\*CI9MK\*CI2NL)  
 JWR=JWR+1  
 S(JJVI, JWR)=0.  
 JXR=JXR+1  
 S(JJVI, JXR)=+(BI12\*CI39MK\*CI40NL+(B/A)\*BI16\*CI56MK\*CI38NL+(A/B)

```

1*BI26*CI38MK*CI56NL+BI66*CI40MK*CI39NL)
JYR=JYR+1
S(JJVI,JYR)=+((A/B)*BI22*CI41MK*CI57NL+BI26*CI42MK*CI43NL+BI26
1*CI43MK*CI42NL+(B/A)*BI66*CI57MK*CI41NL)
JUI=JUI+1
S(JJVI,JUI)=AR12*CI5MK*CI4NL+(B/A)*AR16*CI10MK*CI3NL+(A/B)
1*AR26*CI3MK*CI10NL+AR66*CI4MK*CI5NL
JVI=JVI+1
S(JJVI,JVI)=(A/B)*AR22*CI2MK*CI9NL+2.*AR26*CI7MK*CI7NL+(B/A)
1*AR66*CI9MK*CI2NL-W2*A*BP0*CI2MK*CI2NL
JWI=JWI+1
S(JJVI,JWI)=0.
JXI=JXI+1
S(JJVI,JXI)=BR12*CI39MK*CI40NL+(B/A)*BR16*CI56MK*CI38NL+(A/B)
1*BR26*CI38MK*CI56NL+BR66*CI40MK*CI39NL
JYI=JYI+1
1100 S(JJVI,JYI)=(A/B)*BR22*CI41MK*CI57NL+BR26*CI42MK*CI43NL+BR26
1*CI43MK*CI42NL+(B/A)*BR66*CI57MK*CI41NL-W2*A*BP1*CI41MK*CI41NL
C CALCULATE SUBMATRIX
C WIUR,WIVR,WIWR,WIXR,WIYR,WIUI,WIVI,WIWI,WIXI,WIYI
JJWI=7*NN**2
DO 1200 KI=1,NN
K=KI+INPU1
DO 1200 L2=1,NN
L=L2+INPU2
JUR=0
JVR=1*NN**2
JWR=2*NN**2
JXR=3*NN**2
JYR=4*NN**2
JUI=5*NN**2
JVI=6*NN**2
JWI=7*NN**2
JXI=8*NN**2
JYI=9*NN**2
JJWI=JJWI+1

```



```

DD 1200 M1=1,NN
M=M1+INPU1
DO 1200 N2=1,NN
N=N2+INPU2
JUR=JUR+1

C
C
C
INTEGRAL CI20MK, CI20NL

IF(M-K)1202,1204,1202
1202 CI20MK=0.
GO TO 1205
1204 CI20MK=2.0*M*K*PI**2
1205 CONTINUE
IF(N-L)1206,1208,1206
1206 CI20NL=0.
GO TO 1209
1208 CI20NL=2.0*N*L*PI**2
1209 CONTINUE

C
C
C
INTEGRAL CI17MK, CI17NL

IF(M-K)1212,1214,1212
1212 CI17MK=1.
GO TO 1215
1214 CI17MK=1.5
1215 CONTINUE
IF(N-L)1216,1218,1216
INTEGRAL CI36MK, CI36NL

C
C
CI36MK=CI14MK
CI36NL=CI14NL

C
C
C
INTEGRAL CI55MK, CI55NL

CI55MK=CI18MK
CI55NL=CI18NL

```

```

C
C
C
      INTEGRAL CI35MK, CI35NL

      CI35MK=CI11MK
      CI35NL=CI11NL
      S(JJUR,JUR)=(B/A)*AR11*CI8MK*CI11NL+2.*AR16*CI6MK*CI6NL+(A/B)
      1*AR66*CI11MK*CI8NL-W2*A*B*PO*CI11MK*CI11NL
      JVR=JVR+1
      S(JJUR,JVR)=AR12*CI5MK*CI4NL+(B/A)*AR16*CI10MK*CI3NL+(A/B)
      1*AR26*CI3MK*CI10NL+AR66*CI4MK*CI5NL
      JWR=JWR+1
      S(JJUR,JWR)=0.
      JXR=JXR+1
      S(JJUR,JXR)=(B/A)*BR11*CI44MK*CI31NL+BR16*CI34MK*CI33NL
      1+BR16*CI33MK*CI34NL+(A/B)*BR66*CI31MK*CI44NL-W2*A*B*PI*CI31MK
      2*CI31NL
      JYR=JYR+1
      S(JJUR,JYR)=BR12*CI37MK*CI36NL+(B/A)*BR16*CI55MK*CI35NL+(A/B)
      1*BR26*CI35MK*CI55NL+BR66*CI36MK*CI37NL
      JUI=JUI+1
      S(JJUR,JUI)=-((B/A)*AI11*CI8MK*CI1NL+2.*AI16*CI6MK*CI6NL+(A/B)
      1*AI66*CI11MK*CI8NL)
      JVI=JVI+1
      S(JJUR,JVI)=-((AI12*CI5MK*CI4NL+(B/A)*AI16*CI10MK*CI3NL+(A/B)
      1*AI26*CI3MK*CI10NL+AI66*CI4MK*CI5NL)
      JWI=JWI+1
      S(JJUR,JWI)=0.
      JXI=JXI+1
      S(JJUR,JXI)=-((B/A)*BI11*CI44MK*CI31NL+BI16*CI34MK*CI33NL+BI16
      1*CI33MK*CI34NL+(A/B)*BI66*CI31MK*CI44NL)
      JYI=JYI+1
      500 S(JJUR,JYI)=-((BI12*CI37MK*CI36NL+(B/A)*BI16*CI55MK*CI35NL+(A/B)
      1*BI26*CI35MK*CI55NL+BI66*CI36MK*CI37NL)
      CALCULATE SUBMATRIX
      VRUR,VRVR,VRWR,VRXR,VRUI,VRVI,VRWI,VRXI,VRXI
      JJVR=1*NN**2

```

```

DO 600 K1=1,NN
K=K1+INPUT
DO 600 L2=1,NN
L=L2+INPUT2
JUR=0
JVR=1*NN**2
JWR=2*NN**2
JXR=3*NN**2
JYR=4*NN**2
JUI=5*NN**2
JVI=6*NN**2
JWI=7*NN**2
JXI=8*NN**2
JYI=9*NN**2
JJVR=JJVR+1
DO 600 M1=1,NN
M=M1+INPUT
DO 600 N2=1,NN
N=N2+INPUT2
JUR=JUR+1

```

```

C
C
C      INTEGRAL CI4MK, CI4NL

```

```

IF(M-K)602,604,602
602 CI4MK=0.
GO TO 605
604 CI4MK=0.
605 CONTINUE
IF(N-L)606,608,606
606 CI4NL=0.
GO TO 609
608 CI4NL=0.
609 CONTINUE

```

```

C
C
C      INTEGRAL CI5MK, CI5NL

```

```

C      CI5MK=CI4MK
C      CI5NL=CI4NL
C      INTEGRAL CI3MK, CI3NL
C      IF(M-K)612,614,612
612 CI3MK=1.
GO TO 615
614 CI3MK=1.5
615 CONTINUE
C      IF(N-L)616,618,616
616 CI3NL=1.
GO TO 619
618 CI3NL=1.5
619 CONTINUE
C      INTEGRAL CI10MK, CI10NL
C      IF(M-K)622,624,622
622 CI10MK=0.
GO TO 625
624 CI10MK=2.*M*K*PI**2
625 CONTINUE
C      IF(N-L)626,628,626
626 CI10NL=0.
GO TO 629
628 CI10NL=2.*N*L*PI**2
629 CONTINUE
C      INTEGRAL CI2MK, CI2NL
C      CI2MK=CI3MK
C      CI2NL=CI3NL
C      INTEGRAL CI9MK, CI9NL
C

```

CI9MK=CI10MK  
CI9NL=CI10NL

C  
C  
C

INTEGRAL CI7MK, CI7NL

CI7MK=CI4MK  
CI7NL=CI4NL

C  
C  
C

INTEGRAL CI39MK, CI39NL

CI39MK=CI4MK  
CI39NL=CI4NL

C  
C  
C

INTEGRAL CI40MK, CI40NL

CI40MK=CI4MK  
CI40NL=CI4NL

C  
C  
C

INTEGRAL CI56MK, CI56NL

CI56MK=CI10MK  
CI56NL=CI10NL

C  
C  
C

INTEGRAL CI38MK, CI38NL

CI38MK=CI3MK  
CI38NL=CI3NL

C  
C  
C

INTEGRAL CI41MK, CI41NL

CI41MK=CI3MK  
CI41NL=CI3NL

C  
C  
C

INTEGRAL CI57MK, CI57NL

CI57MK=CI10MK



```

600 S(JJVR,JYI)=-((A/B)*BI22*CI41MK*CI57NL+BI26*CI42MK*CI43NL+BI26
1*CI43MK*CI42NL+(B/A)*BI66*CI57MK*CI41NL)
C CALCULATE SUBMATRIX
C WRUR,WRVR,WRWR,WRXR,WRXR,WRUI,WRVI,WRWI,WRXI,WRXI
JJWR=2*NN**2
DO 700 K1=1,NN
K=K1+INPU1
DO 700 L2=1,NN
L=L2+INPU2
JUR=0
JVR=1*NN**2
JWR=2*NN**2
JXR=3*NN**2
JYR=4*NN**2
JUI=5*NN**2
JVI=6*NN**2
JWI=7*NN**2
JXI=8*NN**2
JYI=9*NN**2
JJWR=JJWR+1
DO 700 M1=1,NN
M=M1+INPU1
DO 700 N2=1,NN
N=N2+INPU2
JUR=JUR+1
C
C INTEGRAL CI20MK, CI20NL
C
IF(M-K) 702,704,702
702 CI20MK=0.
GO TO 705
704 CI20MK=2.0*M*K*PI**2
705 CONTINUE
IF(N-L) 706,708,706
706 CI20NL=0.
GO TO 709

```

```

708 CI20NL=2.0*N*L*PI**2
709 CONTINUE
C
C      INTEGRAL CI17MK,CI17NL
C
      IF(M-K)712,714,712
712 CI17MK=1.
   GO TO 715
714 CI17MK=1.5
715 CONTINUE
      IF(N-L)716,718,716
716 CI17NL=1.
   GO TO 719
718 CI17NL=1.5
719 CONTINUE
C
C      INTEGRAL CI18MK ,CI18NL
C
      CI18MK=0.
      CI18NL=0.
C
C      INTEGRAL CI13MK, CI13NL
C
      CI13MK=0.
      CI13NL=0.
C
C      INTEGRAL CI11MK, CI11NL
C
      CI11MK=CI17MK
      CI11NL=CI17NL
C
C      INTEGRAL CI15MK, CI15NL
C
      CI15MK=CI13MK
      CI15NL=CI13NL
C

```



```

C
C
INTEGRAL CI12MK, CI12NL

CI12MK=CI11MK
CI12NL=CI11NL
S(JJWR,JUR)=0.
JVR=JVR+1
S(JJWR,JVR)=0.
JWR=JWR+1
S(JJWR,JWR)=(B/A)*K11*AR44*CI20MK*CI17NL+2.*K12*AR45*CI18MK
1*CI18NL+(A/B)*K22*AR55*CI17MK*CI20NL-W2*A*B*P0*CI17MK*CI17NL
JXR=JXR+1
S(JJWR,JXR)=H*K11*AR44*CI13MK*CI11NL+A*K12*AR45*CI11MK*CI13NL
JYP=JYP+1
S(JJWR,JYP)=B*K12*AR45*CI15MK*CI12NL+A*K22*AR55*CI12MK*CI15NL
JUI=JUI+1
S(JJWR,JUI)=0.
JVI=JVI+1
S(JJWR,JVI)=0.
JWI=JWI+1
S(JJWR,JWI)=-((B/A)*K11*AI44*CI20MK*CI17NL+2.*K12*AI45*CI18MK
1*CI18NL+(A/B)*K22*AI55*CI17MK*CI20NL)
JXI=JXI+1
S(JJWR,JXI)=-((B*K11*AI44*CI13MK*CI11NL+A*K12*AI45*CI11MK*CI13NL)
JYI=JYI+1
700 S(JJWR,JYI)=-((B*K12*AI45*CI15MK*CI12NL+A*K22*AI55*CI12MK*CI15NL)
C CALCULATE SUBMATRIX
C XRUR,XRVR,XRWR,XRRR,XRYR,XRUI,XRVI,XRWI,XRXI,XRYI
JJXR=3*NN**2
DO 800 K1=1,NN
K=K1+INPU1
DO 800 L2=1,NN
L=L2+INPU2
JUR=0
JVR=1*NN**2
JWR=2*NN**2
JXR=3*NN**2

```

```

JYR=4*NN**2
JUI=5*NN**2
JVI=6*NN**2
JWI=7*NN**2
JXI=8*NN**2
JYI=9*NN**2
JJXR=JJXR+1
DO 800 MI=1,NN
M=M1+INPU1
DO 800 N2=1,NN
N=N2+INPU2
JUR=JUR+1

C
C
C
      INTEGRAL CI44MK, CI44NL
      IF(M-K)802,804,802
      802 CI44MK=0.
      GO TO 805
      804 CI44MK=2.*M*K*PI**2
      805 CONTINUE
      IF(N-L)806,808,806
      806 CI44NL=0.
      GO TO 809
      808 CI44NL=2.*N*L*PI**2
      809 CONTINUE

C
C
C
      INTEGRAL CI31MK, CI31NL
      IF(M-K)812,814,812
      812 CI31MK=1.
      GO TO 815
      814 CI31MK=1.5
      815 CONTINUE
      IF(N-L)816,818,816
      816 CI31NL=1.
      GO TO 819

```

```

818 CI31NL=1.5
819 CONTINUE
C
C   INTEGRAL CI33MK, CI33NL
C
      IF(M-K)822,824,822
822 CI33MK=0.
      GO TO 825
824 CI33MK=0.
825 CONTINUE
      IF(N-L)826,828,826
826 CI33NL=0.
      GO TO 829
828 CI33NL=0.
829 CONTINUE
C
C   INTEGRAL CI34MK, CI34NL
C
      CI34MK=CI33MK
      CI34NL=CI33NL
C
C   INTEGRAL CI39MK, CI39NL
C
      CI39MK=CI33MK
      CI39NL=CI33NL
C
C   INTEGRAL CI40MK, CI40NL
C
      CI40MK=CI33MK
      CI40NL=CI33NL
C
C   INTEGRAL CI56MK, CI56NL
C
      CI56MK=CI44MK
      CI56NL=CI44NL
C

```

C	INTEGRAL CI38MK, CI38NL
C	CI38MK=CI31MK
	CI38NL=CI31NL
C	
C	INTEGRAL CI13MK, CI13NL
C	CI13MK=0.
	CI13NL=0.
C	
C	INTEGRAL CI11MK, CI11NL
C	CI11MK=CI31MK
	CI11NL=CI31NL
C	
C	INTEGRAL CI28MK, CI28NL
C	CI28MK=CI44MK
	CI28NL=CI44NL
C	
C	INTEGRAL CI21MK, CI21NL
C	CI21MK=CI31MK
	CI21NL=CI31NL
C	
C	INTEGRAL CI26MK, CI26NL
C	CI26MK=CI33MK
	CI26NL=CI33NL
C	
C	INTEGRAL CI25MK, CI25NL
C	CI25MK=CI33MK
	CI25NL=CI33NL
C	
C	INTEGRAL CI24MK, CI24NL

C  
CI24MK=CI33MK  
CI24NL=CI33NL  
  
C  
INTEGRAL CI30MK, CI30NL  
  
C  
CI30MK=CI44MK  
CI30NL=CI44NL  
  
C  
INTEGRAL CI23MK, CI23NL  
  
C  
CI23MK=CI31MK  
CI23NL=CI31NL  
S(JJXR,JUR)=(B/A)\*BR11\*CI44MK\*CI31NL+BR16\*CI34MK\*CI33NL+BR16  
1\*CI33MK\*CI34NL+(A/B)\*BR66\*CI31MK\*CI44NL-W2\*A\*BP1\*CI31MK\*CI31NL  
JVR=JVR+1  
S(JJXR,JVR)=BR12\*CI39MK\*CI40NL+(B/A)\*BR16\*CI56MK\*CI38NL+(A/B)  
1\*BR26\*CI38MK\*CI56NL+BR66\*CI40MK\*CI39NL  
JWR=JWR+1  
S(JJXR,JWR)=B\*K11\*AR44\*CI13MK\*CI11NL+A\*K12\*AR45\*CI11MK\*CI13NL  
JXR=JXR+1  
S(JJXR,JXR)=(B/A)\*DR11\*CI28MK\*CI21NL+2.\*DR16\*CI26MK\*CI26NL+(A/B)  
1\*DR66\*CI21MK\*CI28NL+A\*B\*K11\*AR44\*CI21MK\*CI21NL-W2\*A\*BP2\*CI21MK  
2\*CI21NL  
JYR=JYR+1  
S(JJXR,JYR)=DR12\*CI25MK\*CI24NL+(B/A)\*DR16\*CI30MK\*CI23NL+(A/B)  
1\*DR26\*CI23MK\*CI30NL+DR66\*CI24MK\*CI25NL+A\*B\*K12\*AR45\*CI23MK  
2\*CI23NL  
JUI=JUI+1  
S(JJXR,JUI)=-((B/A)\*BI11\*CI44MK\*CI31NL+BI16\*CI34MK\*CI33NL  
1\*BI16\*CI33MK\*CI34NL+(A/B)\*BI66\*CI31MK\*CI44NL)  
JVI=JVI+1  
S(JJXR,JVI)=-((BI12\*CI39MK\*CI40NL+(B/A)\*BI16\*CI56MK\*CI38NL+(A/B)  
1\*BI26\*CI38MK\*CI56NL+BI66\*CI40MK\*CI39NL)  
JWI=JWI+1  
S(JJXR,JWI)=-((B\*K11\*AI44\*CI13MK\*CI11NL+A\*K12\*AI45\*CI11MK

```

1*CI13NL)
  JXI=JXI+1
  S(JJXR,JXI)=-((B/A)*DI11*CI28MK*CI21NL+2.*DI16*CI26MK*CI26NL
  1+(A/B)*DI66*CI21MK*CI28NL+A*B*K11*AI44*CI21MK*CI21NL)
  GO TO 1219
1218 CI17NL=1.5
1219 CONTINUE
C
C
C
  INTEGRAL CI18MK , CI18NL
  CI18MK=0.
  CI18NK=0.
C
C
C
  INTEGRAL CI13MK, CI13NL
  CI13MK=0.
  CI13NL=0.
C
C
C
  INTEGRAL CI11MK, CI11NL
  CI11MK=CI17MK
  CI11NL=CI17NL
C
C
C
  INTEGRAL CI15MK, CI15NL
  CI15MK=CI13MK
  CI15NL=CI13NL
C
C
C
  INTEGRAL CI12MK, CI12NL
  CI12MK=CI11MK
  CI12NL=CI11NL
  S(JJWI,JUR)=0.
  JVR=JVR+1
  S(JJWI,JVR)=0.
  JWR=JWR+1

```

```

S(JJWI,JWR)=+((B/A)*K11*AI44*CI20MK*CI17NL+2.*K12*AI45*CI18MK
1*CI18NL+(A/B)*K22*AI55*CI17MK*CI20NL)
JXR=JXR+1
S(JJWI,JXR)=+(B*K11*AI44*CI13MK*CI11NL+A*K12*AI45*CI11MK*CI13NL)
JYR=JYR+1
S(JJWI,JYR)=+(B*K12*AI45*CI15MK*CI12NL+A*K22*AI55*CI12MK*CI15NL)
JUI=JUI+1
S(JJWI,JUI)=0.
JVI=JVI+1
S(JJWI,JVI)=0.
JWI=JWI+1
S(JJWI,JWI)=(B/A)*K11*AR44*CI20MK*CI17NL+2.*K12*AR45*CI18MK
1*CI18NL+(A/B)*K22*AR55*CI17MK*CI20NL-W2*A*B*P0*CI17MK*CI17NL
JXI=JXI+1
JYI=JYI+1
S(JJWI,JXI)=B*K11*AR44*CI13MK*CI11NL+A*K12*AR45*CI11MK*CI13NL
1200 S(JJWI,JYI)=B*K12*AR45*CI15MK*CI12NL+A*K22*AR55*CI12MK*CI15NL
C CALCULATE SUBMATRIX
C XIUR,XIVR,XIWR,XIXR,XIYR,XIUI,XIVI,XIWI,XIXI,XIYI
JJXI=8*NN**2
DO 1300 KI=1,NN
K=KI+INPU1
DO 1300 L2=1,NN
L=L2+INPU2
JUR=0
JVR=1*NN**2
JWR=2*NN**2
JXR=3*NN**2
JYR=4*NN**2
JUI=5*NN**2
JVI=6*NN**2
JWI=7*NN**2
JXI=8*NN**2
JYI=9*NN**2
JJXI=JJXI+1
DO 1300 MI=1,NN

```

```

M=M1+INPUT1
DO 1300 N2=1,NN
N=N2+INPUT2
JUR=JUR+1

C
C
C
      INTEGRAL CI44MK, CI44NL
      IF(M-K)1302,1304,1302
1302 CI44MK=0.
      GO TO 1305
1304 CI44MK=2.*M*K*PI**2
1305 CONTINUE
      IF(N-L)1306,1308,1306
1306 CI44NL=0.
      GO TO 1309
1308 CI44NL=2.*N*L*PI**2
1309 CONTINUE

C
C
C
      INTEGRAL CI31MK, CI31NL
      IF(M-K)1312,1314,1312
1312 CI31MK=1.
      GO TO 1315
1314 CI31MK=1.5
1315 CONTINUE
      IF(N-L)1316,1318,1316
1316 CI31NL=1.
      GO TO 1319
1318 CI31NL=1.5
1319 CONTINUE

C
C
C
      INTEGRAL CI33MK, CI33NL
      IF(M-K)1322,1324,1322
1322 CI33MK=0.
      GO TO 1325

```



```

1324 CI33MK=0.
1325 CONTINUE
      IF(N-L)1326,1328,1326
1326 CI33NL=0.
      GO TO 1329
1328 CI33NL=0.
1329 CONTINUE
C
C      INTEGRAL CI34MK, CI34NL
C
C      CI34MK=CI33MK
C      CI34NL=CI33NL
C
C      INTEGRAL CI39MK, CI39NL
C
C      CI39MK=CI33MK
C      CI39NL=CI33NL
C
C      INTEGRAL CI40MK, CI40NL
C
C      CI40MK=CI33MK
C      CI40NL=CI33NL
C
C      INTEGRAL CI56MK, CI56NL
C
C      CI56MK=CI44MK
C      CI56NL=CI44NL
C
C      INTEGRAL CI38MK, CI38NL
C
C      CI38MK=CI31MK
C      CI38NL=CI31NL
C
C      INTEGRAL CI13MK, CI13NL
C      CI13MK=0.

```

C	CI13NL=0.
C	INTEGRAL CI11MK, CI11NL
C	CI11MK=CI31MK
	CI11NL=CI31NL
C	INTEGRAL CI28MK, CI28NL
C	CI28MK=CI44MK
C	CI28NL=CI44NL
C	INTEGRAL CI21MK, CI21NL
C	CI21MK=CI31MK
C	CI21NL=CI31NL
C	INTEGRAL CI26MK, CI26NL
C	CI26MK=CI33MK
C	CI26NL=CI33NL
C	INTEGRAL CI25MK, CI25NL
C	CI25MK=CI33MK
C	CI25NL=CI33NL
C	INTEGRAL CI24MK, CI24NL
C	CI24MK=CI33MK
C	CI24NL=CI33NL
C	INTEGRAL CI30MK, CI30NL
C	CI30MK=CI44MK
C	CI30NL=CI44NL

C  
C  
C

INTEGRAL CI23MK. CI23NL

CI23MK=CI31MK

CI23NL=CI31NL

S(JJXI,JUR)=+((B/A)\*BI11\*CI44MK\*CI31NL+BI16\*CI34MK\*CI33NL

1+BI16\*CI33MK\*CI34NL+(A/B)\*BI66\*CI31MK\*CI44NL)

JVR=JVR+1

S(JJXI,JVR)=+(BI12\*CI39MK\*CI40NL+(B/A)\*BI16\*CI56MK\*CI38NL+(A/B)

1\*BI26\*CI38MK\*CI56NL+BI66\*CI40MK\*CI39NL)

JWR=JWR+1

S(JJXI,JWR)=+(B\*K11\*AI44\*CI13MK\*CI11NL+A\*K12\*AI45\*CI11MK

1\*CI13NL)

JXR=JXR+1

S(JJXI,JXR)=+((B/A)\*DI11\*CI28MK\*CI21NL+2.\*DI16\*CI26MK\*CI26NL

1+(A/B)\*DI66\*CI21MK\*CI28NL+A\*B\*K11\*AI44\*CI21MK\*CI21NL)

JYR=JYR+1

S(JJXI,JYR)=+(DI12\*CI25MK\*CI24NL+(B/A)\*DI16\*CI30MK\*CI23NL+(A/B)

1\*DI26\*CI23MK\*CI30NL+DI66\*CI24MK\*CI25NL+A\*B\*K12\*AI45\*CI23MK

2\*CI23NL)

JUI=JUI+1

S(JJXI,JUI)=(B/A)\*BR11\*CI44MK\*CI31NL+BR16\*CI34MK\*CI33NL+BR16

1\*CI33MK\*CI34NL+(A/B)\*BR66\*CI31MK\*CI44NL-W2\*A\*B\*P1\*CI31MK\*CI31NL

JVI=JVI+1

S(JJXI,JVI)=BR12\*CI39MK\*CI40NL+(B/A)\*BR16\*CI56MK\*CI38NL+(A/B)

1\*BR26\*CI38MK\*CI56NL+BR66\*CI40MK\*CI39NL

JWI=JWI+1

S(JJXI,JWI)=B\*K11\*AR44\*CI13MK\*CI11NL+A\*K12\*AR45\*CI11MK\*CI13NL

JXI=JXI+1

S(JJXI,JXI)=(B/A)\*DR11\*CI28MK\*CI21NL+2.\*DR16\*CI26MK\*CI26NL+(A/B)

1\*DR66\*CI21MK\*CI28NL+A\*B\*K11\*AR44\*CI21MK\*CI21NL-W2\*A\*B\*P2\*CI21MK

2\*CI21NL

JYI=JYI+1

1300 S(JJXI,JYI)=DR12\*CI25MK\*CI24NL+(B/A)\*DR16\*CI30MK\*CI23NL+(A/B)

1\*DR26\*CI23MK\*CI30NL+DR66\*CI24MK\*CI25NL+A\*B\*K12\*AR45\*CI23MK

2\*CI23NL

```

C
C  CALCULATE SUBMATRIX
C  YIUR,YIVR,YIWR,YIXR,YIYR,YIUI,YIVI,YIMI,YIXI,YIYI
  JJYI=9*NN**2
  DO 1400 K1=1,NN
    K=K1+INPU1
  DO 1400 L2=1,NN
    L=L2+INPU2
  JUR=0
  JVR=1*NN**2
  JWR=2*NN**2
  JXR=3*NN**2
  JYR=4*NN**2
  JUI=5*NN**2
  JVI=6*NN**2
  JWI=7*NN**2
  JXI=8*NN**2
  JYI=9*NN**2
  JJYI=JJYI+1
  DO 1400 M1=1,NN
    M=M1+INPU1
  DO 1400 N2=1,NN
    N=N2+INPU2
  JUR=JUR+1

```

```

C
C  INTEGRAL CI37MK, CI37NL
C
  IF(M-K)1402,1404,1402
1402 CI37MK=0.
  GO TO 1405
1404 CI37MK=0.
1405 CONTINUE
  IF(N-L)1406,1408,1406
1406 CI37NL=0.
  GO TO 1409
1408 CI37NL=0.
1409 CONTINUE

```

```

C
C      INTEGRAL CI36MK. CI36NL
C
C      CI36MK=CI37MK
C      CI36NL=CI37NL
C
C      INTEGRAL CI55MK. CI55NL
C
C      IF(M-K)1412,1414,1412
C      1412 CI55MK=0.
C      GO TO 1415
C      1414 CI55MK=2.*MK*PI**2
C      1415 CONTINUE
C      IF(N-L)1416,1418,1416
C      1416 CI55NL=0.
C      GO TO 1419
C      1418 CI55NL=2.*NL*PI**2
C      1419 CONTINUE
C
C      INTEGRAL CI35MK. CI35NL
C
C      IF(M-K)1422,1424,1422
C      1422 CI35MK=1.
C      GO TO 1425
C      1424 CI35MK=1.5
C      1425 CONTINUE
C      IF(N-L)1426,1428,1426
C      1426 CI35NL=1.0
C      GO TO 1429
C      1428 CI35NL=1.5
C      1429 CONTINUE
C
C      INTEGRAL CI41MK. CI41NL
C
C      CI41MK=CI35MK
C      CI41NL=CI35NL

```

C	INTEGRAL CI57MK, CI57NL
C	
C	CI57MK=CI55MK
	CI57NL=CI55NL
C	
C	INTEGRAL CI42MK, CI42NL
C	
C	CI42MK=CI37MK
	CI42NL=CI37NL
C	
C	INTEGRAL CI43MK, CI43NL
C	
C	CI43MK=CI37MK
	CI43NL=CI37NL
C	
C	INTEGRAL CI15MK, CI15NL
C	
C	CI15MK=0.
	CI15NL=0.
C	
C	INTEGRAL CI12MK, CI12NL
C	
C	CI12MK=CI35MK
	CI12NL=CI35NL
C	
C	INTEGRAL CI24MK, CI24NL
C	
C	CI24MK=CI37MK
	CI24NL=CI37NL
C	
C	INTEGRAL CI25MK, CI25NL
C	
C	CI25MK=CI37MK
	CI25NL=CI37NL
C	

C	INTEGRAL CI23MK, CI23NL
C	
	CI23MK=CI35MK
	CI23NL=CI35NL
C	
C	INTEGRAL CI30MK, CI30NL
C	
	CI30MK=CI55MK
	CI30NL=CI55NL
C	
C	INTEGRAL CI22MK, CI22NL
C	
	CI22MK=CI35MK
	CI22NL=CI35NL
C	
C	INTEGRAL CI29MK, CI29NL
C	
	CI29MK=CI55MK
	CI29NL=CI55NL
C	
C	INTEGRAL CI27MK, CI27NL
C	
	CI27MK=CI37MK
	CI27NL=CI37NL
	S(JJYI,JUR)=+(BI12*CI37MK*CI36NL+(B/A)*BI16*CI55MK*CI35NL+(A/B)
	1*BI26*CI35MK*CI55NL+BI66*CI36MK*CI37NL)
	JVR=JVR+1
	S(JJYI,JVR)=+((A/B)*BI22*CI41MK*CI57NL+BI26*CI42MK*CI43NL+BI26
	1*CI43MK*CI42NL+(B/A)*BI66*CI57MK*CI41NL)
	JWR=JWR+1
	S(JJYI,JWR)=+(B*KI2*AI45*CI15MK*CI12NL+A*K22*AI55*CI12MK*CI15NL)
	JXR=JXR+1
	S(JJYI,JXR)=+(DI12*CI25MK*CI24NL+(B/A)*DI16*CI30MK*CI23NL+(A/B)
	1*DI26*CI23MK*CI30NL+DI66*CI24MK*CI25NL+A*H*KI2*AI45*CI23MK
	2*CI23NL)
	JYR=JYR+1

```

S(JJYI,JYR)=+((A/B)*DI22*CI22MK*CI29NL+2.*DI26*CI27MK*CI27NL+(B/A)
1*DI66*CI29MK*CI22NL+A*B*K22*AI55*CI22MK*CI22NL)
JUI=JUI+1
S(JJYI,JUI)=BR12*CI37MK*CI36NL+(B/A)*BR16*CI55MK*CI35NL+(A/B)
1*BR26*CI35MK*CI55NL+3R66*CI36MK*CI37NL
JVI=JVI+1
S(JJYI,JVI)=(A/B)*BR22*CI41MK*CI57NL+BR26*CI42MK*CI43NL+BR26
1*CI43MK*CI42NL+(B/A)*BR66*CI57MK*CI41NL-W2*A*B*PI*CI41MK
2*CI41NL
JWI=JWI+1
S(JJYI,JWI)=B*K12*AR45*CI15MK*CI12NL+A*K22*AR55*CI12MK*CI15NL
JXI=JXI+1
S(JJYI,JXI)=DR12*CI25MK*CI24NL+(B/A)*DR16*CI30MK*CI23NL+(A/B)
1*DR26*CI23MK*CI30NL+DR66*CI24MK*CI25NL+A*B*K12*AR45*CI23MK
2*CI23NL
JYI=JYI+1
1400 S(JJYI,JYI)=(A/B)*DR22*CI22MK*CI29NL+2.*DR26*CI27MK*CI27NL+(B/A)
1*DR66*CI29MK*CI22NL+A*B*K22*AR55*CI22MK*CI22NL-W2*A*B*P2*CI22MK
2*CI22NL
C CALCULATE B MATRIX
IJUR=0
IJVR=1*NN**2
IJWR=2*NN**2
IJXR=3*NN**2
IJYR=4*NN**2
IJUI=5*NN**2
IJVI=6*NN**2
IJWI=7*NN**2
IJXI=8*NN**2
IJYI=9*NN**2
DO 1500 M1=1,NN
M=M1+INPU1
DO 1500 N2=1,NN
N=N2+INPU2
IJUR=IJUR+1

```

C



INTEGRAL CIMK. CINL

CIMK=1.  
CINL=1.  
T(IJUR)=0.  
IJVR=IJVR+1  
T(IJVR)=0.  
IJWR=IJWR+1  
T(IJWR)=1.\*A\*B\*CIMK\*CINL  
IJXR=IJXR+1  
T(IJXR)=0.  
IJYR=IJYR+1  
T(IJYR)=0.  
IJUI=IJUI+1  
T(IJUI)=0.  
IJVI=IJVI+1  
T(IJVI)=0.  
IJWI=IJWI+1  
T(IJWI)=0.  
IJXI=IJXI+1  
T(IJXI)=0.  
IJYI=IJYI+1  
1500 T(IJYI)=0.

CALL SIMQ

NI=10\*NN\*\*2  
CALL SIMQ(S,T.NI.KS)  
WRITE(6,2050)KS  
2050 FORMAT(, KS=,13//)  
KN1=2\*NN\*\*2+1  
KN2=3\*NN\*\*2  
KN3=7\*NN\*\*2+1  
KN4=8\*NN\*\*2  
WRITE(6,2055) (T(J),J=KN1,KN2)  
WRITE(6,2055) (T(I),I=KN3,KN4)

```

2055 FORMAT(E12.5)
WRITE(6,2067)F
2067 FORMAT(' FQ=,F10.3)
GO TO 10
3333 CALL EXIT
END
C PEAK-AMPLITUDE AND MODIFIED KENNEDY-PANCU METHODS
C WR(J)=T(J) AND WI(I)=T(I)
REAL M1PIA,N1PIB,M2PIA,N2PIB,M3PIA,N3PIB,M4PIA,N4PIB
10 READ(5,20)FQ
20 FORMAT(F10.4)
IF(FQ)80,80,25
25 READ(5,30)WR1,WR2,WR3,WR4
30 FORMAT(4F10.4)
READ(5,40)WI1,WI2,WI3,WI4
40 FORMAT(4F10.4)
READ(5,50)M1,M2,M3,M4,N1,N2,N3,N4
50 FORMAT(8I5)
READ(5,55)A,B
55 FORMAT(2F10.4)
PI=3.1416
M1PIA=M1*PI*A
M2PIA=M2*PI*A
M3PIA=M3*PI*A
M4PIA=M4*PI*A
N1PIB=N1*PI*B
N2PIB=N2*PI*B
N3PIB=N3*PI*B
N4PIB=N4*PI*B
WRT=WR1*COS(M1PIA)*COS(N1PIB)+WR2*COS(M2PIA)*COS(N2PIB)
1+WR3*COS(M3PIA)*COS(N3PIB)+WR4*COS(M4PIA)*COS(N4PIB)
WIT=WI1*COS(M1PIA)*COS(N1PIB)+WI2*COS(M2PIA)*COS(N2PIB)
1+WI3*COS(M3PIA)*COS(N3PIB)+WI4*COS(M4PIA)*COS(N4PIB)
WT=(WRT**2+WIT**2)**0.5
WXOY1=ABS(WT)
RW=WIT/WRT

```

```

PHA=ATAN(RW)
DELS=WT*PHA
WRITE(6,60)PHA,DELS,FQ
60 FORMAT(' PHA=',F10.4,' DELS=',F10.4,' FQ=',F10.4)
WRITE(6,65) WXOY1
65 FORMAT(' WXOY1',E12.5)
GO TO 10
80 CALL EXIT
END
C NODAL PATTERNS FOR ANG=0,10,30,45,60,90
WRITE(6,35)
35 FORMAT(' X ' Y ' W ' //)
10 READ(5,20,END=220)WMIN1,WMIN2,WM2N1,WM2N2
20 FORMAT(4F10.4)
30 READ(5,30)M1,N1,M2,N2
30 FORMAT(4I5)
PI=3.1416
DO 100 J=1,5
Y=(J-1)*0.4
B=Y/1.6
X=-0.5
36 X=X+0.5
A=X/12.
M1PIA=M1*PI*A
N1PIB=N1*PI*B
M2PIA=M2*PI*A
N2PIB=N2*PI*B
W=WMIN1*COS(M1PIA)*COS(N1PIB)+WMIN2*COS(M1PIA)*COS(N2PIB)
1+W2N1*COS(M2PIA)*COS(N1PIB)+WM2N2*COS(M2PIA)*COS(N2PIB)
W1=ABS(W)
IF(W1.LT.0.01)WRITE(6,40)A,B,W1
IF(A.LT.1.0)GO TO 36
40 FORMAT(3F10.4)
100 CONTINUE
GO TO 10
220 CALL EXIT

```